NATIONAL AND KAPODISTRIAN UNIVERSITY OF ATHENS

SCHOOL OF SCIENCE

DEPARTMENT OF BIOLOGY

Studying and characterization of enzymes and metabolic pathways involved in the decomposition of lignin and lignin-derived compounds

Doctoral Thesis

DAPHNE GEORGIADOU

MSc Agronomist – Biotechnologist

ATHENS 2020

Approval of this Doctoral Thesis by the Department of Biology, of the School of Science of the National and Kapodistrian University of Athens (NKUA) does not constitute in any way an acceptance of the views of the author contained herein by the said academic organization (L. 5343/1932, art. 202).

I hereby expressly declare that this Doctoral Thesis is not the product of partial or total plagiarism.

Seven-member Examination Committee:

Supervisor:

Dimitris G. Hatzinikolaou
Associate Professor of Microbial Biotechnology, Department of Biology, National and Kapodistrian University of Athens.

Members of the Three-member Advisory Committee:

George Diallinas
Professor of Molecular Microbiology, Department of Biology, National and Kapodistrian University of Athens.

Amalia Karagounis – Kyrtsou
Professor Emeritus of Microbiology, Department of Biology, National and Kapodistrian University of Athens.

Members of the Seven-member Examination Committee:

Constantinos E. Vorgias
Professor of Biochemistry, Department of Biology, National and Kapodistrian University of Athens.

Zacharoula Gonou – Zagou
Assistant Professor of Systematics & Ecology of Fungi, Department of Biology, National and Kapodistrian University of Athens.

Iordanis Chatzipavlidis
Associate Professor of Environmental Microbiology, Faculty of Crop Science, Agricultural University of Athens.

Diomi Mamma
Assistant Professor of Biochemical Engineering School of Chemical Engineering, National Technical University of Athens.

Table of contents

List of abbreviations

S.I. (Système International d'Unités) abbreviations for units and standard notations for chemical elements, formulae and chemical abbreviations are used in this work. Other abbreviations are listed below.

ABTS	2,2'-azino-bis(3-ethylbenzothiazoline-6-sulfonic acid)
APS	Ammonium persulfate
CBM	Carbohydrate-binding module
CMC	Carboxymethyl cellulose
CSLH	Corn stover lignin hydrolysate
DMSO	Dimethyl sulfoxide
DNS	3,5-Dinitrosalicylic acid
DyP	Dye decolorizing Peroxidase
DTT	Dithiothreitol
EDTA	Ethylenediaminetetraacetic acid
EPR	Electron Paramagnetic Resonance
FC	Folin – Ciocalteu
GGE	Guaiacyl glycerol-beta-guaiacyl ether
HPLC	High-pressure liquid chromatography
IEA	International Energy Agency
IPTG	Isopropyl β-D-1-thiogalactopyranoside
KatG	Catalase-Peroxidase
LiP	Lignin-dependent Peroxidase
MeOH	Methanol
MCO	Multicopper oxidase
MnP	Manganese-dependent Peroxidase
MSM	Mineral salt medium
NMR	Nuclear magnetic resonance
OprD	Outer membrane porin D
PAGE	Polyacrylamide gel electrophoresis
PCA	Protocatechuic acid
PCR	Polymerase chain reaction
Pk-CopA	*Pseudomonas kilonensis* ZKA7 CopA protein
Pk-DypB	*Pseudomonas kilonensis* ZKA7 DypB protein
Pk-KatG	*Pseudomonas kilonensis* ZKA7 KatG protein
PMSF	Phenylmethylsulfonyl fluoride
SDS	Sodium dodecyl sulfate
SSF	Solid-state fermentation
TBDR	TonB-dependent receptors
TEMED	Tetramethylethylenediamine
TFA	Trifluoroacetic acid
WSLH	Wheat straw lignin hydrolysate

Abstract

Lignocellulose biorefineries can harness the immense amounts of reduced carbon in the structural components of plant cell walls, via the conversion of residual biomass into biofuels and bio-based chemicals. The use of bacterial enzymes for lignocellulose valorization has recently gained growing attention and has been proposed as an alternative approach to the current use of fungal hydrolytic enzymes, due to the lower production cost of bacterial enzymes and their higher stability against the harsh conditions usually employed in biorefineries. Moreover, bacteria naturally endowed or engineered with the ability to funnel diverse lignin-derived molecules into specific high added-value products can replace chemical processes for lignin valorization. The aims of this thesis were to discover novel lignin and plant polysaccharide degrading bacteria, to detect efficient hydrolytic and oxidative enzymes and to elucidate pathways involved in bacterial degradation of lignin. The outcomes of this thesis are expected to aid the efforts towards designing efficient enzymatic and microbial biocatalysts for the complete valorization of lignocellulosic biomass.

To detect aerobic, mesophilic bacterial lignocellulose degraders, five uniformly distributed surface soil samples were collected from Keri Lake, at the island of Zakynthos, in western Greece. This area represents a unique environment, dominated by a marsh mainly composed of reeds, with increased biomass degradation, where, in parallel, for more than 2.500 years asphalt springs release crude oil, rich in aromatic hydrocarbons. For the isolation of bacteria, an enrichment strategy based on organosolv lignin, xylan from birchwood and carboxymethyl amorphous cellulose (CMC), as sole carbon and energy sources was used. A total of 63 colonies were isolated from enrichment cultures of all five soil samples. Characterization of the 16S rRNA gene of all the isolates generated 24 different genera. A wide diversity of *Pseudomonas* species was enriched in organosolv lignin cultures. Complex bacterial consortia were enriched in cultures with xylan or CMC, belonging to Actinobacteria, Proteobacteria, Bacilli, Sphingobacteriia and Flavobacteria. Several individual isolates could target amorphous and crystalline cellulose, or xylan, by expressing the corresponding hydrolytic activities, providing evidence of endoglycolytic, exoglycolytic and xylanolytic enzyme activity. A series of screening tests have featured the ability of strain *Pseudomonas kilonensis* ZKA7 to grow on organosolv lignin, on lignin hydrolysates generated from agricultural residues of corn stover and wheat straw, by implementing a mild alkali pretreatment method, and on lignin-derived aromatic monomers such as ferulic, caffeic and vanillic acid. NMR analysis revealed that this strain was also able to generate structural modifications in corn stover lignin hydrolysate, arising from degradation of lignin aromatic moieties.

Three novel oxidoreductases from strain ZKA7 were selected for investigation of their ligninolytic and oxidative potential, a multicopper oxidase (Pk-CopA), a dye decolorizing peroxidase (Pk-DypB) and a catalase-peroxidase (Pk-katG). The recombinant proteins were expressed as N-terminal 6xHis-fusion proteins in *E. coli* expression system and were purified by nickel affinity chromatography and gel filtration chromatography. Pk-CopA was able to oxidize lignin prepared from alkali pretreated corn stover, in the presence of ABTS as a mediator, generating a new product, as indicated by HPLC analysis. It was also able to oxidize the lignin-associated aromatic monomers ferulic acid, caffeic acid, syringic acid and catechol. Pk-CopA exhibited activity at a higher pH range than most bacterial laccases, retaining over 80% of its optimal activity between pH 4.5 - 6.5. It also exhibited high pH and thermal stability, maintaining 80% of its initial activity after 2 h of preincubation at pH 11and almost 70% of its initial activity within 6 hours of incubation at 60°C.

Pk-DypB was active towards ABTS, while it was able to act at a less acidic pH (6.0) than other characterized dyp-type peroxidases. However, its thermal stability and pH stability under alkaline and acidic conditions were lower than other enzymes. Under the conditions tested, no oxidative activity was detected for Pk-DypB towards lignin hydrolysate from alkali pretreated corn stover. Pk-KatG exhibited both catalase and peroxidase activity though it exhibited higher affinity and catalytic efficiency towards peroxidase substrates than the natural catalase substrate, H_2O_2. The biochemical characterization of Pk-KatG also provides the first report of the oxidation of syringaldazine, a typical substrate of ligninolytic enzymes, by a catalase-peroxidase, as well as the first report of the oxidation of the aromatic monomers catechol and pyrogallol, mediated by the presence of ABTS, and the oxidation of the synthetic dye Remazol Brilliant Blue R, a substrate used to detect ligninolytic activity. These findings may suggest a potential lignin oxidative activity that remains to be investigated.

For the identification of pathways involved in lignin degradation a proteomic analysis was conducted on *Pseudomonas kilonensis* ZKA7 cells, grown on lignin hydrolysate from corn stover, ferulic, caffeic, and vanillic acid, and acetate as a reference substrate. Protein samples were collected from cells grown on each substrate, separated into intracellular and extracellular fractions and subjected to proteomic analysis, using an LC-MS/MS system. Statistical analysis revealed the upregulation of genes involved in upper and central pathways of lignin-derived aromatic monomers degradation, as well as genes encoding transport proteins, transcriptional regulators, stress response proteins, oxidative enzymes and proteins of unknown function.

Περίληψη

Η λιγνινοκυτταρινούχος βιομάζα αποτελεί μία άφθονη και ανανεώσιμη πηγή ανηγμένου άνθρακα που μπορεί να χρησιμοποιηθεί για την παραγωγή βιοκαυσίμων και χημικών τα οποία μέχρι σήμερα παράγονται από το πετρέλαιο. Στα πλαίσια ενός βιοδιυλιστηρίου δεύτερης γενιάς το λιγνινοκυτταρινούχο φυτικό υλικό υπόκειται αρχικά σε προκατεργασία προκειμένου να απομακρυνθεί η λιγνίνη και να αποκτήσουν τα υδρολυτικά ένζυμα πρόσβαση στους πολυσακχαρίτες του φυτικού κυτταρικού τοιχώματος. Τα υδρολυτικά ένζυμα απελευθερώνουν σάκχαρα τα οποία στη συνέχεια ζυμώνονται από μικροοργανισμούς, προς παραγωγή βιοκαυσίμων και χημικών. Έως σήμερα, η λιγνίνη που απομακρύνεται παραμένει σε μεγάλο ποσοστό ανεκμετάλλευτη, ενώ τα μυκητιακής φύσεως υδρολυτικά ένζυμα που χρησιμοποιούνται, έχουν αυξημένο κόστος παραγωγής και παρουσιάζουν χαμηλή σταθερότητα στις αντίξοες συνθήκες ενός βιοδιυλιστηρίου. Η χρήση βακτηρίων που διαθέτουν μεταβολικά μονοπάτια αποικοδόμησης της λιγνίνης και των παραγώγων της αλλά και η χρήση εξειδικευμένων βακτηριακών ενζύμων διάσπασης της λιγνίνης αποτελούν εναλλακτικές μεθόδους αξιοποίησης της λιγνίνης προς την κατεύθυνση της παραγωγής προϊόντων υψηλής προστιθέμενης αξίας. Η χρήση βακτηριακών υδρολυτικών ενζύμων έχει επίσης προταθεί ως εναλλακτική της χρήσης των μυκητιακών, εξαιτίας του χαμηλότερου κόστους παραγωγής των βακτηριακών ενζύμων και της υψηλότερης σταθερότητάς τους σε υψηλές θερμοκρασίες και ακραίες τιμές pH. Ο στόχος αυτής της διατριβής είναι η ανεύρεση νέων βακτηρίων και ενζύμων με ικανότητα αποικοδόμησης της λιγνίνης, η μελέτη του μηχανισμού της βακτηριακής διάσπασης της λιγνίνης και των αρωματικών μονομερών της, και η εξεύρεση βακτηριακών ενζύμων που υδρολύουν την κυτταρίνη και τις ημικυτταρίνες. Τα αποτελέσματα αυτής της έρευνας αναμένεται να βοηθήσουν την προσπάθεια σχεδιασμού αποτελεσματικών μικροβιακών και ενζυμικών βιοκαταλυτών και την εφαρμογή τους για την πλήρη αξιοποίηση της λιγνινοκυτταρινούχου βιομάζας.

Για την απομόνωση αερόβιων, μεσόφιλων βακτηρίων με ικανότητα διάσπασης των συστατικών της λιγνινοκυτταρίνης, χρησιμοποιήθηκαν πέντε επιφανειακά εδαφικά δείγματα της περιοχής Λίμνη Κεριού, από το νησί της Ζακύνθου, τα οποία προστέθηκαν σε καλλιέργειες εμπλουτισμού με μοναδικές πηγές άνθρακα και ενέργειας τη λιγνίνη organosolv, την ξυλάνη σημύδας ή την άμορφη κυτταρίνη CMC. Η περιοχή του Κεριού αποτελεί ένα ιδιαίτερο ενδιαίτημα όπου παρατηρείται εκτεταμένη αποικοδόμηση της φυτικής βιομάζας και κατά τόπους φυσική ανάβλυση πετρελαίου με διαπιστωμένα υψηλό ποσοστό αρωματικών υδρογονανθράκων. Από το σύνολο των πέντε εδαφικών δειγμάτων απομονώθηκαν 63 αμιγείς αποικίες, οι οποίες βάση του χαρακτηρισμού του 16S rRNA γονιδίου ανήκουν σε 24 διαφορετικά γένη. Ένα ευρύ φάσμα βακτηρίων που ανήκουν στο

γένος *Pseudomonas* απομονώθηκαν από καλλιέργειες σε λιγνίνη organosolv, και ποικίλα στελέχη που ανήκουν στα φύλα Actinobacteria, Proteobacteria, Bacilli, Sphingobacteriia και Flavobacteria απομονώθηκαν από καλλιέργειες ξυλάνης και κυτταρίνης, με κυρίαρχα τα είδη του γένους *Microbacterium*.

Για τη μελέτη ανάπτυξης των βακτηριακών στελεχών σε υποστρώματα λιγνίνης παρασκευάστηκαν υδρολύματα λιγνίνης από άχυρο καλαμποκιού και σιταριού, χρησιμοποιώντας μία ήπια αλκαλική μέθοδο προκατεργασίας. Παράλληλα, εξετάστηκε η ικανότητα ανάπτυξης των στελεχών σε εμπορικά σκευάσματα λιγνίνης organosolv και kraft λιγνίνης καθώς και σε πρότυπες μονομερείς και διμερείς αρωματικές ενώσεις λιγνίνης. Σημαντικός αριθμός στελεχών αναπτύχθηκαν στα υποστρώματα λιγνίνης από προκατεργασμένα αγροτικά υπολείμματα. Τα αποτελέσματα ανέδειξαν το στέλεχος *Pseudomonas kilonensis* ZKA7 το οποίο είναι ικανό να αναπτύσσεται σε λιγνίνη από αλκαλικά προκατεργασμένο άχυρο καλαμποκιού και σιταριού, σε λιγνίνη organosolv, και στα αρωματικά μονομερή φερουλικό, καφεϊκό και βανιλλικό οξύ. Η ανάλυση με NMR πρωτονίων έδειξε ότι το στέλεχος αυτό επιφέρει δομικές αλλαγές στο υδρόλυμα λιγνίνης από προκατεργασμένο άχυρο καλαμποκιού, και συγκεκριμένα μείωση των κορυφών που αντιστοιχούν στα αρωματικά πρωτόνια. Επίσης, το στέλεχος *Pseudomonas* sp. ZKA12 είναι ικανό να μεταβολίζει μονομερή λιγνίνης τύπου G- και S-, όπως φερουλικό και συρινγκικό οξύ, και μπορεί να αποτελέσει τη βάση για το μελλοντικό σχεδιασμό ενός μικροοργανισμού που θα αποικοδομεί όλα τα δομικά συστατικά της λιγνίνης. Αρκετά στελέχη ήταν ικανά να αποικοδομούν τη CMC κυτταρίνη, την μικροκρυσταλλική κυτταρίνη Avicel και την ξυλάνη σημύδας σε αμιγείς καλλιέργειες, υποδηλώνοντας τη δράση ενδογλουκανασών, εξωγλουκανασών και ξυλανασών, ωστόσο από το σημείο αυτό και έπειτα η έρευνα επικεντρώθηκε στην μελέτη της διάσπασης της λιγνίνης.

Τρία οξειδοαναγωγικά ένζυμα του στελέχους ZKA7 επιλέχθηκαν για τη διερεύνηση της λιγνινολυτικής και οξειδωτικής τους ικανότητας. Συγκεκριμένα, τα ένζυμα αυτά ήταν μία πολυοξειδάση χαλκού (Pk-CopA), μία υπεροξειδάση αποχρωματισμού χρωστικών τύπου Dyp (Pk-DypB) και μία καταλάση-υπεροξειδάση (Pk-katG). Οι ανασυνδυασμένες πρωτεΐνες παρήχθησαν σε σύστημα υπερέκφρασης *E. coli* και ο καθαρισμός τους πραγματοποιήθηκε με χρωματογραφία συγγένειας και χρωματογραφία μοριακού αποκλεισμού. Η πρωτεΐνη Pk-CopA είχε χαρακτηριστικά λακκάσης και οξείδωσε τη λιγνίνη από αλκαλικά προκατεργασμένο άχυρο, παρουσία ABTS ως ενδιάμεσου μορίου. Επίσης, εμφάνισε ικανότητα οξείδωσης των αρωματικών μονομερών φερουλικό, καφεϊκό και συρινγκικό οξύ καθώς και της κατεχόλης. Η Pk-CopA είχε ενεργότητα σε ένα μεγαλύτερο εύρος pH σε σχέση με τις περισσότερες βακτηριακές λακκάσες, και επέδειξε υψηλή σταθερότητα σε

θερμοκρασίες 60-70°C, και υψηλή σταθερότητα σε αλκαλικό pH, χαρακτηριστικά που καθιστούν το ένζυμο ικανό να αξιοποιηθεί σε διεργασίες ενός βιοδιυλιστηρίου.

Η πρωτεΐνη Pk-DypB εμφάνισε άριστο pH δράσης στην όξινη περιοχή, αλλά σε μεγαλύτερη τιμή σε σύγκριση με χαρακτηρισμένες υπεροξειδάσες τύπου dyp, ωστόσο, η σταθερότητά της σε υψηλές θερμοκρασίες και αλκαλικό και όξινο pH ήταν χαμηλότερη από παρόμοια ένζυμα. Υπό τις εξεταζόμενες συνθήκες, δεν ανιχνεύτηκε οξειδωτική δράση έναντι της λιγνίνης που παρασκευάστηκε από αλκαλικά προκατεργασμένο άχυρο. Η πρωτεΐνη Pk-KatG είχε δράση καταλάσης και υπεροξειδάσης ενώ επέδειξε υψηλότερη συγγένεια και καταλυτική ικανότητα έναντι οργανικών υποστρωμάτων υπεροξειδασών , σε σχέση με το υπεροξείδιο υδρογόνου που αποτελεί φυσικό υπόστρωμα για τις καταλάσες. Η Pk-KatG οξείδωσε το πρότυπο αρωματικό υπόστρωμα syringaldazine και τη συνθετική χρωστική Remazol Brilliant Blue R, υποδηλώνοντας πιθανή λιγνινολυτική δράση του ενζύμου.

Τέλος, η πρωτεομική ανάλυση του στελέχους *Pseudomonas kilonensis* ZKA7 έδειξε ότι τα γονίδια που εμπλέκονται σε περιφερειακά και κεντρικά μονοπάτια αποδόμησης αρωματικών μονομερών της λιγνίνης είναι μεταβολικά ενεργά και επάγονται παρουσία λιγνίνης από αλκαλικά προκατεργασμένο άχυρο. Επίσης, η πρωτεομική ανάλυση ανέδειξε την αυξορύθμιση γονιδίων που κωδικοποιούν πρωτεϊνικούς μεταφορείς, μεταγραφικούς παράγοντες, πρωτεΐνες απόκρισης στο οξειδωτικό στρες, οξειδωτικά ένζυμα και πρωτεΐνες άγνωστης έως τώρα λειτουργίας, των οποίων ο ρόλος αναμένεται να διερευνηθεί μέσα από περαιτέρω πειράματα.

Acknowledgments

Chapter 1

Introduction

Introductory

In the last decades, the fast-growing human population and the consequent accelerating consumption of Earth's resources have raised global concern over our planet's material, energy and environmental sustainability (Ferreira, 2017). While the dependence of the transport and chemical sector on fossil fuels is high (Cherubini, 2010), petroleum's availability is depleting, necessitating the use of alternative sources for the production of fuels and industrial chemicals. What is more, human-induced global warming, driven mainly by the fossil-fuel-based production processes, has strengthened the global response to the threat of climate change and its detrimental consequences (Fleurbaey *et al.*, 2014). Hence, sustainable, and environmentally friendly energy and material sources are required to meet the world's future energy needs.

Biofuels are of considerable interest to researchers, industrial partners and governments, and can provide an alternative to petrol for the transport sector (Hill *et al.*, 2006). Lignocellulosic biomass is the most abundant, inexpensive and fully renewable resource of reduced biomass in the biosphere (Fisher, 2014) and can serve as a raw material for the production of second generation bioethanol and valuable products within a biorefinery (Kamm *et al.*, 2008). Vast amounts of lignocellulosic waste are created annually, through agricultural practice, forestry, industrial processes such as paper and pulp, textile or timber industries, breweries and municipal waste. However, due to the complex and recalcitrant structure of lignocellulose, which consists of cellulose, hemicelluloses and the aromatic heteropolymer of lignin, the conversion technology of lignocellulose materials into energy and bioproducts is costly and ineffective up to now (Menon and Rao, 2012).

The remaining lignin from industries that utilize plant polysaccharides, remains mostly underutilized and is treated as waste (Schoenherr *et al.*, 2018). Lignin stands for the only renewable source in the biosphere for aromatic moieties, therefore, the development of a lignin valorization technology for the production of value-added aromatic chemicals would greatly improve the economics of producing biofuels from lignocellulose (Doherty *et al.*, 2011). Besides, there is still a demand for diminishing the production cost of hydrolytic enzymes used during plant polysaccharide bioconversion into bioethanol, along with the need to optimize their catalytic efficiency (Lynd *et al.*, 2008).

The use of bacteria-based systems and enzymes for lignocellulose valorization has recently gained growing attention (Bugg and Rahmanpour, 2015, Orencio-Trejo *et al.*, 2016). However, the bacterial degradation of lignin is currently insufficiently understood, particularly regarding the oxidative enzymes involved in the initial breakdown of lignin and the release of monoaromatic moieties, the subsequent transport of the monomeric compounds into the bacterial cells, and the transcriptional regulation of the catabolic genes for lignin-derived aromatics. Moreover, despite the recent improvements towards designing efficient enzymes for polysaccharide hydrolysis, the development of an ideal enzyme has not been accomplished yet.

With this thesis, we hope to discover novel bacterial lignocellulose degraders that produce robust oxidative and hydrolytic enzymes, and to elucidate the individual catalytic steps in the bacterial transformation of residual lignin. The knowledge obtained will hopefully add to the efforts for the development of enzymatic and microbial bioengineering strategies towards lignocellulose saccharification and production of lignin-based commodity chemicals. It is our vision to develop potent bacterial-based biorefinery applications to assist the replacement of the fossil fuel-based production of fuels and chemicals with a sustainable alternative, through the complete valorization of residual lignocellulosic biomass.

1.1. The biorefinery concept

Following the oil embargo in the United States in 1973, a serious effort commenced to replace the use of gasoline with biofuels and reduce reliance on energy imports. Governments throughout the world have introduced a series of actions to replace a certain percentage of transportation fuels with renewable fuels (Bowyer, 2017). Furthermore, in 2007, the Executive Committee of the International Energy Agency (IEA) recognized the importance of co-production of chemicals and materials along with bioenergy, and therefore established the IEA Bioenergy Task 42 Biorefinery (de Jong, 2009). The biorefinery concept is based on the sustainable conversion of renewable biomass into biofuels, bioenergy and marketable bio-based products, and was proposed as a potential solution to help moderate the harmful consequences of the growing demand for fuels, energy and chemicals (Figure 1).

Currently, the main producers of bioethanol worldwide, USA and Brazil, utilize edible feedstocks, such as starchy (corn, wheat, barley, cassava and potato) and sucrose-containing materials (sugarcane, sugarbeet and sweet sorghum), to produce first-generation bioethanol. This has generated a serious competition for arable land and water with food crops, raising global socio-economic and environmental concerns (Jambo *et al.*, 2016). Therefore, governments are trying to promote a shift from first-generation towards advanced biofuels, i.e. second-generation cellulosic ethanol derived from lignocellulosic biomass and third-generation biofuels produced from algae or cyanobacteria (Bracmort, 2019).
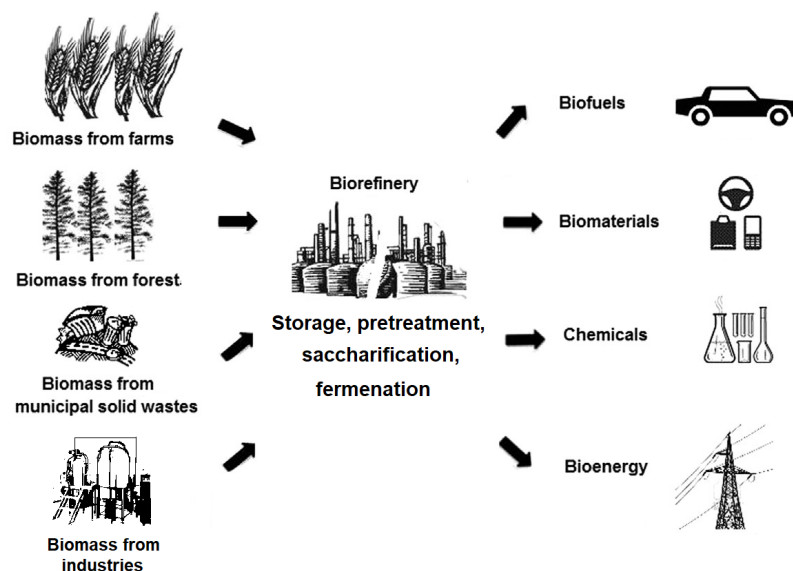
Fig. 1. The lignocellulose biorefinery concept. Adapted from (Kudakasseril *et al.*, 2013).

For many years cellulosic ethanol was produced on a smaller scale in pilot and demonstration facilities, but in 2015 cellulosic ethanol plants began to operate and second-generation biofuels began to be commercialized. As of 2017, 67 lignocellulosic biorefineries operated around the world, with at least 1/3 of them operating at a commercial scale (Figure 2). (Bowyer, 2017).

Fig. 2. Global cellulosic biorefineries. Operational biorefineries are displayed in blue, biorefineries in development are displayed in yellow and suspended biorefineries are displayed in red. Map developed by Dovetail Partners, Inc. – Source: www.dovetailinc.org.

Although cellulosic biofuel requirements are ascending, according to the policies implemented around the world, the volume requirements are hardly met and the biofuel and bio-based chemicals potential of lignocellulose are far greater than current production levels (Bracmort, 2019).

1.1.1 Challenges during enzymatic saccharification of plant biomass and lignin valorization within a biorefinery

Within a biorefinery, the conversion of lignocellulose into biofuels involves three main steps. The first step involves the delignification of plant material and the disruption of cellulose's crystal structure, aiming to enhance the accessibility of hydrolytic enzymes to glucan and xylan (Alvira *et al.*, 2010). Typically, it is achieved either by mechanical, physical or chemical pretreatment processes of plant biomass. After pretreatment, hydrolytic enzymes are used to depolymerize cellulose and hemicelluloses into simple sugars and in the final step, sugars are fermented and converted to ethanol or other fuels and chemicals by microorganisms.

Currently, the main enzymes used for plant polysaccharide hydrolysis are derived from fungi, however, their high production cost, which results from the insufficient quantities produced by fungal strains, accounts for 20-40% of the total cost for cellulosic ethanol production (Naresh Kumar *et al.*, 2019). The high cost of cellulases is one of the major obstacles to commercialization of biomass biorefineries since a large amount of cellulase is consumed for biomass saccharification, i.e. approximately 100 g of enzymes are required per gallon of cellulosic ethanol produced (Zhu *et al.*, 2009). Moreover, higher enzyme catalytic efficiencies, thermostability and inhibitor tolerance are required to render the biorefinery process economically feasible (Zhang and Zhang, 2013).

What is more, the residual lignin is mostly disposed of due to the inefficiency of lignin degradation processes (Malherbe and Cloete, 2002). In some cases, a major portion of lignin is being burned to generate power supplying the internal processes (Ragauskas *et al.*, 2014), with only a small amount of it (2%) being used for the generation of valuable aromatic chemicals (Laurichesse and Avérous, 2014). However, lignin utilization as fuel is not economically rational (Vishtal and Kraslawski, 2011). On the other hand, industrial lignins generated by pretreatment of plant biomass constitute a complex mixture of depolymerization components, therefore, generating a single chemical species from depolymerized lignin mixtures remains challenging. Chemical procedures currently implemented for further lignin fragmentation and transformation into high-value products usually result in the formation of multiple diverse products, which necessitate an extensive and cost-consuming separation process (Schoenherr *et al.*, 2018).

1.1.2 The use of bacterial enzymes and bacteria-based systems for lignocellulose valorization

To improve the microbial saccharification efficiency and reduce the cost of hydrolytic enzymes a lot of strategies have been proposed, such as the use of bacterial hydrolytic enzymes. Their use could overcome the challenges of fungal genetic modification and protein expression of cellulases (Srivastava *et al.*, 2018), since bacterial protein production could be facilitated by the widely available bacterial genetic engineering strategies and potent heterologous protein expression systems (Li *et al.*, 2008). Also, bacterial enzymes, such as xylanases, have an advantage over fungal enzymes, as the former can operate efficiently in neutral or alkaline pH, whereas fungal xylanases have their optimal pH in the acidic range (Chakdar *et al.*, 2016). Another advantage of the industrial use of bacterial enzymes is their higher tolerance and stability against harsh conditions formed during the conversion process

of lignocellulose, such as extreme temperatures, salinity or potential inhibitors (Orencio-Trejo *et al.*, 2016).

Lately, there has also been a growing interest in the identification of microbial enzymes for lignin depolymerization (Bugg and Rahmanpour, 2015). As opposed to chemical procedures currently implemented to valorize lignin, enzymatic catalysis is conducted in water and under mild conditions, avoiding high pressure and temperature and hazardous and expensive chemical catalysts, thus lowering the environmental impact of the process (Hämäläinen *et al.*, 2018). The development of fungal ligninolytic enzymes for large-scale lignin degradation, such as laccases, has been hindered by the challenges of fungal genetic modification and protein expression, their acidic pH preference and lower thermal stability (Baldrian, 2006).

In addition, contrary to the targeted depolymerization of plant polysaccharides, the enzymatic degradation of lignin by fungi takes place with non-specific oxidative enzymes, which act indirectly in a cascade manner, eventually causing the oxidative cleavage of lignin bonds (Abdelaziz *et al.*, 2016). Enzymatic strategies for lignin valorization need to allow highly selective bond-scissions so that the reaction products are produced at a reasonable quantity. There is evidence that bacterial lignin degradation is more specific than with the corresponding fungal systems, thus rendering bacterial enzymes more attractive for applications in biotechnology where specific modifications of lignin are of interest (Vicuña, 1988). In contrast to fungal lignin degradation though, knowledge concerning bacterial ligninolytic enzymes has only recently grown. Therefore, the search and identification of new bacterial enzymes involved in lignin decomposition remain an essential step for the development of effective lignin transformation bioprocesses.

An alternative approach for lignin valorization is the use of microorganisms naturally endowed or engineered with the ability to assimilate a wide range of lignin-derived aromatic compounds as energy and carbon sources, transforming them into a specific metabolite (Xu *et al.*, 2019). Bacterial-based systems of lignin metabolism have only recently gained attention, through the identification of bacteria able to funnel diverse lignin-derived molecules into specific high added value products, such as vanillin, polyhydroxyalkanoates, lipids, pyruvate, etc. The target metabolite is typically produced upstream to the central metabolism and may be readily purified or converted into a commodity chemical (Beckham, 2018).

Biological funneling exploits the biological diversity of aromatic catabolic pathways of microorganisms thereby avoiding the need for separation of heterogeneous lignin

depolymerization components. However, most lignin-degrading bacteria can only assimilate a fraction of lignin-based compounds, therefore, more efficient bacteria and metabolic pathways are in need for the comprehensive utilization of lignin (Xu *et al.*, 2019). Further understanding of the bacterial lignin degradation process will allow pathway engineering and introduction of desired metabolic traits into a single organism. Another challenge in lignin valorization by bacterial systems is the low product titers from lignin-based solutions (Rodriguez *et al.*, 2017). What is more, microbes have low capability in utilizing water-insoluble and/or high-molecular-weight lignin. Hence, the successful valorization of lignin depends also on pretreatment processes that disrupt lignin-enriched substrates into low-molecular-weight and water-soluble species that can be assimilated by bacteria efficiently (Beckham *et al.*, 2016).

1.2 Research aims and objectives

<u>Aims:</u>

1.   To discover novel efficient enzymes and bacteria for lignin valorization and plant polysaccharide hydrolysis that can be employed in an industrial lignocellulose biorefinery process,

2.   To elucidate the proteomic and the genetic basis of the bacterial transformation of industrial lignin and lignin-derived aromatic compounds, in order to identify new ligninolytic enzymes and allow pathway engineering for the production of commodity chemicals from lignin in future studies.

<u>Objectives:</u>

1.   Novel aerobic mesophilic lignocellulose degrading bacteria will be isolated from soil samples collected from Keri Lake, in Zakynthos Island, western Greece, by using an enrichment strategy based on organosolv lignin, xylan from birchwood and amorphous cellulose, as sole carbon and energy sources. The area represents a unique environment with increased biomass degradation, dominated by a marsh mainly composed of reeds, with natural oil seeps at several sites, rich in aromatic hydrocarbons. Our approach is based on the hypothesis that these characteristics favor the natural enrichment of bacteria that have developed the ability i) to utilize lignin-associated aromatic compounds as their carbon and energy source and ii) to withstand inhibitory concentrations of lignin and oil-derived aromatic compounds. In addition, we anticipate that the continuous input of cellulosic and hemicellulosic carbon from decaying biomass may result in the natural selection of microbes that have acquired multiple genes and transcriptional regulators for high-level production of enzymes efficient in plant polysaccharide deconstruction.

2.   The enzymatic and metabolic potential of individual strains will be explored by screening their ability to grow on industrial lignin substrates, lignin-derived aromatic substances, and cellulosic and hemicellulosic substrates. Agricultural residues will also be used for generating lignin substrates, by implementing a laboratory-scale pretreatment method so as to simulate the lignin streams produced by large-scale biorefineries. NMR analysis will reveal any modifications in the lignin substrates following treatment with selected individual strains.

3.   Based on the screening results the most promising bacterial candidates will be used for the identification, heterologous production and characterization of oxidoreductases

possibly involved in the transformation of lignin feedstocks, prepared from chemically pretreated agricultural residues. This approach will be based on the selection of oxidative enzymes for which there is yet no information on their ligninolytic potential. The *in vitro* enzymatic degradation of lignin and formation of any products will be monitored via HPLC. The produced enzymes will be further evaluated for their potential application in a lignin valorization scheme, by studying their properties, such as activity optima, thermal and pH stability, inhibition patterns and ability to oxidize lignin-associated aromatic compounds. The synergistic effect of these enzymes towards lignin transformation will be examined.

4. In parallel, to decipher the genetic basis of ligninolytic genes the complete genomes of 20 in total ligninolytic isolates of this study will be sequenced at the DOE-Joint Genome Institute. These genomes will be comparatively analyzed together with additionally available genomes of known bacterial lignin degraders.

5. To identify oxidative enzymes and metabolic pathways involved in lignin biotransformation a proteomic analysis on a selected ligninolytic strain will be conducted. Protein profiles of lignin grown cells will be compared with cells grown on monoaromatic compounds and reference substrates. Proteins will be separated into intracellular and extracellular fractions and will be subjected to LC-MS/MS analysis in the Protein and Proteome analytical facility of the University of Newcastle.

The following section will review the current knowledge and ongoing research on lignocellulosic biomass bioprocessing.

1.3 Lignocellulose structure

1.3.1 Cellulose

Cellulose is classified as the most abundant organic substance on earth, covering 40-60% of dry plant biomass. Its role is exclusively structural. The high tensile strength of cellulose enables plant cells to withstand osmotic pressure and mechanical stress. Cellulose is a linear polymer made of D-glucose residues, linked by β-1,4-glycosidic bonds. Each glucose residue is rotated 180° around the axis of cellulose's backbone chain, making cellobiose the repeating unit of cellulose (Figure 3) (Zhang and Lynd, 2004).
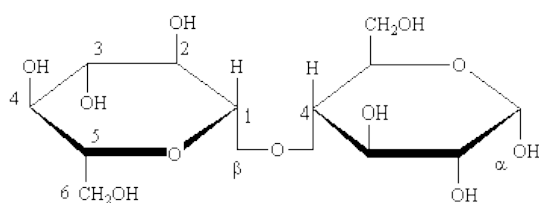
Fig 3. Cellobiose, the repeating unit of cellulose.

Hydroxyl groups on the glucose units can either form intrachain or interchain hydrogen bonds with oxygen atoms on the same or a neighbor chain respectively, holding firmly in parallel linear chains of several hundred to many thousands of glucose residues which in turn form the cellulose microfibrils (Figure 4) (Moon *et al.*, 2011). Within these microfibrils, regions of highly ordered structure create a highly crystalline form, with increased recalcitrance and resistance to chemical and enzymatic degradation (Lee, 1997).
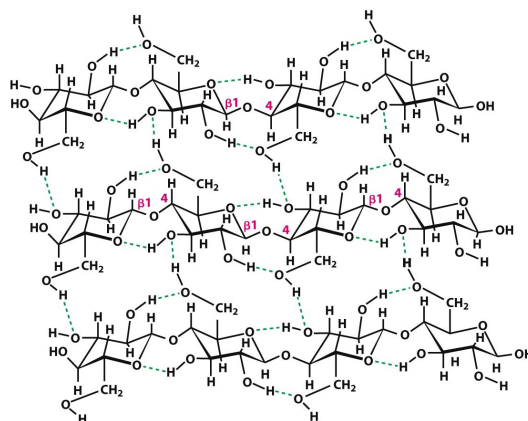
Fig. 4. Cellulose chains formed by glucose residues, connected with β-1,4 glycosidic bonds. Intramolecular hydrogen bonds hold firmly together the cellulose chains, while intermolecular hydrogen bonds stabilize each chain (Berg et al., 2012).

Crystalline cellulose may account for 50-90% of total cellulose in a plant, intertwined with less-ordered regions that form the amorphous part of cellulose. Cellulose's resistance to enzymatic attack is further reinforced by its structural relationship with hemicelluloses and lignin (Fan and Lee, 1983).

1.3.2 Hemicelluloses

Cellulose fibrils are closely associated with hemicellulose chains which are partly buried within and partly coat the surface of the fibrils (Srivastava, 2002). Hemicelluloses are a heterogeneous group of branched and linear polysaccharides with β-1,4 or β-1,3 linked backbones, comprising 20-40% of dry plant biomass. Hemicelluloses content and structure may vary among different plants or type cells of the same plant. Their building blocks can be hexoses such as glucose, mannose, rhamnose and galactose, pentoses such as xylose and arabinose, and glucuronic acid. Hemicelluloses are classified as xylans, mannans, xyloglucans, β-(1-3,1-4)-glucans and galactans (Figure 5) (Ebringerová *et al.*, 2005). As opposed to cellulose, hemicelluloses are random and amorphous with few crystalline structures, so they are relatively easily degraded into monosaccharides.

Xylan is the most prevalent hemicellulose component of hardwoods and grasses, comprised of xylose backbones and classified as homo- or heteroxylans (Chen, 2014). Heteroxylans can be further divided into glucuronoxylans, arabinoxylans, arabinoglucuronoxylans, or glucuronoarabinoxylans based on the structure and abundance of primary functional groups on the side chains (Obel *et al.*, 2007). Mannan-type hemicellulose polysaccharides are generally classified into four groups, homomannans, galactomannans, glucomannans, and galactoglucomannans, based on their backbone structures and galactose side chains. Xyloglucan is composed of a backbone of β-1,4-linked glucose residues, up to 75 % of which are substituted with α-1–6-linked xylose side chains (Ibrahim *et al.*, 2009). β-(1,3,1,4)-glucan constitutes an unbranched homopolymer of glucose connected by mixed β-1,4 and β-1,3-linkages. Plant galactans are minor hemicellulose polysaccharides that can be further divided into sulfated galactans and arabinogalactans. Sulfated galactans have a backbone structure of α-(1,3)- and α-(1,4)-linked sulfated galactose residues. Arabinogalactan is a hemicellulosic polysaccharide present in all types of biomass, but occurring in only minor amounts (typically 1–3 wt %) (Zhou *et al.*, 2017).
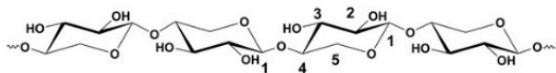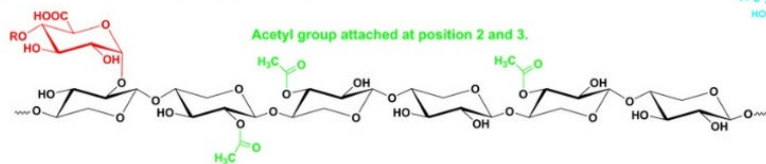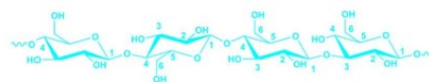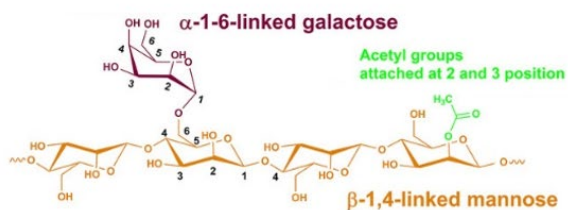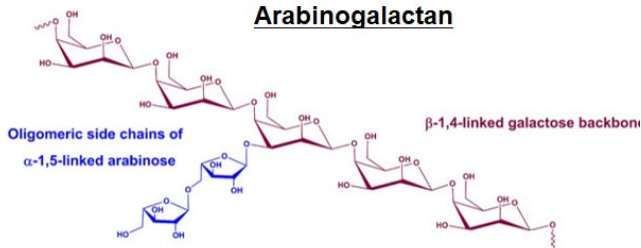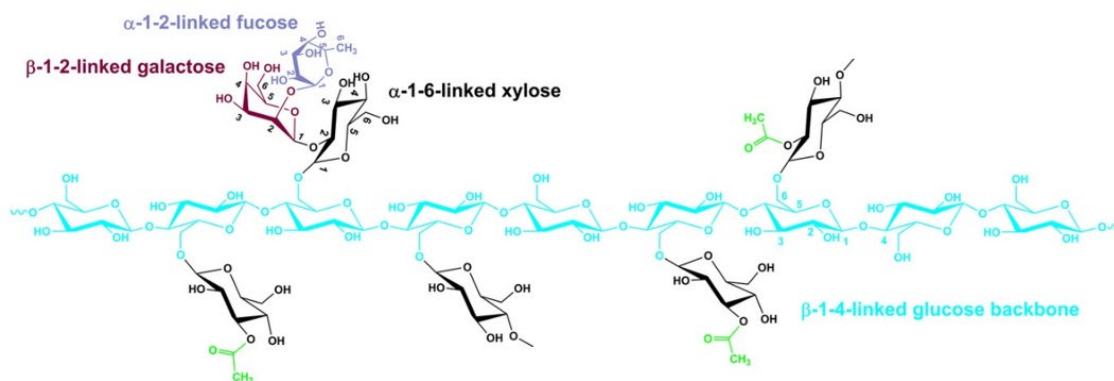
Fig. 5. Structures of various hemicellulose polysaccharides belonging to xylans, mannans, xyloglucans, β-(1-3,1-4)-glucans and galactans. Adapted from (Zhou *et al.*, 2017).

1.3.3 Lignin

Lignin constitutes the most abundant aromatic substance on earth, comprising 10-25% of dry plant biomass. It is an amorphous, overly complicated aromatic heteropolymer, of high molecular weight. It is formed by an enzyme-initiated, free-radical polymerization of three phenylpropane units originating from three monolignols, *p*-coumaryl, coniferyl and sinapyl alcohol, which differ in the number of methoxy groups present on the aromatic ring (0,1,2 respectively) (Figure 6).
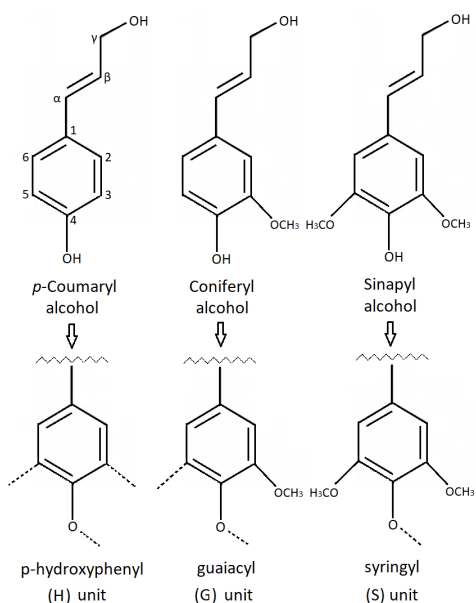
Fig. 6. Lignin monomer units. The three monolignols, *p*-coumaryl, coniferyl and sinapyl alcohol are incorporated into the lignin polymer, corresponding to *p*-hydroxyphenyl (H), quaiacyl (G) and syringyl (S) units.

Once incorporated into the lignin polymer these monomeric units are correspondingly identified as *p*-hydroxyphenyl (H), quaiacyl (G) and syringyl (S) units. Most lignin from softwoods belongs to G type, while lignin from hardwoods is mainly of GS type and grass lignin is of GSH type (Vanholme *et al.*, 2010, Windeisen and Wegener, 2016).

During lignification, the monomeric units are attached to each other through various ether (C-O-C) or carbon-carbon bonds (C-C), creating characteristic motifs. The most frequent lignin substructure is the arylglycerol-β-aryl ether (dimers between two aryl units containing a β-O-4 ether linkage). Other characteristic motifs include biphenyl (dimers containing a 5-5' linkage), phenylcoumaran (dimers containing a β-5' linkage), di-aryl propane (dimers containing a β-1' linkage) and pinoresinol (dimers containing a β-β linkage) (Figure 7). Additionally, it was recently shown that hydroxycinnamates, tricin –a flavonoid compound, and monolignol ferulate conjugates are also co-polymerized into the lignin polymer (Ralph, 2010, Karlen *et al.*, 2016, Lan *et al.*, 2016).
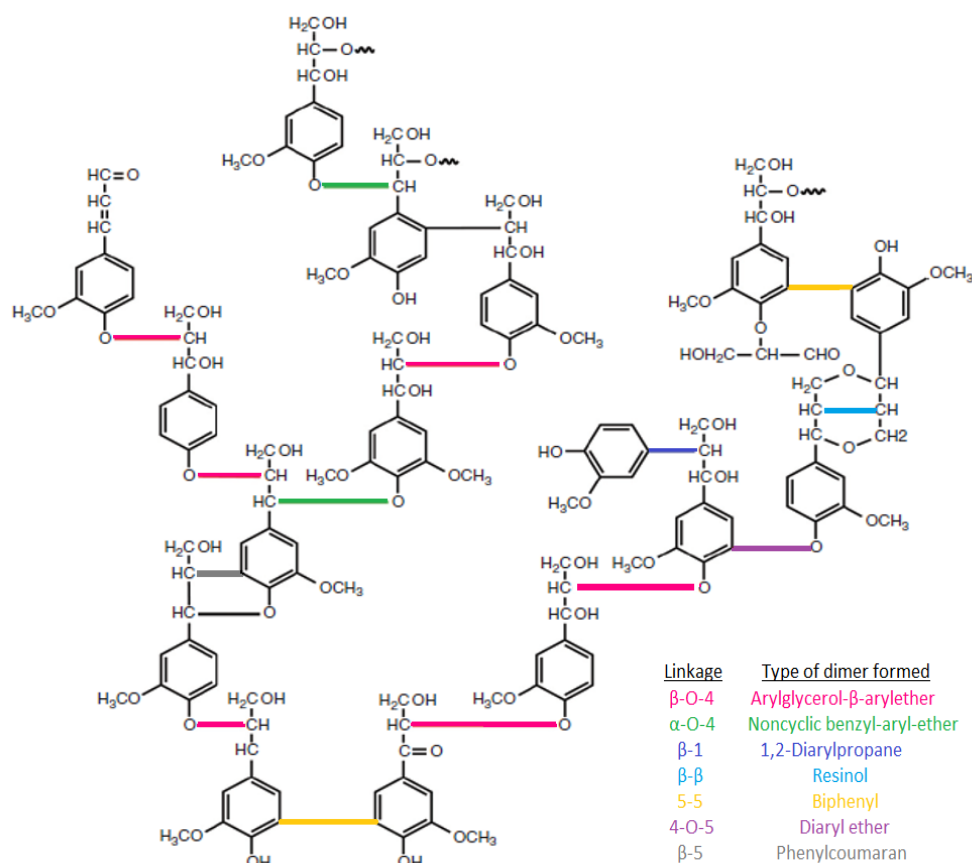
Fig. 7. Simplified schematic illustration of the lignin polymer structure (lignin lacks regularity and orderliness of its repeating units). Common interunit linkages are shown in different colors. Adapted from (Laurichesse and Avérous, 2014).

Lignin imparts strength and rigidity to the plant, binds adjacent cells together, protects the plant from pathogen invasion and plays a crucial role in conducting water in plant stems due to its hydrophobic nature. Lignin properties create several challenges impeding its chemical and biological processing. Hydrophobicity of native and native-like industrial lignins, render these polymers insoluble in water, thus limiting the access of enzymes and chemical catalysts (Bugg and Rahmanpour, 2015). In addition, its complex and random structure resists chemical degradation and does not favor the evolution of ligninolytic enzymes, which are often selective for a particular lignin linkage (Hatfield and Vermerris, 2001). What is more, resistant C-O-C and C-C linkages and formation of lignin-carbohydrate complexes increase the recalcitrance of the plant cell wall. More specifically, C-C linkages resist hydrolytic cleavage and the only hydrolysable units, susceptible to acid or alkaline hydrolysis are the ether units at the α- and β- positions, namely the β-aryl, α-aryl and α-alkyl ether linkages.

1.3.4 Industrial lignins and their properties

Lignin derived from industrial conversion processes is described as industrial or technical lignin. Industrial lignin is produced on a large scale from the pulp and paper industry at estimated $5*10^6$ metric tons annually, supplemented by growing amounts of lignin generated from the industrial production of cellulosic bioethanol. Industrial lignins have highly diverse structural properties that reflect the specific pretreatment process applied (Vishtal and Kraslawski, 2011). Pretreatment methods generally alter the constitution, structure, and/ or molecular weight of lignin, cause a partial degradation of hemicelluloses and alter the crystalline structure of cellulose. Therefore, a pretreatment reduces lignocellulose's recalcitrance, facilitates lignin removal from the plant biomass and improves the efficiency of cellulose utilization (Chen *et al.*, 2017). Pretreatment processes can be generally classified into physical, chemical, physical-chemical, biological methods and their combinations.

1.3.4.1 Kraft lignin

Kraft lignin accounts for approximately 85% of total world industrial lignin production (Tejado *et al.*, 2007). During kraft pulping, plant biomass is treated with a sodium hydroxide and sodium sulfide (Na₂S) aqueous solution, for 1-2 h at 170 °C. During this treatment, the hydroxide and hydrosulfide anions depolymerize 90-95% of the lignin polymer into smaller water/alkali-soluble fragments of different molecular weights (Chakar and Ragauskas, 2004, Strassberger *et al.*, 2014). Kraft lignin is often considered highly condensed, due to loss of benzylic hydroxyl groups in the β-aryl ether structural groups, thus forming a benzylic cation that can form new C-C cross-linking bonds (Bugg and Rahmanpour, 2015). Kraft lignin contains sulfur atoms in an irregular pattern, resulting from the use of sodium sulfide. This fact may restrict its subsequent biodegradation since sulfonated intermediates are unable to enter central metabolic pathways (Asina *et al.*, 2017).

1.3.4.2 Soda lignin

The Soda lignin process is mainly used for processing non-wood feedstocks such as wheat straw, bagasse and kenaf (Biermann, 1996). This pretreatment method uses sodium hydroxide to dissolve the lignin from lignocellulosic biomass generating sulfur-free lignin. Usually pulping is conducted at 140-170 °C in the presence of 13–16 wt% sodium hydroxide (Doherty *et al.*, 2011). Soda lignin from non-wood crops contains high amounts of aliphatic hydroxyl

and carboxyl groups and compared to Kraft lignin is characterized by less extensive cleavage of β-ether linkages and less reactive phenolic units (Asina *et al.*, 2017):

1.3.4.3 Lignosulfonate/sulfite lignin

Another pulping process available is the lignosulfonate/sulfite process. During sulfite pulping, wood chips are treated at 120-150 °C, and 500-700 kPa, using different sulfurous acid salts like sulfites and bisulfites to dissolve lignin. The sulfite process can be further classified into four different pulping methods based on the components of the sulfite cooking liquor. Acid sulfite and bisulfite pulping use high and low H_2SO_3/HSO_3 ratios, respectively. Alkaline sulfite pulping employs equal amounts of NaOH and Na_2SO_3 in the cooking liquor. Neutral sulfite pulping uses a neutral solution of Na_2SO_3 and Na_2CO_3 to soften the lignin and is often coupled with mechanical pulping for a more complete lignin removal (Biermann, 1996). The various types of lignin recovered, termed lignosulfonates, contain about 4–8 % sulfur. Compared to Kraft lignin, lignosulfonates have higher water solubility and broader dispersity, however, the treatment efficiency of sulfite pulping is lower than Kraft pulping and can be only applicable to certain wood species. Consequently, only around 10% of worldwide pulp industries currently use this pretreatment technique (Iglesias *et al.*, 2019).

1.3.4.4 Organosolv Lignin

Organosolv lignin is extracted from biomass through solubilization with organic solvents such as ethanol, methanol and organic acids. This process yields lignin of high purity with low residual carbohydrate content and a relatively higher proportion of β-O-4 linkages (Lora *et al.*, 1989, Bauer *et al.*, 2012). Organosolv pulping is less efficient than methods involving sulfur, therefore organosolv lignin represents a small portion of lignin produced industrially. However, organosolv lignin is relatively less modified and its sulfur-free structure allows for further processing (Doherty *et al.*, 2011).

1.4 Plant cell wall polysaccharide degradation

1.4.1 Cellulolytic enzymes

Aerobic and anaerobic bacteria use different strategies for cellulose degradation (Bayer *et al.*, 1998). Aerobes produce extracellular cellulase enzymes, occasionally present in complexes at the cell surface. Most aerobic individual cellulases carry a carbohydrate-binding module (CBM), joined by a flexible linker to one end of the catalytic domain. CBMs facilitate binding to the cellulose surface thus bringing the catalytic domain close to its substrate. Anaerobes degrade cellulose mostly via complex multienzyme systems, called cellulosomes. Cellulosomes consist of the catalytic enzymes, the scaffoldin molecules, which anchor the enzymes to the cellulosome, and the carbohydrate binding modules (CBM) that maintain close contact with the substrate (Bayer *et al.*, 2004).

Cellulases are distinguished from other glycoside hydrolases by their ability to catalyze the hydrolysis of β-1,4-glucosidic bonds that link two glucosyl residues. Based on their mode of catalytic action cellulases are classified into three major types that display strong synergy in the hydrolysis of cellulose:
i) endoglucanases (EC 3.2.1.4),
ii) exoglucanases, including 1,4-β-D-glucan glucanohydrolases (EC 3.2.1.74) and 1,4-β-D-glucan cellobiohydrolases (EC 3.2.1.91 and 3.2.1.176), and
iii) β-glucosidases (EC 3.2.1.21).

Enzymes involved in the decomposition of cellulose and hemicelluloses belong primarily to the glycoside hydrolases (GH) group (EC 3.2.1.-). Based on their amino sequence and folding similarities GHs are classified into families whose members may have diverse substrate specificities. Endoglucanases belong mainly to the families GH5-GH9, GH12, GH44, GH45, GH48 and GH51, while β-glucosidases belong to GH1, GH3, GH5, GH9 and GH30 families. Enzymes with exoglucanase activity belong primarily to the families GH5, GH6, GH9 and GH48. The Carbohydrate-Active Enzymes database (CAZy; http://www.cazy.org) provides continuously updated information of the GH families (Lombard *et al.*, 2014).

Endoglucanases have an open active site so they can bind and cleave a cellulose molecule at any accessible point along the amorphous parts of the chain (Spezio *et al.*, 1993). They bind randomly, make a few cleavages and then dissociate from the chain, generating oligosaccharides of various lengths and consequently new chain ends. Exoglucanases have their active site inside a tunnel and can only bind at one end of the cellulose chain. They act

progressively on the reducing or nonreducing ends of cellulose polysaccharide chains, liberating either glucose (glucanohydrolases) or cellobiose (cellobiohydrolase) as major products. Exoglucanases can also act on microcrystalline cellulose, presumably peeling cellulose chains from the microcrystalline structure (Teeri, 1997). β-glucosidases have a pocket-shaped active site, which allows them to bind the nonreducing glucose unit and clip off glucose from soluble cellodextrins or cellobiose (Zhang and Zhang, 2013) (Figure 8).

Lately, the importance of lytic polysaccharide monooxygenases (LPMOs, AA10) to the deconstruction of recalcitrant polysaccharides is increasingly recognized (Vaaje-Kolstad *et al.*, 2010). LPMOs have an unusual surface-exposed active site with a tightly bound Cu(II) ion that catalyzes the regioselective hydroxylation of crystalline cellulose, leading to glycosidic bond cleavage. LPMOs show great promise in reducing the cost of conversion of lignocellulosic biomass to fermentable sugars; however, many questions remain about their reaction mechanism and biological function (Beeson *et al.*, 2015).
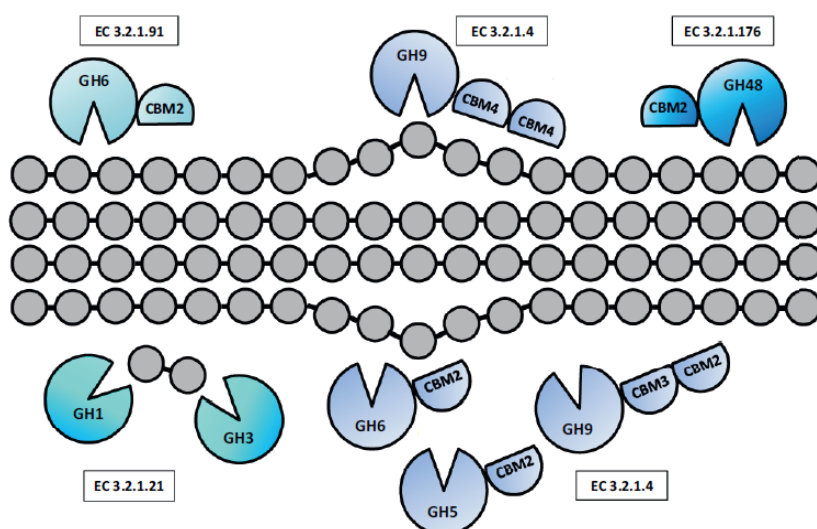
Fig. 8. Simplified schematic illustration of enzymatic systems for cellulose deconstruction of a typical aerobic bacterial strain. Endoglucanases (EC 3.2.1.4), such as GH5, GH6 and GH9 family enzymes, cleave glycosidic bonds randomly at internal amorphous sites in the cellulose polysaccharide chain. Exoglucanases (EC 3.2.1.91 and 3.2.1.176), such as GH6 and GH48 family enzymes, act progressively on the reducing or nonreducing ends of cellulose polysaccharide chains, liberating cellobiose as a major product. β-glucosidases (EC 3.2.1.21), such as GH1 and GH3 family enzymes, act specifically on cellobiose disaccharides and produce glucose. Most cellulases carry a carbohydrate-binding module (CBM) that facilitates binding to the cellulose surface. Adapted from (Lopez-Mondejar *et al.*, 2019).

Critical steps for reducing the costs of plant polysaccharide bioconversion are the reduction of cellulases production cost, the reduction of the loading dosage of enzymes, and the improvement of hydrolysis yields (Lynd *et al.*, 2008). Higher catalytic efficiency of cellulases requires reduced susceptibility to inhibitors, such as cellobiose or glucose, which are known

to inhibit cellobiohydrolases/endoglucanases or β-glucosidases respectively, high hydrolytic ability on insoluble substrates, enhanced stability at elevated temperatures and at extreme pH, and operation in a wide pH and temperature range (Tiwari *et al.*, 2018).

Recent accomplishments in the improvement of enzymes' specific activity and thermostability result from an extensive exploration for novel cellulases in nature's biodiversity, alongside with engineering of currently known enzymes. Current cellulase improvement strategies include directed evolution, rational protein design, and reconstitution of designer cellulosomes or cellulase mixtures. For example, a thermostable β-glucosidase, identified from a random mutant library of the *Paenibacillus polymyxa* β-glucosidase, generated by error-prone PCR, had an 11-fold increase in the half-life of thermo-inactivation at 50°C (Liu *et al.*, 2009). Site-directed mutagenesis improved the activity of the *Thermobifida fusca* endocellulase/exocellulase Cel9A on soluble and amorphous cellulose by 40% (Escovar-Kousen *et al.*, 2004).

The generation of chimeric endoglucanases by fusing a carbohydrate-binding module with two thermophilic endoglucanases enhanced the enzymatic hydrolysis of microcrystalline cellulose up to threefold (Reyes-Ortiz *et al.*, 2013). The addition of accessory enzymes has also been proposed to diminish the inhibitory effect of oligomeric sugars, phenolics, and lignin on cellulases. An optimized cellulase enzyme blend with hemicellulases, pectinases, β-glucosidase, and laccases resulted in a lower requirement of cellulase dosage to effectively hydrolyze 22% (w/v) alkali-pretreated sugarcane bagasse, achieving a higher glucose titer and yield (Xu *et al.*, 2019).

1.4.2 Hemicellulolytic enzymes

The microbial degradation of hemicelluloses imposes several intrinsic challenges, such as the high molecular weight and highly variable structure of the polymer, which is either insoluble or associated with cellulose and lignin. Their complete hydrolysis requires the concerted action of many enzymes that have to work synergistically (Shallom and Shoham, 2003). Hemicellulases are modular proteins, and, in addition to their catalytic domains, include other functional modules, such as carbohydrate-binding modules (CBMs), which facilitate the targeting of the enzymes to the insoluble polysaccharides, and dockerin modules that mediate the binding of the catalytic domains via cohesin–dockerin interactions, either to the microbial

cell surface or to large enzymatic complexes, such as the cellulosome (Bourne and Henrissat, 2001).

Xylanases (EC 3.2.1.8) and β-xylosidases (EC 3.2.1.37) are the main hemicellulases involved in the depolymerization of the xylan backbone, Xylanases hydrolyze the β-1,4 bond in the xylan backbone, yielding short xylooligomers. Most known bacterial xylanases belong to GH10 and GH11 families, but are also found in families GH5, GH8 and GH43. β-Xylosidases are exo-type glycosidases that cleave xylose monomers from the nonreducing end of xylooligomers and xylobiose, found in GH families 1, 3, 5, 10, 30, 39, 43, and 51. Branch-point degrading enzymes of xylan include α-L-arabinofuranosidases (EC 3.2.1.55) and α-D-glucuronidases (EC 3.2.1.131) (Figure 9).

Hemicellulolytic esterases include acetyl xylan esterases (EC 3.1.1.72) and feruloyl esterases (EC 3.1.1.73). Acetyl xylan esterases hydrolyze the ester linkage between acetyl and xylose residues in xylans. Feruloyl esterases hydrolyze the ester bond between the arabinose substitutions and ferulic acid. This latter ester bond is involved in covalent crosslinking between arabinoxylan and lignin (Manju and Singh Chadha, 2011). β-Mannanases (EC 3.2.1.78) hydrolyze mannan-based hemicelluloses and liberate short b-1,4-manno-oligomers, which can be further hydrolyzed to mannose by β-mannosidases (EC 3.2.1.25). (Lombard *et al.*, 2014).

Hemicellulose bioconversion processes into monomeric sugars, for further fermentation into biofuels and chemicals, require the complete spectrum of hemicellulolytic enzymes (Ohara, 2003). However, research on the production of hemicellulases is primarily focused on xylanases, which are specifically required in the paper and pulp industry, for their utility as bleaching agents (Sharma *et al.*, 2010). Xylanases with improved catalytic activities, thermostability, substrate binding, inhibitor tolerance and wide pH range, higher substrate specificities, expressed in high levels, are required for sustainable saccharification of lignocellulose.
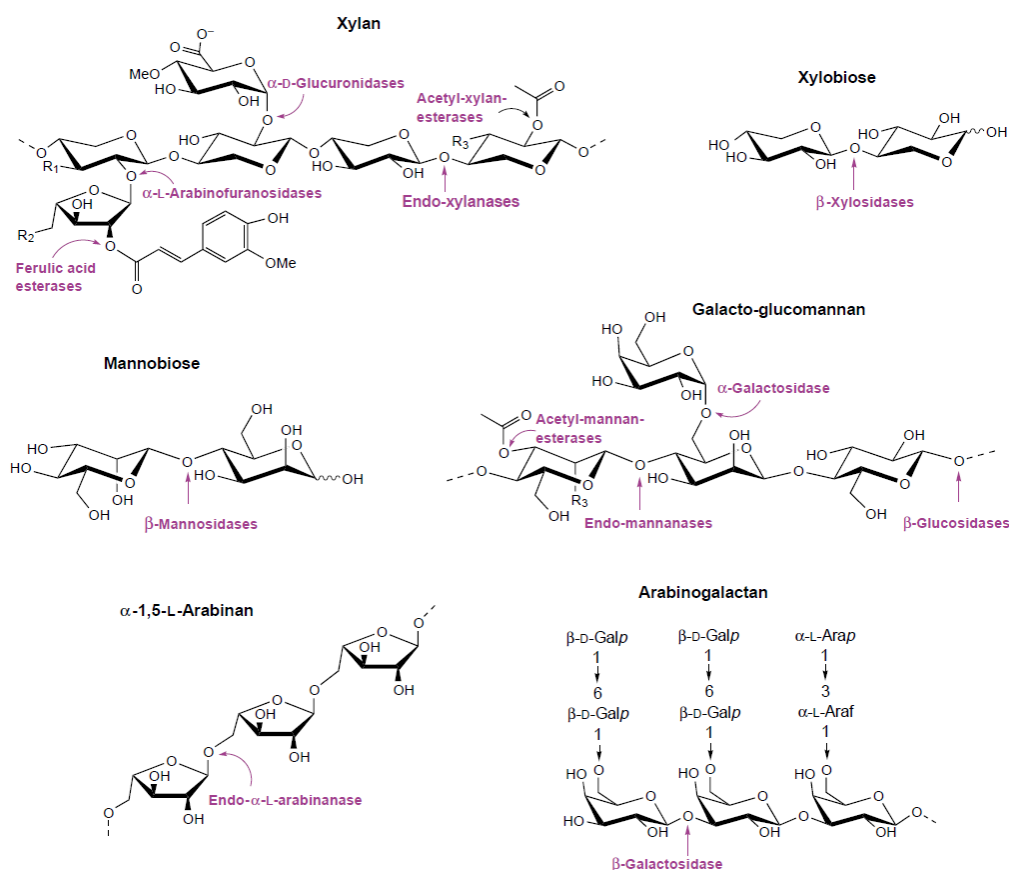
Fig. 9. Hemicellulases involved in the degradation of basic structural components of hemicelluloses. (Shallom and Shoham, 2003).

Most of the commercially available hemicellulases are derived from fungi, though constraints met during mass production and industrial applications have recently led to the development of commercial bacterial xylanases, too (Chakdar *et al.*, 2016). Several xylanases have been isolated and characterized from bacteria and, recently, substantial progress has been achieved in improving their efficiency. A number of bacilli, such as *B. pumilus* and *B. halodurans*, have been proven a potential source of xylanases with considerable activity (Banka *et al.*, 2014, Thomas *et al.*, 2014, Gupta *et al.*, 2015). Thermostable xylanases active at high temperatures, as high as 80-100°, have been found in bacteria, such as *Acidothermus cellulolyticus*, *Geobacillus thermoleovorans*, *Stenotrophomonas maltophila* and *Thermotoga thermarum*, (Barabote *et al.*, 2010, Raj *et al.*, 2013, Shi *et al.*, 2014). Alkali stable xylanases have also been reported from Firmicutes, such as *Bacillus pumilus, Bacillus halodurans*, and *Geobacillus thermoleovorans*, and actinomycetes, such as *Streptomyces* sp. (Verma and Satyanarayana, 2012, Luo *et al.*, 2015)

For large-scale industrial production of xylanases, heterologous expression in bacterial hosts like *E. coli*, *B. subtilis*, and *Lactobacillus* has been widely used. However, the expression of

36

recombinant proteins at high titers can be hindered by factors like expression as inclusion bodies, lactate accumulation, and lack of disulfide bond formation (Ethiraj *et al.*, 2018). A variety of cheap lignocellulose materials, such as wheat bran, wheat straw, rice straw, corncob, corn stalk, and sugarcane bagasse have also been found to induce the production of xylanolytic enzymes, under solid-state fermentation (SSF), in certain bacteria (Heck *et al.*, 2006, Walia *et al.*, 2012).

Site-directed mutagenesis has been used to enhance the thermostability of bacterial xylanases. A point mutation increased not only thermostability but also catalytic efficiency, through a 2-fold improvement in the substrate-binding affinity of the mesophilic *Bacillus circulans* xylanase Bcx (Joo *et al.*, 2011). A combination of directed evolution and a rational approach, using error-prone PCR and site-directed mutagenesis, has also resulted in a 90% increase in catalytic efficiency of *Geobacillus stearothermophilus* xylanase XT6 (Zhang *et al.*, 2010). Although some properties of xylanases have been significantly improved, most enzymes possess only few of the properties required for industrial applications (Verma and Satyanarayana, 2012, Chakdar *et al.*, 2016). Therefore, identifying xylanolytic bacteria with novel xylanases, and adopting protein engineering strategies remain important tools for robust enzymes production.

1.5. Lignin degradation

1.5.1 Ligninolytic bacteria

It is widely accepted that, in nature, lignin decomposition is primarily initiated with fungi, such as white-rot fungi, which secrete extracellular enzymes that depolymerize lignin into lower molecular weight aromatics (Kirk and Farrell, 1987). Few bacteria can degrade fully intact lignified wood cells, although, many bacteria are able to assimilate and use the monomeric constituents of the aromatic lignin polymer as a carbon and energy source, through well-adapted metabolic pathways (Zimmermann, 1990). The extent to which bacteria can cause the decay of native lignin has not been properly assessed, since much of the present knowledge of the mechanism of lignin degradation by bacteria has been obtained using technical lignins and lignin model compounds as substrates. Hence, whether in nature bacteria degrade lignin to use it as a carbon source, or to access the polysaccharide fractions, remains an interesting question.

Bacteria able to metabolize lignin constituents are generally abundant in natural or manmade lignin-rich environments, such as leaf litter, sludge of pulp paper mill, compost soils, decomposing woods, activated sludge and wood-eating insects' guts. These bacteria primarily belong to members of α-, β- and γ-Proteobacteria, such as *Pseudomonas* spp., *Rhizobium* sp., *Sphingobium* sp., *Comamonas* sp., *Burkholderia* sp., *Serratia* sp., and *Enterobacter* sp., members of Actinobacteria, such as *Streptomyces* sp. and *Rhodococcus* spp., and members of Firmicutes, such as *Bacillus* spp., *Paenibacillus* and *Aneurinibacillus* sp. (Xu *et al.*, 2019).

1.5.2 Ligninolytic enzymes

In nature, the complete degradation of lignin is carried out in two stages. The first step involves the decomposition of polymeric lignin by extracellular oxidoreductases, such as laccases, lignin peroxidases, manganese dependent peroxidases and versatile peroxidases. This step is achieved by ligninolytic microorganisms including wood-decaying fungi and a number of bacterial species (Bugg *et al.*, 2011). Degradation of lignin is also mediated by diffusible, oxidative, radical mediator compounds, resulting in the release of low molecular weight (mono-, di- and oligomeric) aromatic products (ten Have and Teunissen, 2001, Brown and Chang, 2014). The second step of lignin degradation involves the incorporation of the small aromatic compounds into the cell, ring fission and mineralization through pathways for aromatic catabolism. This step is achieved by the ligninolytic species themselves or by different, aromatic degrading species. The enzymology of bacterial decomposition of polymeric lignin is not well characterized. Yet, distinctive bacterial extracellular or intracellular enzymes catalyzing similar reactions to those of extracellular fungal ligninolytic enzymes have also been found, as described below (Bugg *et al.*, 2011).

1.5.2.1 Multicopper oxidases

Multicopper oxidases (MCOs) constitute a superfamily of enzymes that are widespread in nature, including plant, insect, fungal, bacterial and archaeal enzymes. These enzymes exhibit a range of functions broadly divided into three categories: cross-linking of monomers, degradation of polymers, and ring cleavage of aromatic compounds. In plants, MCOs are involved in lignin polymerization, fungal MCOs participate in lignin degradation, pigmentation and detoxification and bacterial MCOs are implicated in copper homeostasis, spore formation and pigmentation (Solomon *et al.*, 1996). MCOs catalyze the monoelectronic

oxidation of four substrate equivalents, coupled to the four-electron reduction of oxygen, according to the following reaction:

$$4RH + O_2 \longrightarrow 4R^{\bullet} + 2H_2O$$

MCOs contain four copper atoms per monomer, classified into three types according to their spectroscopic properties: a type I copper atom (T1) which gives an intense blue color to the enzyme, a type II copper atom (T2) which is colorless, and two type III (T3) copper atoms that give a weak absorbance near the UV range. The T2 copper forms a trinuclear Cu cluster with the pair of T3 copper atoms, where binding and reduction of molecular oxygen take place (Leontievsky *et al.*, 1997). The first step in the catalytic mechanism of MCOs involves the reduction of the T1 copper atom and the concomitant oxidation of the substrate. Subsequently, the electrons are transferred to the T2-T3 reaction center cluster, via a cysteine–histidine pathway that is highly conserved among multicopper oxidases, where they finally reduce molecular oxygen to water (Figure 10) (Solomon *et al.*, 1996). The difference in redox potential between the T1 copper atom and the reducing substrate is a measure of the potential for the reaction center to receive electrons (Xu *et al.*, 1996). A putative substrate-binding site is located at the surface of the proteins close to the T1 mononuclear copper center (Vicuña *et al.*, 1987).
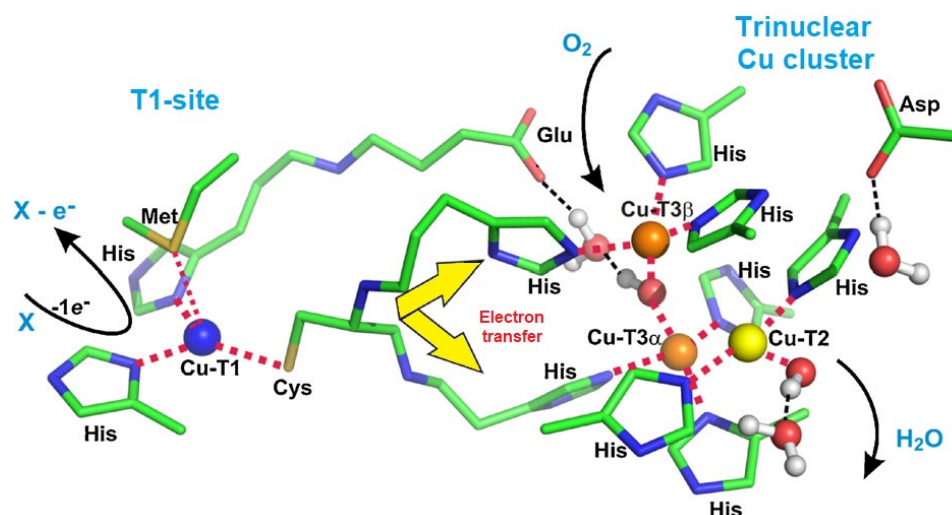
Fig. 10. Representation of the general catalytic mechanism of multicopper oxidases. In the T1-site, reduction of the T1 copper atom (blue sphere) results in the concomitant one-electron oxidation of four substrate equivalents (organic substrates or metal ions). The electrons are transferred via a Cys-(His)$_2$ chain to the trinuclear copper cluster, formed by a type-2 and two type-3 coppers (yellow and orange spheres), where molecular oxygen is reduced, and water is released (Rulíšek and Ryde, 2013).

1.5.2.1.1 Laccases and their function

Laccases (Lac, EC.1.10.3.2) constitute the largest subgroup of MCOs and the most widely studied. They can oxidize a wide range of organic substrates including phenols, polyphenols, anilines, aromatic polyamines, and certain metal ions such as Fe and Mn^{2+}. It has been reported that laccases catalyze the degradation of both β-1 and β-O-4 dimers in lignin, via Cα-Cβ cleavage, Cα oxidation, as well as cleavage of aryl-alkyl C-C bond (Wong, 2009). These enzymes are particularly interesting as they are considered "green" biocatalysts, since they employ O_2 as a co-substrate and generate water as a non-toxic byproduct (Asina *et al.*, 2017). What is more, these enzymes do not require costly cofactors like NADH, NADPH, H_2O_2 or Mn^{2+}, as other oxidoreductases (Koschorreck *et al.*, 2009).

Oxidation of phenolic substrates by laccases involves the removal of one electron from the phenolic hydroxyl groups of the substrate to form phenyl hydroxyl radicals. These radicals may spontaneously reorganize and trigger the cleavage of alkyl side chains of the lignin polymer and the release of aromatic monomers (Kunamneni et al., 2008). Oxidation of non-phenolic substrates often requires the presence of a redox mediator, a molecule that after being oxidized by the enzyme can diffuse into the lignin matrix and nonenzymatically oxidize non-phenolic substrates (Bourbonnais *et al.*, 1998, Camarero *et al.*, 2005). In the presence of mediators, MCOs can oxidize substrates of larger size, of lower diffusion into the active pocket, or of high redox potential, thus widening their range of substrates. Mediators include synthetic molecules such as 2,2′-azino-bis-(3- ethyl-benzothizoline-6-sulphonic acid) (ABTS), 1- hydroxybenzotriazole (HBT), 2,2,6,6,-tetramethyl-1-piperidinyloxy-free radical (TEMPO), or natural molecules such as 4-hydroxybenzoic acid, aniline, phenol, acetosyringone, p-coumaric acid, ferulic acid, syringaldehyde and vanillin (Kudanga and Le Roes-Hill, 2014). The reaction mechanisms for laccase mediators can be classified as hydrogen atom transfer, electron transfer and ionic mechanisms (Fabbrini *et al.*, 2002).

1.5.2.1.2 Bacterial laccases

Laccases have mostly been isolated from fungi and plants, whereas laccases from bacteria have not been extensively studied. One of the most well-known bacterial laccases is the outer endospore coat protein CotA from *Bacillus subtilis* (Enguita *et al*., 2003). Other similar bacterial MCOs include the copper homeostasis protein CueO from *Escherichia coli* (Roberts *et al.*, 2002). Laccase-like activity has also been found in CopA protein from *Pseudomonas syringae* that has been shown to be important for bacterial copper resistance (Mellano and

Cooksey, 1988), and in EpoA from *Streptomyces griseus* that appeared to have a role in cell differentiation (Endo *et al.*, 2002). Laccases have also been discovered from members of the genera *Streptomyces*, *Geobacterial*, *Staphylococcus*, *Lysinibacillus*, *Aquisalibacillus*, *Delfia*, *Enterobacter*, *Proteobacterium*, and *Alteromonas* (Guan et al., 2018).

However, only few bacterial laccases have shown activity against polymeric lignin or lignin model compounds. One such is the halotolerant laccase (SilA) from *Streptomyces ipomoea* CECT 3341, which was shown to degrade lignin present in the eucalyptus kraft pulps, using acetosyringone as a mediator (Eugenio *et al.*, 2011). A laccase from *Strepromyces coelicolor* A3(2) was shown to oxidize lignocellulosic substrates to produce aryl cation radicals that can rearrange and promote repolymerization of the substrate (Majumdar *et al.*, 2014). In the same study, laccases from *Streptomyces lividans* TK24, *Streptomyces viridosporus* T7A, and *Amycolatopsis* sp. 75iv2 were shown to degrade a phenolic model compound into a mixture of different products including vanillin, but were able to oxidize a nonphenolic model compound only in the presence of redox mediators.

The laccase enzyme Lac4 from *Pantoea ananatis* Sd-1 was able to degrade lignin in the presence of ABTS, yielding several compounds such as 4-benzedicarboxaldehyde, benzenepropanoic acid and phenol (Shi *et al.*, 2015). Upon treatment of wheat straw pulp with the laccase from *Thermus thermophilius* HB27 (Tth-laccase) the pulp brightness was increased, suggesting a delignification role for this enzyme (Zheng *et al.*, 2012). Also, CueO laccase from *Ochrobactrum* sp, showed activity towards β-aryl ether and biphenyl lignin dimer model compounds, and lignosulfonates (Granja-Travez *et al.*, 2018).

Bacterial laccases have several unique properties in comparison to fungal laccases, such as stability at high temperature, pH, organic solvents, and salt concentrations (Chauhan *et al.*, 2017, Guan *et al.*, 2018). However, laccases' full potential is still untapped, and some bottlenecks are the lack of selectivity, and compatibility with the rigorous process conditions, the lower redox potential, and their very limited commercial availability (Martínez *et al.*, 2017). Many concerted approaches are being pursued to boost the exploitation of laccases, such as the exploration of the biodiversity of microorganisms living in extreme habitats, enzyme immobilization, recombinant production in homologous or heterologous hosts, protein engineering, and metagenomic analysis (Stanzione *et al.*, 2020).

A few bacterial laccases have been engineered, combining rational and computational design with directed evolution, to attain the selectivity, catalytic efficiency and stability properties required for their industrial utilization. A Glu188Lys mutation at a surface loop of *Bacillus* sp.

HR03 laccase resulted in a higher T_{50} (5 °C higher), while a Glu188Arg mutation resulted in a 3-fold higher k_{cat} and K_m reduced by 25%, with respect to the native enzyme (Mollania *et al.*, 2011). Random and site-directed mutagenesis methods were combined to improve the functional expression of *Bacillus licheniformis* CotA laccase in *E. coli*. A double mutant enzyme Lys316Asn/Asp500Gly showed improved functional expression, higher activity in dimerization of ferulic acid, and a much better decolorization efficiency than the wild-type enzyme (Koschorreck *et al.*, 2009). A site-directed mutagenesis approach in combination with DNA shuffling resulted in the production of two variants of *Bacillus pumilus* laccase-like multi-copper oxidases (LMCOs), carrying the mutations L386Q and G417R/I, both showing higher catalytic efficiency against guaiacol, a lignin model compound (Ihssen *et al.*, 2017). The thermostable spore laccase CotA from the bacterial strain *Bacillus subtilis* LS02 has been heterologously expressed in *Pichia pastoris* strain SMD1168H, achieving a 76-fold increase in laccase activity through sorbitol addition in combination with pH adjustment (Wang *et al.*, 2015). Despite being promising in most of the reported examples, the evolved laccases were only tested at a laboratory scale (Stanzione *et al.*, 2020).

1.5.2.1.3 The structure of bacterial laccases

Common bacterial laccases have three sequentially arranged cupredoxin-like domains, which consist of two β-sheets arranged into a Greek-key barrel. The Greek-key motif has at least seven antiparallel β-strands twisted to form a closed barrel structure, in which some β-strands are adjacent in space but not in sequence (Hakulinen and Rouvinen, 2015). The T1 mononuclear copper centre is located in domain 3, the trinuclear copper cluster (two T3 and one T2 copper ions) is located between domains 1 and 3, while the amino acid residues of domains 2 and 3 are involved in the formation of the substrate-binding pocket (Dwivedi *et al.*, 2011). Two-domain laccases have also been found in *Streptomyces, Amycolatopsis,* and *Nitrosomonas* strains. These enzymes belong to the group denoted as SLACs (small laccases) and form homotrimers to be catalytically active (Figure 11) (Majumdar *et al.*, 2014).
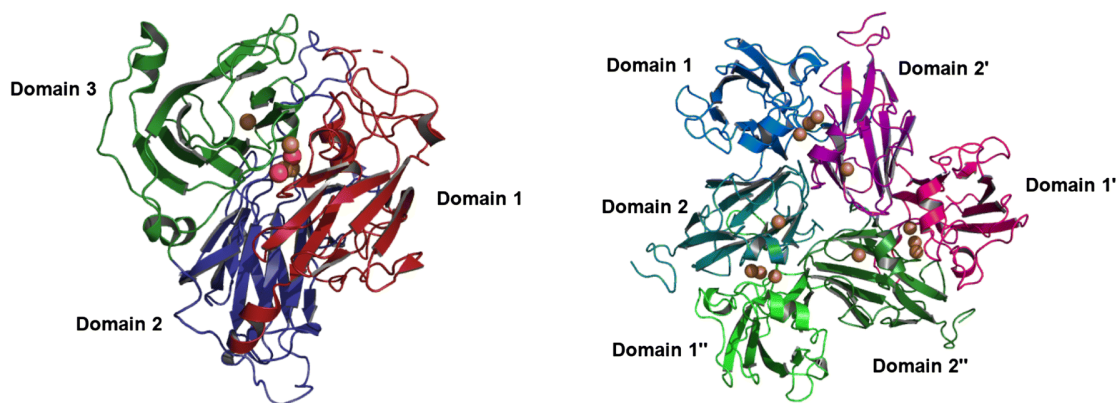
Fig. 11. Representation of the structure of a three-domain laccase from *Bacillus subtilis* (PDB 1GSK) and a homotrimeric two-domain laccase from *Streptomyces coelicolor* (PDB 3CG8). Single orange spheres represent the mononuclear T1-site and the clusters of three orange spheres represent the trinuclear copper site (Arregui *et al.*, 2019).

1.5.2.1.4 Transformation of lignin into value-added chemicals by laccases

The depolymerization ability of laccases can transform the lignin polymer into several phenolic and aromatic compounds for which there is a demand by food, pharmaceutical and cosmetic industries (Moreno *et al.*, 2019). Emerging materials such as engineering plastics, thickeners, fillers, and adsorbents have also been developed through the action of fungal laccases grafting co-polymerization of lignin by-products and acrylic compounds (Mai *et al.*, 2000). Furthermore, wood composite boards have been produced by crosslinking of phenolic compounds in lignin-based materials via laccase action (Widsten and Kandelbauer, 2008). Modifications of cellulosic fibers' properties including hydrophobicity, strength, and color, have been achieved by laccase-assisted grafting of phenolic or other compounds (Chandra and Ragauskas, 2002). What is more, using this enzymatic strategy antimicrobial and antioxidant properties could be incorporated to produce cellulose-based materials for food packaging or sanitary use (Elegir *et al.*, 2008).

1.5.2.2 Heme peroxidases

Heme peroxidases form a superfamily of enzymes responsible for numerous biosynthetic and degradative functions. These enzymes catalyze the oxidation of a range of organic and inorganic compounds while reducing hydrogen peroxide (H_2O_2) to water. They use heme *b* as a cofactor, formed by protoporphyrin IX, a complex cyclic structure that combines with iron, and serves as a mediator for electron transfer between a peroxide molecule and two reducing substrate molecules, according to the reaction:

43

$$H_2O_2 + 2AH_2 \longrightarrow H_2O + 2\text{'}AH$$

where peroxide is reduced to water and the substrate (AH$_2$) is oxidized to the respective radical (Zámocký *et al.*, 2015). Unlike the cytochromes *c*, heme *b* is bound to the protein through non-covalent interactions. The iron in heme *b* containing proteins is bound to the four nitrogens of protoporphyrin and an axial histidine residue (five-coordinated). In some cases there is an additional weak sixth bound to a water molecule or hydroxide (six-coordinated) (Raven, 2013) (Figure 12).
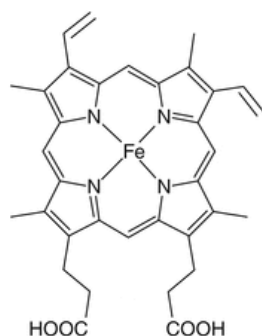
Fig. 12. The structure of heme *b*.

White-rot fungi produce several different kinds of heme-peroxidases for the degradation of lignin: lignin peroxidases, manganese dependent peroxidases and versatile peroxidases: Lignin peroxidases (Lip, EC 1.11.1.14) catalyze the H$_2$O$_2$-dependent oxidative depolymerization of lignin. LiPs are mediator-free peroxidases, relatively nonspecific to their substrates. They are known to oxidize both phenolic and also a variety of non-phenolic lignin components due to their high redox potential, through a scission between the Cα and Cβ atoms of propyl side chains, hydroxylation of benzylic methylene groups and formation of aldehydes or ketones through oxidation of benzyl alcohols (Wong, 2009).

Manganese dependent peroxidases (MnP, EC 1.11.1.13), are more selective than other peroxidases catalyzing mostly Cα-Cβ cleavages, Cα-H -oxidation and alkyl-aryl C-C bond cleavages of phenolics within the lignin structure (Hofrichter, 2002). Mn^{2+} serves as a reducing substrate for MnP to be oxidized to Mn^{3+}, which in turn oxidizes phenolic compounds (Wong, 2009). Versatile peroxidases (VP, EC 1.11.1.16) exhibit multi-functionality combining the enzymatic characteristics of MnP and LiP, thus, being capable of oxidizing high redox potential substrates including phenolic and nonphenolic moieties of lignin. To date, homologs of the above fungal ligninolytic peroxidases have not been found in ligninolytic bacteria, nor in their genomes or proteomes (Salvachúa *et al.*, 2013).

1.5.2.2.1 Dye decolorizing peroxidases and their function

Dye decolorizing peroxidases (DyP, EC 1.11.1.19), a newly discovered family of heme peroxidases, have recently gained attention due to studies pointing towards a role of these enzymes in the microbial degradation of lignin. They comprise a superfamily of peroxidases that show no homology or related features to typical plant or animal peroxidases (Sugano *et al.*, 2007). They are able to catalyze the oxidation of phenolic or nonphenolic lignin compounds, aromatic sulfides, β-carotene, and manganese (Mn^{2+}) (Scheibner *et al.*, 2008, Roberts *et al.*, 2011, Colpa *et al.*, 2014), and can also effectively degrade synthetic dyes such as high redox anthraquinone dyes or azo dyes, an ability they owe their name to (Sugano, 2009).

According to RedOxiBase database, DyP-type peroxidases are sub-classified into the phylogenetically distinct classes A, B, C, and D (Savelli *et al.*, 2019). Enzymes belonging to classes A, B and C are mainly found in bacterial representatives, while class D DyPs are extracellular fungal enzymes. Class B and C DyP protein sequences do not possess any secretion signal peptides, suggesting they are cytoplasmic enzymes. The physiological function and the natural substrates of DyPs remain largely unknown. It has been proposed that A-type DyPs, such as EfeB from *Escherichia coli*, are implicated in the removal of heme-derived iron without degrading the porphyrin tetrapyrrole (deferrochelation) (Rajasekaran *et al.*, 2009).

The catalytic mechanism of DyP-type peroxidases was proposed to be similar to that of the well-characterized heme peroxidases. However, the catalytic cycle may differ among the distinct classes of DyPs (Figure 13). In the resting state, the heme group is in the ferric form ($[Fe^{3+}]Por$). Reaction of H_2O_2 with the resting enzyme oxidizes heme by two equivalents to yield an oxo-ferryl ($Fe^{4+}=O$) porphyrin cation radical (Por^+) complex (Compound I), which successively oxidizes two substrate molecules *via* one-electron abstraction. The two-electron oxidation of heme by H_2O_2 is aided by distal histidine and arginine residues. This mechanism has been detected in B-type and D-type DyPs whereas a different mechanism has been detected in A-type DyPs that results in the formation of a Compound II type intermediate ($[Fe^{4+}=O]Por$) and then the resting heme (Ahmad *et al.*, 2011).
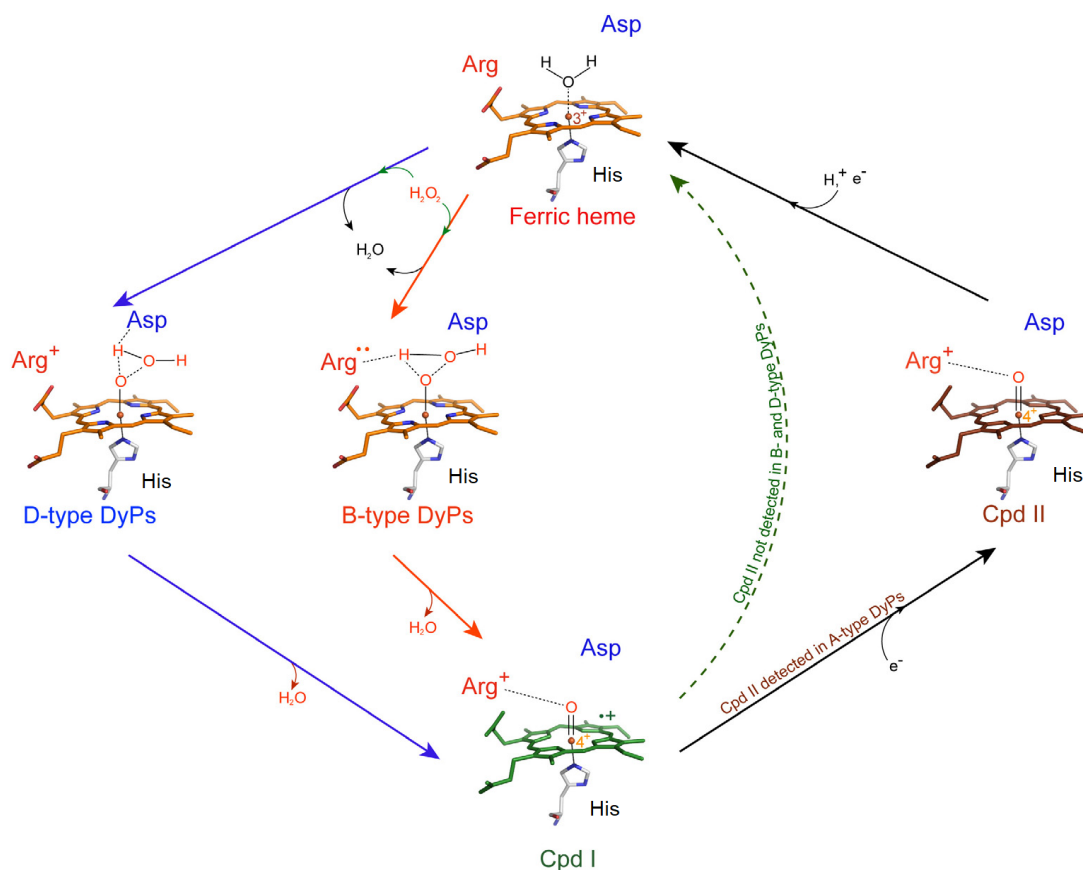
Fig. 13. Peroxidative cycle in DyPs. In B-type and D-type DyPs the two-electron oxidation of heme (red-blue-orange scheme with iron as a red sphere) by H_2O_2 is aided by distal histidine and arginine residues, forming Compound I, an oxo-ferryl porphyrin cation radical complex (Cpd I), which successively oxidizes two substrate molecules *via* one-electron abstraction. In A-type DyPs two successive one-electron reductions of Cpd I by reducing substrates yield first a Compound II (Cpd II) intermediate and then the resting heme (Singh and Eltis, 2015).

1.5.2.2.2 Bacterial dye decolorizing peroxidases

While many fungal DyPs have been studied, only a small number of bacterial DyPs have been characterized, and studies on *in vitro* treatments of industrial lignin with peroxidases are limited (Asina *et al.*, 2017). Dye decolorizing peroxidases DypB from *Rhodococcus jostii* RHA1 (DypB$_{RHA1}$) (Ahmad *et al.*, 2011), Dyp2 from *Amycolatopsis* sp. 75iv2 (Brown *et al.*, 2011) and Dyp1B from *Pseudomonas fluorescens* (Rahmanpour and Bugg, 2015) have been shown to be active in the oxidation of polymeric lignin and lignin model compounds. Recently, the Mn^{2+}-oxidizing activity of DypB$_{RHA1}$ was increased greater than an order of magnitude through the substitution of the distal heme residue Asn246 with alanine (Singh *et al.*, 2013). A dye-decolorizing peroxidase YfeX from *Escherichia coli O157:H7* was able to catalyze the oxidation of ABTS, and the phenolic compounds guaiacol and catechol, and could also decolorize the anthraquinone dye reactive blue 19 (Liu *et al.*, 2017). Bacterial DyPs have also been shown to promote substrate oxidation by oxidizing redox mediators,

such as veratryl alcohol, syringaldehyde and Mn^{+2} (de Gonzalo *et al.*, 2016). The activities of DyP1B and $DyPB_{RHA1}$ towards wheat straw lignocellulose and Kraft lignin respectively have been shown to be boosted in the presence of Mn^{+2} (Ahmad *et al.*, 2011, Rahmanpour and Bugg, 2015).

The dye-decolorizing peroxidase Tfu from *Thermobifida fusca*, belonging to class A DyPs, showed high reactivity towards anthraquinone dyes and a lower activity towards guaiacol, 2,6-dimethoxyphenol and azo dyes (van Bloois *et al.*, 2010). Tfu DyP has also been shown to oxidize the phenolic lignin model dimer guaiacylglycerol-β-guaiacyl ether (GGE). It was shown that oxidation yielded dimeric and trimeric products of the model compound while no cleavage of the ether bond was observed (Rahmanpour *et al.*, 2016). In contrast, the oxidation of GGE by $DypB_{RHA1}$ probably resulted in the cleavage of the Cα-Cβ linkages of the substrate and the subsequent radical coupling of the products formed, yielding guaiacol, guaiacol trimers and vanillin (Ahmad *et al.*, 2011). A more diverse product profile was also observed by the treatment of GGE by the A-type TcDyP from *Thermomonospora curvata*, yielding hydroxylated guaiacol pentamers and cresol dimers (Figure 14) (Chen *et al.*, 2015).
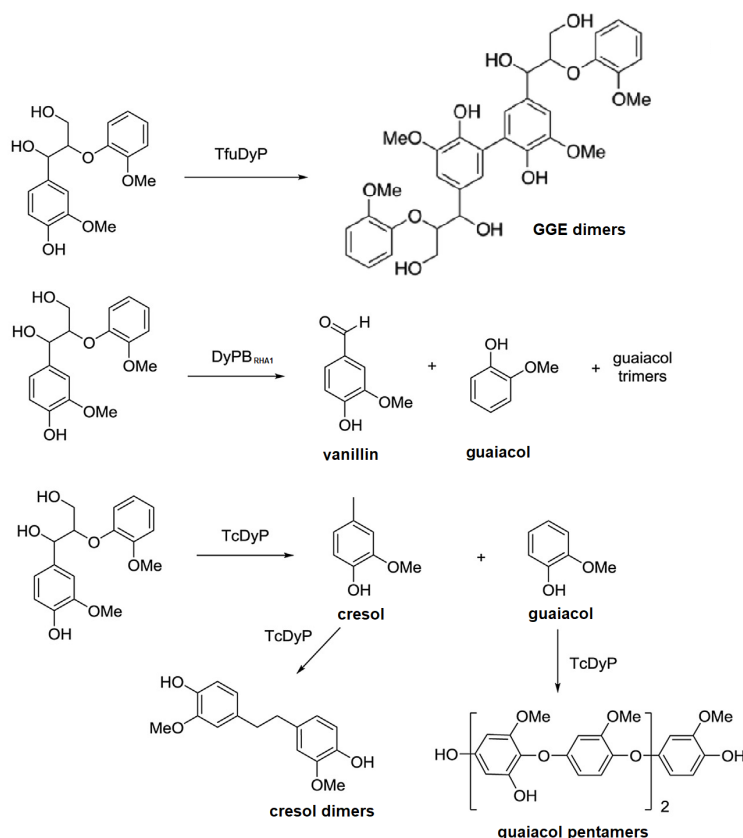
Fig. 14. Oxidation of the β-aryl ether lignin model compound guaiacylglycerol-β-guaiacyl ether (GGE) by different dye-decolorizing peroxidases: TfuDyP from *Thermobifida fusca*, DyPB from *Rhodococcus jostii* RHA1, and TcDyP from *Thermomonospora curvata*. Adapted from (de Gonzalo *et al.*, 2016, Rahmanpour *et al.*, 2016).

1.5.2.2.3 The structure of dye decolorizing peroxidases

The structure of dyp-type peroxidases consists of two domains that contain α-helices and anti-parallel β-sheets. Both domains adopt a unique ferredoxin-like fold and form an active site crevice with the heme cofactor sandwiched in between (Colpa *et al.*, 2014). Some heme-binding residues are conserved among all DyPs and others are conserved within specific DyP classes. In all DyPs, the proximal axial ligand to the heme iron is a histidine, and it is hydrogen-bonded to the carboxylate of an acidic residue. Three residues on the distal face of the heme are also conserved: an acidic residue, usually aspartic acid, an arginine and a phenylalanine (Zámocký *et al.*, 2015) (Figure 15). A GXXDG motif found in their primary sequence of all DyP-type peroxidases, is part of the heme-binding region. The conserved aspartate functions as an acid-base catalyst and is considered important for peroxidase activity, however, Singh and colleagues proposed that instead, a conserved arginine of DypB plays crucial role in peroxidase activity (Singh *et al.*, 2012).
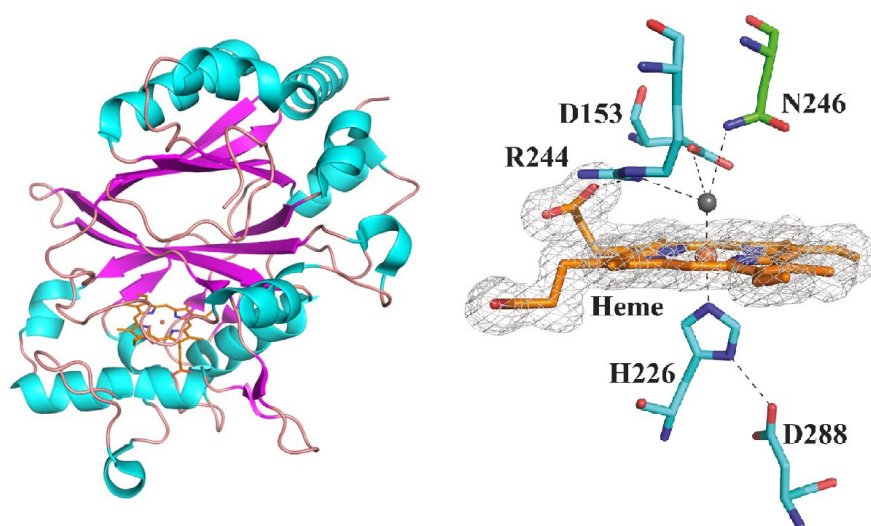
Fig. 15. Tertiary structure and heme-binding pocket of a B-type dye peroxidase DypB of *R. jostii* RHA1 (PDB: 3QNS). β-sheets are represented in purple, a-helices in magenta and loops in salmon. The heme is shown as a stick, nitrogen and oxygen atoms are colored blue and red respectively. Iron is shown as an orange sphere. Conserved residues among all DyPs are shown in cyan. The water molecule is colored dark gray. Adapted from (Roberts *et al.*, 2011, Singh and Eltis, 2015).

1.5.2.2.4 Transformation of lignin into value-added chemicals by peroxidases

Enzymatic polymerization of lignophenols provides a way to turn lignin into phenolic resins that have potential application in adhesives, bonding agents and engineering materials. Researchers have reported the enzymatic polymerization of lignocatechol and lignocresol by a

horse-radish peroxidase, involving the coupling of the grafted catechol and cresol, to give cross-linked polymers (Xia *et al.*, 2003). Despite their potential, the broad industrial application of peroxidase-based bioprocesses has not yet been realized. The use of peroxidases has been hampered by their low availability in sufficient amounts, H_2O_2-related enzyme instabilities and high enzyme cost (Schoenherr *et al.*, 2018).

1.5.2.3 Catalases-peroxidases and their function

Catalase-peroxidases (EC 1.11.1.21), also called KatGs, are bifunctional enzymes, found in bacteria, archaebacteria and a few fungi. They attach heme B as a co-factor and can oxidize various electron donors according to the following chemical reaction:

$$1.\ donor + H_2O_2 \rightleftharpoons oxidized\ donor + 2H_2O\ and$$

$$2.\ 2H_2O_2 \rightleftharpoons O_2 + 2H_2O.$$
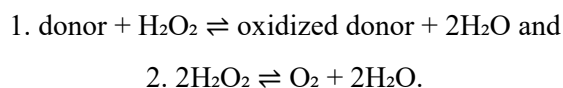
H_2O_2 itself can be utilized as an electron donor, producing $O_2 + H_2O$, but also a variety of other organic or inorganic molecules. These enzymes show catalase and peroxidase activities, but also low levels of NADH oxidase, isonicotinoyl hydrazide INH lyase and isonicotinoyl-NAD synthase activities have also been reported (Singh *et al.*, 2004). Catalases-peroxidases have extensive similarity to plant peroxidases, therefore they are categorized as members of the Class I family of peroxidases.

The catalase and peroxidase reactions involve a common path for oxoferryl Compound I formation, but differ in the path for Compound I reduction back to resting state. Compound I initially has the heme oxidized to the oxoferryl state ($Fe^{4+}=O$) and a porphyrin cation π-radical ($Por^{\circ+}$). In catalases, Compound I is reduced in a single two-electron transfer from H_2O_2, whereas peroxidases undergo two sequential one-electron transfers, usually from organic donors (AH), and involve the intermediate Compound II (Carpena *et al.*, 2005).

1.5.2.3.1 Bacterial catalases-peroxidases

Many bacterial KatGs have been biochemically characterized, however, reports on oxidation of lignin and its derivatives are scarce. A bacterial heme-containing catalase-peroxidase Amyco1 from *Amycolatopsis* sp. 75iv2 was proposed to be associated with lignocellulose degradation, based on a proteomic approach that showed the secretion of this enzyme during incubation with lignocellulosic material, and on its ability to convert the phenolic lignin model compound guaiacyl-glycerol-β-aryl ether (Brown *et al.*, 2011). Also, the bifunctional

Cyanobacterium synechocystis PCC 6803 catalase-peroxidase has shown activity towards *o*-dianisidine, guaiacol and pyrogallol (Jakopitsch *et al.*, 1999).

1.5.2.3.2 The structure of catalases-peroxidases

Bacterial catalase-peroxidases mostly exist as homodimers or homotetramers of ~80 kDa subunits, each composed of two domains (the N-terminal and the C-terminal) with significant sequence similarity, possibly arising from a gene duplication and fusion event (Welinder, 1991). The N-terminal domain contains the active site with a single heme-b cofactor whereas the function of C-terminal domain remains unclear, due to the absence of a heme-binding motif (Yamada *et al.*, 2002). KatGs mostly constitute of α-helices, usually 10 on each domain, with highly conserved residues but also contain a few β-sheets (Carpena *et al.*, 2003). Structures of different KatGs reveal the presence of a peroxidase-conserved proximal and distal heme pocket, including the essential for enzymatic activity triads His/Trp/Asp and His/Arg/Trp, respectively (Bertrand *et al.*, 2004). The heme is buried inside the N-terminal domain and the substrate enters the active site through a narrow channel that prevents the access of large substrates. The side chains of two Glu residues on the surface loops of the molecule distinguish the acidic entrance of the channel (Yamada *et al.*, 2002). At its narrowest part highly conserved residues Asp and Ser, control the access to the distal heme pocket, namely the Arg/His/Trp triad (Smulevich *et al.*, 2006). Another distinctive structural element of KatGs is a covalent bond between the side chains of a Met/Tyr/Trp triad. Mutation of the Trp residue resulted in loss of activity, suggesting a role in catalase activity (Zámocký *et al.*, 2001).

1.6 Bacterial transport systems for lignin-derived aromatics

Once the lignin polymer has been decomposed by extracellular microbial enzymes, the bi- and monoaryls compounds formed are incorporated into the bacterial cell. Proteins that facilitate the transport of lignin derivatives, across the bacterial cell membrane, have not been thoroughly characterized and fewer studies have been conducted on Gram-positive than Gram-negative species concerning aromatic transport (Brink *et al.*, 2019).

1.6.1 Outer membrane transporters

In Gram-negative bacteria, lignin-derived aromatic compounds are reported to be transported across the outer membrane by passive transporters, such as porins and substrate-specific channels, or by active transporters, such as TonB-dependent receptors (Figure 13). The porin OmpW was proven to be required for the nonspecific uptake of naphthalene and various polycyclic aromatic compounds in *Pseudomonas fluorescens* (Neher and Lueking, 2009). Based on the presence of *ompW* gene in many bacteria, OmpW is considered to be ubiquitously involved in nonspecific uptake of hydrophobic compounds, including aromatic hydrocarbons (Kamimura *et al.*, 2017).

In *Pseudomonas* species and other soil bacteria, substrate-specific channels, allow passive diffusion of most water-soluble and small molecules, including aromatic compounds (Tamber *et al.*, 2006). In *Pseudomonas aeruginosa*, OpdK protein belonging to the outer membrane porin D family (OprD) was found to be involved in the uptake of vanillate and related compounds (Biswas *et al.*, 2008). Since many putative opdK homologs have been found among catabolic genes for aromatic compounds, these homologs are assumed to be involved in the uptake of various aromatic compounds (Tamber *et al.*, 2006).

TonB-dependent receptors (TBDRs) are bacterial, outer membrane, active transporters that use the energy in the form of proton motive force, transmitted from the TonB-ExbB-ExbD complex of inner membrane proteins (Figure 16), in order to transport their substrates (Noinaj *et al.*, 2010). Recently, it was shown that genes encoding TBDRs were specifically induced during the growth of *Sphingomonas wittichii* RW1, *Pseudomonas putida* KT2440 and *Novosphingobium pentaromativorans* US6-1 on dibenzodioxin, vanillin and phenanthrene respectively (Hartmann and Armengaud, 2014, Simon *et al.*, 2014, Yun *et al.*, 2014). Coexpression of a putative TBDR gene, located immediately upstream of the vanillate catabolic gene cluster, during the growth of *Pseudomonas aeruginosa* on vanillate, may imply the involvement of TBDR proteins in the outer membrane transport of aromatic compounds (Tamber *et al.*, 2006).
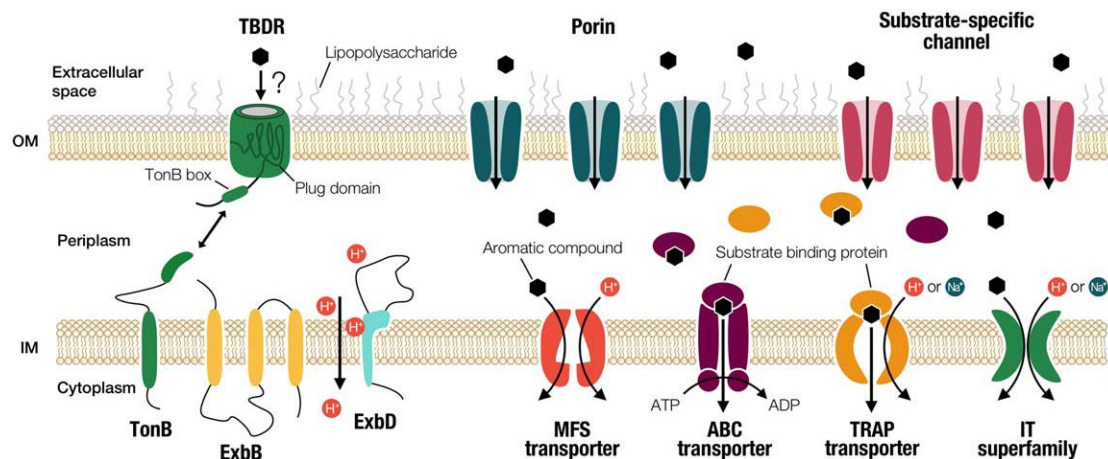
Fig. 16. Putative transport systems for lignin-derived aromatic compounds in Gram-negative bacteria. Aromatic compounds are generally transported across the outer membrane (OM), by passive transporters, such as porins and substrate-specific channels or active transporters such as TonB-dependent receptors (TBDRs), which interact with inner membrane (IM)-localized TonB complex (TonB-ExbB-ExbD). Active transporters belonging to the families of MFS, ABC,TRAP and ion transporters (IT), have been reported to be IM transporters of lignin-derived aromatics (Kamimura *et al.*, 2017).

1.6.2 Inner membrane transporters

The transport of substrates across the bacterial inner membrane is accomplished by active transporters. Members of four different families of active transporters are suggested to be involved in the transport of lignin-derived aromatics, belonging to the superfamily of ATP-binding cassette (ABC) transporters, the major facilitator superfamily of transporters (MFS), the family of tripartite ATP-independent periplasmic transporters (TRAP) and the superfamily of ion transporters (IT).

A gene cluster in *Sinorhizobium meliloti*, designated *pcaMNVWX*, was hypothesized to encode an ABC transport system involved in the uptake of protocatechuate. However, though *pcaM* and *pcaN* mutant strains were unable to grow on protocatechuate, there is still no clear evidence that this transport system incorporates protocatechuate into the cell (MacLean *et al.*, 2011). The MFS transporters involved in the uptake of lignin-derived aromatic compounds reported to date are basically categorized into Family 15: aromatic acid/H1 symporters (AAHS). Many putative active transporters of this family have been described, yet only few have been characterized both *in vivo* and *in vitro* (Kamimura *et al.*, 2017). One of these characterized transporters is PcaK of *P. putida* PRS2000 which was shown to transport p-hydroxybenzoate and protocatechuate using 14C-labeled substrates (Nichols and Harwood, 1997). Although there are a few reports on vanillate MFS transporters, the vanillate transport system remains unclarified.

Salmon and his coworkers reported the involvement of the TRAP transporter TarP in the uptake of lignin-derived aromatics, such as p-coumarate, caffeate, ferulate and cinnamate in *Rhodopseudomonas palustris* CGA009 (Salmon *et al.*, 2013). Recently, it was reported that disruption of the putative IT superfamily gene *gacP* in *Lactobacillus plantarum* WCFS1 greatly reduced the gallate conversion rate, suggesting the involvement of GacP in the uptake of gallate (Reverón *et al.*, 2017).

1.7 Bacterial metabolic pathways of lignin-derived aromatics

Bacterial metabolism of aromatic compounds occurs by a combination of upper metabolic pathways, which "funnel" a variety of compounds into a few key aromatic intermediates, such as catechol, protocatechuate and benzoate (Fuchs *et al.*, 2011), and a central pathway where the intermediates undergo de-aromatization and transformation to different metabolites, such as acetyl-CoA, succinyl-CoA and pyruvate, that enter the tricarboxylic acid cycle (Bugg *et al.*, 2011). Biological funneling has been recently used as a strategy for the conversion of deconstructed lignin into commodity chemicals that maintain the aromatic ring, ring-opened species native to the aromatic catabolic pathways, and products derived after the carbon enters central metabolism. Some of these approaches require extensive metabolic re-routing and introduction of foreign pathways, while others rely on a small number of mutations that redirect aromatic metabolism to the product of interest (Perez *et al.*, 2019). Such processes have proven feasible in the laboratory, and the next challenge would be to scale up production to industrial levels.

The most important lignin catabolic pathways along with examples of strategies for the production of valuable metabolites will be outlined below.

1.7.1 Catabolism of G-type lignin monomers

Degradation of lignin monomers with G-structure, carrying one methoxy group, such as ferulate, can proceed through four different pathways: (i) nonoxidative decarboxylation pathway, (ii) coenzyme A (CoA)-dependent non-β-oxidation pathway, (iii) CoA-dependent β-oxidation pathway, and (iv) side chain reduction pathway. These four pathways are all funneled into vanillic acid for further degradation (Figure 17).

The nonoxidative decarboxylation pathway converts ferulic acid to 4-vinyl guaiacol, via a decarboxylase enzyme (Fdc) that catalyzes the one-carbon cleavage of the side-chain. 4-vinyl guaiacol can be further transformed to vanillin by a vinyl guaiacol dehydrogenase (Vgdh). The demand for natural aroma compounds derived from 4-vinylphenols such as 4-vinylcatechol or 4-vinyl guaiacol is particularly high, especially in the food industry. A few bacteria have been reported to produce 4-vinyl guaiacol as a major metabolite from ferulic acid along with other value added-compounds such as vanillin, vanillic acid and protocatechuic acid. These bacteria include representatives of the genera *Cupriavidus*, *Lactobacillus*, *Enterobacter*, *Streptomyces*, *Bacillus* and *Pseudomonas* (Mishra et al., 2014).
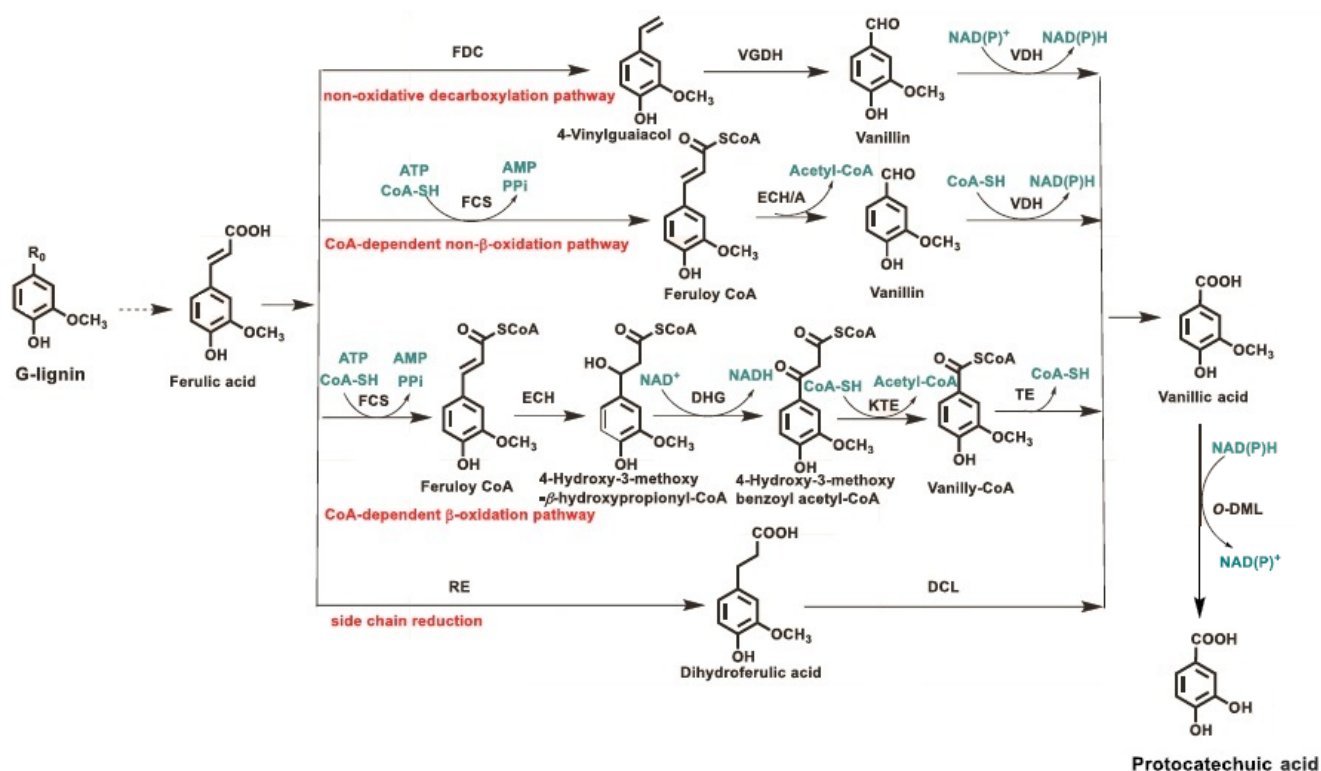
Fig. 17 Bacterial degradation pathways of g-type lignin units, such as ferulic acid. A detailed description is outlined in the text. Adapted from (Xu *et al.*, 2019).

A CoA-dependent non-β-oxidation pathway involved in the degradation of ferulic and caffeic acid implicates a broad substrate specificity hydroxycinnamoyl-CoA synthase (Fcs or FerA), which transforms them into feruloyl CoA and caffeoyl-CoA respectively. Then, a bifunctional enoyl-CoA hydratase/aldolase (Ech or FerB or HCHL) converts these hydrated derivatives into acetyl-CoA and vanillin or 3,4-dihydroxybenzaldehyde respectively (Gasson *et al.*, 1998). This pathway has been reported in *Pseudomonas*, *Amycolatopsis*, *Sphingomonas* and *Rhodococcus* strains (Mitra *et al.*, 1999, Yang *et al.*, 2013).

In a similar CoA-dependent β-oxidation pathway, the resulting feruloyl-CoA is hydrated by Ech to form the intermediate 4-hydroxy-3-methoxyphenyl-β-hydroxypropionyl–CoA, which is further oxidized to 3(4′-hydroxy-3-methoxyphenyl)-3-ketopropionyl-CoA and cleaved by a β-ketothiolase to produce vanillyl-CoA and acetyl-CoA. Vanillyl-CoA is then hydrolyzed to form vanillic acid, with concomitant release of CoA-SH. This pathway has been identified in a *Pseudomonas putida* strain and a *Rhodotorularubra* sp. (Gallage and Møller, 2015)

Chain shortening of the side chain of ferulic acid may also proceed by a reductive mechanism. This catabolic pathway is typical of anaerobic degradation and the proposed reaction mechanism involves initial isomerization of ferulic acid to a transient quinoid intermediate, which is converted into dihydroferulic acid in a reductive step, and subsequently to vanillic acid (Batista, 2014).

Vanillin can be oxidized to vanillic acid by a vanillin dehydrogenase (Vdh). Vanillic acid is transformed into protocatechuic acid *via* demethylation by either a two-component non-heme iron-dependent oxygenase enzyme, vanillate O-demethylase VanAB, found in *Pseudomonas* species (Brunel and Davison, 1988) or by a tetrahydrofolate-dependent O-demethylase LigM, found in *Sphingomonas paucimobilis* SYK-6 (Abe *et al.*, 2005).

Vanillin is one of the most important flavoring agents used in the world. Natural vanillin extracted from vanilla pods provides only about 0.25% of vanillin sold in the market, whereas the remainder is mostly produced through chemical synthesis from lignin or fossil hydrocarbons. Alternatively, vanillin produced by biotechnological approaches in microbial systems, classified as natural vanillin by the European and US food legislation, has a market price that is 300-times higher than the synthetic ''unnatural'' vanillin (Yang *et al.*, 2013). An engineered strain of *Rhodococcus jostii* RHA1 in which the vanillin dehydrogenase gene had been deleted, when grown on minimal medium containing 2.5% wheat straw lignocellulose and 0.05% glucose, was found to accumulate vanillin with yields of up to 96 mg/L after 144 h (Sainsbury *et al.*, 2013).

1.7.2 Catabolism of S-type lignin monomers

The S-lignin compounds, such as syringic acid, carry two methoxy groups on the aromatic ring. A tetrahydrofolate-dependent O-demethylase (DesA) catalyzes the demethylation of

syringate into 3-O-methylgallate (3MGA). 3MGA is metabolized via multiple pathways, involving i) demethylation by LigM O-demethylase into gallate, ii) direct dioxygenation by a 3-O-methylgallate 3,4-dioxygenase (DesZ), into 4-carboxy-2-hydroxy-6-methoxy-6-oxohexa-2,4-dienoate, and iii) direct dioxygenation by two dioxygenases, protocatechuate 4,5-dioxygenase (LigA and LigB) and DesZ, into 2-pyrone-4,6-dicarboxylate (Figure 18).
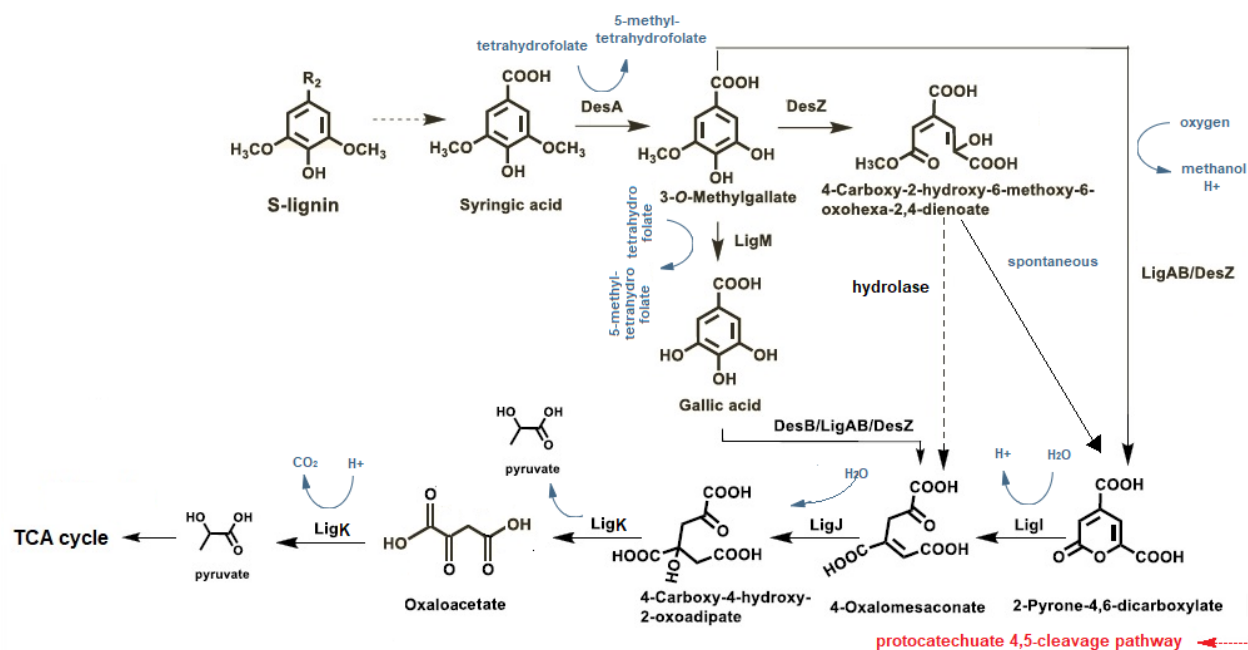
Fig. 18. Bacterial degradation pathways of S-type lignin units, such as syringic acid. A detailed description is outlined in the text. Adapted from (Kasai *et al.*, 2007, Xu *et al.*, 2019).

All three pathways converge at 4-oxalomesaconate, therefore, in this way, syringic acid is assimilated into the protocatechuate 4,5-cleavage pathway and ultimately integrated into the tricarboxylic acid (TCA) cycle (Figure 11) (Masai *et al.*, 2004). Strains that have been shown to possess the syringate degradation pathway include *Sphingomonas paucimobilis* SYK-6 (Kasai *et al.*, 2004) and *Pseudomonas putida* KT2440 (Nogales *et al.*, 2005).

An *E. coli* strain engineered to co-express two demethylase genes *desA*, *ligM* with a GA decarboxylase gene was able to convert syringic acid into pyrogallol, a common raw material used in chemical synthesis of bioactive molecules, yielding about 7.3 mg/L pyrogallol and 18 mg/L GA (Wu *et al.*, 2017).

1.7.3 Catabolism of H-type lignin monomers

The H-lignin compounds carry no methoxy groups on their aromatic ring. *p*-Coumaric acid has been used as a standard model compound for H-lignin units. In herbaceous plants, *p*-coumaric acid is linked to hemicellulose residues with ester linkages and can be released together with ferulic acid under alkaline pretreatment (Mussatto *et al.*, 2007). The aerobic degradation of *p*-coumaric acid in bacteria proceeds mainly via three different pathways i) CoA-dependent β-oxidation pathway, ii) CoA-dependent non-β-oxidation pathway, and iii) CoA-independent pathway (Figure 19).
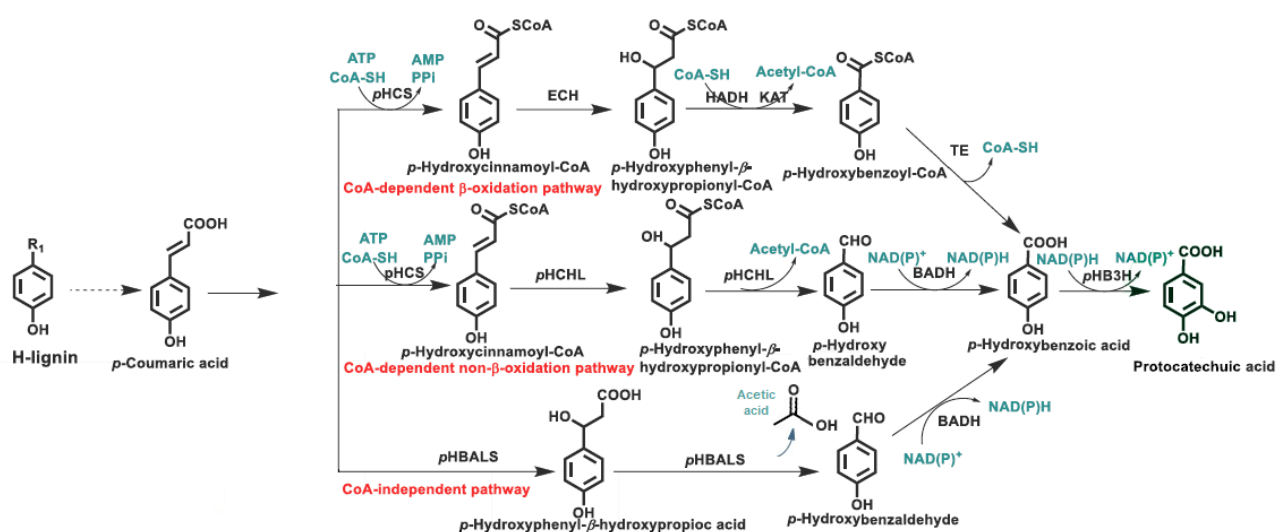
Fig. 19. Bacterial degradation pathways of H-type lignin units, such as syringic acid. A detailed description is outlined in the text. Modified from (Xu *et al.*, 2019).

In the first pathway, *p*-Hydroxycinnamoyl-CoA synthetase (pHCS) activates *p*-coumaric acid by producing *p*-hydroxycinnamoyl-CoA, which is subsequently hydrated, oxidized and cleaved by thiolysis to acetyl-CoA, and *p*-hydroxybenzoyl-CoA. Hydrolysis of this CoA ester yields *p*-hydroxybenzoic acid (pHBA). This pathway has been found in some proteobacteria such as *Aromatoleum* sp. and *Pseudomonas* sp. (Trautwein *et al.*, 2012).

In the CoA-dependent non-β-oxidation pathway, the first two steps are the same as the CoA-dependent β-oxidation pathway, but then, instead of oxidation, the bond between the α- and β-carbons of p-hydroxyphenyl-β-hydroxypropionyl-CoA cleaves in a retro aldol reaction to acetyl-CoA and p-hydroxybenzaldehyde. Oxidation of the latter compound yields *p*HBA. This pathway is found in strains such as *Acinetobacter* sp., *Pseudomonas* sp., *Rhodococcus* sp., *Sphingomonas* sp., and *Sphingobium* sp.. The CoA-independent pathway catalyzes a

similar hydration and retro aldol to form *p*-hydroxybenzaldehyde like the non-b-oxidation pathway, but without formation of the CoA thioester (Jung *et al.*, 2016).

The first three pathways all converge at the intermediate of *p*HBA, which is then converted to protocatechuic acid by *p*-hydroxybenzoate-3-hydroxylase (*p*HB3H). *p*HBA is a useful industrial platform chemical that is generally used as a monomer for liquid crystal polymers and high-performance plastics for electronic devices. Its alkyl ester derivatives, such as paraben, are preservatives used in the pharmaceutical and cosmetic industry (Jung *et al.*, 2016). The biological synthesis of *p*HBA has been accomplished by engineered *Pseudomonas putida* strains deficient in *p*HBA degradation, using substrates such as a xylose-glucose mixture, glycerol or toluene (S. Miller Jr and W. Peretti, 1999, Meijnen *et al.*, 2011, Verhoef *et al.*, 2014). An engineered *Burkholderia glumae* strain BGR1, with a deficiency in *p*HBA degradation and higher expression levels of the rate-limiting enzyme, CoA-synthetase, was able to produce up to 19.8 mM of *p*HBA, by using *p*-coumaric acid as a substrate, through CoA-dependent non-b-oxidation pathway (Jung *et al.*, 2016).

1.7.4 Catabolism of β-aryl ether lignin dimers

The arylglycerol β-aryl ether (β-O-4) bond is the most abundant linkage in lignin, comprising 45–50% and 60 62% of all the intermonomer linkages in softwood and hardwood lignin, respectively (Zakzeski *et al.*, 2010), therefore, its cleavage is considered important during lignin degradation. Guaiacylglycerol-β-guaiacyl ether (GGE) has been used as a model compound to study β-aryl ether degradation in *Sphingomonas* sp. SYK-6 (Figure 20).

Biaryls of β-aryl ether type have two distinct isomeric forms, erythro and threo, each of which has enantiomeric forms, (Akiyama *et al.*, 2000). The four stereoisomers of GGE are stereospecifically converted to two enantiomers of α-(2-methoxyphenoxy)-β-hydroxypropiovanillone (MPHPV), through oxidation of the GGE Cα, catalyzed by three nicotinamide adenine dinucleotide (NADH)-dependent Cα dehydrogenases LigD, LigL and LigN. The ether linkage of the resultant MPHPV is cleaved by enantioselective β-etherases; LigF, LigE and LigP, members of the glutathione transferase superfamily (GSTs; EC 2.5.1.18). The reactions produce α-glutathionyl-β-hydroxypropiovanillone (GS-HPV) and guaiacol upon glutathione (GSH) consumption.

LigG, which belongs to the omega class of GSTs, catalyzes the cleavage of the thioether linkage in (βR)-GS-HPV by transferring glutathione of (βR)-GS-HPV to another molecule of glutathione to produce HPV and glutathione disulfide. Yet, the enzyme that further converts (βS)-GS-HPV, produced by β-etherases LigE and LigP, is still unknown. HPV is further catabolized via vanillate (Masai *et al.*, 1989, Masai *et al.*, 1993, Sato *et al.*, 2009, Tanamura *et al.*, 2011). Genes orthologous to *ligD*, *ligL*, *ligN*, *ligO*, *ligF* and *ligP* have been mainly found in Sphingomonadaceae family, while *ligE* orthologs were more widely distributed among α-proteobacteria (Kamimura *et al.*, 2017).
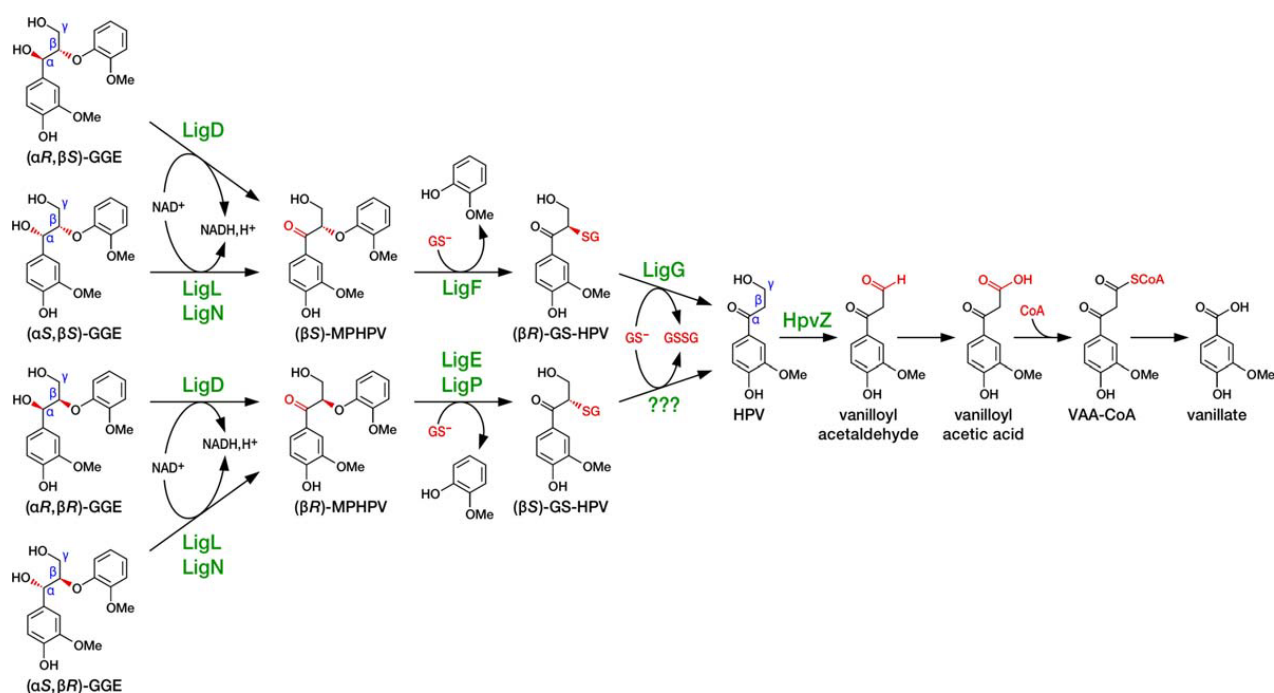
Fig. 20. Bacterial degradation pathway of guaiacylglycerol-β-guaiacyl ether, a model β-aryl ether compound in *Sphingomonas* sp. SYK-6. A detailed description of the pathway is outlined in the text. (Xu *et al.*, 2019).

1.7.5 Catabolism of biphenyl lignin dimers

Biphenyl linkage (5-5) constitutes one of the main components of lignin. Strain *Sphingobium* sp. SYK-6, transforms the biphenyl model compound 5,5'-dehydrodivanillate (DDVA) as shown in Figure 17. DDVA is O-demethylated by a non-heme iron-dependent three-component monooxygenase LigX, consisting of an oxygenase (LigXa), a ferredoxin (LigXc) and a ferredoxin reductase component (LigXd), catalyzing the formation of 2,2',3-trihydroxy-3'-methoxy-5,5'-dicarboxybiphenyl (OH-DDVA) (Yoshikata *et al.*, 2014). OH-DDVA undergoes oxidative *meta*-cleavage by the extradiol dioxygenase LigZ, which produces the meta-cleavage product 4,11-dicarboxy-8-hydroxy-9-methoxy-2-hydroxy-6-oxo-6-

phenylhexa-2,4-dienoate (DCHM-HOPDA). DCHM-HOPDA is further hydrolyzed by LigY to 5-carboxyvanillate, which is decarboxylated to vanillate by LigW or LigW2 (Figure 21) (Masai *et al.*, 2007).
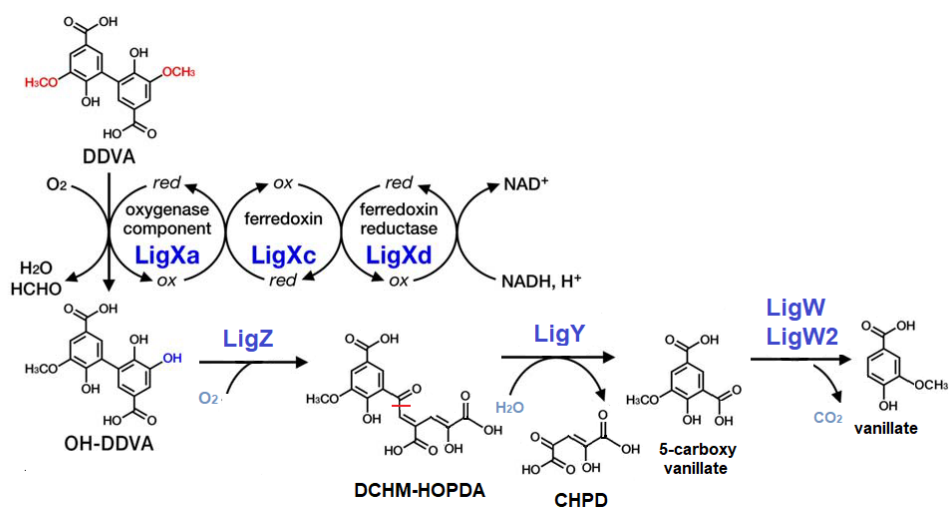
Fig. 21. Bacterial degradation pathway of 5,5'-dehydrodivanillate (DDVA), a model biphenyl compound, by *Sphingomonas* sp. SYK-6. A detailed description of the pathway is outlined in the text. Adapted from (Kamimura *et al.*, 2017).

1.7.6 Protocatechuate and catechol catabolism

Protocatechuic acid and catechol undergo oxidative ring-opening catalyzed by non-heme iron-dependent dioxygenases. The degradation of protocatechuic acid can proceed *via* three different routes: 3,4 *ortho*-cleavage pathway, 4,5 *meta*-cleavage pathway, and 2,3 *meta*-cleavage pathway (Kasai *et al.*, 2009, Kamimura and Masai, 2014, Yamanashi *et al.*, 2015). The degradation of catechol is mainly catalyzed by dioxygenases through either an *ortho*- or a *meta*-cleavage pathway (Kita *et al.*, 1999, Veselý *et al.*, 2007). Various aromatic compounds such as phenol, benzene, benzoate, toluene, naphthalene, etc. can also be funneled into catechol for further degradation (Figure 22).

The catechol and protocatechuate *ortho*-cleavage branches (β-ketoadipate pathway) join at the formation of β-ketoadipate enol-lactone. This molecular intermediate is then converted via enol-lactone hydrolase (PcaD or CatD) into β-ketoadipate. Finally, two further steps convert β-ketoadipate into metabolites of multiple anabolic pathways including the TCA cycle and fatty acid biosynthesis (succinyl-CoA and acetyl-CoA) (Wells and Ragauskas, 2012)

The compound *cis, cis*-muconic acid (*cis, cis*-MA), an intermediate of the β-ketoadipate pathway of the catechol branch, has recently attracted attention because it can be applied as an

intermediate for adipic acid production, the most widely produced dicarboxylic acid, which is a bulk feedstock for fibers and plastics (Vardon *et al.*, 2016). Sonoki *et al.* constructed an engineered *Sphingobium* sp. SME257/pTS084 strain to utilize S-lignin derivatives for cell growth and G-lignin derivatives for *cis, cis*-MA production. This way, hardwood lignin which contained abundant G-lignin and S-lignin components could be utilized comprehensively for *cis, cis*-MA production without additional glucose (Sonoki *et al.*, 2018).
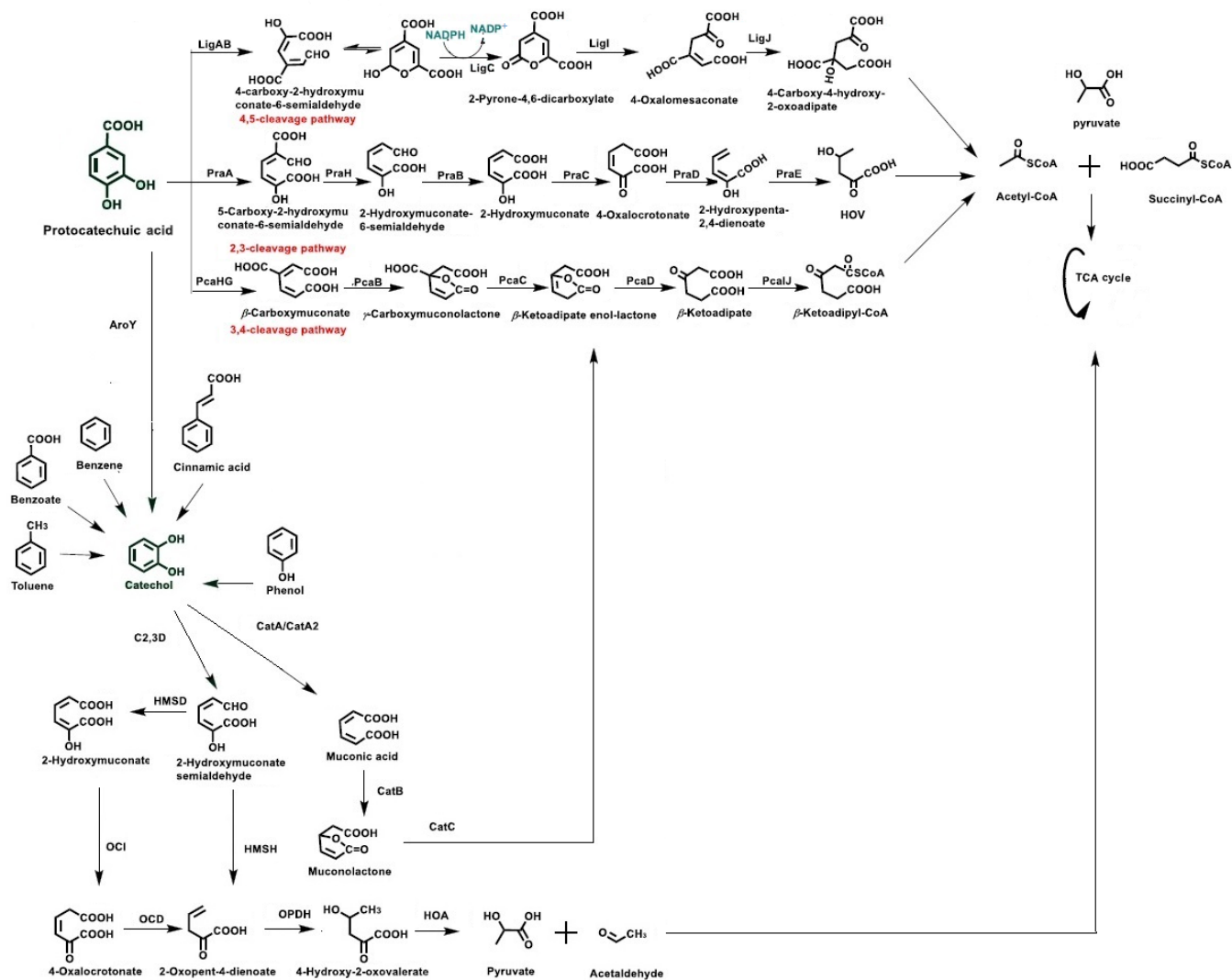
Fig. 22. Bacterial degradation pathways of protocatechuate and catechol. A description is outlined in the text. Adapted from (Xu *et al.*, 2019).

The conversion of aromatic lignocellulosic waste into lipids, suitable for biodiesel applications, and polyhydroxyalkanoates (PHAs), for the production of biodegradable plastics, is also made feasible *via* the β-ketoadipate pathway, by using acetyl-CoA as a precursor. Depolymerized lignin effluents derived from alkali/alkali-peroxide-based pretreatment of corn stover were utilized efficiently by the oleaginous bacterium

61

Rhodococcus opacus PD630, which accumulated 42.1% in oils based on cell dry weight after 48 h (Le *et al.*, 2017). Although the PHA yield was relatively low, *Pseudomonas putida* KT2440 was able to convert lignin-enriched streams derived from pilot-scale biomass pretreatment into medium chain-length polyhydroxyalkanoates (Linger *et al.*, 2014).

Chapter 2

Materials and methods

2.1   Materials

Commercial microorganisms

1. *Escherichia coli* DH5a competent cells, genotype: *fhuA2 lac(del)U169 phoA glnV44 Φ80' lacZ(del)M15 gyrA96 recA1 relA1 endA1 thi-1 hsdR17* (Invitrogen)
2. *Escherichia coli* BL21 DE3 competent cells, genotype: *E. coli B dcm ompT hsdS*(r_B^- m_B^-) *gal* (New England Biolabs)

Chemical Reagents

All chemical reagents used were of analytical grade: ABTS (Applichem), Acrylamide/Bis acrylamide (Sigma - Aldrich), Agarose (Canvax), Avicel microcrystalline cellulose (Sigma - Aldrich), Biphenyl (Merck), Birchwood xylan (Sigma - Aldrich), Caffeic acid (Extrasynthese, Genay), Carboxymethylcellulose (Sigma - Aldrich), Catechol (Extrasynthese), Congo Red (Sigma - Aldrich), Crystal violet (Ferak), Evans blue (Janssen), Ferulic acid (Acros), Folin - Ciocalteu reagent (Merck), Gallic acid (Penta), Guaiacylglycerol-beta-guaiacyl ether (TCI), HCl (Merck), IPTG (Fisher), Kraft lignin (Sigma – Aldrich CAS Number 8068-05-1), Methanol (Merck) Orange G (RAL), Organosolv lignin (Sigma – Aldrich, CAS No. 8068-03-9), Phenol-chloroform-isoamyl alcohol (Sigma - Aldrich) PMSF (Applichem), Pyrogallol (Extrasynthese), Quercetin (Sigma – Aldrich), Remazol Brilliant Blue R (Sigma - Aldrich), Rhodamine B (Sigma - Aldrich), Syringaldazine (Sigma - Aldrich), Syringic acid (Acros), Tannic acid (Merckk), Vanillic acid (Acros), Veratryl alcohol (Fluka).

Vectors and enzymes

pET15b plasmid vector (Novagen)
Restriction enzymes (Takara)
Alkaline phosphatase (Takara)
T4 Ligase (Takara)
Proteinase K (Applichem)
Lysozyme (Applichem)
Phusion DNA polymerase (Thermo Fisher Scientific)
Rnase (Applichem)

DNA-Protein markers

1kb DNA ladder (Nippon Genetics)
N0553G (New England Biolabs)
Lambda DNA – HindIII Digest Ladder (New England Biolabs)
Protein marker P7709s Color Plus Prestained (New England Biolabs)

Commercial kits

Gel Extraction kit (Macherey-Nagel)
NucleoSpin Plasmid Extraction kit (Macherey-Nagel)
Purification of His-tag proteins kit (Macherey-Nagel)

Retins – Ultrafiltration devices

Sephadex G-25 (GE Healthcare)
Amicon Ultra-15 ultrafiltration device (Merck Millipore)
Sephacryl S-200 HR resin (GE Healthcare).

Laboratory equipment

- Autoclave (PBI)
- Shaking Incubators (ZWYR – 240 LABWIT Zhicheng)
- Static incubator (Edelstahl Rostfrei)
- pH meter (Consort P800 / YSI pH 100)
- Laminar flow cabinet (TWO-30, Faster)
- Microplate reader (Multiscan GO – Thermoscientific)
- Spectrophotometer (U-2001 Hitachi)
- Water bath (Clifton)
- Heat block (TS-100 Boeco/ TS-100 Biosan)
- Benchtop centrifuges (Hettich)
- Sonicator (Sonics & Materials Vibra Cell)
- Balance (Orma model BC)
- Precision Balance (Sartorius BL 210s)
- Moisture determination balance (FD 600 – KETT)
- Agarose gel electrophoresis device (Consort EV243)
- UV transilluminator (Bioline)
- Camera gel imaging system (Vilber Lourmat)
- Polyacrylamide gel electrophoresis device (Biorad Pac 100)
- PCR machine (Genius – Techne)
- Laboratory knife mixer
- Sieve-mill
- Freeze-drying machine (Christ Alpha 1-4)
- Vortex (Labinco / Genie 2 Scientific Industries)
- Stirrer (Thermolyne Cimarec 2)
- Distillator (Barloworld Scientific LTD)
- Peristaltic pump (Ismatec)
- UV detector monitor for chromatography (Pharmacia LKB Uvicord SII)
- Microwave (Candy)
- High-Pressure Liquid Chromatography system (Agilent Technologies 1220 Infinity II LC)
- Nuclear Magnetic Resonance spectrometer (Bruker DRX, Department of Pharmacy, National and Kapodistrian University of Athens)
- LC-MS/MS system (Dionex UltiMate 3000 Nano LC system attached to a Bruker maXis 4G Ultra High-Resolution Qq TOF mass spectrometer, Protein and Proteome analytical facility, Newcastle University)

2.1.1 Culture media

Mineral Salt Medium (MSM)

This medium is modified from previous publications, (Trautwein *et al.*, 2012), to match the NaCl concentration measured in Keri Lake ecosystem during October 2013 sampling campaign. The medium containing (g L^{-1}): NH$_4$Cl (0.8), NaSO$_4$ (0.23), NaCl (8.5), KCl (0.5) and distilled water, in the presence or not of a carbon source, was sterilized in autoclave at 121 °C for 15 minutes. After sterilization and cooling the following components were added aseptically, from filter sterile stock solutions (filtered in 0,2 μm filters), in the corresponding final concentrations (g L^{-1}): NaH$_2$PO$_4$.H$_2$O (3.8), NaH$_2$PO$_4$.7H$_2$O (3.0), MgCl$_2$.6H$_2$O (0.32), CaCl$_2$.2H$_2$O (0.03), (mg L^{-1}): Na$_2$-EDTA (5.2), FeSO$_4$.7H$_2$O (2.1), H$_3$BO$_3$ (0.03), MnCl$_2$.4H$_2$O (0.1), CoCl$_2$.6H$_2$O (0.19), ZnSO$_4$.7H$_2$O (0.144), (μg L^{-1}): CuSO$_4$.5H$_2$O (29.0), Na$_2$MoO$_4$.2H$_2$O (36.0), NiCl$_2$.6H$_2$O (24.0), Na$_2$SeO$_3$.5H$_2$O (6.0), Na$_2$WO$_4$.2H$_2$O (8.0), 4-aminobenzoic acid (10.0), D-(+)-biotin (2.0), nicotinic acid (20.0), calcium D(+)-pantothenate (5.0), pyridoxal dihydrochloride (50.0), cyanocobalamine (10.0), thiamin dihydrochloride (10.0). The pH of the medium was adjusted to 6.5 with NaOH/HCl, unless otherwise stated. The compounds used as sole carbon sources in MSM, and the corresponding sterilization methods are listed in Table 1. Their final concentration is stated throughout the text. The corresponding solid media were prepared with the addition of 1.5% (w/v) Agar powder for microbiology, prior to sterilization, except for solid media containing organosolv lignin that contained 2.5% (w/v) Agar powder.

Table 1. Sterilization method of compounds used as carbon and energy sources in this study.

Compound	Sterilization method
Avicel microcrystalline cellulose	Autoclaved separately
Carboxymethylcellulose	Autoclaved separately
Birchwood xylan	Autoclaved separately
Organosolv lignin	Autoclave
Kraft lignin	Autoclave
Lignin hydrolysates from corn stover or wheat straw	Autoclave
Ferulic acid	Filter sterilization in 0.2 μm filters
Caffeic acid	Filter sterilization in 0.2 μm filters
Vanillic acid	Filter sterilization in 0.2 μm filters
Syringic acid	Filter sterilization in 0.2 μm filters
Biphenyl	Autoclave
Guaiacylglycerol-beta-guaiacyl ether	Filter sterilization in 0.2 μm filters
Acetate	Autoclave
Glucose	Autoclaved separately

Nutrient Broth – Nutrient Agar

Composition (g L^{-1}): Meat Extract (3.0), Gelatin Peptone (5.0), pH: 6.8±0.2. To prepare the medium 8.0 grams of Nutrient broth were suspended in one liter of distilled water and sterilized in autoclave at 121 °C for 15 minutes. Nutrient agar (NA) was prepared likewise, by adding in the medium 1.5% (w/v) Agar powder for microbiology prior to sterilization.

Luria Bertani medium (LB) – Luria Bertani Agar

Composition (g L^{-1}): 1% (w/v) Tryptone, (10.0), Yeast extract, (5.0), NaCl (10.0), pH 7.4. To prepare the liquid medium the above components were suspended in distilled water and sterilized in autoclave at 121 °C for 15 minutes. Luria Bertani agar was prepared likewise, by adding in the medium 1.5% (w/v) Agar powder for microbiology prior to sterilization. When necessary, antibiotics were added to the LB medium after sterilization and cooling of the medium, in a final concentration of 100μg mL^{-1}.

2.1.2 Buffers - Solutions

Ringer solution

Composition (g L^{-1}): KCl (0.105), CaCl$_2$ (0.12), NaCl (2.25), NaHCO$_3$ (0.05). The above components were suspended in one liter of distilled water and sterilized in autoclave at 121 °C for 15 minutes.

Phosphate Buffer Saline (PBS)

Composition (g L^{-1}): KCl (0.20), KH$_2$PO$_4$ (0.20), NaCl (8.0), Na$_2$HPO$_4$ (1.15). The above components were suspended in one liter of distilled water and sterilized in autoclave at 121 °C for 15 minutes.

TE Buffer

Composition: 1 mM EDTA pH 8.0, 10 mM Tris-base. The solution was sterilized in autoclave at 121 °C for 15 minutes, when necessary.

Bradford Reagent

Composition: Coomassie brilliant blue G-250 (0.1 g L^{-1}), EtOH (5% v/v), 85% H$_3$PO$_4$ (10% v/v). The above components were added to a glass beaker and stirred for 15 minutes. Distilled water was added to the final volume and the solution was stirred for 40 more minutes. The solution was filtered through Whatman paper and stored in a dark bottle at room temperature.

PMSF protease inhibitor stock solution

A stock solution of 100 mM phenylmethanesulfonyl fluoride (PMSF) was prepared in EtOH and stored at 4 °C.

IPTG stock solution

Stock solutions of isopropyl β-D-1-thiogalactopyranoside (IPTG) were prepared in 1M concentration in distilled water, filter-sterilized, and stored at -20 °C.

Antibiotics stock solution

Ampicillin was prepared in 100 mg mL^{-1} stock solutions, dissolved in distilled water, and stored at -20 °C.

Stock solutions of enzymatic substrates

Stock solutions of 2,2'-azino-bis(3-ethylbenzothiazoline-6-sulphonic acid) (ABTS) were prepared in 10 mM, using distilled water as a solvent. Stock solutions of syringaldazine (SGZ) were prepared at 1 mM concentration in ethanol. Stock solutions of ferulic acid, caffeic acid and quercetin were prepared at 10 mM, using ethanol as a solvent. Stock solutions of syringic acid, vanillic acid, gallic acid, catechol and pyrogallol were prepared at 10 mM, using distilled water supplemented with 5% dimethyl sulfoxide (DMSO). Stock solutions of the dyes Congo red, Evans blue, Orange G, Crystal violet, Rhodamine B and Remazol Brilliant Blue R were prepared at 1 mM in distilled water. All stock solutions were freshly prepared and stored in dark bottles, at 4 °C.

Stock solutions of chemical reagents

Stock solutions of 100 mM in distilled water were prepared for the following compounds: CH_3COOLi, $MgCl_2$, $CaCl_2$, $Ba(OH)_2$, $NiSO_4$, $MnCl_2$, $CuSO_4$, $KAl(SO_4)_2$, NH_4Cl, $CoCl_2$, $Pb(CH_3COO)_2$, sodium citrate dehydrate, EDTA, SDS, PMSF, $CdCl_2$, CrO_3, $AgNO_3$, β-mercaptoethanol, DTT, $HgCl_2$, $ZnCl_2$.

Phosphate buffers

Phosphate buffers in the pH range 5.0-8.0 were prepared by mixing the following stock solutions in the appropriate volumetric ratios: Stock solution A: 0.1 M potassium dihydrogen phosphate (KH_2PO_4) or sodium hydrogen phosphate ($NaHPO_4$), Stock solution B: 0.1 M dipotassium hydrogen phosphate (K_2HPO_4) or disodium hydrogen phosphate (Na_2HPO_4). Distilled water was added in the appropriate amount when necessary, to dilute the buffer.

Phosphate buffers in the pH range 3.0-4.5 were prepared by adding the appropriate volumes of 0.1 M phosphoric acid (H_3PO_4).

Carbonate-Bicarbonate Buffer

Buffers in the pH range 9.2 to 10.8 were prepared by mixing the following stock solutions in the appropriate volumetric ratios: Stock solution A: 0.1 M sodium carbonate (Na_2CO_3), Stock solution B: 0.1 M sodium bicarbonate ($NaHCO_3$). Distilled water was added in the appropriate amount when necessary, to dilute the buffer.

Buffers for DNA Agarose Gel Electrophoresis

TAE Running buffer (50X): 2 M Tris-base, 50 mM EDTA (pH = 8.0), 1 M Glacial acetic acid. Agarose gels were prepared by mixing the appropriate amount of agarose in 1X TAE Running buffer, with the addition of ethidium bromide at a final concentration of 0.2 μg mL^{-1}.

Buffers for Protein Polyacrylamide Gel Electrophoresis (PAGE)

The following buffers were prepared for Native and Denaturating - Sodium dodecyl sulfate (SDS) PAGE:

Table 2. Native PAGE buffers.

Native Page Loading buffer (3X)	0.6 mL 50X Running buffer, 3.0 mL Glycerol, 16 mg Bromophenol blue, 6.4 mL distilled water
Native Page Separating gel buffer	1.5 M Tris-base, adjustment of pH to 8.9 with HCl
Native Page Stacking gel buffer	0.5 M Tris-base, adjustment of pH to 6.8 with HCl
Native Page Separating gel 12% (v/v) acrylamide	3.5 mL distilled water, 4.0 mL 30% Acrylamide/Bis solution, 2.5 mL 1.5 M Native PAGE Separating gel buffer, 35.0 μL 10% Ammonium persulfate (APS), 7.0 μL Tetramethylethylenediamine (TEMED)
Native Page Stacking gel	2.5 mL distilled water, 0.5 mL 30% Acrylamide/Bis solution, 0.5 mL 1.0 M Native PAGE Stacking gel buffer, 20.0 μL 10% APS, 4.0 μL TEMED
Native Page Running buffer (10X)	30.0 g L^{-1} Tris-base, 144 g L^{-1} Glycine

Table 3. SDS PAGE buffers.

SDS PAGE Loading buffer (4X)	4.0 mL 1 M Tris-HCl pH 6.8, 8.0 mL Glycerol, 1.2 g DTT, 1.6 g SDS, 2.0 mL 0.5 M EDTA, 16 mg Bromophenol blue, 5.2 mL distilled water
SDS PAGE Separating gel buffer	1.5 M Tris-base, adjustment of pH to 8.8 with HCl, 3.56 g L^{-1} SDS
SDS PAGE Stacking gel buffer	1.0 M Tris-base, adjustment of pH to 6.8 with HCl, 7.4 g L^{-1} SDS
SDS PAGE Separating	3.4 mL distilled water, 4.0 mL 30% Acrylamide/Bis solution, 2.5 mL

gel 12% (v/v) acrylamide	1.5 M SDS-PAGE Separating gel buffer, 0.1 mL 10% APS, 4.0 μL TEMED
SDS PAGE Stacking gel	1.73 mL distilled water, 0.42 mL 30% Acrylamide/Bis solution, 0.32 mL 1.0 M SDS-PAGE Stacking gel buffer, 25.0 μL 10% APS, 2.5 μL TEMED
SDS PAGE Running buffer (1X)	3.03 g L^{-1} Tris-base, 14.4 g L^{-1} Glycine, 1.0 g L^{-1} SDS, pH = 8.3

Table 4. PAGE Staining / Destaining solutions.

Staining solution	0.2% (w/v) Coomassie Brilliant Blue R-250, 500 mL MeOH filtered through 3MM paper, 100 mL Acetic acid, 400 mL distilled water
Destaining solution	10% v/v Isopropanol, 10% v/v Acetic acid

2.2 Methods

2.2.1 Isolation and identification of lignocellulose degrading bacteria

2.2.1.1 Collection of soil samples from Keri Lake

Keri Lake is situated in the southern part of Zakynthos Island, in western Greece, with its surface lying 1 m above the sea level. Nowadays, this coastal fen is characterized by increased plant biomass degradation along with natural oil seeps at several sites. The vegetation of the area is dominated by the marsh reed *Phragmites australis*, and various peat-forming plants, that form a five-meter thick peat layer below the fen (Avramidis *et al.*, 2017). Surface soil samples (5 - 10 cm depth) were collected from five uniform sites of Keri Lake, exposed to oil, during a sampling campaign conducted in October 2014 (Michas *et al.*, 2017). Soil samples were kept in sterile containers, placed in a portable fridge (4 – 8 °C), and transferred within 24 h to the lab. Soil samples were stored at 4 °C until further processing (maximum storage time in the lab before the commencement of enrichments was 48 h).

2.2.1.2 Isolation of bacterial strains from soil samples

To isolate aerobic lignocellulolytic bacteria, enrichment cultures were performed by suspending 2 g of each soil sample in 20 mL Minimal Salt Medium (MSM), supplemented with either 1% (w/v) carboxymethyl cellulose (CMC), 1% (w/v) birchwood xylan or 1% (w/v) organosolv lignin as sole carbon sources. NaCl concentration was adjusted to match that of the coastal waters of Keri area. Cultures were incubated at 30 °C under continuous shaking

at 180 rpm. Subsequent transfers were carried out (1 mL into 20 mL of fresh medium) at 5 days intervals. At the end of a 30 days enrichment period, 100 μL from suitable dilutions of each final enrichment flask were spread on agar plates containing MSM supplemented with 1% (w/v) of the corresponding carbon source, and plates were incubated at 30 °C under aerobic conditions. Bacterial colonies were selected and were repeatedly streaked and purified on nutrient agar plates. A glycerol stock for each isolated strain was prepared by resuspending bacterial cells grown in NB and pelleted by centrifugation at 4.000 rpm for 5 minutes, in a 20% (w/v) glycerol solution. Glycerol stocks were stored in cryovial tubes, at -20 °C and -80 °C.

2.2.1.3 Identification and phylogenetic analysis of isolated strains

Isolation of genomic DNA was carried out from overnight grown pure bacterial cultures in NB, by using the CTAB method, following the Joint Genome Institute bacterial genomic DNA isolation protocol (William *et al.*, 2012). The purified DNA was used as a template for PCR amplification of the full-length 16S rRNA gene with Phusion DNA Polymerase, using the forward primer 27F (5'-AGAGTTTGATCMTGGCTCAG -3') and reverse primer 1492R (5'-TACGGYTACCTTGTTACGACTT -3'). The temperature profile consisted of 98 °C for 1 min, followed by 35 cycles of denaturation at 98 °C for 10 sec, annealing at 59.5 °C for 30 sec and extension at 72 °C for 50 sec. 16S rRNA gene PCR products (1465 bp) were analyzed on a 1% (w/v) agarose gel, gel-purified using a Gel Extraction kit, following the manufacturer's instructions and sequenced. The obtained sequences were compared to two different databases, Genbank database (16S ribosomal RNA database), by using the BLASTn algorithm (http://blast.ncbi.nlm.nih.gov/Blast.cgi), and EzBioCloud database (http://www.ezbiocloud.net/) (Yoon *et al.*, 2017). Multiple sequence alignments of the isolates' 16S rRNA genes and those of the reference sequences from the Gen-Bank database were generated using the L-INS-i algorithm of MAFFT software. The alignments served as the input for a maximum-likelihood phylogenetic tree using IQTREE version 1.6.10 with Jukes-Cantor chosen as the best-fit model according to BIC. The confidence values of branches were generated using bootstrap analysis based on 1000 iterations.

2.2.1.4 Screening for glycoside hydrolase activities on solid media

All isolates were screened for hydrolytic activities on agar plates containing MSM supplemented with either 1% (w/v) CMC, 1% (w/v) Avicel microcrystalline cellulose or 1% (w/v) birchwood xylan. A cell suspension of each isolate in Ringer solution was spread on

each plate and growth was evaluated after a 5-10 day incubation at 30 °C. Each experiment was conducted in duplicates. Inoculated MSM basal media with no carbon source added, were implemented as control cultures. Once the growth of the bacterial cells was sufficient, agar plates were overlaid with a Congo Red solution, of 1 mg mL^{-1} concentration, and stained for 15 minutes. The Congo Red solution was then replaced by a 1 M NaCl rinsing solution for 15 minutes. The appearance of a clearance zone around the bacterial colonies indicated hydrolysis of the substrate and thus cellulolytic or xylanolytic activity (Teather and Wood, 1982).

2.2.1.5 Preparation of lignin hydrolysates by alkaline pretreatment of plant biomass

Agricultural residues from corn stover and wheat straw, provided by a local producer in the province of Phthiotis, central Greece, were used to prepare a lignin substrate for subsequent use in the screening process of bacterial isolates. Each raw material, consisting of stem and leaves, was air-dried and subjected to mechanical treatment, involving homogenization in a mixer and grinding through a sieve-mill (0.7 mm). Subsequently, an aqueous solution (10% w/v) of the milled material was heated at 90 °C for 30 minutes, to remove impurities, followed by a thorough washing on a sieve (160 μm) using tap and distilled water. The washed solid material was dried at 50 °C, until constant weight. 20 g of each dried material was further dried in a moisture balance while their moisture content was determined. Alkaline (soda) pretreatment was carried out by adding 0.1 g NaOH per gram of dry biomass, in an aqueous solution, at a solid-liquid mass ratio of 1:6. The slurry was heated at 95 °C for 3 hours, under continuous stirring. Finally, the solution was filtered through a 160 μm sieve to separate the black liquor of solubilized lignin from the solid residues of plant material. The final alkali solubilized lignin was subjected to the following analysis: Total carbon (TC), total inorganic carbon (TIC) and total nitrogen (TN) content were simultaneously determined, applying the high-temperature (720°C) catalytic combustion (Pt/Al2O$_3$) oxidation method (Bekiari and Avramidis, 2014) using a Shimadzu TOC analyzer (TOC-VCSH) coupled to a chemiluminescence detector (TNM-1 TN unit) (Department of Geology, University of Patras). Reducing sugars content was measured by the DNS method (Miller, 1959) while total dissolved solids were determined by evaporation of the hydrolysate solution. For ^{1}H NMR spectroscopy an aqueous solution of each lignin hydrolysate containing around 0.5 g L^{-1} Total Organic Carbon, was centrifuged and the supernatant was concentrated in a rotary evaporator and dissolved in deuterated water. $_1$H NMR spectra were recorded on a Bruker DRX 400 MHz spectrometer, at 300 K (Department of Pharmacy, National and Kapodistrian University of Athens). Hydrolysates were stored at -20 °C until use.

2.2.1.6 Growth studies on lignin substrates and selected aromatic carbon sources

Growth on media containing lignin substrates or selected aromatic compounds as sole carbon sources was evaluated for isolates from lignin enrichment cultures, and isolates belonging to the classes of α-Proteobacteria and Actinobacteria. Bacterial strains were inoculated into nutrient agar plates and grown at 30 °C. Plates were flooded with Ringer solution and cells were harvested by scraping. Cell suspensions were used for the inoculation of 5 mL liquid cultures of MSM supplemented with one of the following carbon sources, in the corresponding concentration of Total Organic Carbon (g L^{-1}): corn stover lignin hydrolysate (0.5), wheat straw lignin hydrolysate (0.5), (both prepared as described in § 2.2.1.5), ferulic acid (1.0), caffeic acid (1.0), vanillic acid (1.0), syringic acid (1.0), biphenyl (0.9) and guaiacylglycerol-beta-guaiacyl ether (GGE) (0.6). No further data about the isomer composition of GGE were available. Commercial Kraft lignin was added at a concentration of 0.1 % (w/v). The inoculum volume was adjusted so as to achieve a 0.2 initial optical density in the liquid cultures. Cells were also inoculated on solid media containing MSM supplemented with 0.2% (w/v) organosolv lignin. Three replications were conducted for each carbon source. Inoculated liquid and solid MSM basal media with no carbon source added, were implemented as control cultures. Liquid cultures were incubated at 30 °C on a rotary shaker at 180 rpm for 14 days and samples were withdrawn for determining the optical density in a microplate reader (600 nm). Complete media without inocula, incubated under the same conditions, served as blank samples. Solid media were incubated at 30 °C, for 14 days. Strain *Pseudomonas putida* KT2440 was used as a model strain during the growth tests.

2.2.1.7 Growth study on high and low molecular weight Kraft lignin

Kraft lignin was further fractionated into high and low molecular weight lignin to test the ability of selected isolates to grow in these two fractions. A Sephadex G-25 gel filtration column, with a molecular mass cutoff limit of 5.000 Da, was used for the fractional separation of a 2% (w/v) aqueous solution of Kraft lignin. Elution was conducted with distilled water, collecting two fractions corresponding to high (> 5.000 Da) and low molecular kraft lignin (<5.000 Da). Suspended solids in the resulting fractions were determined by evaporation of the hydrolysate solution.

2.2.1.8 Determination of temperature, pH and nitrogen source effect on bacterial growth and degradation of phenolic compounds in lignin hydrolysates

Strains *Pseudomonas kilonensis* ZKA7 and *Rhodococcus pyridinivorans* ZKA49 were selected for further study of their growth in lignin hydrolysates from alkaline pretreatment of corn stover and wheat straw. Strains were cultured in MSM supplemented with 0.5 g L^{-1} TOC of either corn stover lignin hydrolysate (CSLH) or wheat straw lignin hydrolysate (WSLH), as sole carbon sources. Cell suspensions in PBS of ZKA7 and ZKA49, grown in NA plates, were used for the inoculation of two replicates for each treatment described below. The effect of temperature was tested by incubating the bacterial cultures at temperatures 27 °C, 32 °C, 37 °C and 42 °C, at 180 rpm. Maximum specific growth rate (μ_{max}) was calculated based on modified Gompertz function (Zwietering *et al.*, 1990). The effect of pH was tested by adjusting the above media to pH values, 5.0, 6.0, 7.0 and 8.0, using solutions of 5 N NaOH and 2 N HCl. Cultures were incubated at 30 °C, at 180 rpm. To test the effect of the nitrogen source, one of the following nitrogen sources was added in MSM: NH$_4$Cl, KNO$_3$, NH$_4$NO$_3$, tryptone or yeast extract, in an equivalent amount of N (0.21 g L^{-1} N), as calculated in basic MSM. pH was adjusted to 6.5 and cultures were incubated at 30 °C, at 180 rpm. Bacterial growth was monitored by measuring the optical density of cultures, at 600 nm, in a microplate reader, at intervals of 0, 2, 4, 6, 8, 10, 12, 24 and 48 hours. Control samples for all treatments described above included inoculated MSM without a carbon source. Non-inoculated complete media, incubated under the same conditions, served as blank samples.

In addition, at each sampling point, 50 μL of culture were removed and the supernatant was assayed for total phenolic content using the Folin - Ciocalteu assay. The principle of this assay is based on the oxidation of phenolic compounds and the concomitant reduction of phosphomolybdate and phosphotungstate acid complexes, present in the Folin – Ciocalteu reagent, under alkaline conditions (Singleton and Rossi, 1965). The formation of blue chromophores constituted by the phosphomolybdenum / phosphotungstic complex is proportional to the concentration of phenolic compounds of a sample, while alkaline conditions are achieved by the addition of Na$_2$CO$_3$. The assay was conducted in a final volume of 200 μL by adding the following reagents: 20 μL of culture supernatant in an appropriate dilution, 10 μL Folin - Ciocalteu reagent, 140 μL of distilled water, and 30 μL of a 20% (w/v) Na$_2$CO$_3$ solution. The reaction was incubated at room temperature for 2 hours and the absorption of the samples was measured at 760 nm in a microplate reader. The same reaction with distilled water instead of culture supernatant served as blank sample. A standard curve of gallic acid was designed by conducting the assay with the following concentrations of gallic acid (mg L^{-1}): 10, 20, 30, 50, 75 and 100, prepared in distilled water.

2.2.1.9 Identification of structural changes in lignin hydrolysates treated by bacterial strains

Strains *Pseudomonas kilonensis* ZKA7 and *Rhodococcus pyridinivorans* ZKA49 were inoculated in MSM supplemented with 0.5 g L^{-1} TOC of CSLH or WSLH, pH 6.5. The same medium without the addition of bacterial inoculum served as control sample. Cultures and control samples were incubated at 30 °C on a rotary shaker at 180 rpm and growth of the bacterial strains was monitored by measuring the optical density at 600 nm. Samples were withdrawn during late stationary phase and after centrifugation the supernatant was collected, concentrated in a rotary evaporator and dissolved in deuterated water. Samples were used for $_1$H NMR analysis performed on a Bruker DRX 400 MHz spectrometer, at 300 K (Department of Pharmacy, National and Kapodistrian University of Athens).

2.2.2 Production and characterization of potential lignin-degrading enzymes

2.2.2.1 Detection of genomic sequences encoding potential ligninolytic enzymes

To identify putative lignin-oxidizing enzymes a BLAST search was performed in the genome sequences of strains closely related to *Pseudomonas kilonensis* ZKA7, as at that point its genome sequence was not available. BLAST searches were performed in the Protein Database of the National Center for Biotechnology Information (http://blast.ncbi.nlm.nih.gov/Blast.cgi), using the algorithm blastp and *Pseudomonas brassicacearum* as target taxon. The amino acid sequences of the following proteins were used as queries: (1) CopA multicopper oxidase, from *P. syringae* pv. tomato (Uniprot Acc. No. P12374), (2) Dyp1B peroxidase from *Pseudomonas fluorescens* Pf-5 (Uniprot Acc. No. Q4KAC6), and (3) Catalase-peroxidase from *Amycolatopsis* spp. (NCBI Reference Sequence: WP_101435509.1). A multicopper oxidase-encoding gene *copA*, a DyP-type peroxidase-encoding gene *dypB* and a catalase-peroxidase-encoding gene *katG* encoded in *P. brassicacearum* species were selected for further study of their lignin-oxidizing potential. The rationale of this choice is explained in Results and Discussion (§ 3.9).

2.2.2.2 *In silico* analysis of proteins CopA, DypB and KatG

The amino acid sequences of the three proteins selected for further study were examined for protein homology with characterized homologues, retrieved from NCBI, Uniprot/SwissProt or RedOxiBase protein databases and literature. Multiple sequence alignments were generated using the CLC Main Workbench 5.5 (https://digitalinsights.qiagen.com) and MAFFT software version 7 (Katoh and Standley, 2013). The alignment of representative dyp-type

peroxidases, generated by MAFFT, was used for the construction of a maximum-likelihood phylogenetic tree using IQTREE version 1.6.10 (Nguyen *et al.*, 2014). The Isoelectric Point Calculator algorithm was used to compute the pI of proteins (Kozlowski, 2017). The genomic organization of the *copA*, *dypB* and *katG* genes was analyzed using the DOE Joint Genome Institute portal (https://genome.jgi.doe.gov/portal/), upon receiving the genome sequence of *Pseudomonas kilonensis* ZKA7. The secondary and tertiary structure of the proteins was predicted by Phyre2 web portal (Kelley *et al.*, 2015). Visualization and analysis of protein structures was performed with UCSF Chimera program V.1.13.1 (Pettersen *et al.*, 2004).

2.2.2.3 Amplification and plasmid cloning of genes *copA*, *dypB* and *katG*

The presence and location of signal peptides for CopA, DypB and KatG proteins was predicted using the corresponding amino acid sequences from closely related microorganisms and the SignalIP 4.1 Server (Petersen *et al.*, 2011). CopA contained a signal peptide spanning from residue 1 till 33 of the full protein, while no signal peptide was predicted for DypB or KatG. A set of degenerate primers was designed for each gene, based on their complete open reading frame, removing the sequence of any signal peptide, and adding the appropriate restriction recognition site (Table 5).

Table 5. Primer sequences used for PCR amplification of genes *copA*, *dypB* and *katG*. Added restriction sites are indicated in bold.

Primers	Primer sequence (5´-3´)	Restriction enzyme
Forward *copA*	TATC**CTCGA**GATGACCRGCCCKGGCCAGCCCAAC	XhoI
Reverse *copA*	GATA**CTCGA**GTCATTCCTGCACCCGAACTTCACGGA	XhoI
Forward *dypB*	TATC**CTCGA**GATGAGTTACTACCAGCCCGGCATTCTC	XhoI
Reverse *dypB*	GATA**CTCGA**GTTACCGGGCCAGGGCSCGCARATC	XhoI
Forward *katG*	GTA**GGATCC**GGCAAACGAATCGAAATG	BamHI
Reverse *katG*	GTA**GGATCC**TCACCKSAGATCAAACCGATC	BamHI

Genes *copA*, *dypB* and *katG* were amplified by PCR using the above set of primers and Phusion DNA Polymerase, following manufacturer's instructions. The temperature profile for *copA* consisted of 98 °C for 3 min, followed by 35 cycles of denaturation at 98 °C for 10 sec, annealing at 69 °C for 30 sec and extension at 72 °C for 52 sec. The temperature profile for *dypB* consisted of 98 °C for 3 min, followed by 35 cycles of denaturation at 98 °C for 10 sec, annealing at 68 °C for 30 sec and extension at 72 °C for 27 sec. The temperature profile for *katG* consisted of 98 °C for 3 min, followed by 35 cycles of denaturation at 98 °C for 10 sec, annealing at 62 °C for 30 sec and extension at 72 °C for 68 sec. PCR products were run on a 1% agarose gel and gel-purified using a Gel Extraction kit (MN), following the

manufacturer's instructions. Restriction digestions of the purified flanked genes and vector pET15b were conducted with XhoI for cloning of *copA* and *dypB* and with BamHI for cloning of *katG*. Restriction digestions with XhoI were incubated at 37 °C for 2 h, and those with BamHI at 30 °C for 2 h, according to the manufacturer's instructions. Following digestion, the vector was dephosphorylated to decrease the background of non-recombinants due to self-ligation of the vector, by treatment with alkaline phosphatase for 15 min at 37 °C, according to the manufacturer's instructions. Digested inserts and vectors were run on a 1% w/v agarose gel and gel purified prior to ligation. Ligation of digested inserts and vector was performed by T4 ligase and incubation at 4 °C for 16 h, following the manufacturer's instructions. The resulting recombinant plasmids are shown in Figure 23. Ligation reactions without insert DNA were used as negative control samples.
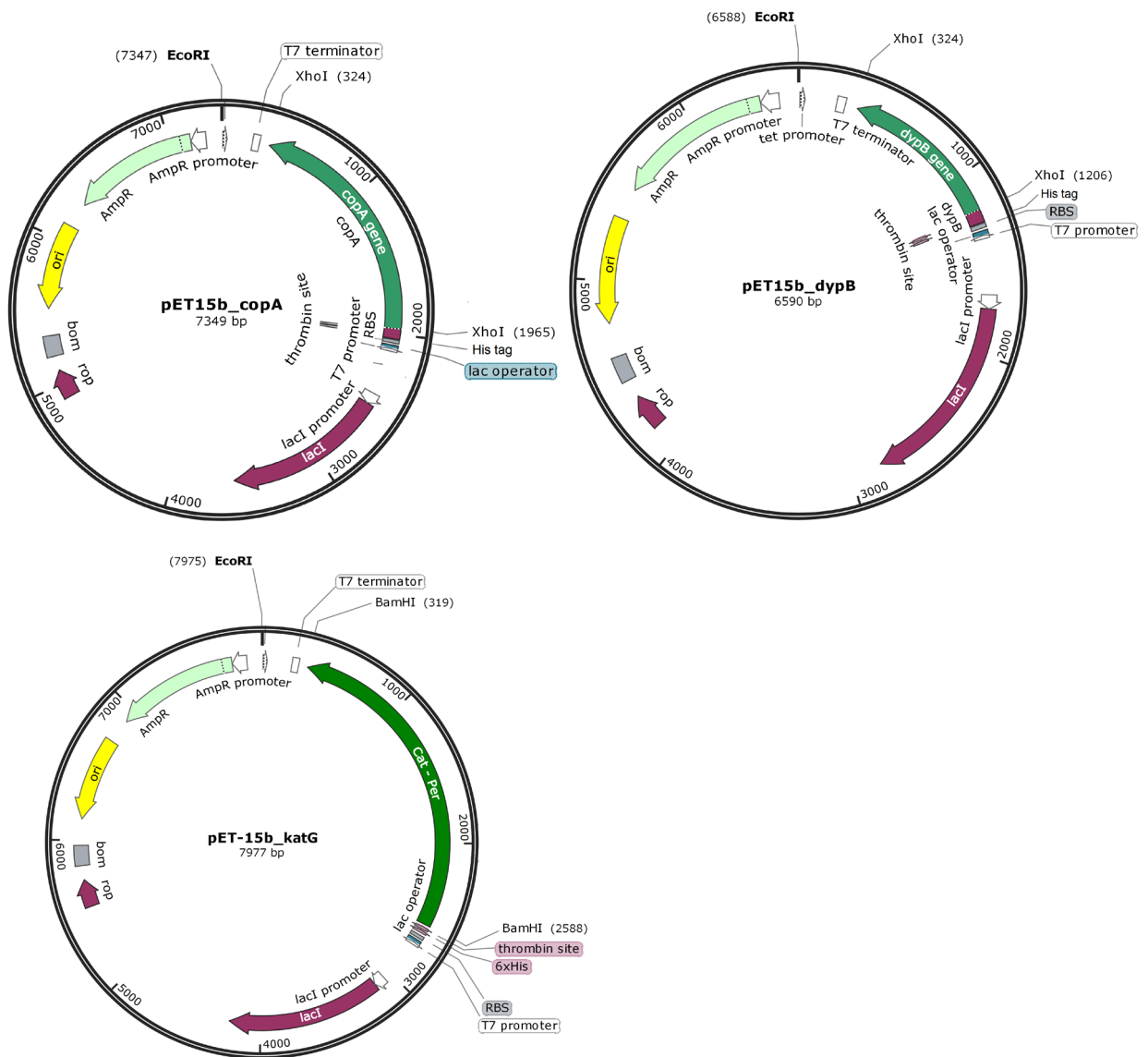
Fig. 23. Cloning of target genes *copA*, *dypB* and *katG* in pET15b plasmid vectors. Target genes were cloned under the control of T7 promoter, fused with histidine tags, and expressed using the T7 RNA Polymerase/Promoter System, in *E. coli* BL21 DE3 competent cells.

2.2.2.4 Transformation of recombinant plasmids into host cells

The recombinant plasmids were transformed into *E. coli* DH5a competent cells, which serve as hosts for maintaining plasmids. The transformation protocol used was as follows: 1-5 μL of ligation reaction were mixed gently with 100 μL of *E. coli* DH5a competent cells and incubated for 30 min on ice. Cells were heat-shocked at 42 °C, for 90 min and immediately cooled on an ice bath for 2 min. 100 μL of LB were added to the reaction and cells were incubated at 37 °C for 1 h, at 180 rpm. Finally, cells were spread on LB agar plates supplemented with 100 μg/mL ampicillin and incubated at 37 °C for 16 h. Positive clones and correct orientation of inserts was verified by a combination of colony PCR with plasmid DNA PCR or restriction digest of plasmid DNA. Colony PCR and plasmid reactions were conducted by using either a pair of modified T7 promoter and T7 terminator primer (Table 6), or pairs of a modified T7 primer with the appropriate amplification primer of each gene. PCR reactions were conducted using Phusion DNA Polymerase, following the manufacturer's instructions. PCR temperature profiles were set according to the primer pair and template DNA used. Plasmids were extracted by using NucleoSpin Plasmid Extraction kit, following the manufacturer's instructions. The recombinant plasmids were sequenced with T7 universal primers. Bacterial colonies carrying the correct clone were further inoculated in 5 mL of LB supplemented with 100 μg/mL ampicillin and incubated at 37 °C for 16 h. After overnight incubation, cells were pelleted by centrifugation at 4.000 rpm for 5 minutes, and resuspended in a 20% (w/v) glycerol solution. Glycerol stocks were stored in cryovial tubes, at -20 °C.

Table 6. T7 primer sequences used in colony or plasmid PCR for verification of positive clones and correct orientation of target genes. Primer sequences were modified from T7 universal primers to match the annealing temperature of *copA*, *dypB* and *katG* gene amplification primers.

Primer	Modified primer sequence (5´-3´)
T7 Promoter (Forward)	TAATACGACTCACTATAGGGGAATTGTG
T7 Terminator (Reverse)	GCTAGTTATTGCTCAGCGGTGG

2.2.2.5 Overexpression and purification of recombinant proteins

Recombinant plasmids harboring *copA*, *dypB* and *katG* genes were transformed into *E. coli* BL21 DE3 cells for protein expression, using the transformation protocol described above. For the expression of the recombinant proteins 10mL of LB broth, supplemented with 100 μg/mL ampicillin, were used as a starter culture, inoculated with a recombinant colony of *E. coli* BL21 DE3 cells. Starter cultures were incubated at 37 °C overnight, at 180 rpm and then gradually scaled-up, first to 150 mL until optical density reached ~1.0 and then to 1,5 L

cultures of LB broth supplemented with 100 μg/mL ampicillin, incubated at 37 °C until optical density reached 0.6 - 0.7. Protein expression was induced by adding IPTG to a final concentration of 0.45 mM and overnight incubation at 18 °C, at 180 rpm. CopA overexpression was supported with the addition of 0.25 mM of filter-sterilized $CuCl_2$, and was conducted at a lower speed (100 rpm) to achieve a fully copper-loaded enzyme. To assess in the first place the production of the recombinant proteins, culture aliquots (~5 mL) were retrieved before the addition of the IPTG inducer and after overnight induction, and their optical density was determined. Cells in these samples were collected by centrifugation at 11.000 g, for 5 min, and were suspended in the appropriate volume of SDS-PAGE loading buffer, so as to achieve an OD of 40 in 50 μL of SDS-PAGE loading buffer. Cells were lysed by boiling for 10 min, followed by centrifugation at 11.000 g for 10 min. 10 μL from the top liquid of the samples were run in a 12% (w/v) SDS-polyacrylamide gel to verify the production of the recombinant proteins. Cells produced after overnight induction of proteins were collected by centrifugation at 10000 x g, at 4 °C, for 20 min and, if necessary, stored at -20 °C, until use. Cell pellets were resuspended in lysis buffer (10 mM imidazole, 300 mM NaCl, 50 mM $NaHPO_4$, pH 8.0), in the presence of 0.5 mM PMSF, and were disrupted by sonication until complete lysis. The sonicator was programmed at 12 sec cycles (3 sec ON and 9 sec OFF). The samples were immersed in an ice bath during sonication, to avoid overheating of protein samples. Cell lysis was followed by centrifugation at 15.000 g, at 4 °C, for 30 min, and collection of supernatant that contains the soluble proteins.

The expressed proteins, carrying a His-tag, were purified by nickel affinity chromatography in a nickel agarose resin of commercial kit "Purification of His-tag proteins", following the manufacturer's instructions. Proteins were eluted with 10 mL of elution buffer, consisted of 50 mM sodium phosphate, 300 mM NaCl, 250 mM imidazole, pH 8.0, generating 10 protein fractions of 1 mL each. The eluted protein fractions (1 μL from each protein fraction) were analyzed by SDS-PAGE, in a 12% (w/v) polyacrylamide gel. Protein bands were visualized by staining the gels with PAGE staining solution for 30 min, followed by rinsing at regular intervals with destaining solution (§ 2.1). Purified protein fractions containing the desired recombinant protein were pooled, concentrated and resuspended in a 50 mM phosphate buffer, pH 6.0, using Amicon ultrafiltration devices, with a 10 kDa molecular mass cutoff, following the manufacturer's instructions. Proteins CopA and DypB were further purified by gel filtration chromatography using a Sephacryl S-200 HR resin. The column was equilibrated with a 20 mM MOPS buffer, pH 7.0. Elution was performed with the same buffer at a flow rate of 1.0 mL/min. The chromatograms were recorded by UV absorbance at 280 nm. Oxidative activity of eluted protein fractions was tested with ABTS assay as described in

§2.2.15. Fractions containing the desired active protein were pooled and concentrated using Amicon ultrafiltration devices with a 10 kDa molecular mass cutoff as described above. Protein purification was verified by SDS and native PAGE in 12% (w/v) polyacrylamide gels. Protein concentration was estimated at all stages, using the Bradford protein assay, using bovine serum albumin (BSA) as a standard, and by measuring the absorbance at 595 nm (Bradford, 1976). Copper reconstitution in CopA was performed by incubating an aliquot of the enzyme with excess $CuCl_2$ (approx. ten times the molar concentration of the enzyme), in a 20 mM MOPS buffer, pH 7.0, in the presence of 1 mM glutathione, at 4 °C, for 1-2 h, as previously described (Cortes et $al.$, 2015). Following copper reconstitution, the concentration of CopA, removal of salts and exchange of buffer were conducted using ultrafiltration devices with a 10 kDa cut-off limit. The absorption spectra of the proteins were determined in the range of 200 to 700 nm in a microplate reader. Protein samples of CopA, DypB and KatG were stored at 4 °C in a 50 mM phosphate buffer pH 6.5 or a 20 mM MOPS buffer pH 7.0, and at -20 °C in the above buffers supplemented with 50% (v/v) glycerol.

2.2.2.6 Kinetic characterization of recombinant proteins

The oxidation of ABTS and syringaldazine (SGZ) was used for the kinetic characterization of CopA, DypB and KatG. Protein KatG was also characterized for catalase activity, using H_2O_2 as a substrate. The enzymatic assays were initially standardized using different amounts of enzyme and substrate so as to achieve linearity in product formation. The optimal concentration of $CuCl_2$ for CopA was determined by using different concentrations in the range 0-10 mM. Optimal H_2O_2 concentration for assaying the peroxidative activity of DypB and KatG and the catalase activity of KatG was determined by using different concentrations in the range 0-30 mM and 0-100 mM, respectively. Optimum pH for ABTS, SGZ and H_2O_2 activity were determined in 100 mM phosphate buffer in the pH range 3.0 – 8.0. Temperature optima were determined by incubation of the ABTS reaction at temperatures ranging from 30 °C to 60 °C, in 100 mM phosphate buffer in the optimum pH of each enzyme. The standard assay reactions were conducted as shown in Table 7, unless otherwise stated:

Table 7. Standard assay reactions for recombinant enzymes.

Enzyme	Substrate	CuCl$_2$	H$_2$O$_2$	Buffer
CopA	1.0 mM ABTS	0.5 mM	-	100 mM phosphates pH 5.5
	0.05 mM SGZ	0.5 mM	-	100 mM phosphates pH 7.0
DypB	0.01 mM ABTS	-	1.0 mM	100 mM phosphates pH 6.0
	0.05 mM SGZ	-	1.0 mM	100 mM phosphates pH 7.0
KatG	0.1 mM ABTS	-	10 mM	100 mM phosphates pH 5.5
	0.01 mM SGZ	-	2 mM	20mM MOPS pH 7.0
	20 mM H$_2$O$_2$	-	-	100 mM phosphates pH 6.5
	5 mM o-dianisidine	-	5 mM	20mM MOPS pH 7.0

ABTS, SGZ and o-dianisidine oxidation were measured spectrophotometrically at 420, 525 and 460 nm respectively. Hydrogen peroxide (H$_2$O$_2$) decomposition by KatG was measured spectrophotometrically at 240 nm. The molar extinction coefficients (ε) used in the assays were 36 mM^{-1} cm^{-1} for ABTS, 65 mM^{-1} cm^{-1} for SGZ, 39.4 mM^{-1} cm^{-1} for H$_2$O$_2$ and 11.3 mM^{-1} cm^{-1} for o-dianisidine. All assays were performed in triplicates, in 96-well microplates using a microplate reader. Blank reactions were conducted with heat-inactivated enzymes at boiling point, for 15 minutes. The initial reaction rate was calculated based on the slope of the linear part of the plot representing absorption against time minus the corresponding slope of the blank reaction. Kinetic parameters of the purified enzymes were determined using different concentrations of substrates: ABTS: 0.1-5.0 mM for CopA, 0.01-1.0 mM for DypB, 0.05-5 mM for KatG, SGZ: 1.0 – 50 mM, H$_2$O$_2$ for KatG 0.2 mM-30 mM, at temperature and pH optima. K$_M$ and V$_{max}$ were estimated by nonlinear regression, using SigmaPlot v.12.0, by fitting the data to the Michaelis–Menten equation: $V = V_{max} [S] / Km + [S]$, where V represents the initial reaction rate and [S] represents the substrate concentration in the following reaction:

$$E + S \rightleftarrows ES \rightarrow E + P$$

K$_M$, the Michaelis constant, provides an estimation of the affinity of the enzyme for a substrate and is operationally defined as the substrate concentration at which initial rates are half of the maximum velocity (V$_{max}$). Substrate inhibition effect of KatG by syringaldazine was described by the equation $V = V_{max} [S] / (K_M + [S] + ([S]^2 / K_{SI}))$, and the Ksi substrate inhibition constant was determined. The catalytic constant k$_{cat}$ is defined as the number of moles of substrate transformed per minute per mole of enzyme under optimum conditions,

and was quantified using the equation $V_{max} = k_{cat} [E]$, where $[E]$ represents molar concentration of enzyme. One unit of enzyme activity (U) was defined as the amount of enzyme that oxidizes 1 μmol of substrate per minute. Specific activity (U/mg) was expressed as units of activity per milligram of protein.

2.2.2.7 Determination of pH and temperature effect on enzyme stability

The thermal stability of expressed enzymes was determined by preincubating the recombinant enzymes at temperatures ranging from 40 °C to 70 °C. At time zero, enzymes CopA and DypB were assayed for ABTS activity, at optimum conditions for each enzyme, apart from temperature that was set at 30°C, and their initial reaction rate was calculated. Similarly, the thermal stability of KatG was determined by using the standard H_2O_2 assay. The remaining activity of the enzymes was measured at various time intervals by withdrawing an aliquot from each preincubated enzyme, cooling of the preincubated aliquot on ice, and conducting the standard ABTS or H_2O_2 assay. Similarly, pH stability was determined by preincubating the enzymes in 50 mM phosphate buffers in the pH range 3-5, or in 50 mM Na_2CO_3 / $NaHCO_3$ buffers in the pH range 10-11, at 30 °C, by withdrawing an aliquot from each preincubated enzyme at various time intervals and conducting the ABTS or H_2O_2 assay accordingly. All assays were performed in triplicates, in 96-well microplates using a microplate reader. Activities at time zero were set as 100% and the residual activity was expressed as percentage of the initial reaction rate.

2.2.2.8 Determination of chemical reagents effect on enzyme activity

The effect of various chemical reagents on the oxidizing activity of the recombinant enzymes was investigated. To test the effect of different chemical reagents the standard ABTS reaction for CopA and DypB or the standard H_2O_2 reaction for KatG, using instead 10 mM H_2O_2, was supplemented with the following compounds in a final concentration of 10 mM: CH_3COOLi, $MgCl_2$, $CaCl_2$, $Ba(OH)_2$, $NiSO_4$, $MnCl_2$, $CuSO_4$, $KAl(SO_4)_2$, NH_4Cl, $CoCl_2$, $Pb(CH_3COO)_2$, sodium citrate dehydrate, EDTA, SDS, PMSF, $CdCl_2$, CrO_3, $AgNO_3$, β- mercaptoethanol, DTT, $HgCl_2$ and $ZnCl_2$. Reactions were conducted in 50 mM MOPS buffer pH 6.5, to avoid interaction of phosphates with the reagents used. Blank reactions for each reagent were assayed by replacing the amount of enzyme added with distilled water. The initial reaction rate of the assays in the absence of chemical reagents was defined as 100% and the residual activity in their presence was expressed as percentage of the initial reaction rate. Chemical reagents causing a significant decrease in enzyme activity at 10 mM (<20% remaining

activity) were further tested for their effect at a final concentration of 1 mM. All assays were performed in triplicates, in 96-well microplates, using a microplate reader.

2.2.2.9 Determination of recombinant enzymes' substrate specificity

Enzymatic activity towards different substrates was determined. Substrates tested included the lignin-related aromatic compounds ferulic acid, caffeic acid, syringic acid, vanillic acid, catechol and pyrogallol, and the dyes Congo red (CR), Evans blue (EB), Orange G (OG), Crystal violet (CV), Rhodamine B (RB) and Remazol Brilliant Blue R (RBBR). The λ_{max} of each substrate was determined by analyzing its UV/Vis spectrum in a microplate reader. Enzymatic activity against the substrates was assayed in 100 mM phosphate buffer, pH 6.0, supplemented with either 0.5 mM $CuCl_2$ for CopA or 1.0 mM H_2O_2 for DypB, or 10 mM H_2O_2 for KatG, at a final concentration for each substrate as follows: ferulic, syringic and vanillic acid 40 μM, caffeic acid 4 μM, catechol and pyrogallol 200 μM, CR 25 μM, EB 10 μM, OG 50 μM, CV 10 μM, RB 1 μM, RBBR 100 μM. Oxidation of Mn^{2+} was assayed in 100 mM potassium sodium tartrate buffer pH 5.0, $MnCl_2$ at a concentration range of 0.1-2 mM, supplemented with 0.5 mM $CuCl_2$ for CopA or 1.0 mM H_2O_2 for DypB, or 10 mM H_2O_2 for KatG. All assays were performed in triplicates, in 96-well microplates, at 30 °C, in the dark. Control reactions were conducted with heat-inactivated enzymes at boiling point, for 15 minutes. Enzymatic activity was monitored spectrophotometrically, using a microplate reader, by recording the absorption spectra of each reaction at regular intervals and measuring the decrease in absorbance of each substrate. Oxidation of Mn^{2+} was monitored at 238 and 270 nm. The following molar extinction coefficients (ε) were used to compute specific activity: ferulic acid ε_{310nm} = 15.000 M^{-1} cm^{-1}, caffeic acid ε_{310nm} = 14.000 M^{-1} cm^{-1}, syringic acid ε_{265nm} = 8.800 M^{-1} cm^{-1}, vanillic acid ε_{285nm} = 5.800 M^{-1} cm^{-1}, pyrogallol ε_{265nm} = 2.640 M^{-1} cm^{-1}, CR ε_{492nm} = 33.000 M^{-1} cm^{-1}, EB 605 nm ε_{605nm} = 86.000 M^{-1} cm^{-1}, OG ε_{476nm} = 20.900 M^{-1} cm^{-1}, CV ε_{590nm} = 75.800 M^{-1} cm^{-1}, RB ε_{554nm} = 106.000 M^{-1} cm^{-1}, RBBR 595 nm ε_{595nm} = 8.270 M^{-1} cm^{-1}. For each substrate, (ε) values indicated above were identified spectrophotometrically at the corresponding λmax. One unit of enzyme activity (U) was defined as the amount of enzyme that oxidizes 1 μmol of substrate per minute. Specific activity (U/mg) was expressed as units of activity per milligram of protein.

2.2.2.10 Lignin decomposition assay

The ligninolytic activity of enzymes CopA and DypB was evaluated on solubilized lignin from alkali pretreated corn stover prepared as outlined in § 2.2.1.5. Enzymatic assays for lignin decomposition were initially standardized with different amounts of lignin substrate and enzyme. The effect of copper and peroxide concentration on the assay was also examined. The standard lignin assays were subsequently conducted with alkali lignin from corn stover at a concentration range of 1-20 mM (assuming carbon accounts for 50% of lignin's molecular mass), in 100 mM phosphate buffer pH 6.0, with 0.5 mM $CuCl_2$ for CopA, or 25 mM H_2O_2 for DypB, with the total volume kept at 1.0 mL, in the presence or not of 1.25 mM ABTS as mediator. Synergism between the two enzymes was assayed by adding the enzymes in tandem or successively after one of incubation with the first enzyme, using the reaction conditions stated above, in the absence of ABTS. Reactions were incubated at 30 °C for 24-48 h, under agitation, in the dark. Control reactions were performed with heat-inactivated enzyme at boiling point for 15 min. Samples were withdrawn at regular intervals, filtered through a 0.45 μm PVDF filter and stored at -20 °C. Reactions were analyzed by reverse-phase HPLC by initially trying different columns, solvents and elution methods to standardize the method of analysis. Standard analysis was then performed in a C18 reverse-phase column (Discovery Bio Wide Pore C18, 25 cm x 4.6 mm, 5 μm, Sigma-Aldrich), at 310 nm, at a flow rate of 1.0 mL/min using Buffer (A): 5% MeOH, 0.05% H_3PO_4, Milli-Q water, and Buffer (B): 100% MeOH, with a gradient elution method as follows (Buffer A-B percentage): 100–0% for 5 min, 70–30% for 25 min, 0–100% for 30 min, 0–100% for 10 min, 100–0% for 5 min, giving a total time of 75 min per run.

2.2.3 Identification of enzymes and pathways involved in degradation of lignin and lignin-derived aromatic compounds by proteomic analysis

2.2.3.1 Genome sequencing of strain *Pseudomonas kilonensis* ZKA7

Strain *Pseudomonas kilonensis* ZKA7 was chosen for a comparative proteomic analysis, to identify proteins and pathways involved in lignin and lignin-derived monoaromatic compounds' decomposition. To aid the identification of proteins the genome of this strain was extracted and sequenced. Genomic DNA was isolated using the JGI CTAB protocol for bacterial genomic DNA isolation (William *et al.*, 2012). DNA sample quality was initially verified by electrophoresis on a 0.8% agarose gel using the Lambda DNA – HindIII Digest Ladder (fragments size range 125 – 23.130 bp), to ensure that DNA fragments were not

heavily degraded and to assess the degree of the samples purity. DNA concentration and purity was also assessed by measuring the absorbance of samples at 260 nm, 280 nm, 230 nm, in a microplate reader. Prior to shipping the sample for sequencing, the 16S rRNA gene was amplified by PCR, as described in § 2.2.1.3, and sequenced. The draft genome of the strain was generated at the DOE Joint Genome Institute (JGI) using the Pacific Biosciences (PacBio) sequencing technology (Eid et al. 2008). A >10kpb Pacbio SMRTbellTM library was constructed and sequenced on the PacBio RS2 platform, which generated 122,954 filtered subreads totaling 638,444,966 bp. All general aspects of library construction and sequencing performed at the JGI can be found at http://www.jgi.doe.gov. The raw reads were assembled using HGAP (smartanalysis/2.3.0 p5, HGAP 3) Chin *et al.* (2013). Structural and functional annotation was performed using the DOE-JGI Microbial Genome Annotation Pipeline (MGAP v.4) (Huntemann *et al.*, 2015). Annotation and analysis of genome were also performed by RAST (Rapid Annotations using Subsystems Technology) (Aziz *et al.*, 2008).

2.2.3.2 Growth of strain *Pseudomonas kilonensis* ZKA7 on selected substrates

The growth curve of strain *Pseudomonas kilonensis* ZKA7 for each substrate selected for proteomic analysis was obtained as follows: Strain ZKA7 was inoculated into a nutrient agar plate and grown at 30 °C, overnight. The plate was flooded with PBS and cells were harvested by scraping. The cell suspension was used for the inoculation of 25 mL liquid cultures of MSM medium, supplemented with one of the following carbon sources, in the corresponding concentration of Total Organic Carbon (g L^{-1}): corn stover lignin hydrolysate (1.5), prepared as described in § 2.2.1.5, ferulic acid (1.0), caffeic acid (1.0), vanillic acid (1.0) or acetate (0.5) (reference substrate). Each final medium was supplemented with trace elements and vitamins, and pH was adjusted to 6.5. The inoculum volume was adjusted in order to achieve a 0.2 initial optical density in the culture and cultures for each medium were conducted in duplicates. Cultures were incubated at 30 °C on a rotary shaker at 180 rpm for 48 h and samples were withdrawn at regular intervals for determining the optical density in a spectrophotometer (600 nm).

2.2.3.3 Trial concentration of extracellular protein fractions from lignin cultures

We performed different protocols in order to establish the concentration method that would be used for concentrating the extracellular protein fractions derived from lignin cultures. Among

the methods tried were: TCA / acetone precipitation, Chloroform / methanol precipitation, ultrafiltration with ultrafiltration devices with a cut-off limit of 3.000 Da. The challenge that arose was that all methods used caused the precipitation or the accumulation of lignin that was previously solubilized in the hydrolysate. This fact rendered impossible the further assessment of the protein content of the samples. Most importantly SDS-PAGE was not possible, since the samples did not enter into the separating gel under all conditions examined. Therefore, the extracellular protein fractions from lignin cultures were excluded from the proteomic analysis.

2.2.3.4 Preparation of samples for proteomic analysis

A single colony of *Pseudomonas kilonensis* ZKA7 was transferred from NA plates to 10 mL liquid precultures of MSM containing CSLH, ferulic acid, caffeic acid, vanillic acid or acetate as sole carbon sources, prepared as described in § 2.2.3.2. Precultures were incubated at 30 °C, at 180 rpm until middle exponential phase and then 1 mL was transferred to 10 mL of fresh corresponding medium (2nd preculture). The transfer to fresh medium was repeated twice. The 3rd preculture was used for the preparation of the inoculum to be used for the inoculation of 150 mL of final cultures of each corresponding medium, in three replicates. Cultures were incubated at 30 °C, at 180 rpm until middle-late exponential phase and harvested for proteomic analysis.

Cells were used for the analysis of intracellular proteins and were pelleted by centrifugation at 4.000 rpm for 20 minutes. Cultures' supernatants were collected for the analysis of extracellular proteins and were filter sterilized in 0.2 μm filters and stored in 4 °C until further treatment. Cells were washed three times and resuspended in a lysis buffer containing 100 mM Tris, 5 mM MgCl$_2$, pH 7.5. Protease inhibitor PMSF was added at a final concentration of 0.5 mM and cells were disrupted by sonication in an ice bath until complete lysis. After cell lysis, samples were centrifuged at 11.000 rpm, at 4 °C, for 30 minutes and the supernatant was collected. Both intracellular and extracellular protein fractions were concentrated using ultrafiltration devices with a 3.0 KDa molecular mass cutoff (Merck Millipore) and diluted in a protein storage buffer having a final concentration 125 mM Tris – HCl (pH 6.8), 3 mM DTT and 25% (v/v) glycerol. Protein samples were stored at -20 °C until further treatment. Protein quantitation of samples was conducted by the Bradford method at all preparation stages.

In order for the protein samples to be stable during their transport to the University of Newcastle, they were loaded and stored onto a denaturating electrophoresis gel as follows: 50μg of each concentrated protein sample were mixed with SDS-PAGE loading buffer and subjected to SDS polyacrylamide gel electrophoresis on a 12% polyacrylamide gel. For each

replicate of protein sample, two or three technical replications were loaded onto the gel. Electrophoresis was performed until protein samples had traveled for approximately 1 cm onto the separating gel. Protein bands were visualized with SDS- PAGE staining buffer, after 30 min of staining, and overnight destaining in SDS- PAGE destaining buffer. A gel slice bearing all the protein bands was cut from each lane by using a sterile razor blade. Gel slices were stored in eppendorfs at 4 °C, with the addition of 30-50 µL of sterile distilled water until their transport to the University of Newcastle for proteomic analysis.

2.2.3.5 Proteomic Analysis

In Gel Digestion of protein samples

SDS PAGE protein bands were excised with a clean scalpel (wiped with lint-free tissue after each cut). Each band was diced into 1x1x1 mm cubes and transferred to a clean microcentrifuge tube. Gel pieces were destained by the excess addition of a destaining buffer containing 50 mM ammonium bicarbonate and 50% (v/v) Acetonitrile. The destaining buffer was removed and exchanged 3 times, or until the gel pieces were clear. A molecular weight marker band was also excised as a digest control. Proteins were reduced with 10 mM DDT for 30 min at 60 °C to break disulphide bridges. This was followed by alkylation with 50 mM iodoacetamide for 30 min at room temperature in the dark to prevent disulphide reformation. Gel pieces were washed in 50 mM ammonium bicarbonate and then dehydrated with 3 washes of 100 µL of acetonitrile. Residual moisture was removed from gel pieces in a vacuum drier. Proteins were digested by the addition of trypsin added at a ratio of 30:1 (protein: trypsin), buffered with 50 mM ammonium bicarbonate and incubated for 16 hours at 37 °C. The digest was stopped by the addition of 10% trifluoroacetic acid (TFA) to a final concentration of 0.5%, shaken for 30mins, at 750 rpm. The liquid containing hydrophilic peptides was transferred to a fresh microcentrifuge tube. 80% Acetonitrile with 2% TFA was then added to the gel pieces and shaken for 30 min at 750rpm. This dehydrates the gel pieces and removes hydrophobic peptides from the gel. The solution containing hydrophobic peptides was pooled with the hydrophilic peptide mix. The peptide solution was dried in a centrifugal evaporator, peptides were dissolved in 3% acetonitrile, 0.1% TFA. The resulting peptide solutions were desalted using home packed C18 stage tips (REF BELOW). The sample was dissolved in 50 µL of 3% acetonitrile, 0.1% TFA giving the final concentration of ~1µg/µL.

NanoLC-MS/MS

1 µg of a protein digest was separated with a 97 min. nonlinear gradient (3-40%, 0.1% formic acid) using an UltiMate 3000 RSLCnano HPLC. Samples were first loaded onto a 300µm x 5mm C18 PepMap C18 trap cartridge in 0.1% formic acid at 5 µl/min and passed on to an in house made 75µmx25cm C18 column (ReproSil-Pur Basic-C18-HD, 3 µm, Dr. Maisch GmbH) at 400nl/min. The eluent was directed to an Ab-Sciex TripleTOF 6600 mass spectrometer through the AB-Sciex Nano-Spray 3 source, fitted with a New Objective FS360-20-10 emitter. For data-dependent data acquisition (DDA), MS1 data were acquired within a range of 400-1250m/z (250ms accumulation time), followed by MS2 of Top 30 precursors with charge states between 2 and 5 (total cycle time 1.8s). Product ion spectra (50ms accumulation time) were acquired within a range of 100-1500m/z, using rolling collision energy for precursors that exceed 150 cps. Precursor ions were excluded for 15s after one occurrence.

For Data Independent Acquisition (SWATH) MS1 data was acquired over a range of 400-800 m/z. The same m/z range was then covered with 83 variable SWATH windows, with a minimum size of 4Da. To calculate this, a DDA file was taken at random, and all MS1 data averaged into a single spectrum. The ion current was then divided into variable bins containing roughly the same number of precursors. https://sciex.com/support/knowledge-base-articles/how-to-use-the-swath-variable-calculator-excel-sheet (areas of low ion intensity have wider windows and vice versa). Windows were overlapped by 0.5 Da to avoid losing data at the edges of a window. Ions were accumulated for 250ms in MS1. Each SWATH window was accumulated for 25 ms (high sensitivity mode) giving a total duty cycle of 2.325 s. SWATH and DDA were acquired with identical chromatography settings. This maximized the reproducibility of the data and improved spectral library matching of SWATH data.

The acquired DDA data were searched against the protein sequence database available from Uniprot Database (https://www.uniprot.org/), concatenated to the Common Repository for Adventitious Proteins v.2012.01.01 (cRAP, ftp://ftp.thegpm.org/fasta/cRAP), using ProteinPilot (AbSciex, v5, parameters used: cysteine alkylation: iodoacetamide, digestion enzyme: trypsin, Parent Mass Error of 20ppm, fragment mass error of 30ppm). The individual search results were exported (using PeakView 2.2), in a spectral library format, as *.tsv files. The confidence cut-off representative to FDR<0.01 was applied to the search result file.

SWATH data processing

All 36 SWATH data files were imported to PeakView2.1 SWATHmicroApp, along with the.tsv spectral library. Firstly, data from the spectral library were aligned to the SWATH data by chromatographic retention. This was done by manual selection of 50 peptides throughout the gradient. Each peptide had to be present in each SWATH file in addition to having an intensity greater than 1e4. SWATH data was processed with the following settings: Number of transitions per peptide: 6, Peptide confidence threshold: 99%, False discovery rate: 1.0%, XIC width: 50ppm. Data was exported in .txt format. Text files were then uploaded to Perseus v1.6.2.3 for further manipulation.

2.2.3.6 Differential expression analysis

Raw data were analyzed using the Perseus software. Statistical analysis for intracellular and extracellular samples was performed separately. Data were Log2 transformed and filtering of rows (proteins) was conducted based on valid values. Sample correlation and inspection of data quality were performed with histograms, Pearson correlation and PCA. Normalization was implemented by Z-score, by column (condition) using the median. Data quality was visualized with histograms. Student's T-tests were performed with FDR=0.01, and 250 randomizations. Post-hoc tests on significant differentially expressed proteins (DEPs) were performed with FDR=0.01. Enrichment analysis (fisher's exact test) for DEPs was performed with Blast2GO.

2.2.4 Genomic sequencing of lignin-degrading bacterial strains

Along with the genome of *Pseudomonas kilonensis* ZKA7, the genomes of 14 more strains of this study, able to grow on lignin or lignin-derived aromatic compounds were sequenced for a future comparative genomic analysis of lignin-degrading bacterial strains. Selected strains were *Pseudomonas* sp. ZKA3, *Pseudomonas* sp. ZKA3, *Pseudomonas* sp. ZKA12, *Cellulomonas* sp. ZKA19, *Cellulosimicrobium* sp. ZKA21, *Rhodococcus* sp. ZKA33, *Pseudomonas* sp. ZKA37, *Pseudomonas* sp. ZKA39, *Stenotrophomonas* sp. ZKA40, *Cellulosimicrobium* sp. ZKA48, *Rhodococcus* sp. ZKA49, *Pseudomonas* sp. ZKA50, *Pseudomonas* sp. ZKA55. Genomic DNA was isolated following the procedure described in §2.2.3.1.

Chapter 3

Results and discussion

3.1 Identification and phylogenetic analysis of bacterial strains isolated from enrichment cultures

An enrichment strategy based on organosolv lignin, xylan from birchwood and amorphous cellulose, as sole carbon and energy sources was used to isolate aerobic, mesophilic bacteria from five uniformly distributed soil samples of Keri Lake, in Zakynthos Island (Appendix Figure A1). The area is dominated by a marsh mainly composed of reeds, with increased biomass degradation, where, in parallel, asphalt springs release crude oil for more than 2.500 years. Previously reported hydrocarbon analyses of surface oil samples from the study area showed an increased content in aromatic hydrocarbons (Palacas *et al.*, 1986, Pasadakis *et al.*, 2016). Our approach was based on the assumption that these characteristics create a unique habitat where indigenous microbial populations are able to use lignin-derived aromatic compounds from plant biomass as their sole carbon and energy source and that they can withstand high concentrations of aromatics derived from lignin and aromatic hydrocarbons from oil. In addition, the long term presence of decaying biomass may favor the selection of microbes that harbor a complete set of highly expressed hydrolytic enzymes towards cellulose and hemicelluloses.

A total of 63 colonies were isolated from enrichment cultures of all five soil samples, named ZKA1 to ZKA63. All isolates were deposited at Athens University Bacterial & Archaea Culture Collection (ATHUBA) under the Accession numbers ATHUBa1401 to ATHUBa1463 (http://m-biotech.biol.uoa.gr/ATHUBintex.html). Among them, 19 were isolated from lignin, 23 from xylan and 21 from cellulose enrichment cultures. Solid media were dominated by bacteria while fungal colonies were scarcely observed. Characterization of the 16S rRNA gene of all the isolates generated 24 different genera. All isolates shared >97% identity with their closest counterparts (Appendix Table A1), and their 16S rRNA sequences were deposited in GenBank database (Accession numbers: MT683172 to MT683234).

16S rRNA gene sequences of the isolates and their related strains were used to generate a maximum-likelihood phylogenetic tree (Figure 24). The three main clusters formed by Bacteroidetes phylum, Firmicutes-Actinobacteria phyla and Proteobacteria phylum were differentiated into subclusters of Flavobacteria and Sphingobacteriia classes, Actinobacteria and Bacilli classes, gamma-beta (γ-β) and alphaproteobacteria classes, respectively, indicated by high bootstrap values of branching points (100%).

Fig. 24. Phylogenetic tree from maximum likelihood analysis of 16S rRNA gene of Keri Lake isolates and their most similar GenBank sequences. Distance matrices were calculated by the Jukes-Cantor model. Bootstrap values expressed as percentages of 1000 replications are shown at the branch points. Colored circles indicate the origin of the bacterial strains according to the substrate used as sole carbon and energy source in enrichment cultures; purple: organosolv lignin isolates, yellow: birchwood xylan isolates, green: carboxymethyl-cellulose isolates.

Strains of the gamma class primarily belonged to the *Pseudomonas* genus, though the sequence analysis could not reliably distinguish their species. This fact is consistent with previous studies, reporting that phylogenetic affiliation of pseudomonads based on 16S rRNA gene alone can generate misclassifications (Moore *et al.*, 1996). Thus, further analysis of more housekeeping genes is required to correctly assign these strains. Two isolates, ZKA22

92

and ZKA40, though identified as *Stenotrophomonas* species (belonging to γ-proteobacteria), clustered in the class of β-proteobacteria. Similarly, the xanthomonads group, from which some strains were later reclassified as stenotrophomonads, was previously reported to cluster either to beta- or gamma-proteobacteria, depending on the treeing algorithm and the number of rDNA sequences included (Dworkin *et al.*, 2006). Strains ZKA1, ZKA2, ZKA8, ZKA22, ZKA36, ZKA38 and ZKA47 were excluded from further experiments due to the opportunistic pathogenicity of their closest counterparts, based on their 16S rRNA sequence.

Several ecosystems naturally exposed to oil are known in Western Greece, nonetheless, to our knowledge, this is the first report on the isolation of microorganisms from one such. Soil samples from Keri Lake were characterized by the presence of oil and heavily decomposed plant material. It is common for soil habitats, such as those with high phenolic content or those with increased biomass decay, to host microbes that have developed resistance and the ability to utilize the respective compounds. In fact, a metagenomic analysis on up to three-meter depth sediments from oil-exposed sites in Keri area identified an abundance of genes involved in the anaerobic degradation of phenolic compounds (Michas et al., 2017). Despite the limitations introduced by the enrichment technique, the number of different bacterial genera encountered was high, possibly reflecting the rich microbial diversity of Keri area ecosystem.

3.2 Distribution of genera based on the enrichment carbon source

The results revealed a distinct distribution of strains isolated from lignin enrichments mainly among gamma- and secondarily among beta-proteobacteria. Lignin enriched isolates were dominated by pseudomonads, followed by *Achromobacter* spp. and *Bordetella* spp. (Figure 25). A more complex bacterial diversity was detected among strains enriched in xylan and CMC cultures. Strains belonging to the class of Actinobacteria, alpha-Proteobacteria, Bacilli, Sphingobacteriia and Flavobacteria were exclusively encountered in these substrates, accompanied by members of the gamma- and beta-Proteobacteria. *Microbacterium* was the most representative genus in xylan enrichment cultures, followed by *Sphingobacterium*, *Cellulosimicrobium*, *Paracandidimonas* and *Sphingobium*. Strains of the genera *Pseudomonas*, *Enterobacter*, *Klebsiella*, *Stenotrophomonas*, *Bordetella*, *Advenella*, *Ochrobactrum*, *Shinella*, *Sphingomonas* and *Cellulomonas* were equally abundant among xylan isolates. Strains enriched in CMC cultures were dominated by *Pseudomonas*, *Bacillus*, *Microbacterium* and *Rhodococcus* species. Members of the genera *Alcanivorax*, *Advenella*,

Paracoccus, *Ancylobacter*, *Fictibacillus*, *Sinomicrobium* and *Parapedobacter* were also recovered from CMC cultures.
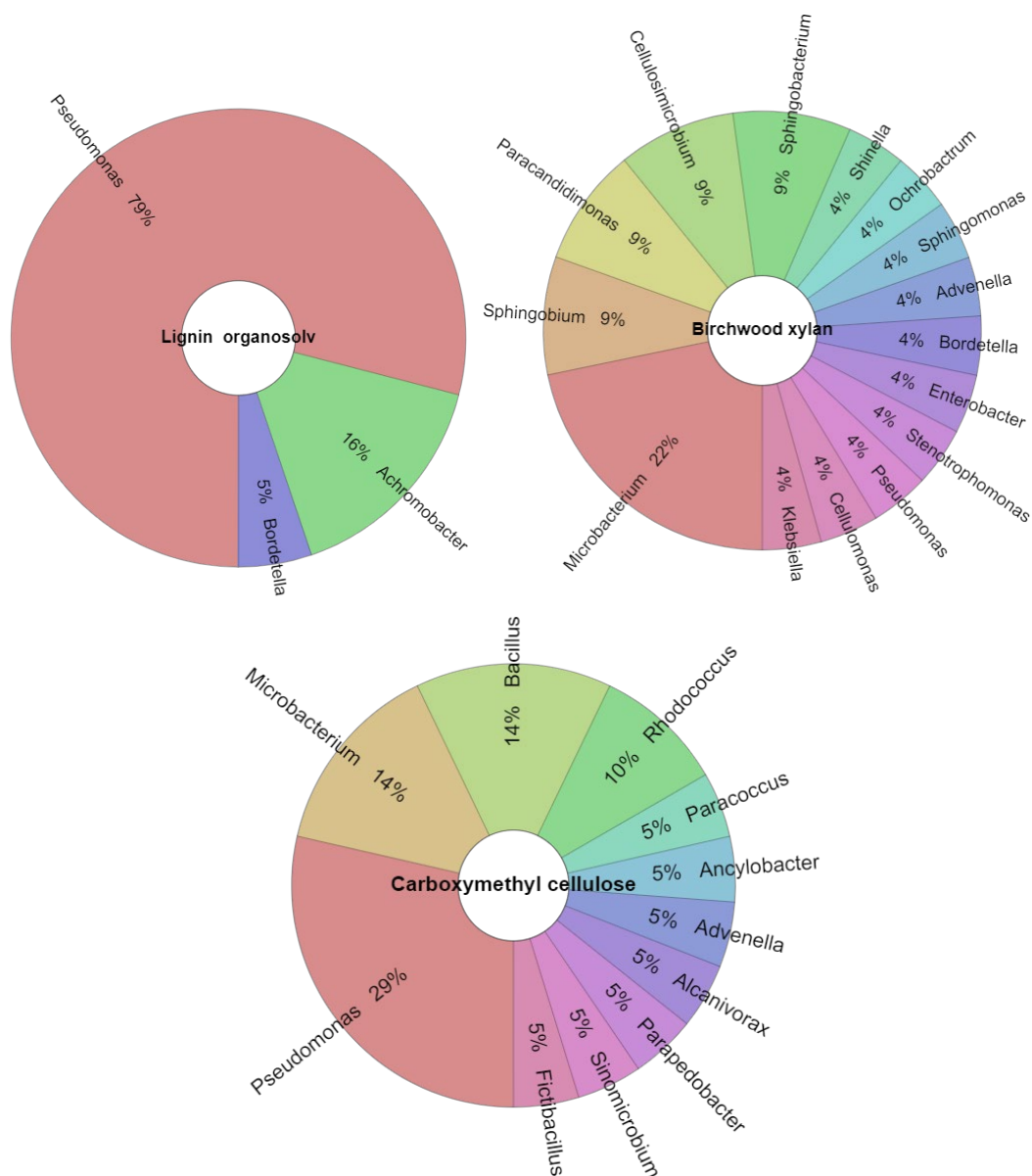
Fig. 25. Substrate distribution of bacterial genera enriched from Keri Lake.

Bacteria belonging to the Proteobacteria phylum are commonly isolated from lignin and lignin model compounds enrichment studies (Brink *et al.*, 2019). Among them, many strains fall into the *Pseudomonas* genus, as reported by several studies (Bandounas *et al.*, 2011, Hirose *et al.*, 2013, Ravi *et al.*, 2017). Although it is difficult to discriminate between the numerically abundant strains in the natural environment and strains that display opportunistic traits in the enrichment cultures, *Pseudomonas* species are indeed widespread in soil, rhizosphere, aquatic habitats and areas polluted with man-made and natural toxic chemicals

(Jiménez *et al.*, 2010). Large sets of unique catabolic genes for a wide range of substrates, transporters, regulators and stress response systems are features accounting for the great metabolic versatility and adaptability to diverse environmental conditions of members of this genus (Dos Santos *et al.*, 2004).

The organosolv pretreatment of lignocellulosic feedstocks constitutes an alternative chemical process of delignification, with the use of organic solvents or their aqueous solutions. Lignin recovered by this method is relatively purer compared to other technical lignins, due to its sulfur-free structure, and lower ash and carbohydrate content (Zhao *et al.*, 2009). However, the high phenolic content of such industrial byproducts can disrupt microorganisms' cell membranes and threaten the cells' viability (Murinova and Dercova, 2014). Although the effect of organosolv pretreatment on the valorization of sugars, and the use of lignin as fuel or as a precursor for chemicals have been extensively studied (Zhao *et al.*, 2009, de la Torre *et al.*, 2013), little is known about the microbial utilization of organosolv lignin. There is only one report on the bacterial utilization of effluents obtained from organosolv pretreatment of pine, enriched with degraded oligosaccharides and lignin, by the oleaginous soil bacterium *Rhodococcus opacus* DSM 1069 (Wells *et al.*, 2015). Here we report the isolation of several bacterial strains from organosolv lignin cultures, containing no supplementary carbon sources. Further assessment of these strains in pure cultures on organosolv lignin will be provided in the following text.

Xylan is the major component of hemicelluloses, contributing over 70% of their structure. Similar to our findings, commonly reported bacteria that produce xylanases include members of genera such as *Bacillus*, *Cellulomonas*, *Micrococcus*, *Staphylococcus*, *Paenibacillus*, *Arthrobacter*, *Microbacterium*, *Rhodothermus* and *Streptomyces* (Chakdar *et al.*, 2016). CMC is an artificial, amorphous and soluble form of cellulose, whose depolymerization is correlated with endo-1,4-β-glucanases and β-glucosidases. Its depolymerization is a prerequisite but not proof of native, crystalline cellulose decomposition that involves exoglycolytic activity, too, a trait of real cellulose degraders (Koeck *et al.*, 2014). However, bacteria enriched in this study have been repeatedly isolated as truly cellulolytic, such as members of the genera *Cellulomonas*, *Bacillus*, *Pseudomonas*, *Streptomyces*, *Micromonospora*, *Rhizobium*, *Sphingomonas*, *Ochrobactrum*, *Arthrobacter*, *Alcaligenes* and *Serratia* (McDonald *et al.*, 2012). Detailed evidence of individual isolates' ability to express cellulolytic and hemicellulolytic activities is provided in the screening test outlined below.

3.3 Cellulose and xylan hydrolytic activity of individual bacterial isolates

To further assess their activity against plant polysaccharides all strains were subsequently grown on plates with CMC amorphous cellulose, Avicel microcrystalline cellulose or xylan from birchwood, as sole carbon sources, and were subjected to the Congo red assay for qualitative observation of hydrolase activity. In most cases, three to five days were required for the strains to grow on the substrates and express the corresponding glycoside hydrolase (GH) activity. Almost half of the isolates, regardless of their origin in enrichment cultures, could sufficiently grow on all three carbon sources and produced hydrolysis zones after staining with Congo red (Figure 26).

Degradation of CMC indicates the combined activity of endo-1,4-β-glucanases (EC 3.2.1.4), enzymes that randomly hydrolyze internal bonds of amorphous regions of cellulose, generating new ends, with activity of β-glucosidases (EC 3.2.1.21), enzymes that hydrolyze cellodextrins and cellobiose to glucose. Avicel is a form of insoluble microcrystalline cellulose, with a lower molecular mass and relatively low accessibility. Hydrolysis zones on Avicel agar plates provide evidence of exoglycolytic enzyme activity. Exoglucanases (or Avicelases) act on the reducing (EC 3.2.1.176) or nonreducing (EC 3.2.1.91) chain ends of cellulose, releasing cellobiose or glucose as main products. Clearing zones around colonies on xylan agar plates treated with Congo Red that specifically binds to β-1,4 glycosidic linkages, are indicative of endo-β-1,4-xylanases (EC 3.2.1.8) that release xylooligomers from the xylan backbone and β-xylosidases (EC 3.2.1.37) that further hydrolyze oligomers to xylose.

Strains *Cellulomonas* sp. ZKA19, *Cellulosimicrobium* spp. ZKA17 and ZKA48, *Sphingobacterium* sp. ZKA44, *Klebsiella* sp. ZKA20, *Microbacterium* spp. ZKA15, ZKA21, ZKA30 and ZKA43, and *Bacillus* spp. ZKA58 and ZKA60 showed the ability to deconstruct all three substrates tested. The broad substrate hydrolyzing phenotype was also observed in strains ZKA6, ZKA9, ZKA10, ZKA11, ZKA37, ZKA41 and ZKA55, members of the genus *Pseudomonas*. Strains *Advenella* sp. ZKA31, *Fictibacillus* sp. ZKA59, *Ochrobactrum* sp. ZKA24, *Paracoccus* sp. ZKA29, *Parapedobacter* sp. ZKA34 and *Shinella* sp. ZKA23 could also target all three substrates tested. Strains *Enterobacter* sp. ZKA62, *Rhodococcus* sp. ZKA 33 and *Sphingobium* sp. ZKA14 and ZKA25 could process both CMC and xylan, but not Avicel cellulose. Strains *Bordetella* sp. ZKA4 and ZKA45 could process CMC and xylan too. Strains *Alcanivorax* sp. ZKA52 and *Ancylobacter* sp. ZKA53 could only hydrolyze CMC.

Strains *Paracandidimonas* sp. ZKA16 and ZKA18 could only utilize xylan. *Sinomicrobium* sp. ZKA54 could only hydrolyze CMC.
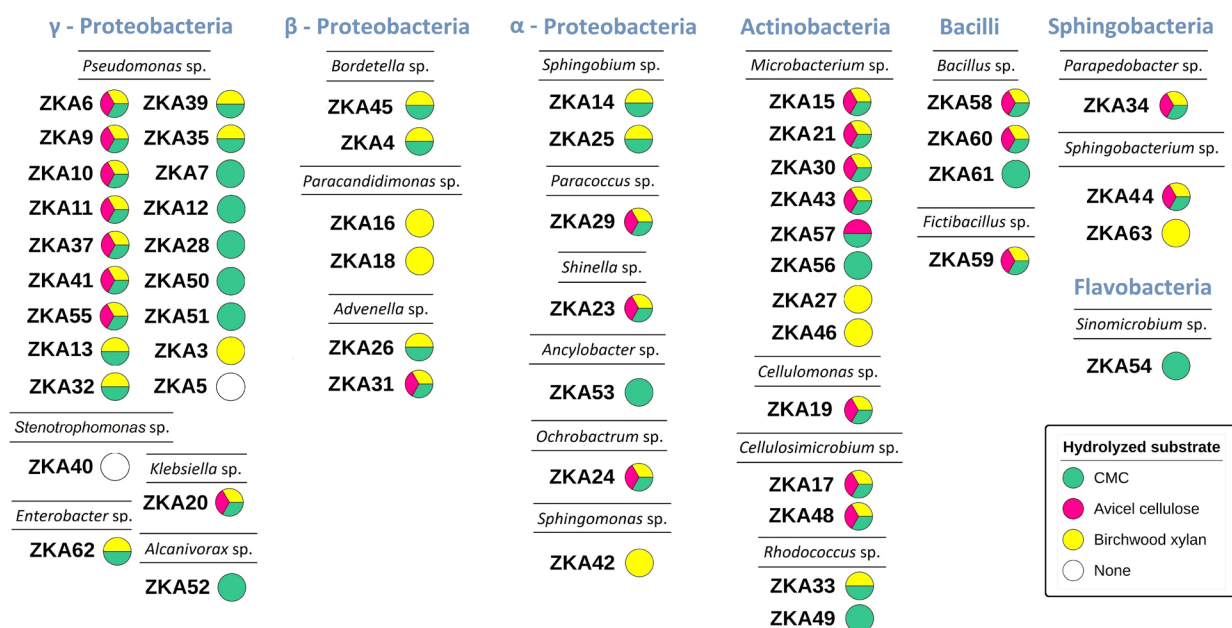
Fig. 26. Glycoside hydrolase activity of bacterial isolates, as indicated by the Congo red assay. Colored circles indicate the presence of hydrolysis zones produced by bacterial cells on plates of amorphous CMC cellulose (green color), Avicel microcrystalline cellulose (red color) or birchwood xylan (yellow color), used as sole carbon sources. Uncolored circles indicate lack of ability to grow on either of these substrates.

Cellulases and xylanases are important components of enzyme cocktails for the biorefining of lignocellulosic biomass. Many available commercial cocktails have inadequate glucosidase and xylanase activities, and also require a stronger activity of xylosidases, too, to prevent end-product inhibition (Dumon *et al.*, 2012). Mesophilic representatives of some of the above genera have been shown to produce GHs with remarkable properties, such as a β-xylosidase from *Cellulomonas fimi* with high activity at 100°C and strong alkaline pH (Kane and French, 2018). A halotolerant endoglucanase from *Bacillus subtilis* BEC-1 showed maximum activity at 60 °C and high activity in the pH range 3-7 (Zhu *et al.*, 2011). A GH10 xylanase from *Cellulosimicrobium* sp. HY-12 and an alkali-tolerant GH10 xylanase from *Microbacterium trichothecenolyticum* HY-17 showed their optimum activity at 60°C, as well (Oh *et al.*, 2008, Kim *et al.*, 2014).

The reports on characterized hydrolases showing experimental cellulolytic or xylanolytic activity for most of the genera of this study are scarce, according to data available in the Carbohydrate Active Enzymes database (CAZy) (Lombard *et al.*, 2014). Some isolates, belonging to *Pseudomonas*, *Advenella*, *Fictibacillus*, *Ochrobactrum*, *Paracoccus* and *Shinella* genera showed multienzymatic activity although their relatives, according to CAZy database,

contain on average few GHs per genome. The above results suggest that certain isolates of Keri Lake may have distinctive potential for processing plant cell-wall poly- and oligosaccharides. Other genera, such as *Parapedobacter*, *Paracandidimonas* and *Sinomicrobium* had no entries in CAZy database, also reflecting the low number of cultivated representatives. Quantitative estimation of the enzymes' hydrolyzing activity and characterization of their properties would further evaluate their industrial potential. However, from this point forward, we decided to focus our efforts on studying the strains' oxidative activity towards lignin since literature on lignin biodegradation was less mature than plant polysaccharide hydrolysis.

3.4 Characterization of lignin hydrolysates prepared from alkali pretreated plant biomass

A weak aqueous solution of sodium hydroxide was used for the alkaline pretreatment of corn stover and wheat straw, in order to prepare a lignin substrate to be used for further screening of bacterial isolates (Figure 27). Residual carbohydrates were almost eliminated in the resulting lignin hydrolysates (black liquor), as indicated by the very low sugar content. The corn stover lignin hydrolysate (CSLH) contained 50.1 g/L dissolved solids, of which 24.1 g/L amounted to total organic carbon and 0.41 g/L to total inorganic carbon. The wheat straw lignin hydrolysate (WSLH) contained 43.5 g/L dissolved solids of which 22.7 g/L amounted to total organic carbon and 0.47 g/L to total inorganic carbon. Total nitrogen was equal to 0.56 g/L and 0.32 g/L for CSLH and WSLH respectively.
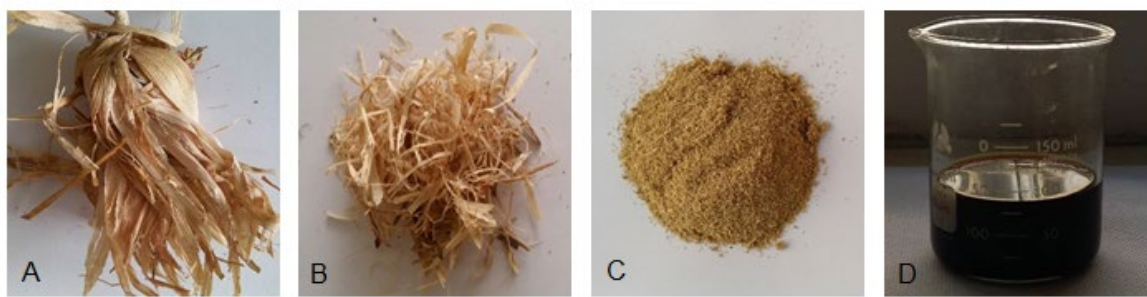
Fig. 27. Isolation of lignin from agricultural residues using an alkaline pretreatment method. Raw materials (A) were air-dried and subjected to mechanical treatment, involving homogenization in a mixer (B) and grinding through a sieve-mill (C). An aqueous solution (10% w/v) of the milled material was heated at 90 °C for 30 minutes, to remove impurities, followed by a thorough washing on a sieve using tap and distilled water. The washed solid material was dried at 50 °C, until constant weight. Alkaline pretreatment was carried out by adding 0.1 g NaOH per gram of dry biomass, in an aqueous solution, at a solid-liquid mass ratio of 1:6. The slurry was heated at 95 °C for 3 hours, under continuous stirring. The final solution was filtered through a 160 μm sieve to separate the black liquor of solubilized lignin (D) from the solid residues of plant material.

Spectra of both lignin hydrolysates obtained by ^{1}H NMR are shown in Figure 28. Although resonances in lignin spectra may shift depending on conditions or solvents chosen, the presence of typical lignin resonances can be observed (Li and Lundquist, 1994, Seca *et al.*, 2000, She *et al.*, 2010). A non-exhaustive list of signal assignments of lignin structures based on literature data is shown in Table 8.

A peak at 8.4 ppm in the ^{1}H NMR spectra may be assigned to phenolic hydroxyl groups. Signals around 6.4 and 6.9 ppm can be attributed to aromatic protons in syringylpropane (S) and guaicylpropane (G) units respectively. The signal at 6.9 ppm in both substrates is more intense than the signal at 6.5 ppm suggesting that guaiacyl units are more abundant than syringyl units. Signals around 7.4-7.6 ppm are typically assigned to aromatic protons located in positions 2 and 6 in structures containing a carbonyl $C\alpha=O$ group, to aromatic protons in positions 2 and 6 of p-hydroxyphenyl (H) units conjugated with a double bond, to protons in $C\alpha=C\beta$ structures, and aromatic protons in p-coumaric and ferulic acids. A strong signal at 5.4 ppm found in CSLH, less discernible in WSLH, could be assigned to aliphatic H_α protons in dimers containing β-5 bonds, suggesting that structures like phenylcoumaran may be present in CSLH. The broad peak at 4.8 ppm belongs to deuterated water. Signals at 4.6 ppm could be attributed to aliphatic H_β protons of residual β-O-4 structures. Signals in the region 3.5-4.4 ppm can be assigned to side-chain H_γ protons in aryl-glycerol units and methoxyl protons (-OCH$_3$). Signals around 2.6 ppm can be due to benzylic protons in β-β structures, such as resinol, and signals in the region 2.0-2.3 ppm can be assigned to aromatic and aliphatic acetate groups.
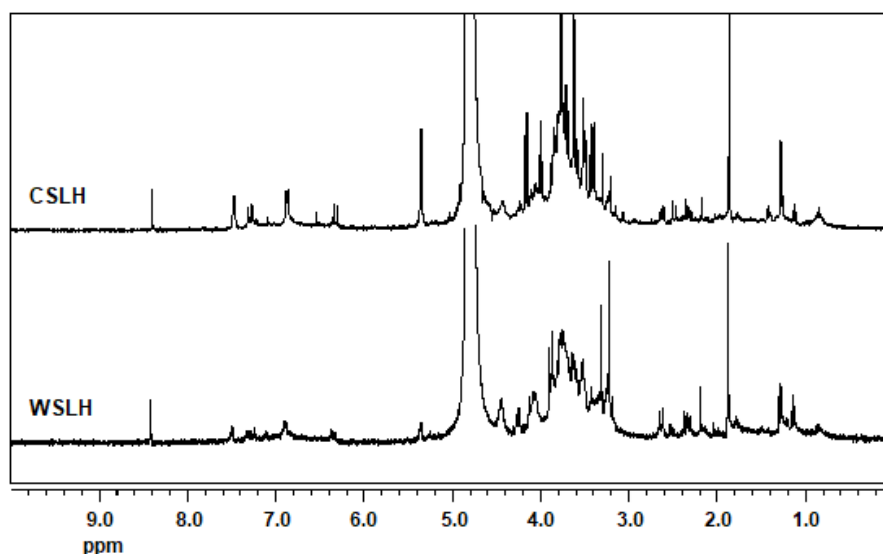
Fig. 28. ^{1}H NMR spectra of lignin hydrolysates obtained from alkali pretreated corn stover (CSLH) and wheat straw (WSLH). Samples were dissolved in D$_2$O and recorded on a Bruker DRX 400 MHz spectrometer, at 300 K.

Table 8. Signals observed in a typical ^{1}H NMR spectrum of lignin, based on literature data.

Probable assignment	δ ^{1}H NMR (ppm)
Carboxylic acid	11.0-14.0
formyl protons in benzaldehyde or cinnamaldehyde units	9.4-11.0
unsubstituted phenolic hydroxyl group protons	8.5-9.4
substituted phenolic hydroxyl group protons	8.0-8.5
▪ aromatic H$_2$ and H$_6$ protons in structures containing a carbonyl Cα=O group ▪ aromatic H$_2$ and H$_6$ protons in p-hydroxyphenyl (H) units conjugated with a double bond ▪ vinyl protons in Cα=Cβ structures ▪ aromatic protons in p-coumaric and ferulic acids	7.4-7.6
aromatic protons in guaicylpropane (G) units	7.0
aromatic protons in syringylpropane (S) units	6.5
aliphatic H$_α$ protons in β-O-4, β-5, β-β and β-1 structures	4.6-6.3
aliphatic H$_β$ protons in β-O-4 structures	4.2-4.6
aliphatic H$_γ$ protons in β-O-4, β-5 and β-β structures	4.2-4.4
methoxyl protons	3.7-3.8
aliphatic H$_β$ protons in β-β, β-5, β-1 structures	2.8-3.1
protons in β-β structures	2.6
Phenolic and aliphatic acetate groups	2.0-2.3
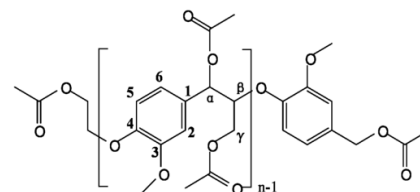
Alkaline pretreatment is a scalable, economically viable approach to isolate a lignin-enriched stream from intact lignocellulosic biomass and retain the majority of the polysaccharides in the residual solids for subsequent processing into biofuels (Salvachúa *et al.*, 2015). Corn stover and wheat straw constitute major crop residues in Greece, therefore they can serve as an abundant biomass feedstock for microbial bioconversion. The pretreatment conditions used in this study were chosen in terms of optimal yield of total sugars released by a commercial cellulase-hemicellulase cocktail, based on previous experiments in our laboratory, therefore provide a stream for parallel carbohydrate conversion into bioethanol.

During alkaline pretreatment the alkali labile lignin linkages, such as α- and β- aryl ethers, and glycosidic bonds in carbohydrates are disrupted, causing the dissolution and degradation of lignin and hemicelluloses with lower alkali stability (Chen *et al.*, 2013). Typically, lignin from Gramineae plants is highly soluble in alkali, leading to a high extraction yield of lignin in the hydrolysates, even with mild alkaline pretreatment conditions, essentially free of polysaccharides (Sun *et al.*, 1996). Consistent with the assignments made for lignin signals of this study is the fact that grass lignins are characterized mostly as guaicyl-type. The main substructures found in native corn stover and wheat straw lignin are β-O-4' alkylaryl ethers,

followed by lower amounts of phenylcoumarans, resinols and spirodienones. The presence of p-coumarates and ferulates in corn stover and wheat straw lignin has also been previously demonstrated (del Rio *et al.*, 2012, Sammons *et al.*, 2013, Min *et al.*, 2017). Further analysis would confirm the estimated assignments of proton NMR signals.

3.5 Bacterial growth studies on substrates of technical lignins

Certain strains were screened for their ability to grow on mineral salt medium supplemented with lignin hydrolysates from alkali pretreated corn stover or wheat straw, commercial Kraft lignin or commercial organosolv lignin, as sole carbon sources. Selected strains included lignin-enriched isolates, strains of Actinobacteria class, by reason of the numerous documented reports concerning degraders of lignin and lignin-derived compounds belonging to this class (Bugg *et al.*, 2011), and α-Proteobacteria since one of the best-characterized strains, known for its ability to degrade a plethora of lignin-derived compounds, *Sphingobium* sp. SYK-6, belongs to this class (Masai *et al.*, 2007). Strain *Pseudomonas putida* KT2440, known for its wide aromatic substrate – utilizing activity and its ability to grow in alkaline pretreatment liquors from corn stover (Linger *et al.*, 2014, Belda *et al.*, 2016, Ravi *et al.*, 2017) was used as a control strain.

Certain microbes exhibited sufficient growth in CSLH and WSLH, while for others growth levels were minor (Figure 29). The maximum optical density for most of the isolates that grew well in CSLH and WSLH was reached within 24 or 48 hours of incubation. No growth was observed in control samples inoculated with each strain, in the absence of a lignin carbon source. Higher growth levels in CSLH were obtained by *Pseudomonas kilonensis* ZKA7, followed by *Bordetella* sp. ZKA4, *Shinella* sp. ZKA23, *Cellulosimicrobium* spp. ZKA17 and ZKA48, *Microbacterium* sp. ZKA21, *Rhodococcus* spp. ZKA49 and ZKA33 and *Microbacterium* sp. ZKA46. Most of these strains exhibited higher growth levels in WSLH too. Strain ZKA23 showed the highest growth rate in WSLH, followed by ZKA48, ZKA46, ZKA7, ZKA4, ZKA17 and ZKA49. *Pseudomonas* strains ZKA37, ZKA6, ZKA5, ZKA13, ZKA3, ZKA39 and *Stenotrophomonas* sp. ZKA40 also showed adequate growth in CSLH, but for some of them cell growth in WSLH was proportionally lower than others. For *Pseudomonas putida* KT2440 growth in both substrates was less significant, similarly to the rest of pseudomonads and isolates tested. Most strains were unable to grow in Kraft lignin, and only *Shinella* sp. ZKA23, *Microbacterium* sp. ZKA30, *Pseudomonas* sp. ZKA3 and *Sphingobium* sp. ZKA25 displayed distinguishable but relatively low growth in this medium.
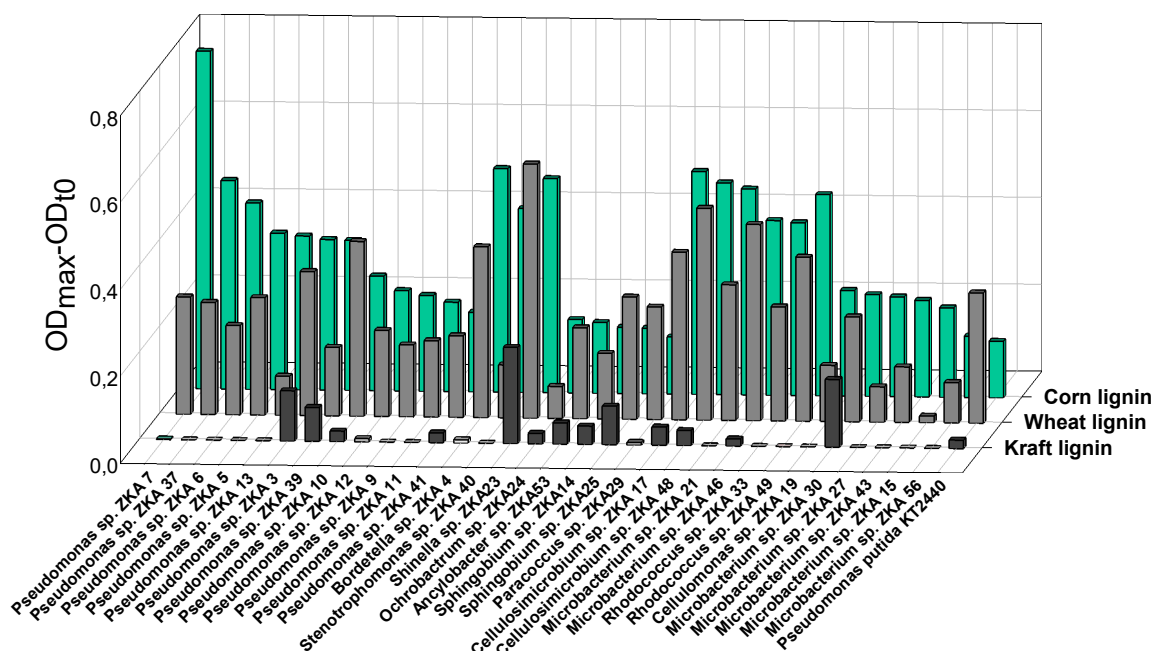
Fig. 29. Growth of selected Keri Lake isolates in technical lignins. Isolates were grown in mineral salt medium supplemented with 0.5 g L^{-1} TOC of lignin hydrolysates (LH) either from alkali pretreated corn stover or wheat straw, or commercial kraft lignin, as sole carbon sources. Growth is expressed as the difference between the maximum and initial optical density.

Growth on organosolv lignin on solid media was verified only for pure cultures of strains ZKA3, ZKA6, ZKA7, ZKA37 and ZKA41, all of which were enriched in the same medium and belong to the *Pseudomonas* genus (Figure 30). No growth was observed for these strains in control samples, in the absence of a carbon source. Perhaps degradation of this polymeric substrate in the enrichment cultures was achieved by the synergistic effect of diverse strains, or perhaps organic compounds present in the soil samples or derived from dead microbial biomass supported the growth of certain bacterial isolates.

In contrast to technical lignins that are pretreated more severely, such as Kraft lignin, alkali lignin generated with mild conditions in this study was more compatible with bacterial growth. It is only recently that a few studies have reported the bacterial utilization of lignin effluents derived from alkali pretreated corn stover. Solid lignin from chemically, mechanically and enzymatically pretreated corn stover, subjected to base-catalyzed depolymerization under mild temperatures (<140°C) and base concentrations (1% NaOH), generated high concentrations of monomeric and dimeric lignin-derived compounds, which were readily metabolized by bacterial strains *Pseudomonas putida* KT2440 and *Corynebacterium glutamicum* ATCC13032 (Rodriguez *et al.*, 2017). Li and colleagues enhanced by 10-fold the production of polyhydroxybutyrate (PHB) from *Cupriavidus*

necator culture growing on alkaline pretreatment liquor from corn stover, by adding an oxidative enzyme-mediator-surfactant system (Li *et al.*, 2019). *Pseudomonas putida* KT2440 was able to convert lignin-enriched streams derived from alkaline pretreatment of corn stover into medium chain-length polyhydroxyalkanoates (*mcl*-PHAs), which can have applications as bioplastics (Linger *et al.*, 2014). Strain *Rhodococcus jostii* PD630 was also able to grow and produce substantial yields of triacylglycerols (TAG) on the hydrolysate of corn stover following a two-stage alkaline pre-extraction with an alkaline hydrogen peroxide post-treatment of plant biomass (Le *et al.*, 2017).
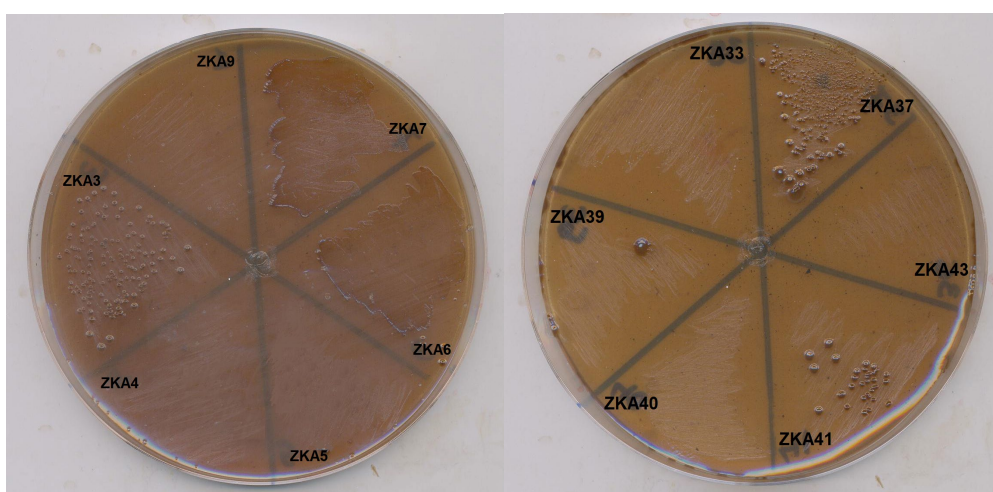
Fig. 30. Growth of selected Keri isolates on solid media containing MSM supplemented with 0.2% organosolv lignin. Figures depict growth for strains ZKA3, ZKA6, ZKA7, ZKA37 and ZKA41. No growth was observed for these five strains on MSM basal media without a carbon source added. No growth was observed for the rest of the bacterial strains tested (see text for the full list of strains tested).

In this study, growth levels in WSLH were in most cases slightly lower than in CSLH. It is possible that a higher lignin content in CSLH, as indicated by the more intense peaks in ^{1}H NMR spectra (Figure 28), supports higher growth levels of bacteria. Inhibitory compounds formed during alkaline pretreatment of wheat straw may also suppress bacterial growth (Jönsson and Martín, 2016). The impact of the pretreatment conditions used in this study on the isolated lignin from both plants is still unclear and needs further investigation. Although bacterial degradation of chemically untreated wheat straw lignin has been reported (Zeng *et al.*, 2012, Sainsbury *et al.*, 2013), reports on bacterial assimilation of alkali lignin from wheat straw are scarce. Three Streptomyces species were able to further decolorize alkali-lignin derived frow wheat straw, which was previously treated with the same strains in solid-state conditions (Hernández *et al.*, 2001). Yang and colleagues constructed a bacterial consortium, comprised of strains from genera *Halomonas* and *Bacillus*, which was effective in treating

wheat straw black liquor derived from a paper pulp mill, with high pH value and COD load (Yang *et al.*, 2008).

On the other hand, during the Kraft process, non-specific chemical reactions generate a variety of compounds, rendering Kraft lignin highly irregular (Mathews *et al.*, 2015). Sulfur compounds introduced into the lignin molecule during this process may act as bacterial cell growth inhibitors or have negative effects on extracellular oxidoreductases involved in the decomposition of lignin. Besides, the higher molecular weight (Mw) of kraft lignin in comparison to the lower Mw of more fragmented soda or organosolv lignins (Constant *et al.*, 2016) may further hamper its assimilation by bacteria (Ravi *et al.*, 2019). To test this assumption, Kraft lignin was size-fractionated using gel filtration chromatography, yielding two fractions, corresponding to high (> 3.000 g/mol) and low molecular weight Kraft lignin (<3.000 g/mol). Isolates selected above were examined for their ability to grow in MSM supplemented with either fraction, in a final concentration of 0.1 (w/v) of Kraft lignin. Still, almost the same growth pattern presented in Figure 29 was recorded either in low or high molecular weight fraction (data not shown).

Only a small number of aerobic mesophilic bacteria have been reported to degrade Kraft lignin, some being isolated from pulp and paper industry waste where the Kraft process is implemented. Some of them, also, fall into genera highlighted in this work, such as *Pseudomonas putida* NX-1, *Ochrobactrum tritici* NX-1 and *Rhodococus jostii* RHA1 (Sainsbury *et al.*, 2013, Xu *et al.*, 2018). However, the chemical composition and functionality, purity and molar mass of technical lignins used are highly variable, depending on the origin of lignin and the conditions of the pretreatment process used (Ragauskas *et al.*, 2014).

The above results feature the potential of certain isolates to proliferate in lignin effluents derived from a mild alkaline pretreatment of residual plant biomass, in a laboratory-scale biorefinery process. Growth of bacteria in lignin-rich waste streams, generated with low energy input, without removal of potential inhibitors or extra carbon sources added, apart from the addition of a small amount of a mineral salt medium, could reduce the overall cost of a biological effluent treatment process. Even strains with lower growth levels in these substrates may still funnel a portion of carbon into valuable metabolites rather than allocate it into biomass. Future work will elucidate any structural changes on lignin or bioproducts formed by microorganisms of this study.

3.6 Bacterial growth studies on selected aromatic carbon sources

To further elucidate their metabolic capabilities, the above-selected strains were cultivated in liquid cultures of different monoaryls or biaryls as sole carbon sources. Eight out of twelve *Pseudomonas* strains showed the ability to assimilate ferulic acid, which correlated well with growth in caffeic and vanillic acid, too (Table 9). The most actively growing species in these carbon sources (indicated by ++++ in Table 9) were strains ZKA3, ZKA7, ZKA10 and ZKA37. Strain *Pseudomonas putida* KT2440, used as a control strain, was able to grow on ferulic, caffeic and vanillic acid among the substrates tested.

Interestingly, *Pseudomonas* sp. ZKA12 was the only strain, amongst all strains tested, able to metabolize syringic acid under those conditions. Among isolates of Actinobacteria class, two *Rhodococcus* strains, ZKA33 and ZKA49, were able to rapidly metabolize vanillic acid, and strain *Microbacterium* sp. ZKA46 was able to slowly grow on biphenyl. Alpha-proteobacterium *Ancylobacter* sp. ZKA53 was also able to grow on biphenyl. No growth was observed for the rest of the tested isolates on any carbon source.

For a small number of strains, such as ZKA12 and ZKA11, the ability to assimilate aromatic monomers with guaicyl and/or syringyl structure, respectively, did not accord with their relatively lower growth levels on lignin hydrolysates. Perhaps some strains cannot depolymerize oligomeric or dimeric aromatic compounds found in lignin hydrolysates. Other strains, such as ZKA4, ZKA23, ZKA17, ZKA48 and ZKA21 could efficiently metabolize lignin hydrolysates despite their inadequacy in utilizing the aromatic monomers or dimers used in this study. It might be possible that these strains preferentially degrade other lignin constituents such as the propanoid side chains rather than the aromatic moieties of lignin, or they might show lower tolerance towards the aromatic compounds used in this study.

Table 9. Growth of selected bacterial strains on different aromatic compounds. Isolates were grown in mineral salt medium supplemented with the corresponding compound as a sole carbon source, in a final concentration of TOC (g L^{-1}): ferulic, caffeic, vanillic and syringic acid: (1.0), biphenyl (0.9), GGE (0.6). Growth is expressed as follows: (++++): OD>0.6 in 24h, (+++): OD>0.6 in 24-48h, (++): OD>0.6 in 48-96h, (+): OD>0.4 in 96-168h, (-): no growth, ND: not determined.

Class	Isolate	Ferulic acid	Caffeic acid	Vanillic acid	Syringic acid	Biphenyl	GGE
γ-Proteobacteria	*Pseudomonas* sp. ZKA3	++++	++++	++++	-	-	-
	Pseudomonas sp. ZKA5	-	-	-	-	-	-
	Pseudomonas sp. ZKA6	+++	+++	+++	-	-	-
	Pseudomonas sp. ZKA7	+++	++++	+++	-	-	-
	Pseudomonas sp. ZKA9	-	-	-	-	-	-
	Pseudomonas sp. ZKA10	++++	++++	++++	-	-	-
	Pseudomonas sp. ZKA11	++	++	++	-	-	-
	Pseudomonas sp. ZKA12	++	+++	+++	++	-	-
	Pseudomonas sp. ZKA13	++	+++	+++	-	-	-
	Pseudomonas sp. ZKA37	++++	++++	++	-	-	-
	Pseudomonas sp. ZKA39	-	-	-	-	ND	ND
	Pseudomonas sp. ZKA41	-	-	-	-	-	-
	Pseudomonas putida KT2440	+++	+++	+++	-	-	-
β-Proteobacteria	*Stenotrophomonas* sp. ZKA40	-	-	-	-	-	-
	Bordetella sp. ZKA4	-	-	-	-	-	-
Actinobacteria	*Microbacterium* sp. ZKA15	-	-	-	-	-	-
	Cellulosimicrobium sp. ZKA17	-	-	-	-	-	-
	Cellulomonas sp. ZKA19	-	-	-	-	-	-
	Microbacterium sp. ZKA21	-	-	-	-	-	-
	Microbacterium sp. ZKA27	-	-	-	-	-	-
	Microbacterium sp. ZKA30	-	-	-	-	-	-
	Rhodococcus sp. ZKA33	-	-	+++	-	-	-
	Microbacterium sp. ZKA43	-	-	-	-	-	-
	Microbacterium sp. ZKA46	-	-	-	-	+	-
	Cellulosimicrobium sp. ZKA48	-	-	-	-	-	-
	Rhodococcus sp. ZKA49	-	-	+++	-	-	-
	Microbacterium sp. ZKA56	-	-	-	-	-	-
α-Proteobacteria	*Sphingobium* sp. ZKA14	-	-	-	-	-	-
	Shinella sp. ZKA23	-	-	-	-	-	-
	Ochrobactrum sp. ZKA24	-	-	-	-	-	-
	Sphingobium sp. ZKA25	-	-	-	-	-	-
	Paracoccus sp. ZKA29	-	-	-	-	-	-
	Ancylobacter sp. ZKA53	-	-	-	-	+	-

Our results show that the degradation of hydroxycinnamates, such as ferulate and caffeate, is a common trait among pseudomonads, but not among the rest of the bacterial strains tested. Ferulic acid bears a guaiacyl nucleus and is co-polymerized into the lignin polymer by covalently bonding to xylan side-chain residues (Karlen *et al.*, 2016). Catabolic pathways involved in the degradation of ferulate and its precursor caffeate, found in several *Pseudomonas* strains, involve funneling into vanillate, further demethylated into protocatechuate, and generating tricarboxylic acid (TCA) cycle intermediates that can be transformed into added-value chemicals (Xu *et al.*, 2019). Previous reports on the degradation of ferulic acid mainly involve members of gamma-proteobacteria, such as *Pseudomonas*, *Acinetobacter, Aeromonas, Azotobacter,* and *Enterobacter* and few actinobacteria such as *Rhodococcus*, *Thermomonospora* and *Amycolatopsis*. Representatives from other phyla also include strains from genera such as *Cupriavidus*, *Flavobacterium,* and *Rhizobium* (Salvachúa *et al.*, 2015).

Syringic acid carries two methoxy groups on its aromatic ring (S- lignin), rendering its degradation more difficult than lignin molecules with a guaiacyl (G-) or p-hydroxyphenyl (H) structure, carrying one or none methoxy group respectively (Xu *et al.*, 2019). This is also reflected by the low number of studies that report the catabolism of syringate by aerobic bacterial species. Some of these include the well-studied lignin degrader *Sphingomonas paucimobilis* SYK-6, and the bacterial isolates *Pandoraea norimbergensis* LD001, *Pseudomonas* sp. LD002, *Bacillus* sp. LD003, *Serratia* sp. JHT01, *Serratia liquefacien* PT01, *Pseudomonas chlororaphis* PT02, *Stenotrophomonas maltophilia* PT03, and *Oceanimonas doudoroffii* JCM21046T (Katayama *et al.*, 1988, Bandounas *et al.*, 2011, Numata and Morisaki, 2015, Tian *et al.*, 2016). The ability of strain ZKA12 to assimilate a wider range of lignin-derived aromatics with guaiacyl and syringyl nuclei would be of significant benefit for designing a single organism with multiple metabolic pathways for lignin degradation.

Biphenyl occurs naturally in crude oil and its degradation proceeds through a pathway that converts biphenyl into benzoate, further metabolized by a catechol *ortho-* or *meta*-cleavage pathway. Cleavage of unsubstituted biphenyls, however, does not correlate with the ability to cleave the C-C biphenyl linkage of lignin-derived compounds, as the corresponding hydrolases involved share no sequence similarity or substrate specificity (Peng *et al.*, 1999). Some of the few bacterial strains known to utilize biphenyl as a sole carbon source belong to genera such as *Microbacterium*, *Ochrobactrum*, *Pseudomonas, Rhodococcus* and *Sphingobium* (Taylor et al., 2012, Tian et al., 2016). Our results are not consistent with these

reports as only strain *Microbacterium* sp. ZKA46 was able to utilize biphenyl. However, to our knowledge, this is the first report of biphenyl utilization by an *Ancylobacter* species.

Guaiacylglycerol-β-guaiacyl ether (GGE) is a model dimer for the study of lignin degradation. The ether link of this compound constitutes the most abundant linkage of the lignin polymer. However, enzymes with Cα-dehydrogenase and β-etherase activity, involved in the degradation of β-aryl ether dimers, rarely occur in nature and are mainly found in Sphingomonadaceae family or the broader class of α-proteobacteria, respectively (Kamimura *et al.*, 2017). Still, none of the isolates of this study belonging to this class could use GGE as a sole carbon source. So far, very few bacterial strains have been reported to degrade GGE, such as *S. paucimobilis* SYK-6, *Novosphingobium* sp. MBES04, *Bacillus atrophaeus* B7, *Bacillus pumilus* C6 and *Trabulsiella* sp. IIPTG13 (Masai *et al.*, 1989, Huang *et al.*, 2013, Ohta *et al.*, 2015, Suman *et al.*, 2016). Notably, among them, only strains SYK-6 and IIPTG13 were able to use GGE as a sole carbon and energy source.

Based on the results of the screening methods, corroborated by literature data, we decided to select two strains, *Pseudomonas kilonensis* ZKA7 and *Rhodococcus pyridinivorans* ZKA49, to further investigate their oxidative enzymatic activity and the pathways involved in lignin degradation. Strain ZKA7 was the most promising strain based on the higher growth levels in CSLH medium and on its ability to grow in organosolv lignin and degrade the aromatic monomers ferulic, caffeic and vanillic acid. Also, *Pseudomonas* strains are highly versatile in terms of their ability to degrade aromatic compounds and have been repeatedly used as model microbes for lignin biodegradation studies (Jiménez *et al.*, 2010). Strain ZKA49 was chosen among actinobacteria of this study since it could assimilate vanillic acid and exhibited sufficient growth levels in CSLH medium. Actinobacteria are considered of great importance in the process of degradation of recalcitrant and relatively complex polymers naturally found in litter and soil, such as lignin and humic acid (Godden *et al.*, 1992, Bugg *et al.*, 2011). Similar to their capacity to produce valuable compounds, such as antibiotics, it has been stated that actinomycetes may also produce attractive enzymes for biotechnological applications (Prakash *et al.*, 2010).

3.7 Effect of temperature, pH and nitrogen source on bacterial growth and degradation of phenolic compounds in lignin hydrolysates

The effect of temperature, pH and nitrogen source on the growth of the strains ZKA7 and ZKA49 in MSM complemented with CSLH and WSLH was examined. In parallel, to monitor the degradation of the lignin phenolic content during bacterial growth we used the Folin-Ciocalteu assay, a relatively rapid method that gives a rough approximation of total phenolic content. The results are expressed in terms of percent reduction in the total phenolic content in culture supernatants during early stationary phase (after approximately 10-12 h of incubation), to avoid any possible interference of the FC reagent with proteins from bacterial cell autolysis during later phases (Everette *et al.*, 2010). Initial phenolic content in both substrates was on average 35 mg/L gallic acid equivalents. No degradation of phenolics was verified for non – inoculated samples.

Temperature effect

Strain ZKA7 was able to grow efficiently on CSLH and WSLH in the temperature range 27-37 °C, with almost undifferentiated growth levels (Figure 31A). A higher temperature (42 °C) had a more profound negative effect on CSLH growth than on WSLH growth. Higher maximum specific growth rate values (μ_{max}) were calculated in the range 27-32 °C, reaching 0.22 h^{-1} for CSLH and 0.28 h^{-1} for WSLH, with a tendency to decrease with an increase in temperature. Degradation of phenolics in CSLH and WSLH reached their highest levels at 27 °C (approx. 38% and 26% reduction in phenolic content respectively), only slightly higher than degradation levels at 32 °C, and declined significantly with increasing temperature.

Growth of strain ZKA49 was obtained in the range 27- 42 °C in both CSLH and WSLH, with only small differences in growth levels between the temperatures tested (Figure 31B). A higher μ_{max} was observed at 27 °C for CSLH (0.13 h^{-1}) which declined at higher temperatures, and at 32 °C for WSLH (0.16 h^{-1}), only marginally higher than μ_{max} obtained at 27 °C (0.15 h^{-1}). Degradation of phenolics by strain ZKA49 peaked at 32 °C in both substrates (approx. 17 % reduction in phenolic content) and declined by rising of temperature.
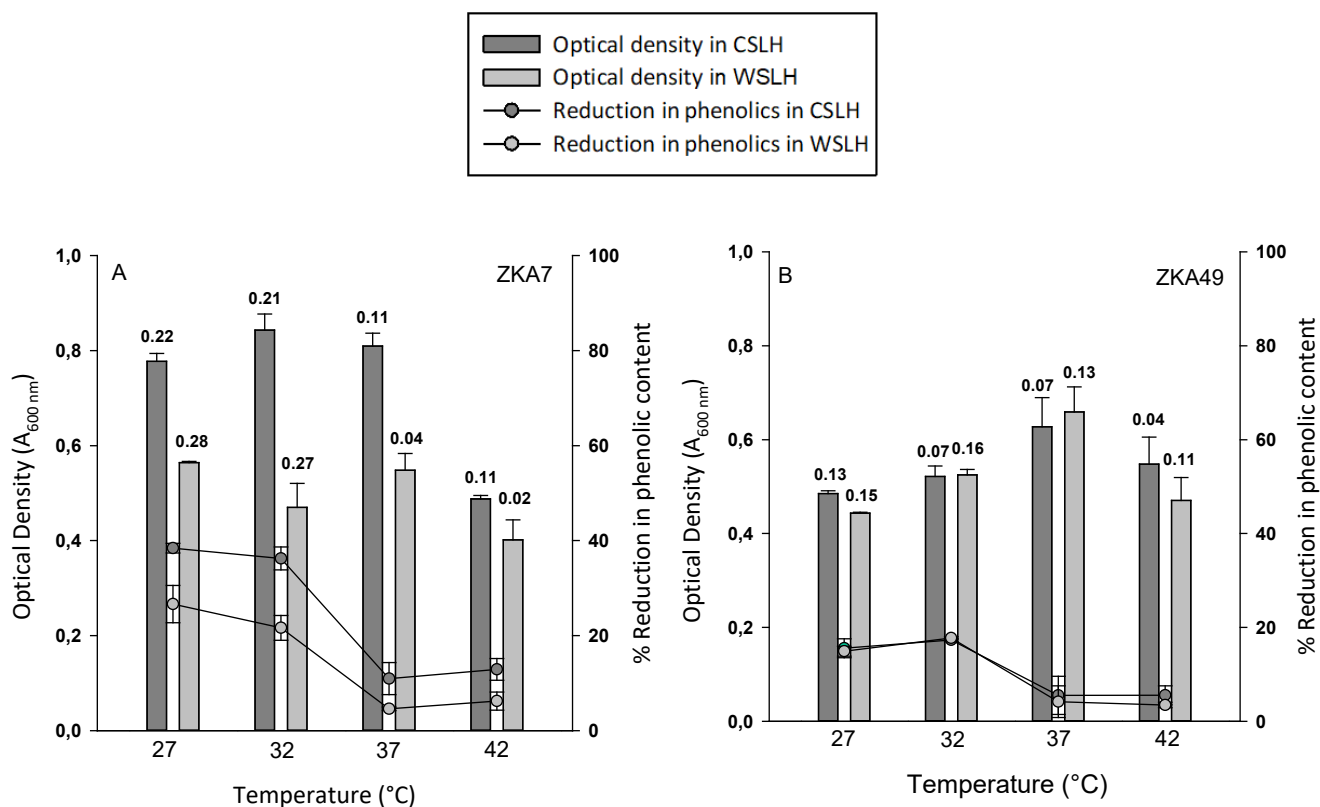
Fig. 31. The effect of temperature on the growth and degradation of lignin phenolic substances of strains (A): *Pseudomonas kilonensis* ZKA7 and (B): *Rhodococcus pyridinivorans* ZKA49, grown on MSM supplemented with 0.5 g L^{-1} TOC of corn stover lignin hydrolysate (CSLH) or wheat straw lignin hydrolysate (WSLH) as sole carbon and energy sources. pH of cultures was adjusted at 6.5. Numbers above bars indicate μ_{max} values (h^{-1}). Error bars indicate the standard deviation of two biological replicates.

Overall, the growth of both strains was characterized by a short lag phase, and exponential growth was observed in most cases during the first 12 hours (data not shown). Both strains showed high specific growth rates in the temperature range 27 °C - 32 °C, yet at higher temperatures growth was slower. Unlike fungi that require longer cultivation periods for their primary growth phase, bacteria usually grow rapidly on lignin, from a few hours to a few days. This fact would be of practical significance in a biorefinery process since liquid effluents cannot be stored on-site for a long time.

Growth patterns of strains ZKA7 and ZKA49 are typical of mesophilic microbes and possibly reflect their adaptation to moderate temperatures like those of Keri Lake. Overall, variation in temperature in the range 27-42 °C had little effect on growth levels, although a more profound, negative effect on phenolics degradation efficiency was observed at temperatures 37-42 °C for both strains and substrates. Perhaps these temperature changes alter the catalytic activity of the enzymes involved in the degradation of lignin phenolic compounds, by affecting the formation of the enzyme-substrate complex and the subsequent formation of

110

products, and/or by affecting the enzymes thermal inactivation. Under these conditions, 30 °C was chosen as an optimal temperature for both strains.

pH effect

Strain ZKA7 was able to grow efficiently in the pH range 6.0 – 8.0 in CSLH and WSLH, while at acidic pH 5.0 growth was completely inhibited (Figure 32A). In CSLH, pH values close to neutral had little effect on the reduction of phenolics, which peaked at pH 7.0 (approx. 37% reduction in phenolic content). In WSLH, the degree of phenolics degradation peaked at pH 6.0 (approx. 28% reduction in phenolic content) and was slightly reduced in the pH range 7.0 – 8.0. At pH 5.0 degradation of phenolics was negligible in both substrates.
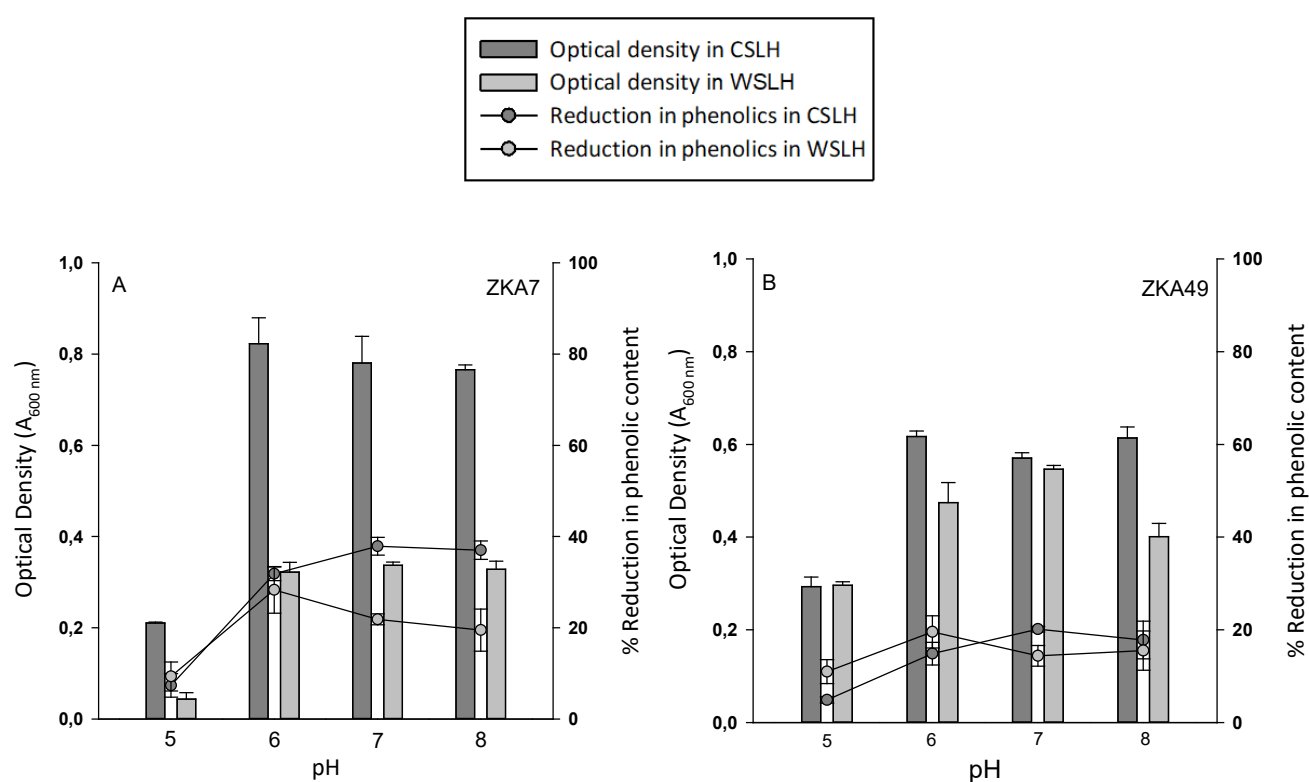
Fig. 32. The effect of pH on the growth and degradation of lignin phenolic substances of strains (A): *Pseudomonas kilonensis* ZKA7 and (B): *Rhodococcus pyridinivorans* ZKA49, grown on MSM supplemented with 0.5 g L^{-1} TOC of corn stover lignin hydrolysate (CSLH) or wheat straw lignin hydrolysate (WSLH) as sole carbon and energy sources. Temperature was adjusted at 30 °C. Error bars indicate the standard deviation of two biological replicates.

Growth of strain ZKA49 in CSLH was not affected by a change of pH in the range 6.0 – 8.0, while in WSLH, growth at pH 8.0 was slightly lower (Figure 32B). Growth levels remained marginal at pH 5.0 in both media. Similar patterns of phenolics degradation were observed in the pH range 6.0-8.0, while at pH 5.0 degradation levels were minimal. The Gompertz model could not fit all the experimental data obtained, therefore μ_{max} was omitted.

Overall, both strains were able to use lignin hydrolysates from alkali pretreated corn straw and wheat straw as sole carbon sources under neutral and slightly acidic or slightly alkaline pH (6.0-8.0). Changes in pH in the range examined did not exert a profound effect on the growth or phenolics degradation efficiency of both strains. However, a more acidic pH (5.0) severely inhibited the growth of ZKA7 cells and significantly suppressed the growth of ZKA49 cells. Perhaps at lower pH values the charge and solubility of the lignin substrate is affected, thus preventing its binding to an enzyme's active site. Besides, pH can also affect the ionization state of amino acids of extracellular ligninolytic enzymes, thereby affecting their catalytic efficiency. Based on these results, the optimized pH value chosen for both strains was 6.5.

In contrast to fungi that require lower pH values for growth and enzyme activity, bacteria can grow at more alkaline pH values. To our knowledge, there are no literature data on optimum pH values for bacterial degradation of alkali lignin from corn stover or wheat straw. However, it has been generally reported that the optimum bacterial pH for degradation of alkaline lignin such as Kraft lignin lies in the range from 7 to 8.5, whereas a higher optimum pH range (9-10) for Kraft lignin was reported for strain *Pandoraea* sp. B-6 (Shi *et al.*, 2013). The ability of bacterial strains to grow and degrade lignin under alkaline conditions would be of benefit for the development of an effective lignin biotreatment process, since pH values of lignin effluents produced by biorefinery industries are usually high due to the wide use of alkaline pretreatment methods.

Nitrogen source effect

Strain ZKA7 was able to use all three inorganic nitrogen sources added in CSLH and WSLH: ammonium (NH_4^+), nitrate (NO_3^-) and ammonium nitrate (NH_4NO_3) (Figure 33A). Phenolics degradation levels remained stable on either source of inorganic nitrogen used. No growth was observed in control samples containing each one of the three inorganic nitrogen sources used, without a carbon source added. Cultures in CSLH and WSLH supplied with an organic nitrogen source, either yeast extract or tryptone, exhibited higher growth rates as was expected, since organic nutrients may also supply carbon and energy. However, the degradation rates of phenolics showed no variation, compared to those recorded on inorganic nitrogen sources.

Similarly, all three different inorganic nitrogen sources tested allowed growth of strain ZKA49, though growth levels on CSLH with KNO_3 as a nitrogen source was slightly lower

(Figure 23B). No significant variation on the phenolics degradation levels was observed between the different inorganic nitrogen sources. No growth was detected in control samples containing each one of the three inorganic nitrogen sources used, without a carbon source added. The organic sources of nitrogen had a positive effect on the growth of ZKA49 in CSLH and WSLH, though, in the presence of tryptone the rates of phenolics degradation were marginally diminished. The Gompertz model could not fit all the experimental data obtained, therefore μ_{max} was omitted.
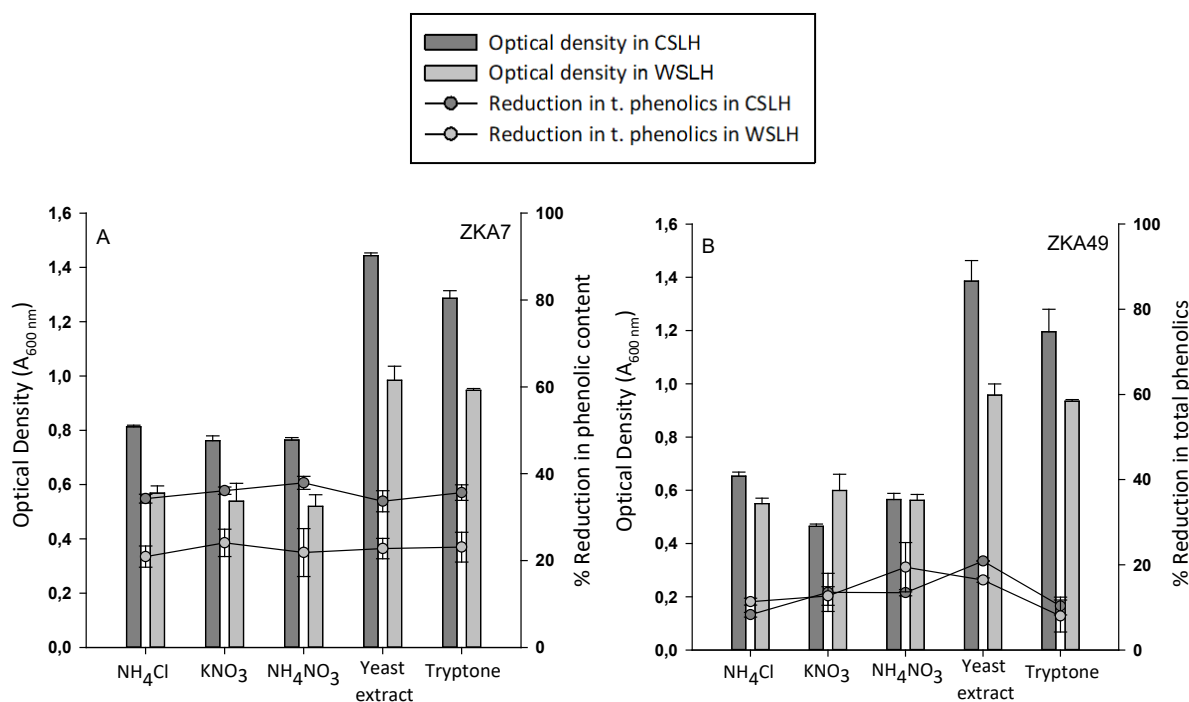
Fig. 33. The effect of different nitrogen sources on the growth and degradation of lignin phenolic substances of strains (A): *Pseudomonas kilonensis* ZKA7 and (B): *Rhodococcus pyridinivorans* ZKA49, grown on MSM supplemented with 0.5 g L^{-1} TOC of corn stover lignin hydrolysate (CSLH) or wheat straw lignin hydrolysate (WSLH) as sole carbon and energy sources. Temperature was adjusted at 30 °C, and pH at 6.5. Error bars indicate the standard deviation of two biological replicates.

Growth levels of both strains on control samples containing only an organic nitrogen source, in the absence of lignin hydrolysates as a carbon source, were almost 50% lower than those obtained when lignin hydrolysates were added (data not shown).

Overall, strains ZKA7 and ZKA49 showed similar growth responses to ammonium and nitrate inorganic nitrogen sources. Supplementation of the media with an organic nitrogen source improved the cell abundance of both strains, though, the corresponding phenolics reduction levels were not substantially altered. Other studies reported that bacterial strains achieved a more enhanced lignin degradation or solubilization rate in the presence of an

organic nitrogen source or organic carbon cosubstrate (Barder and Crawford, 1981, Giroux *et al.*, 1988). However, the requirements for additional growth supporting substrates may vary significantly according to the microorganism used and the nature of the lignin substrate. The carbon and nitrogen source selection may also affect the induction of ligninolytic enzymes, therefore, the role of nutritional regulation on the degradation of lignin hydrolysates of this study needs further research.

More parameters, significant for optimizing the growth and lignin degradation activities of these microbes, such as agitation speed, inoculum size or the addition of different amounts of carbon or nitrogen sources, have yet to be analyzed. Besides, phenolic structures of lignin measured by FC assay only account for a percentage of the lignin aromatic structure. Cleavage of non-phenolic moieties, which comprise the bigger portion in lignin, is a better indicator of enzymatic degradation (Wong, 2009). However, a robust approach for comprehensive analysis of lignin depolymerization has not yet been developed, and multiple methods are usually employed to detect structural and compositional changes of technical lignins, such as FT-IR, pyrolysis-GC-MS, quantitative ^{31}P and 2D HSQC NMR analysis. In this study lignin depolymerization by the two isolates was further investigated by ^{1}H NMR spectroscopy as outlined below.

3.8 Detection of structural modifications in bacterial treated lignin hydrolysates using ^{1}H NMR spectroscopy

To further identify any structural changes in lignin hydrolysates due to bacterial metabolism, culture supernatants of ZKA7 and ZKA49 cells grown in CSLH and WSLH were collected in the late stationary phase and subjected to proton NMR spectroscopy. Changes were determined by comparing the relative signal intensities in culture supernatants with the corresponding supernatants from non-inoculated media, which served as control samples.

A signal with a chemical shift at 8.4 ppm in control samples of both CSLH and WSLH, possibly belonging to phenolic hydroxyl groups protons, was absent from culture supernatants of both strains (Figure 34A-D). A prominent decrease in intensity of aromatic protons signals (6.3-7.5 ppm) was observed in the CSLH culture of ZKA7, compared to the control sample (Figure 34A), while aromatic proton signals were also relatively depleted in the WSLH culture of the same strain (Figure 34B). Certain aromatic signals were also slightly reduced in cultures of ZKA49 (Figure 34C-D), although they are less discernible.

Within the aliphatic oxygenated side-chain region (2.8-6.0 ppm), a signal at 5.4 ppm, possibly belonging to aliphatic H$_\alpha$ protons of a β-5, β-O-4 or β-1 structure, was diminished in the

CSLH culture of ZKA7 and slightly diminished in the CSLH culture of ZKA49 (Figure 34A,C). However, a weaker signal observed in the same region in control samples of WSLH was relatively retained during the growth of both strains in this medium (Figure 34B,D). A signal at 4.3 ppm, observed only in WSLH medium, perhaps belonging to aliphatic Hγ protons, was also slightly diminished in the cultures of both strains (Figure 34B,D). Signals between 3.4-4.1 ppm, possibly attributed to aliphatic Hβ/Hγ protons in β-O-4, β-5 and β-β structures and methoxyl protons, were also reduced in the CSLH culture of ZKA7 (Figure 34A). In the same range, signals remained relatively constant in the rest of the examined samples.

A   **CSLH**

ZKA7

Control

|' ' ' ' '|' ' ' ' '|' ' ' ' '|' ' ' ' '|' ' ' ' '|' ' ' ' '|' ' ' ' '|' ' ' ' '|' ' ' ' '|
      9.0   8.0   7.0   6.0   5.0   4.0   3.0   2.0   1.0
ppm

B   **WSLH**

ZKA7

Control

|' ' ' ' '|' ' ' ' '|' ' ' ' '|' ' ' ' '|' ' ' ' '|' ' ' ' '|' ' ' ' '|' ' ' ' '|' ' ' ' '|
      9.0   8.0   7.0   6.0   5.0   4.0   3.0   2.0   1.0
ppm

C   CSLH

ZKA49

Control

| ' ' ' ' | ' ' ' ' | ' ' ' ' | ' ' ' ' | ' ' ' ' | ' ' ' ' | ' ' ' ' | ' ' ' ' | ' ' ' ' |
         9.0   8.0   7.0   6.0   5.0   4.0   3.0   2.0   1.0
   ppm

D   WSLH

ZKA49

Control

| ' ' ' ' | ' ' ' ' | ' ' ' ' | ' ' ' ' | ' ' ' ' | ' ' ' ' | ' ' ' ' | ' ' ' ' | ' ' ' ' |
         9.0   8.0   7.0   6.0   5.0   4.0   3.0   2.0   1.0
   ppm
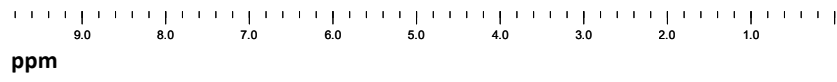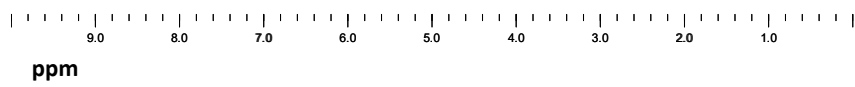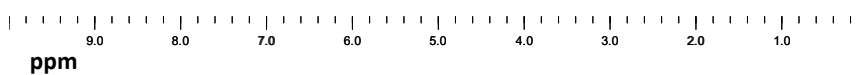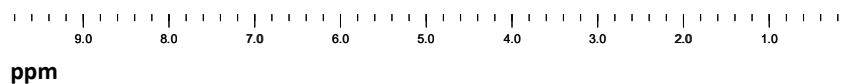
Fig. 34. ^{1}H NMR spectra from culture supernatants of bacterial strains *Pseudomonas kilonensis* ZKA7 and *Rhodococcus* pyridinivorans ZKA49. Each strain was grown on mineral salts medium supplemented with 0.5g L^{-1} TOC lignin hydrolysate from alkali pretreated corn straw (CSLH) or wheat straw (WSLH) as sole carbon sources and energy (upper trace). Supernatants of the corresponding non – inoculated media served as control samples (lower trace). Samples were dissolved in D$_2$O and recorded on a Bruker DRX 400 MHz spectrometer, at 300 K. The broad peak at 4.8 ppm belongs to deuterated water. For signal assignments of lignin structures also see Table 1, §3.4.

117

In the aliphatic side chain region, changes were also observed between 2.3 – 2.6 ppm, where small peaks were almost completely absent in spectra from culture supernatants of ZKA7 in CSLH and WSLH, and ZKA49 supernatants in WSLH (Figure 34 A,B,D), while only some of them were reduced in CSLH cultures of ZKA49 (Figure 34C). These protons may be attributed to protons in β-β structures and phenolic acetate groups. A peak at 1.3 ppm found in the control samples of both substrates was absent from the culture supernatants of both strains in CSLH and of strain ZKA49 in WSLH (Figure 34A,C,D). The same signal became slightly weaker in the culture supernatant of ZKA7 in WSLH (Figure 34B).

Proton–NMR enables the identification of a number of important residual lignin structural features and of major inter-monomeric linkage types in the lignin polymer (Lundquist *et al.*, 1977, Lundquist, 1987, Li and Lundquist, 1994). Some protons have wide ranges of expected chemical shifts, and the actual δ value depends on the solvent used, the concentration, temperature, etc. Therefore, it is not possible to venture a completely accurate assignment of each signal. However, results suggest that strain ZKA7 causes a significant degradation of lignin aromatic moieties during its growth in cultures of CSLH, while a less extensive degradation pattern on aromatic moieties was observed in WSLH cultures of the same strain and cultures of ZKA49 on both media. Depleted aromatic signals may account for aromatic protons located ortho to carbonyl groups, aromatic protons in p-coumarates and ferulates, and aromatic protons of guaiacyl or syringyl units.

Both strains were shown to remove a signal possibly belonging to phenolic hydroxyl groups, suggesting the degradation of lignin phenolic compounds. Results also suggest that ZKA7 may favor the C-C cleavage of intemonomeric linkages of β-O-4, β-5, β-β or β-1 structures, while the action of ZKA49 may be less drastic towards these linkages. Finally, both strains were also shown to decrease signals of aromatic or aliphatic acetate groups that may naturally exist in lignin. Considering these results, ZKA7 conferred more extensive changes in the structure of CSLH, therefore, this strain-substrate combination was chosen for further analysis and detection of ligninolytic enzymes.

3.9 Genomic sequences encoding potential ligninolytic enzymes in *Pseudomonas kilonensis* ZKA7

To detect and characterize potential lignin-oxidizing enzymes the genome sequences of bacterial strains belonging to *Pseudomonas brassicacearum* spp., closely related to *Pseudomonas kilonensis* ZKA7 based on 16S rRNA gene, were examined in search of oxidoreductases, using a multicopper oxidase, a dye decolorizing peroxidase and a catalase-

peroxidase sequence as queries. Multicopper oxidases and dye decolorizing peroxidases were chosen due to the documented role of the corresponding fungal enzymes in lignin decomposition, while studies on *in vitro* treatments of industrial lignin with bacterial multicopper oxidases and peroxidases were limited. What is more, studies on bacterial lignin modifying catalases-peroxidases were scarce.

The multicopper oxidase CopA of *Pseudomonas syringae* pv. tomato (Uniprot / Swiss-Prot Acc. No. P12374) was chosen as query, a plasmid-encoded protein that belongs to a copper - resistance operon (cop) and participates in copper homeostasis by sequestration of copper in the periplasm (Cha and Cooksey, 1991). This protein had no assigned function in relation to lignin and other aromatic substrates. Peroxidase gene prediction was carried out by using Dyp1B dye decolorizing peroxidase from *Pseudomonas fluorescens* Pf-5 as query (Uniprot / Swiss-Prot Acc. No. Q4KAC6), which has shown activity for oxidation of guaiacol, Mn(II) and Kraft lignin (Rahmanpour and Bugg, 2015). Catalase-peroxidase gene prediction was carried out by using the protein sequences of catalase-peroxidase from *Amycolatopsis* sp. (NCBI Ref. Seq. WP_101435509.1), based on the report of an extracellular catalase-peroxidase Amyco1 from *Amycolatopsis* sp. 75iv2 able to degrade the lignin model compound guaiacylglycerol-β-guaiacol ether, and its proposed role in lignocellulose degradation (Brown *et al.*, 2011).

BLAST search in the NCBI database with CopA sequence as a query, yielded a gene encoding a copper-resistance protein CopA, sharing ~76% sequence identity, and a multicopper oxidase with three cupredoxin domains (including cell division protein FtsP and spore coat protein CotA), sharing ~33% sequence identity. One dyp-type peroxidase was encoded in the target species, displaying ~83% sequence identity with Dyp1B, and a catalase-peroxidase KatG, displaying ~68% sequence identity with Amyco1. Proteins CopA, Dyp, and KatG were selected for further investigation in this study, hereafter denoted as **Pk-CopA, Pk-DypB and Pk-KatG**, respectively.

3.10 Sequence analysis of expressed proteins

Further *in silico* analysis of expressed proteins was conducted upon receiving the full genome sequence of strain *Pseudomonas kilonensis* ZKA7. Pk-CopA was annotated as a CopA family copper-resistance protein, Pk-DypB as a putative iron-dependent peroxidase, and Pk-KatG as a catalase-peroxidase HPI (hydroperoxidase I). Table 10 shows characterized proteins with higher identities to Pk-CopA, Pk-DypB and Pk-KatG.

Table 10. Characterized homologues of Pk-CopA, Pk-DypB and Pk-KatG.

Protein / Uniprot Acc. No	Identities with characterized proteins				
	Identity	Protein / Strain	Uniprot Acc. No	Known functions	Reference
Pk-CopA / A0A2U1BL75	77%	CopA / *P. syringae* pv. tomato	P12374	Mediates Cu resistance by sequestration of Cu in the periplasm along with the copper-binding protein CopC	(Cha and Cooksey, 1991)
	32%	EpoA / *Streptomyces griseus*	Q93HV5	Oxidation of *N,N*-dimethyl-*p*-phenylenediamine sulphate	(Endo *et al.*, 2003)
	25%	CotA, Spore coat protein / *Bacillus subtilis*	P07788	Involved in brown pigmentation during sporogenesis	(Enguita *et al.*, 2003)
	25%	MCO, Multicopper oxidase / *Staphylococcus aureus*	Q69HT9	Copper homeostasis and oxidative stress response, low phenoloxidase and ferroxidase activities	(Sitthisak *et al.*, 2005)
	24%	CueO, Blue copper oxidase / *Escherichia coli* K12	P36649	Periplasmic detoxification of copper.	(Roberts *et al.*, 2002)
Pk-DypB / A0A2U1BTQ4	83%	Dyp1B, Dyp-type peroxidase / *Pseudomonas fluorescens* Pf-5	Q4KAC6	Oxidation of guaiacol, Mn(II) and Kraft lignin	(Rahmanpour and Bugg, 2015)
	33%	YfeX, Dye-decolorizing peroxidase / *Escherichia coli* O157:H7	Q8XBI9	Oxidation of guaiacol and catechol and dye-decolorizing activity towards reactive blue 19	(Liu *et al.*, 2017)
	33%	YfeX, Dye-decolorizing peroxidase / *Escherichia coli* K12	P76536	Peroxidase activity and dye-decolorizing activity towards alizarin red and Cibacron blue	(Dailey *et al.*, 2011)
	29%	DypB, from *Rhodococcus jostii* RHA1	Q0SE24	Oxidation of lignin and Mn^{2+}	(Singh *et al.*, 2012)
	26%	Dyp2B, Dyp-type peroxidase / *Pseudomonas fluorescens* Pf-5	Q4KA97	Oxidation of Mn^{2+}, phenol, dichlorophenol and pyrogallol	(Rahmanpour and Bugg, 2015)
	25%	DyP, Dye-decolorizing peroxidase Tfu_ / *Thermobifida fusca* YX	Q47KB1	Activity towards anthraquinone and azo dyes, Kraft lignin, guaiacol and 2,6-dimethoxyphenol	(van Bloois *et al.*, 2010) (Rahmanpour *et al.*, 2016)
	21%	EfeB, Deferrochelatase/peroxidase / *Escherichia coli* K12	P31545	Peroxidase activity on guaiacol	(Miethke *et al.*, 2013)
Pk-KatG / A0A2U1BX77	77%	KatG, catalase-peroxidase / *Burkholderia pseudomallei* K96243	Q939D2	Catalase and peroxidase activity, NADH oxidase, isoniazid hydrazine lyase and isonicotinoyl-NAD synthase activity	(Singh *et al.*, 2008)
	74%	KatG, catalase-peroxidase / *Burkholderia cenocepacia* strain ATCC BAA-245	Q4F6N6	Catalase and peroxidase activity. Peroxidase activity towards o-dianisidine, ABTS and pyrogallol	(Charalabous *et al.*, 2007)
Pk-KatG / A0A2U1BX77	65%	KatG, catalase-peroxidase / *Mycobacterium*	P9WIE5	Catalase and broad-spectrum peroxidase	(Johnsson *et al.*, 1997)

	tuberculosis strain ATCC 25618		activity, protection against toxic ROS, perhaps involved in DNA repair	
65%	KatG, catalase-peroxidase / *Mycolicibacterium smegmatis* strain ATCC 700084	A0QXX7	Catalase and peroxidase activity. May play a role in the intracellular survival of mycobacteria	(Marcinkeviciene *et al.*, 1995)
58%	KatG, catalase-peroxidase / *Synechocystis* sp. PCC 6803	P73911	Catalase and broad-spectrum peroxidase activity, NADH oxidase, isoniazid hydrazine lyase and isonicotinoyl-NAD synthase activity.	(Jakopitsch *et al.*, 1999)
56%	KatG, catalase-peroxidase / *Archaeoglobus fulgidus* strain ATCC 49558	O28050	Catalase and broad-spectrum peroxidase activity, NADH oxidase, INH lyase and isonicotinoyl-NAD synthase activity	(Singh *et al.*, 2008)

Pk-CopA contains a signal peptide belonging to the twin-arginine translocation (tat) pathway, spanning from residue 1 till 33 of the full protein, and was assigned as a periplasmic protein. No signal peptide sequence was predicted for Pk-DypB or Pk-KatG, suggesting they constitute cytoplasmic proteins. The isoelectric point (pI) of the proteins was calculated from their corresponding amino acid sequences (Table 11). All three proteins have a calculated acidic isoelectric point, consistent with their characterized homologues.

Table 11. Characteristics of native and recombinant proteins Pk-CopA, Pk-DypB and Pk-KatG.

Protein	Amino acid residues		Molecular Weight (Da)		Theoritical pI	
	Recomb.	**Native**	**Recomb.**	**Native**	**Recomb.**	**Native**
Pk-CopA	580	577	65.106	64.780	5.60	5.65
Pk-DypB	315	292	34.482	31.946	5.28	4.89
Pk-KatG	779	755	85.246	82.628	5.30	5.09

The multiple sequence alignment of Pk-CopA with selected well-studied bacterial, fungal and plant multicopper oxidases reveals four highly conserved motifs rich in histidine residues, **H**-x-**H**-G-x (position 100-104 of Pk-CopA), **H**-x-**H** (position 142-144), **H**-P-x-**H**-L-**H**-G (position 510-516) and **H**-C-**H**-x(3)-**H** (position 555-561), responsible for binding of four copper ions (Figure 35).
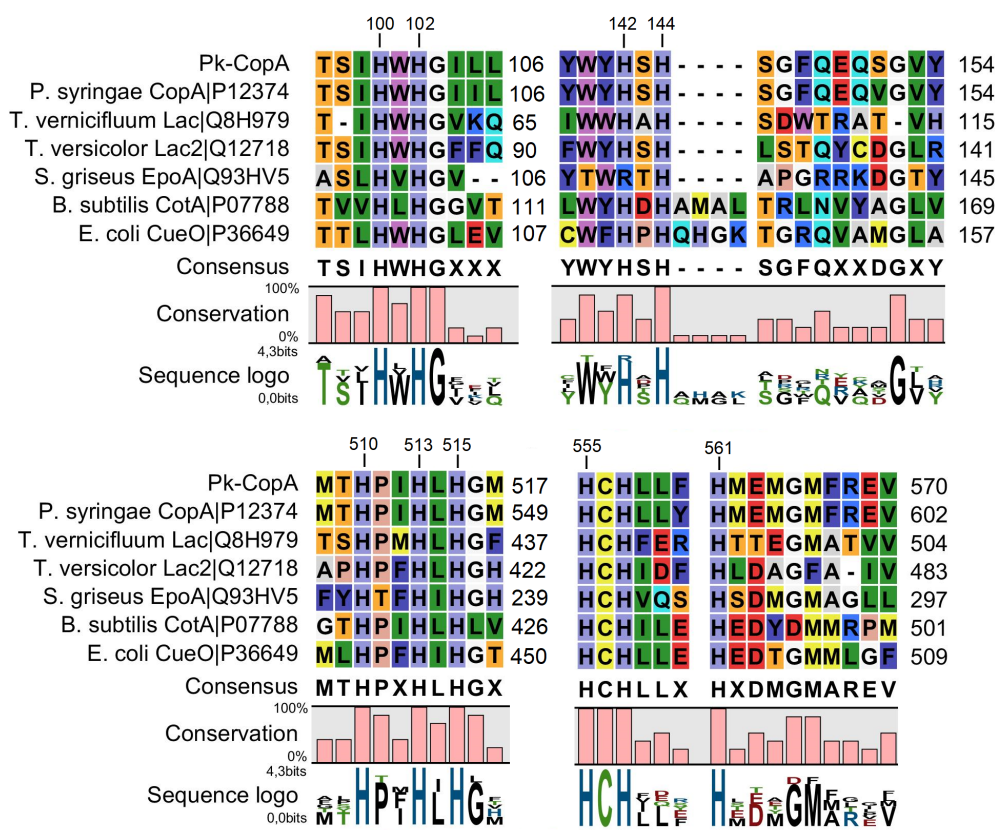
Fig. 35. Conserved amino acid sequences in multicopper oxidases. Aminoacid sequences were retrieved from UniProt/SwissProt database and correspond to: *Pseudomonas kilonensis* ZKA7 Pk-CopA (this study, Acc. No. A0A2U1BL75), *Pseudomonas syringae* CopA (Acc. No. P12374), *Toxicodendron vernicifluum* Lac (Acc. No. Q8H979), *Trametes versicolor* Lac2 (Acc. No. Q12718), *Streptomyces griseus* EpoA (Acc. No. Q93HV5), *Bacillus subtilis* CotA (Acc. No. P07788), *Escherichia coli* CueO (Acc. No. P36649). Consensus sequences were constructed using CLC Main Workbench 5.5. Aminoacids with common properties are colored with similar colours: basic R, H, K, acidic D, E, polar hydroxylic S, T, polar amidic N, Q, aromatic Y, F, W, non-polar aliphatic I, L, V, A, non-polar P, G, sulfur-containing C, M.

Multiple amino acid sequence alignment of Pk-DypB with other characterized DyP-type peroxidases showed the presence of the conserved motif GXXDG (position 130-134 of Pk-DypB) and conserved amino acid residues H203 and R220, required for correct protein folding and formation of the active site of DyP enzymes (Figure 36). Following a maximum likelihood analysis, DyP sequences derived from RedOxiBase database, belonging to four different classes (A to D), were accordingly grouped into four main clusters. DyP from *P. kilonensis* ZKA7 was grouped in class B with high bootstrap support, therefore it was designated as a DypB protein (Figure 37).
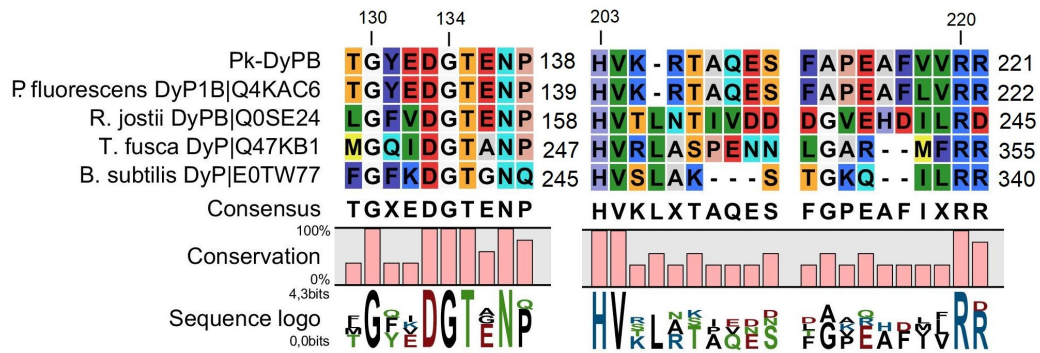
Fig. 36. Conserved amino acid sequences in dyp-type peroxidases. Amino acid sequences were retrieved from UniProt/SwissProt database and correspond to *Pseudomonas kilonensis* ZKA7 Pk-DypB (this study, Acc. No. A0A2U1BTQ4), *Pseudomonas fluorescens* Pf-5 DyP1B (Acc. No. Q4KAC6), *Rhodococcus jostii* RHA1 DyPB (Acc. No. Q0SE24), *Thermobifida fusca* DyP (Acc. No. Q47KB1), *Bacillus subtilis* DyP (Acc. No. E0TW77). Consensus sequences were constructed using CLC Main Workbench 5.5. Aminoacids with common properties are colored with similar colours: basic R, H, K, acidic D, E, polar hydroxylic S, T, polar amidic N, Q, aromatic Y, F, W, non-polar aliphatic I, L, V, A, non-polar P, G, sulfur-containing C, M.
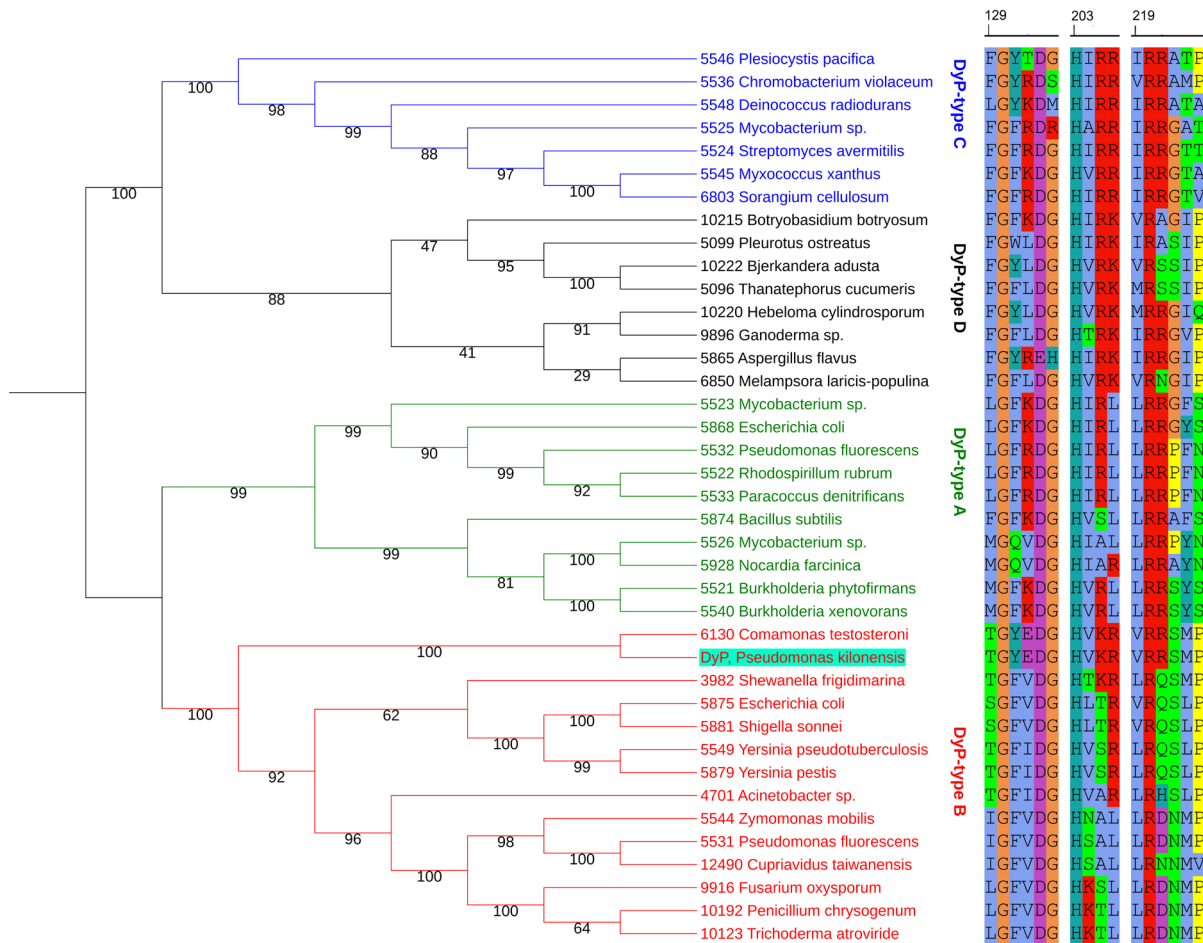
Fig. 37. Phylogenetic relationships among DyP-type peroxidases from bacteria and fungi and the corresponding multiple sequence alignment of conserved regions. Enumeration of aminoacid sequences corresponds to DyP protein from *Pseudomonas kilonensis* ZKA7 (Pk-DypB). Aminoacid sequences were derived from Redoxibase database. Multiple sequence alignments were generated using the L-INS-i algorithm of MAFFT software. The alignments served as the input for a maximum-likelihood phylogenetic tree using IQTREE version 1.6.10 choosing LG+F+I+G4 chosen as the best-fit model according to BIC. Bootstrap values expressed as percentages of 1000 replications are shown at the branch points.

123

Protein Pk-KatG contains the conserved triad Arg-Trp-His (R88-W91-H92 numbering in Pk-KatG, Figure 38), found in the distal heme pocket, essential for hydrogen peroxide reduction and oxidation. It also contains the conserved triad His-Trp-Asp (H283-W334-D395 numbering in Pk-KatG, Figure 38), found in the proximal heme pocket, where the imidazole ring of histidine strongly coordinates the iron ion (Zámocký *et al.*, 2001). The amino acid sequences of Pk-KatG and characterized catalases-peroxidases were highly identical along their entire lengths, however, there was a short insertion in the sequence of Pk-KatG, between P199 and E215 which other KatGs did not possess (not shown). A more extensive analysis would reveal any structural and catalytic consequences of this insertion in Pk-KatG.
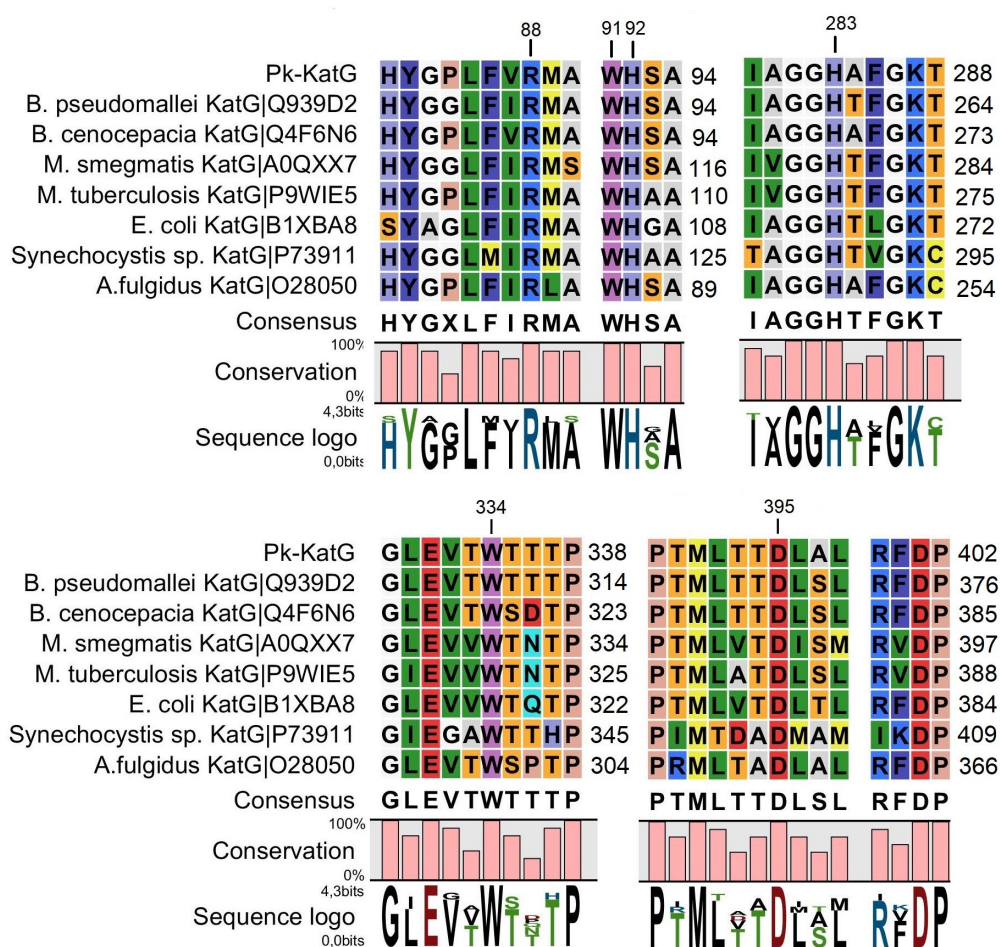
Fig. 38. Multiple amino acid sequence alignment of Pk-KatG with characterized catalase-peroxidases. Amino acid sequences were retrieved from UniProt/SwissProt database and correspond to: *Pseudomonas kilonensis* Pk-KatG (this study, Acc. No. A0A2U1BX77), *Burkholderia pseudomallei* KatG (Acc. No. Q939D2), *Burkholderia cenocepacia* KatG (Acc. No. Q4F6N6), *Mycolicibacterium smegmatis* KatG (Acc. No. A0QXX7), *Mycobacterium tuberculosis* KatG (Acc. No. P9WIE5), *Escherichia coli* KatG (Acc. No. B1XBA8), *Synechocystis sp.* KatG (Acc. No. P73911) and *Archaeoglobus fulgidus* KatG (Acc. No. Q28050). Numbers on top correspond to Pk-KatG amino acid sequence. Consensus sequences were constructed using CLC Main Workbench 5.5. Aminoacids with common properties are colored with similar colours: basic R, H, K, acidic D, E, polar hydroxylic S, T, polar amidic N, Q, aromatic Y, F, W, non-polar aliphatic I, L, V, A, non-polar P, G, sulfur-containing C, M.

3.11 Genomic organization of Pk-CopA, Pk-DypB and Pk-KatG encoding genes

In the genome of *P. kilonensis* ZKA7, downstream of *Pk-copA* gene, three open reading frames were identified with the same orientation, annotated as copper-resistance proteins CopB, CopC and CopD (Figure 39), forming part of a *cop* operon required for copper resistance (Adaikkalam and Swarup, 2005). *copA* and *copB* genes generally encode P-type ATPases which are responsible for the active transport of a variety of cations across biological membranes driven by energy from ATP hydrolysis. *cop* operons are identified in many bacterial genera such as *Pseudomonas*, *Xanthomonas*, *Agrobacterium*, *Enterococcus hirae*, *Escherichia, Rhodobacter*, *Bordetella* and others, comprised of differently ordered sets of *cop* genes (Nawapan *et al.*, 2009). In *Pseudomonas syringae* pv *tomato* strain PT23.2, the *cop* operon is located on a plasmid and consists of periplasmic proteins CopA and CopC, and outer membrane protein CopB, that were proposed to mediate sequestration of copper outside of the cytoplasm as a copper-resistance mechanism (Cha and Cooksey, 1991). In *Enterococcus hirae*, CopA is responsible for Cu uptake under Cu-limiting conditions, while CopB is an efflux pump that excretes Cu when the intracellular concentration of Cu is in excess. In this strain, the expression of the cop operon is modulated by cytoplasmic Cu levels through the coordinated action of the CopY transcriptional repressor and a Cu chaperone, CopZ (Solioz and Stoyanov, 2003).
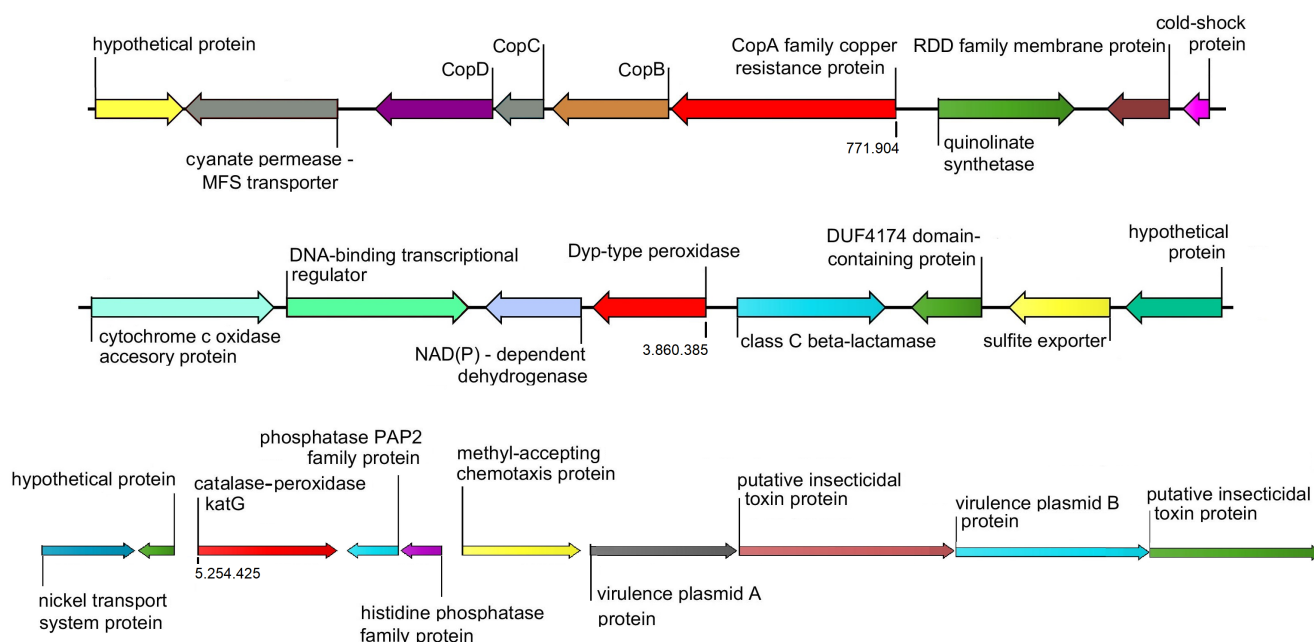
Fig. 39. Genomic organization of Pk-CopA, Pk-DypB and Pk-KatG encoding genes (red arrows), in the *Pseudomonas kilonensis* ZKA7 chromosome. Arrow orientation indicates the transcription direction. The numbering of nucleotide sequences is shown below the genes of this study.

A NAD(P)- dependent dehydrogenase belonging to the short-subunit alcohol dehydrogenase family is located downstream of *dypB* gene (Figure 39). Such enzymes play an important role in lipid, amino acid, carbohydrate, cofactor, hormone and xenobiotic metabolism as well as in redox sensor mechanisms (Kavanagh *et al.*, 2008). The genomic organization of genes encoding the B-type DyPs among different or same species is highly diverse, suggesting different physiological roles, some of which may not involve a peroxidase activity. In some bacteria, such as *Rhodococcus jostii*, the *dypB* gene is cotranscribed with *enc* gene, encoding a protein that assembles to form encapsulin, a bacterial nano-compartment enclosing a large central cavity, to which DyPB is targeted and packaged (Rahmanpour and Bugg, 2013).

In *P. kilonensis* ZKA7 genome, *katG* gene is located downstream of a gene cluster encoding five proteins (not shown) of a nickel transport system and upstream of a gene cluster encoding a chemotaxis protein and putative insecticidal toxin proteins. Nickel is an essential cofactor for a number of enzymes, which among other functions, are also reported to be involved in the detoxification of superoxide anion radicals which act as reactive oxygen species (Eitinger and Mandrand-Berthelot, 2000). Perhaps the function of KatG and the genes located upstream and downstream of it are part of a mechanism that is used for infection against insects and protection against the redox stress generated by the host. In other bacterial genomes, such as in most *Mycobacterium* species, the *katG* gene is preceded by the *furA* gene, a member of the Fur (ferric uptake regulator) family (Master *et al.*, 2001). In general, the catalase function of KatGs is rationalized as protection against H_2O_2, however, the physiological role and importance of the peroxidatic reaction in its anti-oxidant process remain unclear, in large part because the identity of the enzyme's *in vivo* peroxidatic substrates remain unknown.

3.12 Protein overexpression and purification

The recombinant proteins Pk-CopA, Pk-DypB and Pk-KatG were overexpressed as N-terminal His6- fusion proteins in *E. coli* expression system. A 33-residue N-terminal signal for periplasmic translocation was removed from the coding sequence of Pk-CopA. Overexpression of Pk-CopA was aided by the addition of 0.25 mM CuCl$_2$, and conducted under microaerobic conditions to achieve a fully loaded copper enzyme (Durão *et al.*, 2008). All three overexpressed proteins were found in soluble form in the cell extract after IPTG induction and disruption of cells (Appendix Figure A2). The overexpressed proteins were purified by nickel affinity chromatography and the protein fractions obtained were assessed by SDS PAGE (Figure 40). Pk-CopA migrated at ~65 kDa, Pk-DypB at ~30 kDa and Pk-KatG at ~80 kDa, close to the expected molecular mass of the recombinant proteins (Figure

40). The appropriate eluted protein fractions for each protein (No. 7-8-9 for Pk-CopA, 9-10-11 for Pk-DypB and No. 7-8-9 for Pk-KatG) were pooled into one source and concentrated using ultrafiltration devices with a cut-off limit of 10 kDa. Proteins Pk-CopA and Pk-DypB were further purified based on their molecular weight, by gel filtration chromatography.
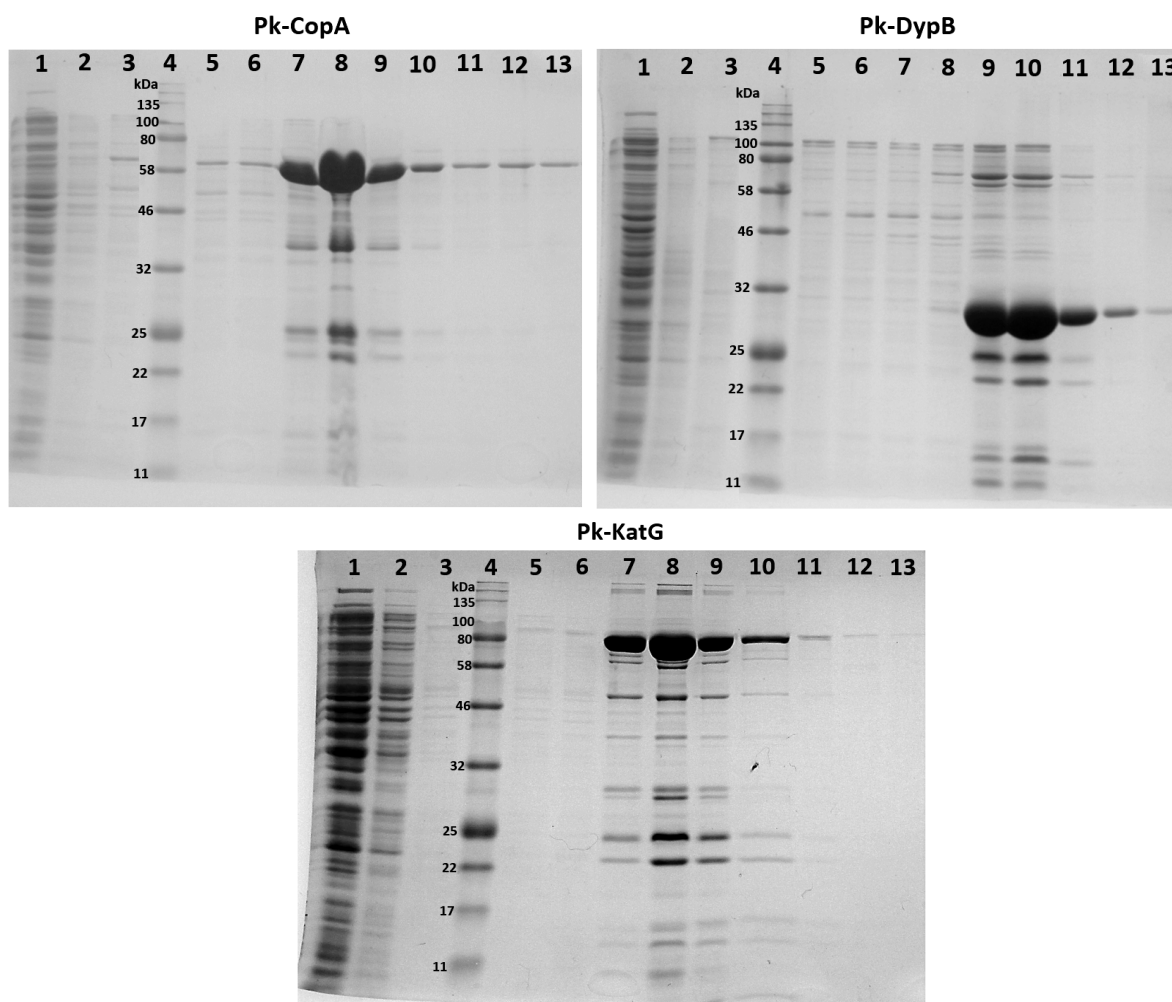
Fig. 40. SDS-PAGE analysis of recombinant proteins Pk-CopA, Pk-DypB and Pk-KatG carrying a six-histidine tag, during purification by nickel chromatography. Lane 1: Column flow-through, Lane 2: First wash of column, Lane 3: Second wash of column, Lane 4: Standard molecular mass protein marker. Lanes 5-13: Eluted protein fractions. Elution of proteins was achieved by applying a high concentration of imidazole (250 mM).

The chromatograms obtained by gel filtration chromatography are shown in Figure 41. The elution volumes of the recombinant proteins suggest that, in vitro, Pk-CopA existed as a monomeric protein and that Pk-DypB existed in the form of hexamers (non-reduced MW of ~180 kDa).   Multicopper oxidases usually form monomers, though laccase-like multicopper oxidases (LCMOs) in *Streptomyces* species can be active as dimers or trimers (Fernandes, 2014). Diverse oligomeric states have been reported for dyp-type peroxidases, ranging from monomers to hexamers (Colpa *et al.*, 2014).
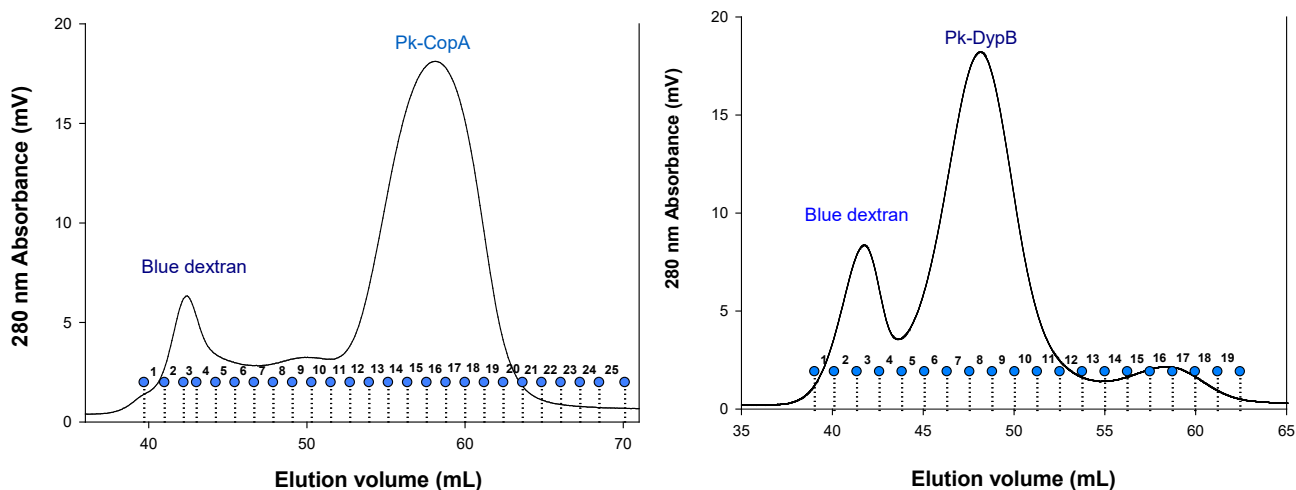
Fig. 41. Purification of expressed enzymes Pk-CopA and Pk-DypB by gel-filtration chromatography, on a Sephacryl S-200 HR resin, using blue dextran as standard. The peak of Pk-CopA in the chromatogram corresponds to its monomeric form (65 kDa), while the peak of Pk-DypB corresponds to its hexameric form (~180 kDa). Drop lines correspond to the numbers of the eluted protein fractions.

Following purification by gel filtration chromatography, the eluted protein fractions of Pk-CopA and Pk-DypB were assayed for ABTS activity to verify the presence of the recombinant proteins. Selected protein fractions (14-18 for Pk-CopA and 7-9 for Pk-DypB) were pooled into one source and further concentrated using ultrafiltration devices with a cut-off limit of 10 kDa. The purified proteins were >95% apparently homogeneous as determined by SDS- and native polyacrylamide gel electrophoresis (Figure 42).
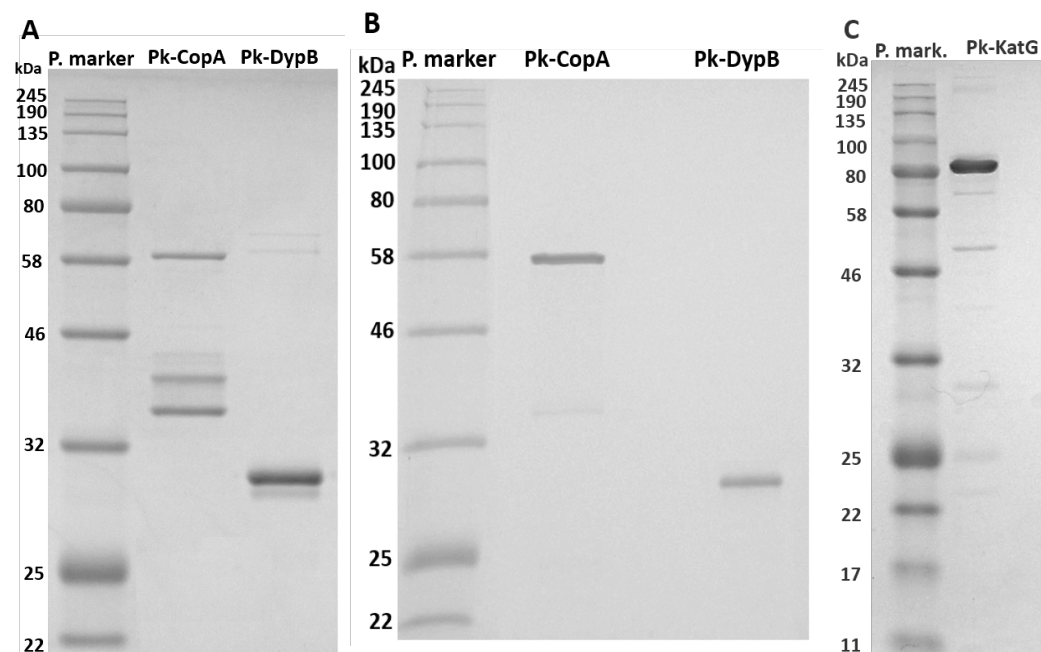
Fig. 42. (A): SDS-PAGE and (B): Native PAGE of recombinant proteins Pk-CopA and Pk-DypB following purification by nickel and gel filtration chromatography and concentration using ultrafiltration devices (10Kda cut-off limit), (C): SDS-PAGE of the recombinant protein Pk-KatG following purification by nickel chromatography and concentration using ultrafiltration devices (10Kda cut-off limit).

3.13 Spectral properties of recombinant proteins

Multicopper oxidases require four canonical Cu atoms to catalyze the oxidation of a substrate. The type I Cu is detected by its blue color and absorption maximum at around 600 nm. Type II copper confers no colour but is detectable by Electron Paramagnetic Resonance spectroscopy (EPR). Type III copper is a pair of copper atoms that give a weak absorbance in the near UV and have no EPR signal (Solomon *et al.*, 1996). Compared to fully copper-loaded "blue" multicopper oxidases/laccases that display an intense blue color, the purified Pk-CopA enzyme displayed a blue-gray color. The UV/vis spectrum of Pk-CopA displayed a peak at 600 nm, corresponding to the T1 copper center, and a A_{280}/A_{600} absorbance ratio of 36.5 (Figure 43). This ratio is used to differentiate blue laccases (A_{280}/A_{600} 15-30) from yellow laccases that may have a copper content similar to the typical blue enzymes, however, under normal aerobic conditions, their copper centers might not be in the oxidized state in resting enzymes, and show lower absorbance at ~600 nm (Leontievsky *et al.*, 1997). White laccases might contain other metal ions (for example, Zn^{2+} or Fe^{3+}), and show higher A_{280}/A_{600} absorbance ratios, too (Das *et al.*, 2020). However, often, a yellow or white laccase may oxidize non-phenolic compounds in the absence of a mediator, or exhibit a more desirable pH or thermal profile than its "blue" counterpart (Xu *et al.*, 2007).
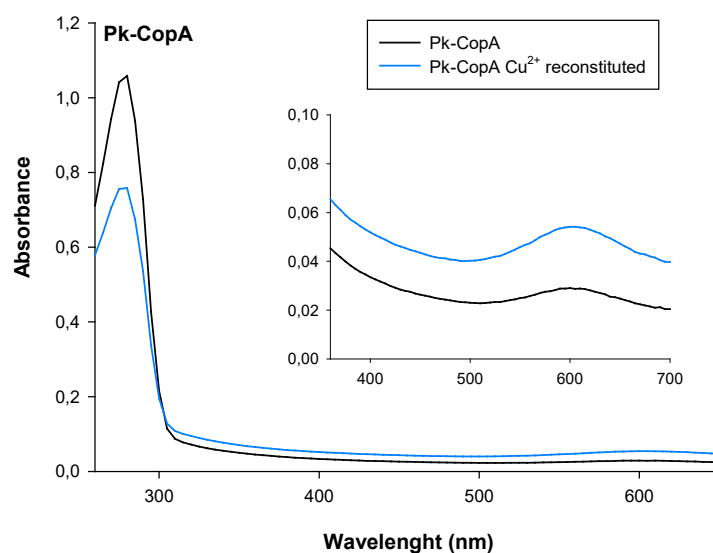
Fig. 43. UV/vis spectrum of purified Pk-CopA protein prior to (black line) and after copper reconstitution (blue line). The enzyme was dissolved in 100 mM potassium phosphate buffer pH 6.0 (blank subtracted). Inset: Wavelength amplification between 350 and 700 nm.

Still, Pk-CopA was only functional upon the addition of exogenous Cu^{2+} salts in the enzymatic assays. This fact may suggest incomplete incorporation of copper in Pk-CopA, attributed to culture conditions during enzyme overexpression, or depletion of some of the copper centers during the purification process. In fact, static incubation for overnight expression of CotA laccase in *E coli* has increased the yield of fully copper-loaded enzyme, due to an increased intracellular accumulation of copper under anaerobic growth conditions (Durão *et al.*, 2008).

To fully reconstitute Pk-CopA with copper, an aliquot of the enzyme was preincubated with excess $CuCl_2$ in the presence of reduced glutathione, as previously described. Concentration of the enzyme and removal of excess Cu was performed in ultrafiltration devices. After copper reconstitution, the enzyme acquired a more intense blue color and showed a typical UV/vis spectrum of blue laccases, with a A_{280}/A_{600} absorbance ratio equal to 14 (Figure 43, inset). However, the presence of glutathione along with copper led to the formation of an insoluble precipitate that complicated the further study of the enzyme. Besides, following the reconstitution treatment, the enzyme's specific activity towards ABTS was not improved. Therefore, further study of Pk-CopA was performed by supplementation of cupric cations ($CuCl_2$) in each enzymatic assay.

The purified enzymes Pk-DypB and Pk-KatG displayed a red-brownish color, typical of proteins carrying a heme prosthetic group in their active site. No hemin was added to the growth medium therefore the recombinant proteins Pk-DypB and Pk-KatG were capable of incorporating heme provided by the host cell, similarly to other heme-containing proteins expressed in *E. coli* (Jakopitsch *et al.*, 1999). The visible absorption spectrum of both enzymes showed a Soret band at 405 nm, which is common in porphyrin compounds. Two less intense peaks are also observed at 505 and 630 nm (Figures 44-45). The A_{405}/A_{280} ratio of Pk-DypB was 1.32, which is close to values reported for fully loaded with heme dyp-type peroxidases (van Bloois *et al.*, 2010). In the presence of 1 mM hydrogen peroxide the Soret band was reduced in amplitude, indicating the presence of a redox-active heme-containing enzyme.
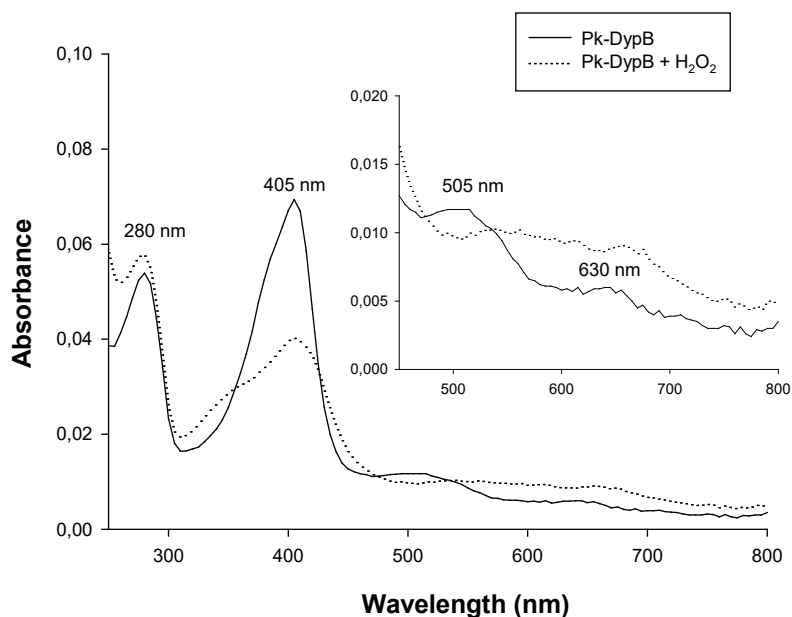
Fig. 44. UV/vis spectrum of purified Pk-DypB in the absence (solid line) and in the presence (dashed line) of 1 mM H_2O_2. The reduction of the peak amplitude at 405 nm in the presence of H_2O_2 indicates the presence of heme in its oxidized –active- form. The enzyme was dissolved in 20 mM MOPS buffer pH 7.0 (blank subtracted). Inset: Wavelength amplification between 450 and 800 nm.

The A_{405}/A_{280} ratio for the purified Pk-KatG was 0.5, consistent with values reported for wild type and recombinant catalase-peroxidases. A_{405}/A_{280} values in the range 0.3-0.65 are typical of catalase-peroxidases carrying two heme molecules per tetrameric enzyme molecule or one heme molecule per homodimer (Calandrelli *et al.*, 2008), a feature that is in contradiction to models proposing a higher heme content of catalase-peroxidases, i.e. one heme molecule per monomer (Welinder, 1991).

Fig. 45. UV/vis spectrum of purified Pk-KatG.The enzyme was dissolved in 20 mM MOPS buffer pH 7.0 (blank subtracted). Inset: Wavelength amplification between 450 and 700 nm.

3.14 Kinetic characterization of recombinant proteins

3.14.1 Determination of optimal activity conditions

The oxidative activity of the recombinant proteins was initially assayed against two model aromatic substrates, ABTS and syringaldazine (SGZ) (Figure 46). All three enzymes catalyzed the oxidation of ABTS but only Pk-CopA and Pk-KatG oxidized SGZ. No peroxidase activity was detected for Pk-KatG towards the usual for catalase-peroxidases substrate o-dianisidine. Pk-CopA was dependent upon exogenous Cu^{2+} salts for activity, while Pk-DypB and Pk-KatG required H_2O_2 for their peroxidative activity. The catalase activity of Pk-KatG was also confirmed following the consumption of H_2O_2 as a substrate.

Fig. 46. Aromatic azo compounds used for the kinetic characterization of the recombinant enzymes, non-phenolic compound ABTS (2,2'-azino-bis(3-ethylbenzothiazoline-6-sulfonic acid) and phenolic compound syringaldazine.

The optimum enzyme and substrate concentrations for kinetic studies were determined with constant substrate concentration and different amounts of enzyme, and then constant amounts of enzyme and varying substrate concentrations. Based on the linear part of the plots of the initial reaction rate against substrate concentration a suitable substrate concentration was chosen for further kinetic studies of the enzymes (Appendix Figure A3). The effect of Cu^{2+} on the activity of Pk-CopA and the effect of H_2O_2 concentration on the activity of Pk-DypB and Pk-KatG towards ABTS was tested. The activity of Pk-CopA initially increased with increasing concentrations of $CuCl_2$ up to 0.5 mM, after which the enzyme's activity declined. Therefore, 0.5 mM $CuCl_2$ was selected as the optimal concentration. (Appendix Figure A4). The concentrations of 1.0 mM and 10 mM of H_2O_2 were chosen as optimal for further kinetic study of Pk-DypB and Pk-KatG towards ABTS.

Optimal pH values were determined for the ABTS assay of each enzyme. Pk-CopA showed optimal activity at pH 5.5 and over 80% of its optimal activity between pH 4.5 - 6.5. For Pk-DypB, optimal activity was reached at pH 6.0, maintaining almost 80% of its optimal activity between pH 5.5 - 7.0 (Fig 47A). The optimum pH for the ABTS reaction of Pk-KatG was 5.5, maintaining approximately 60% of its optimal activity between pH 4.5 - 6.5. In comparison to

Pk-CopA and Pk-KatG, the peroxidase Pk-DypB had a relatively sharper pH optimum curve in the acidic pH range 3.0-5.5 and a broader curve in the neutral-alkaline pH range 6.5-8.0. Activity of Pk-CopA and Pk-KatG towards syringaldazine was observed in a narrow pH range, with a maximal activity at pH 7.0 for both enzymes (Figure 47B). The optimum pH for the enzymatic reaction of Pk-KatG with H_2O_2 as substrate was 6.5 (Figure 47C).
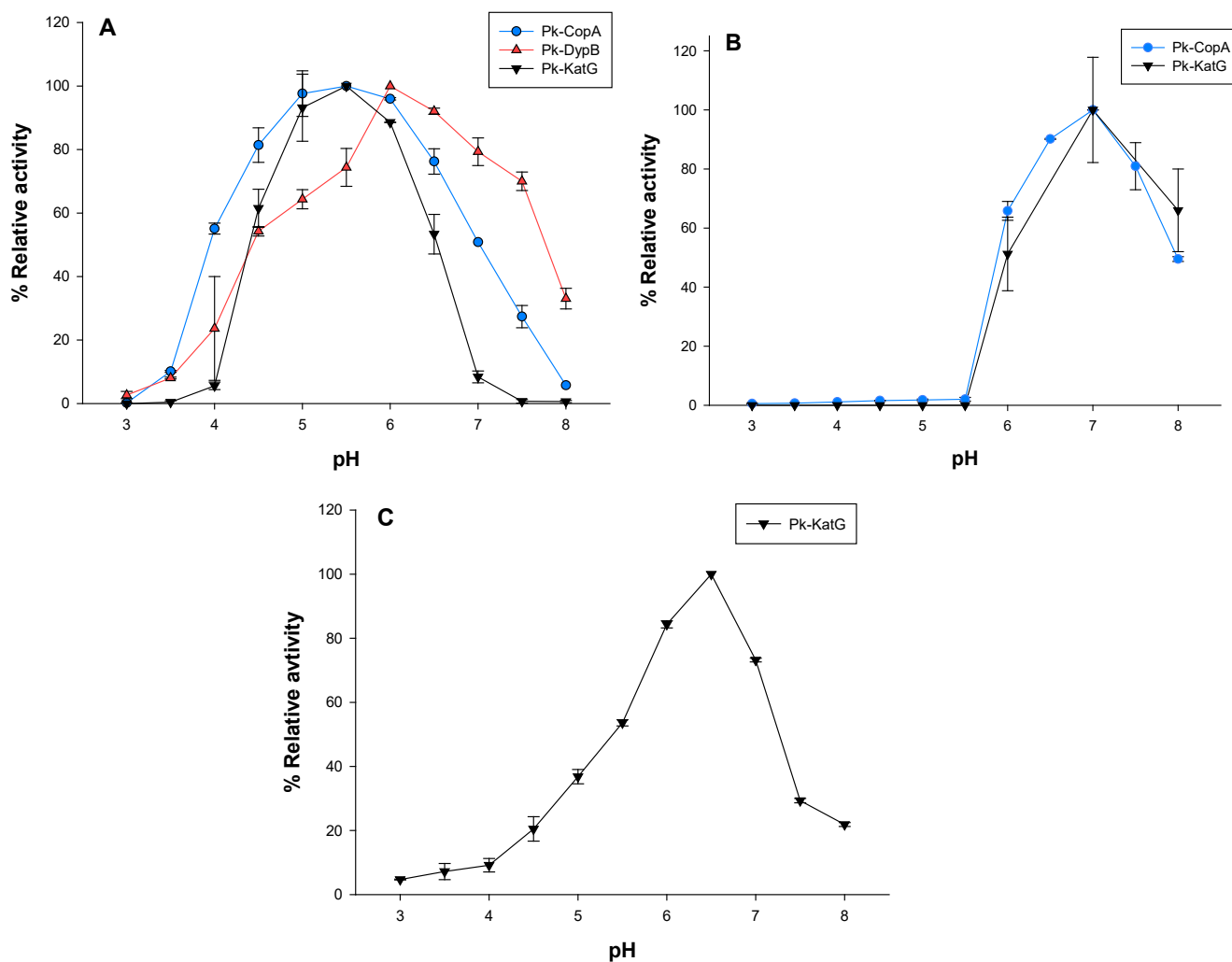
Fig. 47. The effect of pH on the activity of enzymes (A): Pk-CopA, Pk-DypB and Pk-KatG towards ABTS, (B): of enzymes Pk-CopA and Pk-KatG towards syringaldazine, and (C): of enzyme Pk-KatG towards H_2O_2. Assays were conducted in phosphate buffers, at 30 °C, in the presence of optimized concentrations of substrates.

Optimal temperature values were determined for the ABTS assay of Pk-CopA and Pk-DypB and for the H_2O_2 assay of Pk-KatG. Pk-CopA showed optimal activity at 45°C and retained over 70% of its optimal activity between 40°C - 60°C (Figure 48). For Pk-DypB, optimal activity was reached at 40°C, maintaining almost 80% of its optimal activity between 30°C - 45°C. Comparing the two enzymes above their temperature optima, Pk-CopA had a relatively

broader optimum curve than Pk-DypB, whose loss of activity was more rapid with increased temperature. In contrast, below their temperature optima, Pk-DypB retained a relatively higher proportion of its optimum activity than Pk-CopA. The optimum temperature for the reaction of Pk-KatG towards H_2O_2 was 35 °C. However, the temperature dependence was minimal, as even at 45 °C the enzyme retained 97% of its maximum activity.
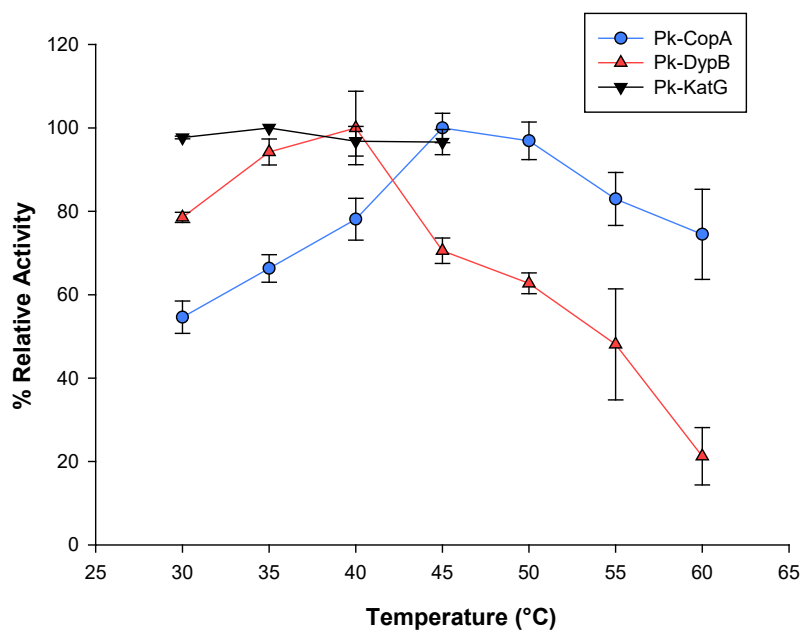
Fig. 48. The effect of temperature on the activity of enzymes Pk-CopA and Pk-DypB, using ABTS as a substrate, and of Pk-KatG using H_2O_2 as a substrate. Temperature effect was assayed in the pH optima of each reaction.

The optimal pH value for ABTS oxidation by Pk-CopA (5.5) was higher than those reported for most bacterial laccases, which mainly have their pH optima in the range 3.0-4.5, except for certain *Streptomyces* spp, whose optima are found at more alkaline pH (8.0) (Table 12). Only recently, in parallel to our study, a research group published their results on two CopA proteins from *Pseudomonas putida* KT2440 and *Pseudomonas fluorescens* Pf-5 (Granja-Travez and Bugg, 2018). Even these proteins exhibited a more acidic optimal pH value of ~4.0 for ABTS. Most fungal laccases also display their optimum activity in the pH range of 3.0–5.5 and they become essentially inactive as the pH is approaching neutral and alkaline values (Baldrian, 2006). Although several studies have reported the improvement of the optimum pH of fungal laccases, most engineered fungal laccases still have an optimum pH at acidic pHs (Novoa *et al.*, 2019). Similarly, most bacterial dyp-type peroxidases have their optimal pH against ABTS at a lower range (3.0-5.0) than the optimal pH value of Pk-DypB (6.0) (Table 12). Likewise, the optimal pH range of most DyPs reported from fungi lies within the pH range 3.0-4.5 (Linde *et al.*, 2014, Fernández-Fueyo *et al.*, 2015).

The peroxidase activity of Pk-KatG towards ABTS was optimal at pH 5.5, similarly to other reported enzymes such as the catalase-peroxidases of *K. pneumoniae* KP1, *C. synechocystis sp*. PCC 6803, and *B. cenocepacia*, while other enzymes exhibited maximal activity under more acidic conditions (pH 4-5) (Table 12). KatG showed a narrower pH range for maximal activity, which is typical of catalases-peroxidases (Nadler *et al.*, 1986). Similar optimum pH values for the catalase activity of Pk-KatG towards H_2O_2 (6.5) were observed in other references, such as KatGs from *B. pseudomallei*, *E. coli* K12, *M. tuberculosis* and *R. capsulatus* B10 that showed maximum activity at pH = 6.0-6.5 (Table 12).

The optimum pH for Pk-CopA activity towards syringaldazine corresponds to those reported for other laccases (Table 12). The pH optima of high redox potential fungal laccases towards phenolic substrates such as syringaldazine or 2,6-Dimethoxyphenol (DMP) are close to 5.0, while no activity is reported above pH 7.0–8.0 (Scheiblbrandner *et al.*, 2017). There are no reports on SGZ oxidation by catalase-peroxidases, as will be described below.

Overall, Pk-CopA and Pk-DypB could operate in a relatively wide pH range, maintaining over 50% of their optimal activity at pH range 4.0-7.0 and 4.5-7.5 respectively, while a relatively narrower pH range was obtained for the peroxidative reaction of Pk-KatG (4.5-6.5). Enzymes with high activity at neutral/alkaline pH are highly desirable, especially for their applications in specific industrial processes such as degradation of lignin from alkali-pretreated biomass.

The optimal temperatures for Pk-CopA (45 °C) and Pk-DypB activity (40 °C) were in line with mesophilic temperatures at which strain *P. kilonensis* ZKA7 thrives in its natural environment. However, activities at high temperatures have been reported for laccases from mesophilic bacteria too, such as spore coat CotA from *B. subtilis* (75 °C), whose physiological role may require activity and resistance at extreme conditions. Still, Pk-CopA had a broad optimal temperature curve, maintaining over 70% of its optimal activity at 60 °C. The optimal temperature of bacterial dyp-type peroxidases range between 30 °C and 65 °C (Table 12). Particularly DyPs from *T. curvata*, *B. subtilis* and *P. putida* showed optimal activity at 30 °C, while BsDyP from *B. subtilis* and *Streptomyces griseosporeus* SN9 DyP protein showed optimal activity at 50 °C and 65 °C, respectively. Pk-DypB was more susceptible to changes in temperature than Pk-CopA, however, it maintained almost 60% of its optimal activity at 50 °C.

The catalase activity of Pk-KatG was independent of temperature, as the activation energy for the oxidation of H_2O_2 to H_2O and O_2 by catalases is very low (2500-7100 kJ/mol), thus temperature is a minor factor for catalysis (Aebi, 1984). Accordingly, the catalase-peroxidase

from the bacterium *Oceanobacillus oncorhynchi* 20AG showed optimum activity at temperatures of 25-35 °C, nevertheless retained more than 80% of its activity, even when the reaction was carried out at 60 °C (Calandrelli *et al.*, 2008).

None of the recombinant enzymes of this study had detectable oxidation activity of Mn^{2+} to Mn^{3+}. This was inconsistent with previous reports on laccase and DypB catalyzed oxidation of Mn^{2+} (Gorbacheva *et al.*, 2009, Ahmad *et al.*, 2010). The Mn^{2+} oxidation by laccases has been proposed to provide H_2O_2 for extracellular reactions performed by ligninolytic enzymes, suggesting a laccase-peroxidase cooperation relevant to the biodegradation of lignin (Schlosser and Höfer, 2002). Moreover, enzymatic Mn^{2+} oxidation plays an important role in the function of the ligninolytic enzymes, since Mn^{3+} is a strong oxidant and can oxidize some non-phenolic substructures of lignin, such as guaiacyl and syringyl model lignin compounds (Hammel *et al.*, 1989, Rahmanpour and Bugg, 2015).

Table 12. Overview of characterized bacterial multicopper oxidases, dyp-type peroxidases and catalase-peroxidases. (*):Heterologously expressd in *E. coli*, (**):Heterologously expressd in *P. pastoris*.

Organism-Enzyme	Substrate	Km (mM)	Kcat (s⁻¹)	Kcat/Km (mM⁻¹ s⁻¹)	T opt. (°C)	pH opt.	Thermal stability	pH stability	Reference
Multicopper oxidases / Laccases									
Bacillus subtilis, CotA*	ABTS	0.106	16.8	158.5	75	3.0	50% /80°C /2h		(Martins *et al.*, 2002)
	SGZ	0.018	3.7	205		7.0			
Bacillus licheniformis Laccase*	ABTS	0.007	83	11.800	85	4.2	43%/ 70°C /1h	100% /pH 5.0–7.0	(Koschorreck *et al.*, 2008)
	SGZ	0.043	100	2.300		7.0			
Bacillus subtilis cjp3, Laccase*	ABTS				80	5.0	>80% / 20-80°C		(Qiao *et al.*, 2017)
Stenotrophomonas maltophilia, Laccase	ABTS	0.7			40	4.5	25%/ 50°C/30min	stable at pH 6.0-9.0/1h	(Galai *et al.*, 2009)
	SGZ	0.05			40	7.0			
Agrobacterium sp. S5-1, Laccase*	ABTS	0.231	32.8	142.1	50	4.5	50%/ 40°C />12 h 50%/ 70°C/30 min	stable at pH 2-9	(Si *et al.*, 2015)
Marinomonas mediterranea, Lac*	ABTS	1.84	4.5	2.4					(Tonin *et al.*, 2016)
Streptomyces cyaneus - Lac	ABTS	0.38			70	4.5			(Arias et al., 2003)
Streptomyces coelicolor, SLAC	ABTS	0.4	4	10	60	4.0			(Machczynski *et al.*, 2004)
Streptomyces psammoticus - Lac	ABTS	0.39			45	8.5			(Niladevi *et al.*, 2008)
Streptomyces ipomoea, SilA	ABTS	0.40	9.99	25		5.0			(Molina-Guijarro *et al.*, 2009)
Streptomyces sviceus, Ssl1	ABTS	0.36	7.38	20.5		4.0			(Gunne and Urlacher, 2012)
	SGZ	15.8	0.06	4*10⁻³		8.0			
Streptomyces sp., SCLAC	ABTS	0.43	8.45	17.6		8.0			(Lu *et al.*, 2013)
	SGZ	5.58	4.88	0.83	40				
Klebsiella pneumonia, Laccase*	ABTS			0.19	35	4.0	30-70°C	5.0-9.0	(Liu *et al.*, 2017)
Thermus thermophilus, Laaccase**	ABTS	0.036	0.37	10.3	90	4.5	>75%/80°C/4h	>95%/pH 4-11//12 h	(Liu *et al.*, 2015)
	SGZ	0.027	1.0	37					
Pseudomonas putida KT2440-CopA	ABTS	0.49	2.4	4.9			60%/50°C/6h		(Granja-Travez and Bugg, 2018)
	SGZ	0.03	1.28	49.2					
Pseudomonas fluorescens Pf-5-CopA	ABTS	0.21	2.2	10.5					
	SGZ	0.05	1.22	24.4					

Organism-Enzyme	Substrate	Km (mM)	Kcat (s⁻¹)	Kcat/Km (mM⁻¹ s⁻¹)	T opt. (°C)	pH opt.	Thermal stability	pH stability	Reference

Organism-Enzyme	Substrate	K_m (mM)	K_{cat} (s^{-1})	K_{cat}/K_m ($mM^{-1} s^{-1}$)	T opt. (°C)	pH opt.	Thermal stability	pH stability	Reference
					Dyp-type Peroxidases				
Thermomonospora curvata –TcDyP*	ABTS	0.015	260	17.000	30	3.0	70%/60°C/1h		(Chen *et al.*, 2015)
Bacillus subtilis – DyP*	ABTS	0.166		70	30	4.0	stable for 53 h at 40°C	stable for 16 h at pH 5.0	(Santos *et al.*, 2014)
Bacillus subtilis – BsDyP*	ABTS				50	3.0			(Min *et al.*, 2015)
Streptomyces griseosporeus SN9– *DyP**					65	8.5	50% /60°C/2h	stable for 48 h at pH 7.0 and 10.0	(Rekik *et al.*, 2015)
Pseudomonas fluorescens Pf-5 -Dyp1B*	ABTS	1.13	13.5	12					(Rahmanpour and Bugg, 2015)
Pseudomonas putida – PpDyP*	ABTS	2.5		8	30	5.0	stable for 53h at 40°C	stable for 16 h at pH 5.0	(Santos *et al.*, 2014)
Vibrio cholera – DyP*	ABTS	0.18	500	2.700		4.0??			(Uchida *et al.*, 2015)
Streptomyces avermitilis -DyP*	ABTS	0.79	1.21	1.71		4.5	stable for 2h at 30°C		(Sugawara *et al.*, 2017)
Amycolatopsis sp.– DyP*	ABTS	0.013	87	6.600					(Singh and Eltis, 2015)
Rhodococcus jostii RHA1 – DypB* (B)	ABTS					3.6			(Roberts *et al.*, 2011)
Pseudomonas aeruginosa PKE117- DyPPa*	Reactive Blue 5					3.5	83% / at 60°C/4h	stable at 6.5–7.0	(Li *et al.*, 2012)
					Ctatalase-Peroxidases				
Archaeoglobus fulgidus DSM 4304, KatG*	ABTS	0.016	17	1.060		4.5			(Singh *et al.*, 2008)
	H_2O_2	3.8	7.770	2.040		6.0-6.5			
Bacillus stearothermophilus IAM11001, KatG*	ABTS	0.031	11	355		4.0			
	H_2O_2	3.7	4300	1.160		6.0-6.5			
Escherichia coli K12, KatG*	ABTS	0.024	25	1.040		4.25			
	H_2O_2	4.2	2.950	700		6.0-6.5			
Burkholderia pseudomallei KatG*	ABTS	0.3	7.9	26		4.5			
	H_2O_2	4.5	5.680	1.260		6.5			
Rhodobacter capsulatus B10, KatG*	ABTS	0.016	7.7	481		5.0			
	H_2O_2	3.7	6.640	1.800		6.0-6.5			
Synechocystis sp. PCC 6803, KatG*	ABTS	0.007	13	1.860		4.25			
	H_2O_2	3.1	7.630	2.460		6.0-6.5			
Escherichia coli, KatG*	ABTS	0.09	20	222					(Moore *et al.*, 2008)
Mycobacterium tuberculosis, KatG*	ABTS	0.83	12	14.5		4.75			(Ndontsa *et al.*, 2012)
	H_2O_2								
Oceanobacillus oncorhynchi, KatG	H_2O_2	24	3.500	7.1 _ 105	40	9.0	50%/ 60°C /4h	Stable at pH 5.0-10.0 after 1 h	(Calandrelli *et al.*, 2008)
Cyanobacterium	H_2O_2	4.9	714			6.5			(Jakopitsch *et al.*,

synechocystis KatG*	ABTS	5.5	1999)
Klebsiella. pneumoniae KP1- KpCP	ABTS	5.5	(Hochman and Goldberg, 1991)
B. cenocepacia J2315 - KatG	ABTS H$_2$O$_2$	5.2-5.7 6.0	(Charalabous *et al.*, 2007)

3.14.2 Kinetic parameters of recombinant enzymes

The kinetic parameters of Pk-CopA, Pk-DypB and Pk-KatG were measured under the optimal reaction conditions by using ABTS and SGZ as substrates, applying nonlinear regression in the obtained data (Appendix Figure A5). The catalase activity of Pk-KatG was characterized using H_2O_2 as a substrate. Pk-CopA had higher affinity for SGZ (K_M 22 μM) than ABTS (K_M 2.8 mM), and a higher k_{cat}/K_M value for SGZ (92.6 mM^{-1} s^{-1}) than ABTS (5.2 mM^{-1} s^{-1}) (Table 13). Syringaldazine values correspond well with literature data on bacterial laccases, except for *Bacillus licheniformis* laccase that exhibited a 25 fold higher catalytic efficiency than Pk-CopA (k_{cat}/K_M 2.300 mM^{-1} s^{-1}) (Table 12). The K_M constant of Pk-CopA for SGZ is slightly higher than some of the lowest K_M values reported for fungal enzymes, such as the laccase from *Melanocarpus albomyces* (K_M 1.8 μM) (Kiiskinen *et al.*, 2004) or the laccase from *Pleurotus ostreatus* D1 (K_M 8.7 μM) (Pozdnyakova *et al.*, 2006), but lower than many other fungal enzymes with a K_M in the range 23-350 μM, suggesting high affinity of syringaldazine with the active site of Pk-CopA. However, much higher turnover numbers are usually recorded among fungal laccases for SGZ, reporting k_{cat} values as high as 650 s^{-1} for laccase from *Pleurotus pulmonarius* (Marques De Souza and Peralta, 2003), suggesting higher consumption rates and catalytic efficiency by such enzymes. Catalytic efficiency of Pk-CopA towards ABTS was among the lowest between bacterial laccases, though comparable with CopA proteins from *P. putida* and *P. fluorescens* (Table 12).

Table 13. Kinetic parameters of recombinant enzymes Pk-CopA, Pk-DypB and Pk-KatG. Abbreviations: ABTS: 2,2'-*azino-bis* (3-ethylbenzothiazoline-6-sulphonic acid), SGZ: syringaldazine. The turnover number (k_{cat}) is defined as the number of substrate molecules converted to product per unit of time by an enzyme molecule when the enzyme is fully saturated with substrate. The k_{cat}/K_M ratio describes the enzyme-substrate interaction and can be used as a measure for the catalytic efficiency of an enzyme.

Enzyme	Substrate	K_M (mM)	V_{max} (mU μg^{-1})	k_{cat} (s^{-1})	k_{cat}/K_M (mM^{-1} s^{-1})
Pk-CopA	ABTS	2.8	13.3	14.5	5.2
	SGZ	$2.2 \cdot 10^{-2}$	1.9	2.0	92.6
Pk-DypB	ABTS	$6.4 \cdot 10^{-3}$	0.8	0.5	72
	H_2O_2	6.1	2.7	6.5	1.1
Pk-KatG	ABTS	$7.1 \cdot 10^{-2}$	3.7	8.7	122
	SGZ	$8.7 \cdot 10^{-3}$		0.6	67.1

Pk-DypB had a 200 fold lower K_M for ABTS than Pk-CopA (6.4 μM) and higher catalytic efficiency (k_{cat}/K_M value of 72 mM^{-1} s^{-1}). Although its K_M value is the lowest reported among many bacterial dyp-type peroxidases, its catalytic efficiency remains significantly lower than

other enzymes, such as TcDyP from *Thermomonospora curvata* that displayed almost a 250-fold higher k_{cat}/K_M value (Table 12). Still, Pk-DypB displayed a six-fold higher k_{cat}/K_M value for ABTS than its homolog protein Dyp1B from *P. fluorescens* (Table 12).

The enzyme Pk-KatG was able to consume H_2O_2, but at concentrations greater than 100 mM an inhibition of its activity was observed. Due to the two-step reaction mechanism of catalysis, catalase-peroxidases do not follow the standard Michaelis-Menten pattern: $E + S \rightleftarrows E\text{-}S \rightarrow E + P$ and the terms K_M, V_{max} and k_{cat} cannot be applied to the observed data as in monofunctional catalases. Therefore, the apparent K_M (6.1 mM), and k_{cat} (6.5 s^{-1}) were calculated at lower substrate concentrations where the standard Michaelis-Menten equation is applicable (Table 12) (Singh *et al.*, 2008). Its K_M value is in the same range with other bacterial KatGs, however, the Kcat constant and the k_{cat}/K_M ratio are three and two, respectively, orders of magnitude lower than those reported for other KatGs, such as KatG from *A. fulgidus* DSM 4304 (k_{cat} 7.770 s^{-1}) and KatG from *Synechocystis* sp. PCC 6803 (k_{cat} 7.630 s^{-1}) (Table 12). Lower k_{cat} values reflect a slower reaction rate of Pk-KatG, perhaps attributed to a different conformation of the enzyme's active site, which renders binding of H_2O_2 more difficult.

The K_M constant of Pk-KatG for ABTS was 71 µM and the k_{cat}/K_M constant 122 mM^{-1} s^{-1}. A broad K_M range is reported for ABTS (7-830 µM) (Table 12), indicating a different binding affinity for ABTS to the active site of the different KatG enzymes. Unlike the kinetic parameters of the catalase activity, k_{cat} and k_{cat}/K_M values for the peroxidase activity are consistent with those previously reported for bacterial laccases (k_{cat} range 7.7-20 s^{-1} and k_{cat}/K_M range 14-1860 mM^{-1}s^{-1}) (Table 12).

The turnover number (k_{cat}) values for catalase activity reported in the literature are much higher than those recorded for peroxidase activity (Table 12). Catalase activity involves H_2O_2 oxidation, whereas peroxidase activity involves oxidation of an exogenous electron donor. It has been shown that even under conditions that favored peroxidase activity (in the presence of an electron donor, low pH and low H_2O_2 concentration) the catalase activity was stimulated up to 14-fold (Ndontsa *et al.*, 2012). In the case of Pk-KatG, most H_2O_2 consumed is probably directed to the oxidation of an electron donor, such as the ABTS molecule, rather than the production of O_2, as indicated by the higher k_{cat} and k_{cat}/K_M constants for peroxidase activity. This enzyme, therefore, appears to be a ***more efficient peroxidase than catalase***.

At concentrations of SGZ higher than 25 µM a substrate inhibition effect was observed for Pk-KatG (Appendix Figure A5F). The substrate inhibition effect appears in about 20% of enzymes and occurs when the substrate, owing to its structure, can bind both to the catalytic site of the enzyme and a second, non-catalytic or allosteric site resulting in the creation of a non-functional complex formed of the enzyme molecule with two substrate molecules attached simultaneously at different positions (Yoshino and Murakami, 2015). The K_{SI} constant was determined at 28.4 µM, meaning that at quite a low concentration of SGZ the enzyme begins to inactivate. This phenomenon has not been described in the literature for syringaldazine before, therefore, there are no reports for K_{SI} values.

ABTS has been used as a model substrate for oxidoreductases while syringaldazine, a methoxy activated phenol, has been considered a specific substrate for laccases (Fernandes, 2014). What is more, multicopper oxidases have been assigned as laccases provided that the four copper atoms are present in the typical formation of type-1, type-2 and type-3 copper centers (Reiss *et al.*, 2013). However, the definition of laccase remains unclear, since not all laccases can oxidize syringaldazine, for example, EpoA from *Streptomyces griseus* does not oxidize it, while SLAC from *S. cyaneus* exhibited very low affinity (Endo *et al.*, 2003, Machczynski *et al.*, 2004). To account for the potential multiplicity of multicopper oxidases the term "laccase-like multicopper oxidase" (LMCO) has been proposed (Reiss *et al.*, 2013). Based on Pk-CopA amino acid sequence that contains conserved motifs involved in the binding of four copper atoms, its spectroscopic properties and the laccase-specific capability to oxidize syringaldazine, ***Pk-CopA can be assigned as a laccase-like multicopper oxidase***. What is more, peroxidases with syringaldazine oxidase activity have been claimed to be specifically involved in delignification (Peyrado *et al.*, 1996). Notably, this is the first report of the oxidation of syringaldazine by a catalase-peroxidase, suggesting a potential ability of the enzyme to react with lignin itself.
.

3.15 Thermal stability of recombinant enzymes

Thermal stability of the three recombinant enzymes was evaluated by preincubating the enzymes under various temperatures and by measuring their residual activity, using the ABTS reaction for Pk-CopA and Pk-DypB, and the H_2O_2 reaction for Pk-KatG. Interestingly, Pk-CopA retained almost 70% of its initial activity within 6 hours of preincubation at 60°C and about 50% of its initial activity at 65 °C. At 70 °C the enzyme retained its activity for 30 minutes and then gradually lost its activity, retaining a 35% after 2.5 h (Figure 49A).
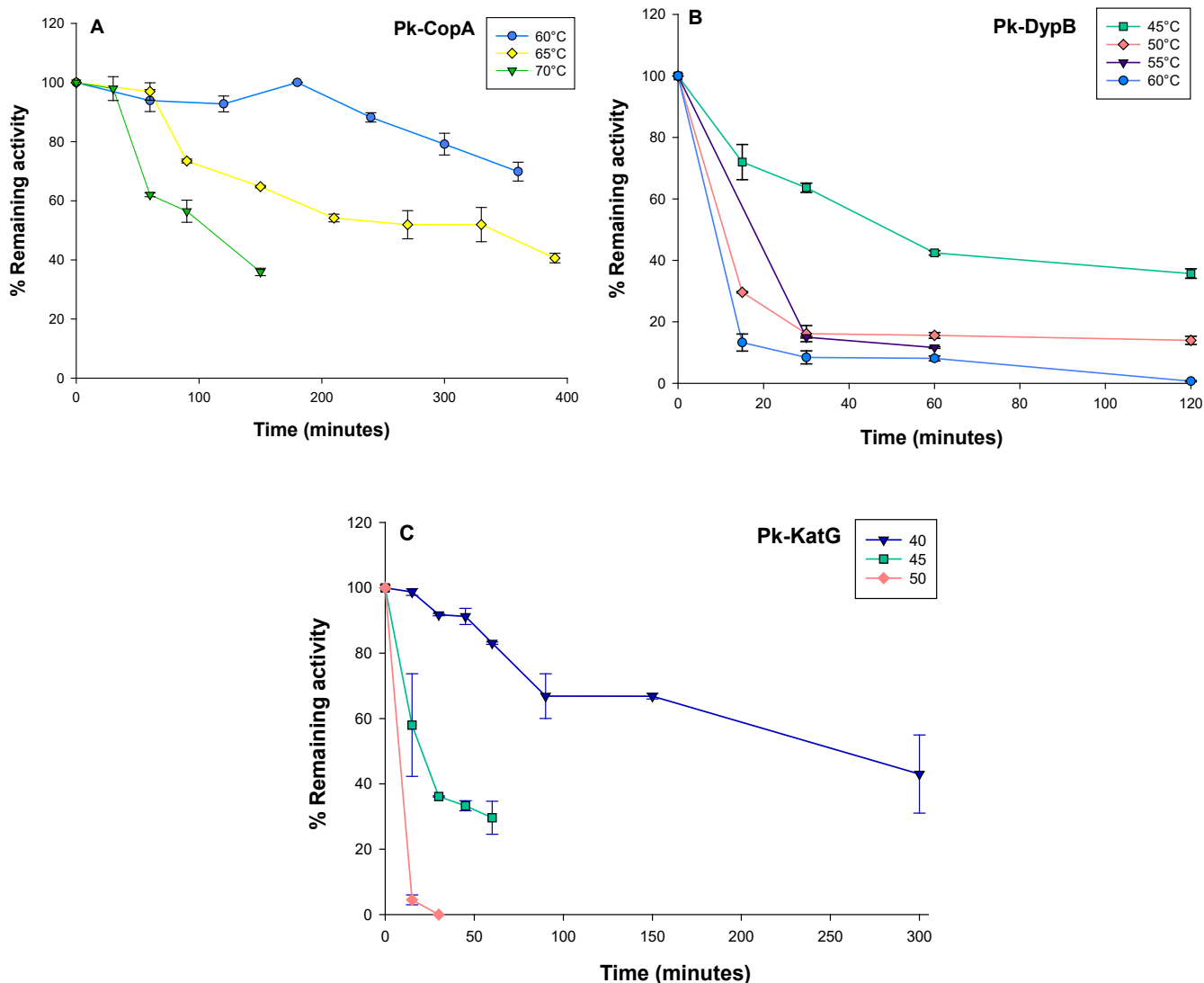
Fig. 49. Thermal stability of recombinant enzymes (A): Pk-CopA, (B):Pk-DypB and (C): Pk-KatG. Results are expressed as residual activity after preincubating the enzymes at different temperatures, and conducting the ABTS assay for Pk-CopA and Pk-DypB, or the H_2O_2 assay for Pk-KatG, at the indicated times, at 30°C, at optimal conditions for each enzyme.

Pk-DypB retained 40% of its initial activity after preincubation for 2 h at 45 °C, while at 50 °C its activity was drastically reduced at 30%, within 15 min of preincubation. Within 1 h preincubation at 55 °C and 60 °C, Pk-DypB retained only 10% of its initial activity (Figure 49B). Pk-KatG retained 65% of its initial activity after 2.5h incubation at 40 °C, and 40% up to 5h. When incubated at 45 °C, the enzyme retained 30% of its initial activity after 1h, while at 50 °C an immediate loss of activity was observed within the first 15 min (Figure 49C). After incubation at higher temperatures, 55 °C and 60 °C, enzymatic activities diminished within minutes (data not shown).

143

Temperature causes some of the weak, non-covalent bonds necessary for maintaining the enzyme's structure to break, thus altering an enzyme's three-dimensional conformation (Daniel *et al.*, 2008). Furthermore, the pKa values of the amino acids are temperature dependent. Ionizable residues are key components of many enzyme active sites, interacting with adjacent ionized residues (e.g ionic bonds), polar residues, or even water molecules (Daniel and Danson, 2013). A shift in the pKa of these residues can have a great impact on both the active site and the overall conformation and activity of the enzyme. Thermal stability of enzymes is considered an industrially important property, allowing higher reaction temperatures, higher reaction rates, lower enzyme loads and longer process duration (Gunne and Urlacher, 2012).

Though originating from a mesophilic organism Pk-CopA demonstrated high stability at elevated temperatures 60-65 °C. The thermal stability of laccases can vary significantly with the growth temperature range of the source organism. Moreover, several physicochemical factors are suggested to be the causes for protein thermostability, such as protein packing, hydrophobicity, increased helical fold content, increased content of internal hydrogen bonds and salt bridges, distribution of charged residues on the enzyme's surface and proportion of certain amino acids (Kumar and Nussinov, 2001). Several factors have been proposed to account for the thermostability of some laccases, including surface distribution of charged residues, higher proline content, and increased hydrophobic interactions between the cupredoxin-like domains 1 and 2, responsible for higher degree of domain packing (Enguita *et al.*, 2003).

Thermal stability among different laccases varies significantly (Table 12). At 70°C the half-life of Pk-CopA was 90 min, while for the *Bacillus licheniformis* laccase, whose optimal activity temperature was 85°C, was less than 1 h. Similarly, the half-life of *Agrobacterium sp. S5-1* laccase at 70°C was 30 min. Other bacterial laccases, with stability at extreme temperatures are *T. thermophilus* laccase with a half-life more than 14 h at 80 ºC, and *S. coelicolor* laccase that retains activity after boiling and treatment with SDS (Machczynski *et al.*, 2004, Miyazaki, 2005). CopA protein from *P. putida* KT2440, a close homologue of Pk-CopA, maintained 60% of its initial activity after 6h at 50°C, while comparable stability after 6h was recorded for Pk-CopA at 65 °C. Bacterial laccases generally exhibit a higher degree of stability at increased temperatures, than their fungal counterparts (Chauhan *et al.*, 2017). The half-life of several fungal laccases at 70 °C ranges between 10 and 60 min, though strains with much high thermostability are reported, such as laccase from *Pycnoporus* sp. SYBC-L1, with a half-life of 37 h (Wang *et al.*, 2010).

Pk-DypB demonstrated lower thermostability than other reported bacterial dyp-type peroxidases, such as TcDyp from *T. curvata* that maintained 70% of its initial activity after 1 h at 60 °C, Dyp from *S. griseosporeus* whose half-life at 60 °C was 2 h, and DyPPa from *P. aeruginosa* that retained 83% of its activity after 4 h at 60 °C (Table 12). High thermal stability was also exhibited by *Svi*DyP from *Saccharomonospora viridis* DSM 43017 that showed 63% residual activity after 4 h of incubation at 50°C, and more than 60% residual activity after 2 h of incubation at 60°C (Yu *et al.*, 2014).

The stability properties of Pk-KatG are consistent with existing references. While monofunctional catalases exhibit remarkable temperature stability, retaining their activity even at 80 °C (Singh *et al.*, 2008), the bifunctional catalase-peroxidases are more sensitive in temperature. Catalase-peroxidases from several mesophilic bacteria, such as *Mycobacterium sp.* JC1 DSM 3803, *E. coli* K12 and *Rhodobacter capsulatus* B10, are completely inactivated within 60-90 sec when incubated at 65 °C (Ro *et al.*, 2003, Singh *et al.*, 2008). Other enzymes such as the catalase-peroxidase of *Bacillus pumilus* ML 413 and the catalase-peroxidase of *O. oncorhynchi* 20AG were more stable, maintaining 30% and 50% of their activity after 10 h and 4 h of incubation at 60 °C (Calandrelli *et al.*, 2008, Philibert *et al.*, 2016).

3.16 pH stability of recombinant enzymes

Similarly to thermal stability, pH stability of the three recombinant enzymes was evaluated by preincubating the enzymes under various pH conditions and by measuring their residual activity, using the ABTS reaction for Pk-CopA and Pk-DypB, and the H_2O_2 reaction for Pk-KatG. After 2 h of preincubation at pH 10 and 11 Pk-CopA retained 100% and 80% of its initial activity, respectively (Figure 50A). At pH 4 its activity was stable after 2 h, while at pH 3 its activity drastically dropped to 11% after 15 min of preincubation. Pk-DypB displayed maximum stability at pH 9, maintaining approximately 50% of its initial activity after 5 h of preincubation. At more alkaline conditions Pk-DypB was less stable, losing 50% and 80% of its initial activity within 45 min at pH 10 and 11. At acidic pH, Pk-DypB was almost completely inactivated within 1 h at pH 3 and 4, and lost 65% of its initial activity at pH 5.0 (Figure 50B). The activity of Pk-KatG was diminished in the first 15 min of incubation at pH 3.0 and 4.0. At pH 5.0 the enzyme was stable for up to 2.5h. In the alkaline pH range, the enzyme retained almost 50% of its activity after 5h and 30 min of incubation at pH 10 and pH 11, respectively (Figure 50C).
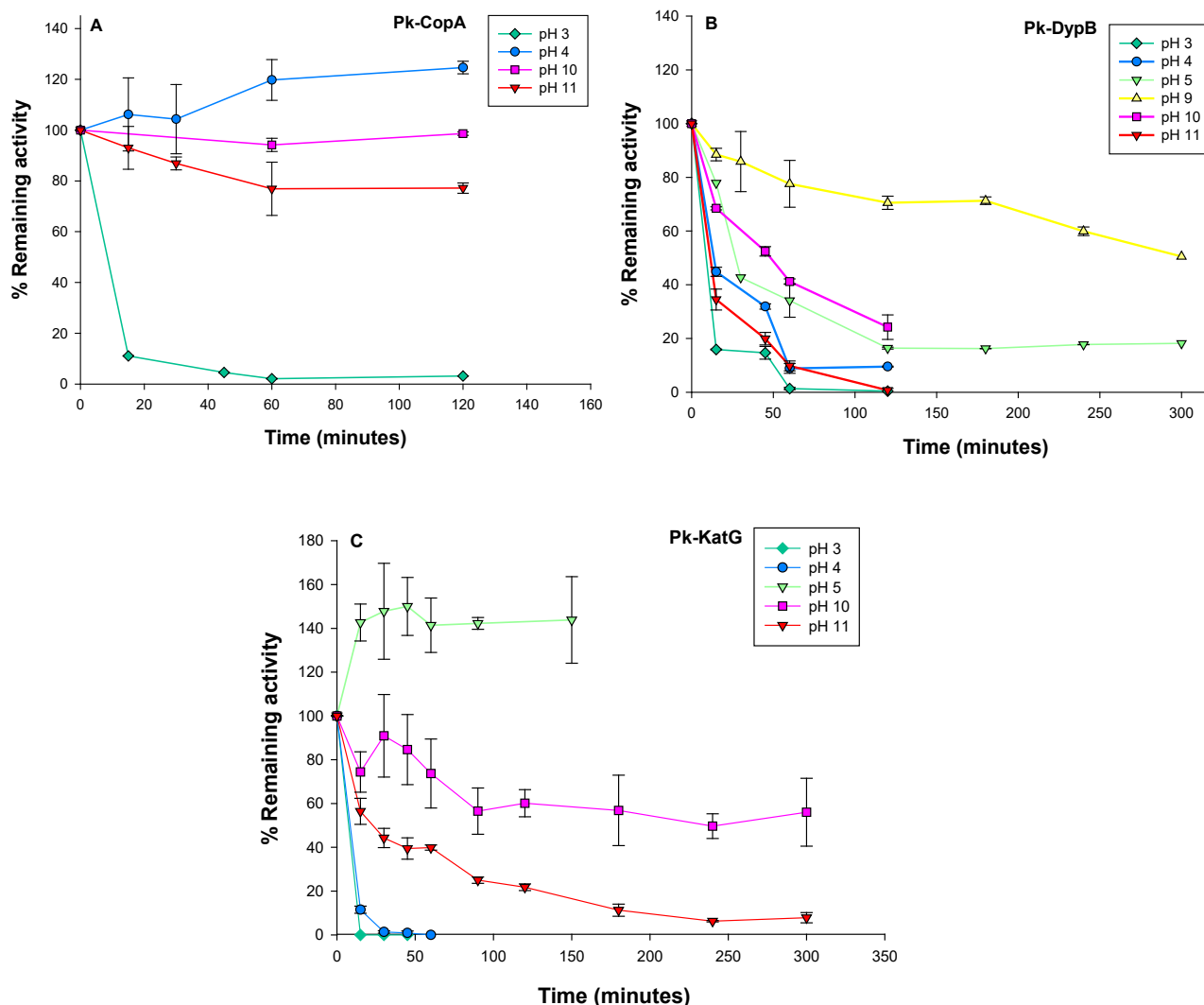
Fig. 50. pH stability of recombinant enzymes (A): Pk-CopA, (B): Pk-DypB and (C): Pk-KatG. Results are expressed as residual activity after preincubating the enzymes in 50 mM phosphate buffers in the pH range 3-5, or in 50 mM Na_2CO_3 / $NaHCO_3$ buffers in the pH range 10-11 and conducting the ABTS assay for Pk-CopA and Pk-DypB or the H_2O_2 assay for Pk-KatG, at the indicated times, at 30°C, at optimal conditions for each enzyme.

Pk-CopA was stable over a broad pH range. Tolerance of enzymes to extreme pH values is an important feature for industrial applications. Especially, enzymes with high stability and activity at alkaline conditions are required for the treatment of alkali pretreated lignin pulps (Gunne and Urlacher, 2012). Although the pH stability of different laccases can vary, bacterial laccases are generally more stable at high pH than fungal laccases, whose stability is higher at acidic pH (Baldrian, 2006, Ogola *et al.*, 2015). The laccase Ssl1 from *Streptomyces sviceus* retained 80% residual activity after 5 days of incubation at pH 11. At pH 4 Ssl1 lost

65% activity within 1 day and at pH 3 it was almost completely inactivated within 30 min (Gunne and Urlacher, 2012). The rLac laccase from *K. pneumonia* retained 41%, 34%, and 32% residual activity after 20 h incubation at pH 4.0, 10.0, and 11.0, respectively, at 4 °C (Liu *et al.*, 2017). The stability of laccases at high pH values has been explained by the fact that inhibition of the trinuclear cluster by hydroxide ions reduces auto-oxidation of laccase and thereby stabilizes the enzyme (Alcalde, 2007). It has also been suggested that thermostable enzymes can commonly withstand extreme alkalinity or acidity or chemical denaturation, too (Haki and Rakshit, 2003). Circular dichroism experiments could provide information on the folding or unfolding processes of Pk-CopA as a function of experimental conditions used in this study, and therefore on the underlying mechanisms for some of its properties, such as temperature and pH optima, thermal and pH stability.

Pk-DypB was not stable in the acidic pH range but showed higher stability at alkaline pH 9.0. Other bacterial dyp-type peroxidases exhibited higher stability at pH 5.0, such as DyP from *B. subtilis* and PpDyP from *P. putida* that were stable for 16 h, or at a neutral-alkaline pH range, such as DyP from *S. griseosporeus* SN9 that was stable for 48 h at pH 7.0 and 10.0 (Table 12). Pk-KatG was stable over a pH range of 5.0-10.0, a property common to catalases-peroxidases such as the enzyme of the bacterium *K. pneumoniae* KP1 with stability at pH 5.2-10.8 (retention of at least 50% of activity) and the catalase-peroxidase of *B. pumilus* ML 413 which is stable at pH range 6-11, retaining 50% of its activity even after 12h at pH 11 (Hochman and Goldberg, 1991, Philibert *et al.*, 2016).

3.17 Effect of chemicals on enzyme activity

The effect of metal ions, denaturants and metal chelating agents on the activity of the recombinant enzymes was assayed at a final concentration of 10 mM. Pk-CopA was strongly activated in the presence of Al^{3+}, Na^+ and Hg^{2+}, which caused a 1.7-2.5-fold increase in its activity (Figure 51A). Enzyme's activity was slightly increased in the presence of Li^+, Mg^{2+}, Ca^{2+}, Ni^{2+} and Mn^{2+}, reaching 105-125% of its initial activity, and remained almost unaffected (more than 75% remaining activity) by Ba^{2+}, NH_4, PMSF, Cd^{2+}, Zn^{2+} and β-mercaptoethanol. The presence of EDTA, SDS, Ag^{+1} and DTT partially inhibited its activity (30-60% remaining activity), while Co^{2+} and Cr^{6+} caused complete inhibition of the enzyme's activity, even at a final concentration of 1 mM. The effect of Cu^{2+} and Pb^{2+} at a final concentration of 10 mM could not be assessed due to the formation of a highly absorbing product, therefore

their effect was assayed at 1 mM final concentration, where a slight activation effect was observed for Pk-CopA.
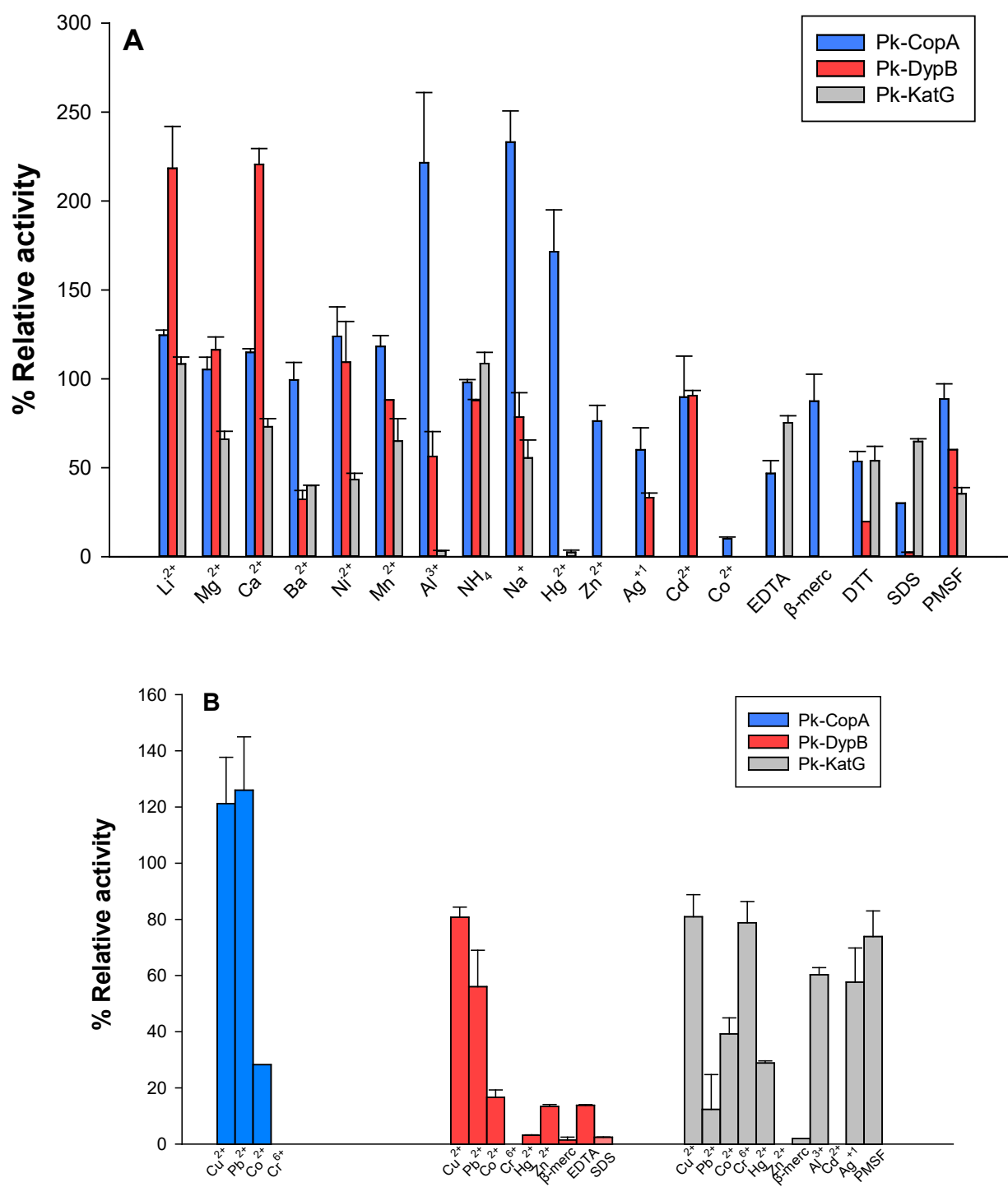
Fig. 51. Effect of chemical reagents on enzymatic activity of recombinant enzymes at a final concentration of (A): 10 mM or (B): 1 mM. Relative activity is expressed as percentage of the initial reaction rate of the ABTS assay, conducted in 50 mM buffer, pH 6.5.

A two-fold increase in Pk-DypB activity was recorded in the presence of 10 mM Li^+ and Ca^{2+}. A slight increase of activity was observed in the presence of Mg^{2+} and Ni^{2+}, reaching 110-115% of the enzyme's initial activity. Activity was almost unaffected by Mn^{2+}, NH_4, Na^+ and Cd^{2+} and partially inhibited by Ba^{2+}, Al^{3+} and Ag^{+1}. Complete inhibition was observed with Hg^{2+}, Zn^{2+}, β-mercaptoethanol, EDTA, SDS, Co^{2+} and Cr^{6+}, even at a lower concentration of 1 mM.

The activity of Pk-KatG towards H_2O_2 was marginally activated by 10 mM of Li^+ and NH_4^+ and was partially inhibited by Mg^{2+}, Ca^{2+}, Ba^{2+}, Ni^{2+}, Mn^{2+}, Alum, Na^+, EDTA, SDS, DTT, and PMSF. Complete inhibition of activity was recorded in the presence of β-mercaptoethanol, Co^{2+}, Cd^{2+}, Zn^{2+}, Ag^{+1} and Hg^{2+}. At a final concentration of 1 mM β-mercaptoethanol, Cd^{2+} and Zn^{2+} completely inactivated the enzyme, while all other modulators had a negative but milder effect on the enzyme activity (Figure 51B).

The effect of various activators and inhibitors on enzymatic activity is an important parameter, especially in the case of industrial processes. Such molecules may be present within the water or the other chemicals and solutions utilized in industrial applications or may even result from the corrosion of the equipment used (Pereira *et al.*, 2017). Metal ions can cause structural changes in enzymes by reacting with the amino or carboxyl groups of amino acids and affecting either positively or negatively the enzymatic activity. Heavy metals such as Hg^{2+}, Co^{2+}, Mn^{2+}, Ag^{2+}, Cu^{2+} and Pb^{2+} often form complexes with the catalytic amino acids' active groups and due to their large size, prevent the substrate from reaching the active site (Ishida *et al.*, 1980). Some metals tend to interact with specific residues, such as Cu^{2+} that interacts with histidine and Ba^{2+} that interacts with a series of residues including arginine, glutamine, proline, serine and valine (Bush *et al.*, 2008). Monovalent and divalent ions can also act as electron-pair acceptors (electrophiles), thus helping to stabilize the electron density during the catalytic process or as electron-pair donors (nucleophiles) and as a result have a regulatory role for the active site, helping the recognition and activation of the substrate and enhancing catalysis (Andreini *et al.*, 2008).

Laccase-like multicopper oxidases (LCMOs) have been reported to be affected by metal ions, such as Ca^{2+}, Mn^{2+}, Co^{2+}, Cu^{2+}, Zn^{2+}, Mg^{2+}, Ni^{2+} and Hg^{2+}, but the profiles of inhibition or activation are variable among enzymes (Galai *et al.*, 2009, Si *et al.*, 2015). For instance, Cu^{2+} inhibited SilA from *Streptomyces ipomoea* and activated the LCMO from *S. cyaneus*, Zn^{2+} inhibited LCMO from *S. cyaneus* while it activated *S. psammoticus* LMCO (Niladevi *et al.*,

2008, Molina-Guijarro *et al.*, 2009). It has been proposed that mercury or cobalt can replace the type I copper in MCOs (Larrabee and Spiro, 1979). Interestingly, the presence of 10 mM Hg^{2+} had an activating effect on the enzymatic activity of Pk-CopA. In contrast to our results, mercury (Hg^{2+}) inhibited the ABTS activity of SCLAC from *Streptomyces* sp. even at the concentration of 1 mM (Lu *et al.*, 2013). Unlike Pk-DypB, DypB from *R. jostii* RHA1 was found to show 5.4-fold greater activity in the ABTS assay in the presence of 1 mM $MnCl_2$, suggesting that Mn^{2+} acts as a cofactor or mediator for DypB (Roberts *et al.*, 2011).

EDTA is a chelating agent for various metal ions, such as Cu^{2+} and Fe^{3+} (Oviedo and Rodríguez, 2003). Therefore, EDTA constitutes a common inhibitor of multicopper oxidases and heme-containing peroxidases or catalases-peroxidases, as also observed in our study. Among characterized bacterial MCOs, EDTA has also inhibited LCMOs from *Streptomyces* species (Arias *et al.*, 2003, Endo *et al.*, 2003, Suzuki *et al.*, 2003). Fe(II)-EDTA complexes can also react with H_2O_2 to produce hydroxyl radicals, which may further affect the conformation of the peroxidase Pk-DypB (McCord and Day, 1978).

DTT and β-mercaptoethanol are reducing agents that reduce the disulfide bonds between cysteine residues. Pk-CopA and Pk-KatG contain no disulfide bonds since they only carry one cysteine residue. Pk-DypB contains two cysteine residues, however, the distance between the two cysteines, as predicted by the enzyme's structure are not in close proximity (9.89Å) to form a disulfide bond (data not shown). Nevertheless, in the presence of β-mercaptoethanol Pk-DypB and Pk-KatG had their activities completely hindered, while Pk-CopA was minimally affected. A stronger inhibition effect was observed for Pk-CopA by DTT in comparison to β-mercaptoethanol, which was accordingly milder for Pk-DypB and Pk-KatG. The results suggest that the inhibition mechanism exerted by the reducing agents is different. In fact, it has been previously reported that DTT and β-mercaptoethanol can interact with protein domains in the absence of disulfide bonds, causing slow-reversible inhibitions by chelation of essential metal cofactors (Yang *et al.*, 1996), perhaps also applying in the case of this study.

SDS is a denaturing agent that strongly binds to the positively charged and the hydrophobic residues of proteins through its sulfate groups and alkyl chains, respectively, unfolding the three-dimensional structure of proteins and thereby modifying their functionality (Hansen *et al.*, 2009). PMSF is a protease inhibitor that binds specifically to the active site serine residue in serine proteases. The presence of 10 mM PMSF did not affect the activity of Pk-CopA, while it caused a partial inhibition of Pk-DypB and Pk-KatG (60 and 36% remaining activity, respectively, with control samples performed with ethanol, which was used as a solvent for

PMSF). PMSF is also a general electrophile and could potentially react with exposed nucleophiles in an unfolded or partially unfolded protein.

3.18 Oxidation of lignin-associated aromatic substrates

The recombinant enzymes were tested for their ability to oxidize lignin-associated monoaromatic compounds, shown in Figure 52. Pk-CopA showed higher oxidative activity towards ferulic and caffeic acid, oxidizing 43% and 28% of each substrate correspondingly, following a 24-hour incubation of the enzymatic reaction (Figure 52). Lower oxidizing activity was observed towards vanillic acid (5%) and syringic acid (9%). Pk-DypB showed negligible activity towards caffeic (1%) and vanillic acid (2%). No oxidation effect was observed by Pk-KatG, however, the addition of ABTS in the enzymatic reaction caused the oxidation of the four phenolic acids in a percentage of 40%, 13%, 30% and 13%, respectively, after a 24-hour incubation of the enzymatic reaction. All control samples containing heat-inactivated protein samples showed no changes throughout the corresponding spectra.
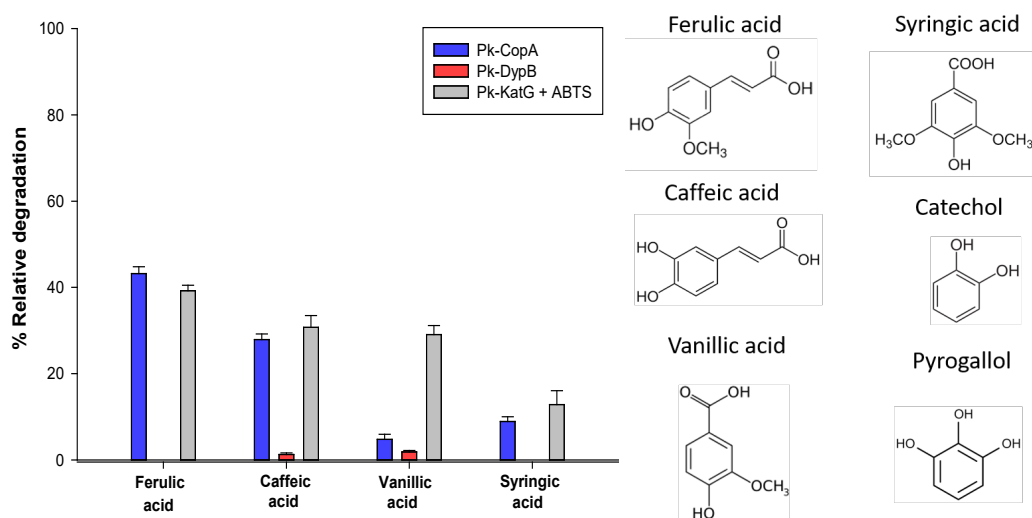
Fig. 52. Oxidative activity of enzymes Pk-CopA, Pk-DypB and Pk-KatG towards lignin-related monoaromatic compounds. Degradation of substrates is expressed as the decrease in absorbance at λmax of each substrate, within a 24-hour incubation of each enzyme at 30 °C, in the dark. Reactions were performed with a 4μM final concentration for caffeic acid and 40 μM for the rest of the substrates, in 100 mM phosphate buffer pH 6.0, supplemented with 0.5 mM $CuCl_2$ for Pk-CopA, 1.0 mM H_2O_2 for Pk-DypB and 10 mM H_2O_2 for Pk-KatG. ABTS was added in Pk-KatG reactions at a final concentration equal to that of each aromatic acid. Control reactions were performed with heat-inactivated enzymes.

Under the influence of Pk-CopA and Pk-KatG, catechol showed a change in color from colorless to brown, with a gradual increase in the absorbance of catechol UV spectrum within

1 h of incubation, while the respective control reactions of heat-inactivated protein did not produce any changes (Figures 53A-B). Pk-KatG was also active against pyrogallol, producing an additional peak at 300 nm in the UV spectrum (Figure 53C), absent from control samples.
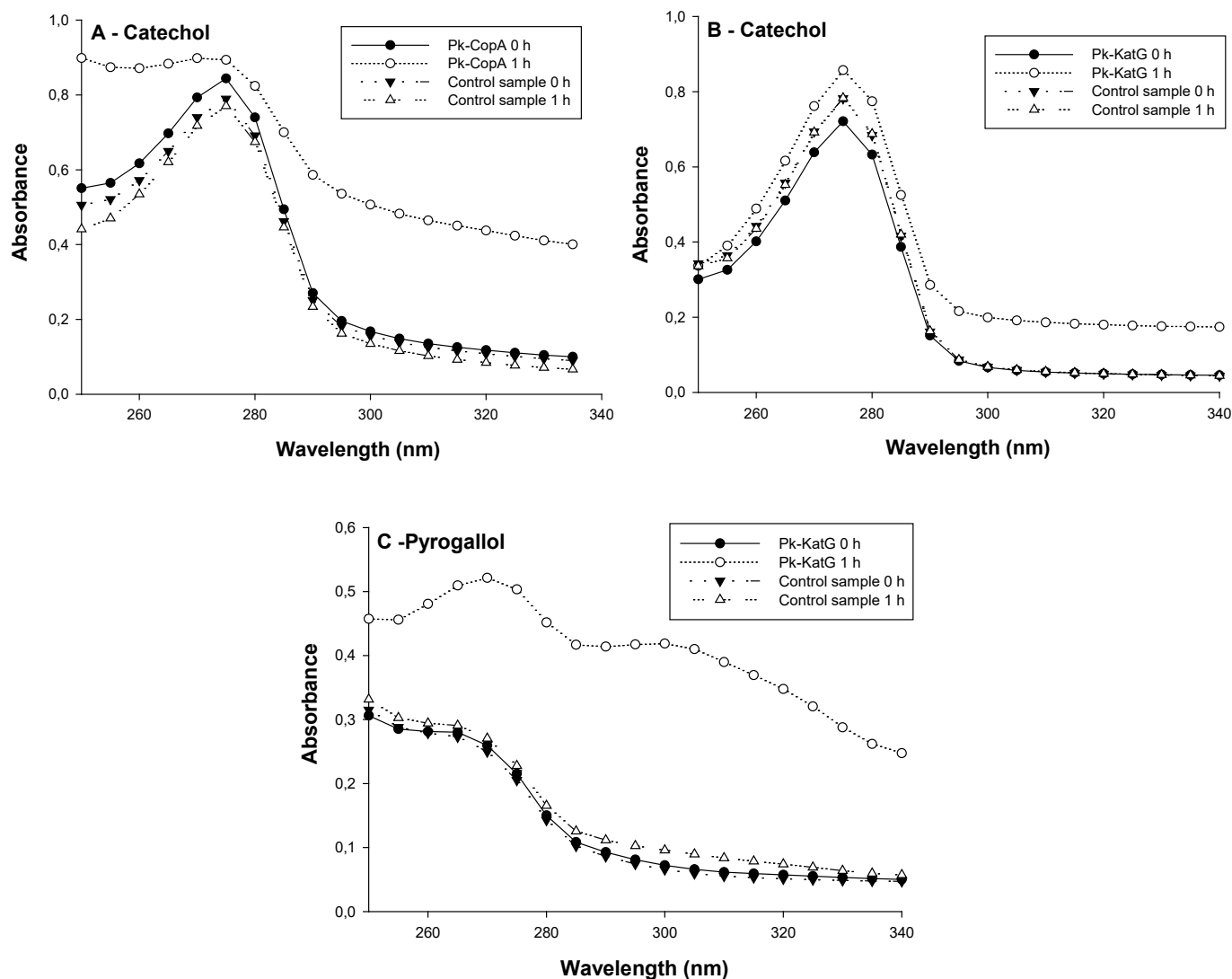
Figure 53. UV spectra of enzymatic reactions of (A): Pk-CopA and (B): Pk-KatG, with catechol and (C): Pk-KatG with pyrogallol, following a one-hour incubation. Reactions were performed at 30 °C, in the dark, in 100 mM phosphate buffer, pH 6.0, supplemented with 0.5 mM $CuCl_2$ for Pk-CopA and 10 mM H_2O_2 for Pk-KatG, with a 200 μM final substrate concentration. Control reactions were performed with heat-inactivated enzymes.

The specific activity of the enzymes towards each substrate was determined (Table 14). The highest specific activity for Pk-CopA was observed towards ferulic acid, and towards pyrogallol for Pk-KatG. The specific activity of Pk-KatG towards pyrogallol was quite higher than that of the catalase-peroxidase of *Synechocystis sp.* PCC 6803 (0.13U/mg).

Table 14. Specific activities of recombinant enzymes towards lignin-related monoaromatic compounds. One Unit of enzyme was defined as the amount of enzyme that catalyzed the conversion of 1 μmol of substrate per minute of reaction. ND: not determined.

Substrate	Specific activity (Units/mg protein)		
	Pk-CopA	Pk-DypB	Pk-KatG + ABTS
Ferulic acid	$0.05 \pm 2 \cdot 10^{-3}$	-	$0.05 \pm$
Caffeic acid	$0.03 \pm 8 \cdot 10^{-3}$	$0.08 \cdot 10^{-2} \pm 4 \cdot 10^{-5}$	$0.02 \cdot 10^{-1} \pm$
Vanillic acid	$0.02 \pm 2 \cdot 10^{-3}$	$0.02 \cdot 10^{-1} \pm 10^{-3}$	$0.04 \pm$
Syringic acid	$0.02 \pm 7 \cdot 10^{-3}$	-	$0.02 \pm$
Catechol	ND	-	ND
Pyrogallol	-	-	3.47

Phenolic compounds are typical substrates for laccases due to their low redox potential, which allows electron abstraction from the hydroxyl groups by the T1 copper site. Specifically, *ortho*-substituted compounds such as caffeic acid, catechol, guaiacol, pyrogallol, gallic acid and protocatechuic acid are good substrates for most laccases, in contrast to *para*- (such as *p*-cresol and hydroquinone) or *meta*-substituted compounds (such as *m*-phenylenediamine, orcinol and resorcinol) (Baldrian, 2006). The removal of one electron can lead to the formation of unstable phenoxy radicals accompanied by reactions such as quinone formation, crosslinking, demethylation and ring cleavage (Chandra and Chowdhary, 2015). An endospore coat protein CotA laccase from *Bacillus licheniformis* was able to oxidize syringic acid to 2,6-dimethoxy-1,4-benzoquinone, but failed to oxidize coumaric, cinnamic and vanillic acid. Reactions of this enzyme with ferulic, caffeic and sinapic acid mainly resulted in the formation of dimerization products (Koschorreck *et al.*, 2008). ***However, this is the first proof of a CopA protein being able to oxidize monoaromatic lignin constituents such as ferulic, caffeic and syringic acid, or catechol***.

Although bacterial dye-decolorizing peroxidases can catalyze the direct oxidation of high redox potential lignin model compounds, such as guaiacyl glycerol-β-guaiacol ether, (Chen and Li, 2016), so far, to our knowledge, activity towards the lignin-associated monoaromatic acids used in this study has not been reported. Our results also suggest that ABTS acted as a redox mediator for the Pk-KatG-catalyzed oxidation of the phenolic acids used in this study. Brown and coworkers had also reported the ABTS mediated oxidation of guaiacylglycerol-β-

guaiacol ether by the catalase-peroxidase Amyco 1 (Brown *et al.*, 2011). The ability of Pk-KatG to react with lignin, in the presence or not of a mediator remains to be investigated.

3.19 Decolorization of synthetic dyes

To assess the oxidative activity of the recombinant enzymes towards compounds with lignin-like structure we used synthetic dyes with aromatic chromophores, classified as azo, triarylmethane, xanthene and anthraquinone dyes (Figure 54).
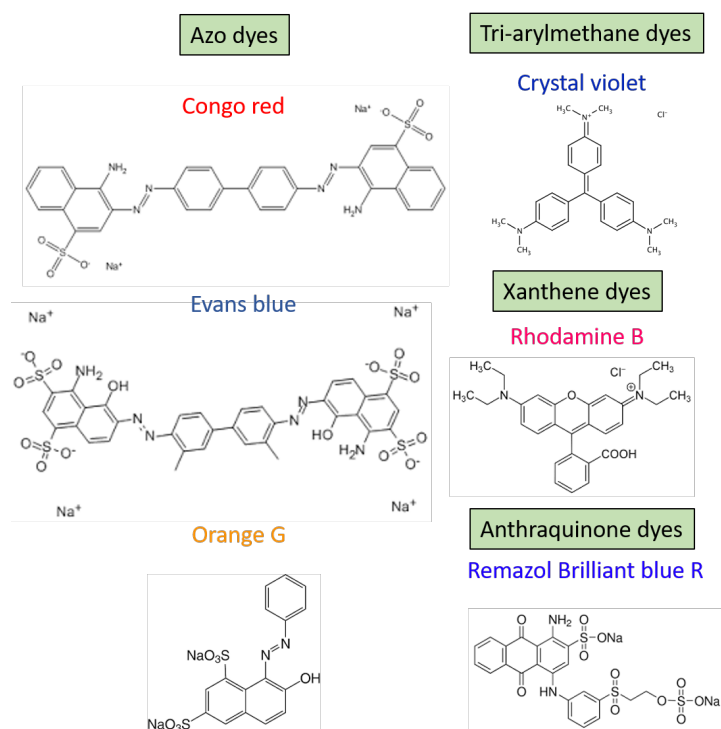
Figure 54. Synthetic dyes used as enzymatic substrates in this study.

Under the assay conditions used in this study (pH 6.0, 30 °C), Pk-CopA could significantly decolorize the azo dyes Congo red (37% decolorization) and Evans blue (19%), within one-hour incubation with each substrate (Figure 55). A lower conversion rate was observed for the triphenylmethane dye Crystal violet (4 %) and the anthraquinone dye Remazol Brilliant blue R (RBBR) (4%). No activity was observed towards the azo dye Orange G or the xanthene dye Rhodamine B. Pk-DypB caused approximately a 3.5% decrease in absorbance of Congo red, Rhodamine B and RBBR. No activity was observed towards Orange G or Crystal violet. Pk-KatG could decolorize Orange G (10%), Evans blue (15%), Rhodamine (42%) and RBBR (11%).
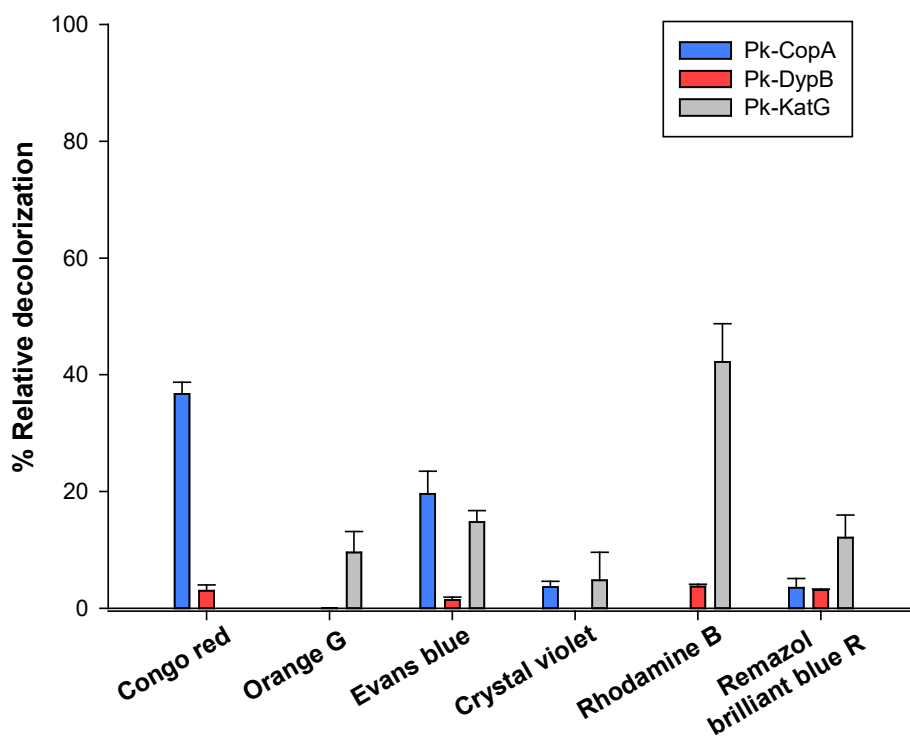
Figure 55. Oxidative activity of enzymes Pk-CopA, Pk-DypB and Pk-KatG towards recalcitrant synthetic dyes. Decolorization of dyes is expressed as the decrease in absorbance at λmax of each substrate, within 1 h of incubation of each enzyme with each substrate, at 30° C, in 100 mM phosphate buffer, pH 6.0, supplemented with either 0.5 mM $CuCl_2$ for Pk-CopA, 1.0 mM H_2O_2 for Pk-DypB or 10 mM H_2O_2 for Pk-KatG. Final concentration of substrates was as follows: Congo red 25μM, Orange G 50μM, Evans Blue, Crystal Violet and Rhodamine B 10μM, Remazol BBR100μM.

The specific activity of the enzymes towards each dye was determined (Table 15). The highest specific activity for enzymes Pk-CopA and Pk-DypB was observed towards Congo red, while for Pk-KatG towards RBBR. One should bear in mind that decolorization rates of dyes may be underestimated in case the product has a similar absorption spectrum (Lončar *et al.*, 2016).

Pk-CopA could decolorize the bis azo dyes Congo red and Evans blue but no decolorization was observed for the mono azo dye Orange G. Perhaps the presence and the location of different functional groups in dye structure affects the degradation of certain dyes. Besides their substrate specificities, the activity of laccases towards reducing substrates correlates with the difference between the substrates' E° and that of laccases' T1 copper atom. Laccases have been shown to decolorize anthraquinone dyes more efficiently than other classes of dyes, due to the lower redox potential of these dyes (Zeng *et al.*, 2011). *Streptomyces psammoticus* LMCO was tested against 10 different dyes, but was effective only for RBBR (Niladevi and Prema, 2008). Cyclic voltammetric experiments would elucidate the redox chemistry of these compounds and the redox potential of the enzymes of this study.

Table 15. Specific activities of recombinant enzymes Pk-CopA, Pk-DypB and Pk-KatG towards synthetic dyes. Specific activities were calculated within one hour of incubation of the enzymes with each dye, in the presence or not of ABTS as a redox mediator. One unit of enzyme was defined as the amount of enzyme that catalyzed the conversion of 1 μmol of substrate per minute of reaction.

Substrate	Specific activity (Units/mg protein)		
	Pk-CopA	Pk-DypB	Pk-KatG
Congo red	$3.0 \cdot 10^{-2}$	$5.3 \cdot 10^{-3}$	-
Orange G	-	-	$5.0 \cdot 10^{-2}$
Evans blue	$9.0 \cdot 10^{-3}$	$1.0 \cdot 10^{-3}$	$2.0 \cdot 10^{-2}$
Crystal violet	$9.5 \cdot 10^{-4}$	-	-
Rhodamine B	-	$6.1 \cdot 10^{-4}$	$2.0 \cdot 10^{-2}$
Remazol Brilliant Blue R	$2.8 \cdot 10^{-3}$	$6.8 \cdot 10^{-4}$	$2.6 \cdot 10^{-1}$

Dyp –type peroxidases owe their name to their ability to decolorize synthetic dyes. Azo, di/tri-arylmethane, xathene, indigoid, carotenoid, anthraquinone and pathalocyanrine dyes constitute substrates of DyPs. Previous studies have shown that anthraquinone-type dyes are more susceptible to biodegradation by dye-decolorizing peroxidases, too (Lončar *et al.*, 2016). Our results do not comply with these results as Pk-DypB showed quite low specific activity towards anthraquinone dye RBBR. DyP protein from *Saccharomonospora viridis* DSM 43017 could decolorize efficiently several triarylmethane dyes, anthraquinonic, and azo dyes under neutral to alkaline conditions (Yu *et al.*, 2014). A Dyp protein from *Pseudmonas aeruginosa* PKE117 displayed maximal activity towards anthraquinone dyes such as RBBR but no enzymatic activity was observed towards azo dyes (Li *et al.*, 2012).

Interestingly, Pk-KatG decolorized structurally different dyes, with a variable decolorization rate and a higher specific activity towards RBBR, although much lower than the specific activity of the typical fungal monofunctional peroxidase of *Pleurotus ostreatus* NFFA (6 U/mg) (Shin *et al.*, 1997). To our knowledge, this is the first report of a catalase-peroxidase's ability to oxidize synthetic dyes, therefore, these results expand the substrate range of catalase-peroxidases towards recalcitrant aromatic dyes. Oxidation of RBBR by Pk-KatG might also be correlated with lignin biodegradation, as it is commonly used as a substrate to evaluate the ligninolytic activity of fungal oxidative enzymes.

3.20 Enzymatic oxidation of lignin from alkali pretreated corn stover

To investigate their lignin-degrading capacity the recombinant enzymes Pk-CopA and Pk-DypB were assayed against lignin hydrolysate from alkali pretreated corn stover (CSLH), and the reactions were analyzed by reverse-phase HPLC. Following incubation of Pk-CopA with CSLH, in the presence of ABTS as a mediator, a time-dependent change was observed in the chromatogram of lignin (Figure 56). Specifically, a peak at 33.5 min corresponding to CSLH was diminished over 16 h, a smaller peak initially present at 35.6 min was absent, while a new peak at 39 min was formed. Incubation of control sample, containing heat-inactivated enzyme, did not yield any significant changes in the chromatogram.

Incubation of Pk-CopA with CSLH, in the absence of ABTS did not produce any changes either (data not shown). Under the conditions studied, the reaction of Pk-DypB with CSLH, in the absence of ABTS, after 1 h of incubation led to a slight reduction of the lignin peak, without yielding any product peaks, yet over 2 h hours of incubation a reconfiguration of this peak was observed. These results were not always confirmed and therefore are omitted. The synergy between enzymes Pk-CopA and Pk-DypB was also investigated by adding the two enzymes in the reaction either in tandem or successively. The results obtained suggested that the activity of Pk-CopA was inhibited by the presence of H_2O_2, which is required for the activity of Pk-DypB (data not shown). Further investigation of the applied conditions is required to address this matter.
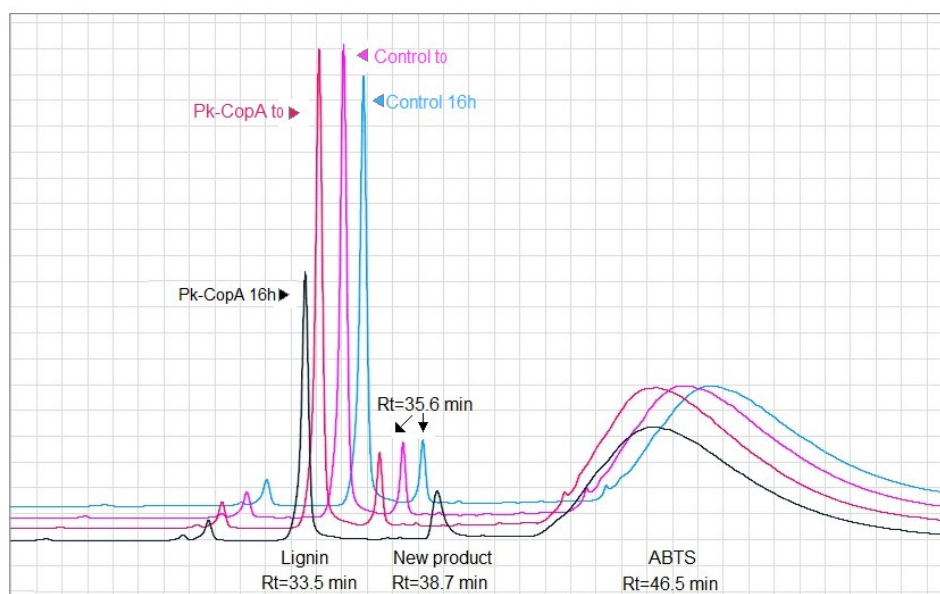
Fig. 56. HPLC chromatogram of the reaction of Pk-CopA with lignin from alkali pretreated corn stover. Enzymatic assays for which results are shown were conducted in the presence of 0.5 mM $CuCl_2$ and 1.25 mM ABTS, in 100 mM phosphate buffer pH 6.0. Control reactions were performed with heat-inactivated enzyme at boiling point for 15 min. Reactions were analyzed using a C18 reverse-phase column with UV detection at 310nm.

ABTS has allowed the oxidation of lignin by Pk-CopA that initially may have been hindered by lignin's lower diffusion into the active site of the enzyme, or its high redox potential. The oxidation of large molecules such as lignin can be inhibited by their high redox potential, or steric hindrance (Bourbonnais and Paice, 1990). It is suggested that laccases first oxidize accessible phenolic moieties in lignin, generating phenoxy radicals, leading to quinone formation, crosslinking, or other reactions (Barreca *et al.*, 2003). Redox mediators, such as ABTS used in this study, are oxidized by laccases and then diffuse in the surrounding medium, causing the oxidation of non-phenolic moieties of lignin, too (Strong and Claus, 2011). This mechanism can lead to other reactions such as peroxygenation, demethoxylation, Cα-Cβ cleavage, or aromatic ring-opening (Xu *et al.*, 1997).

Our work establishes that the multicopper oxidase Pk-CopA can catalyze the oxidation of polymeric lignin derived from alkali pretreated corn stover. Collection of the product formed, and mass spectrometry (MS) analysis will reveal its structure. In fact, during the completion of this work, CopA protein from *P. putida* KT2440 was shown to oxidize Ca-lignosulfonate, a product derived from softwood during the sulfite pulping method for manufacturing paper, thus confirming the oxidative ability of CopA protein towards lignin (Granja-Travez and Bugg, 2018). The reaction of this protein with Ca-lignosulfonate yielded vanillic acid as a product. In the same study, it was proven that CopA from *P. putida* KT2440 and CopA from P. *fluorescens* Pf-5 can oxidize the lignin model compounds guaiacylglycerol-beta-guaiacyl (GGE) and 2,2′-dihydroxy-3,3′-dimethoxy-5,5′-dicarboxybiphenyl (DDVA), yielding oxidized dimerized products.

Bacterial DyPs known to act on polymeric lignin include DyPB from *Rhodococcus jostii* RHA1, and two DyPs from *Pseudomonas fluorescence* Pf-5: DyP1B and DyPA (Ahmad *et al.*, 2011, Rahmanpour and Bugg, 2015). All three enzymes were able to act towards alkali Kraft lignin, however, the identity of any products formed from Kraft lignin is not known. The results of Pk-DypB towards lignin may suggest an initial depolymerization of the substrate countered by repolymerization reactions. Oxidoreductases often catalyze the repolymerization of phenolic compounds (Ghoul and Chebil, 2012). The balance between depolymerization and repolymerization depends on several factors, such as the structure and redox potential of the substrate and the enzyme, and the reaction temperature and pH (Hämäläinen *et al.*, 2018), Thus, a thorough investigation of these parameters is required to analyze the reactions of oxidative enzymes towards polymeric lignin.

3.21 Enzymes and pathways involved in degradation of lignin and lignin-derived aromatic compounds

Bacterial isolate *Pseudomonas kilonensis* ZKA7 was implemented as a research model to elucidate proteins putatively involved in the degradation of lignin and lignin-derived monoaromatic compounds. Annotation and analysis of the ZKA7 genome revealed genes related to pathways for the degradation of ferulate, vanillate, benzoate, protocatechuate, as well as genes that could be ralated to the degradation of xenobiotic compounds such as atrazine, caprolactam, chloroalkenes, chlorobenzene, furfural, toluene and others. To detect differentially expressed proteins a comparative proteomic study was performed on ZKA7 cells grown on lignin hydrolysate from alkali pretreated corn stover (CSLH), ferulic acid, caffeic acid, vanillic acid and acetate (reference sample). Protein samples were withdrawn from each substrate during the middle-late exponential phase and were separated into intracellular and extracellular protein samples (growth curves shown in Appendix Figure A6). Extracellular protein samples derived from lignin cultures could not be further analyzed due to technical reasons associated with lignin's nature, and therefore were not subjected to proteomic analysis. Protein samples were subjected to LC-MS/MS analysis and data were acquired by the SWATH method that allows comprehensive detection and quantitation of even low abundance compounds in complex samples (Gillet *et al.*, 2012).

There were 1794 proteins detected, representing 30% of the total proteins encoded by strain *P. kilonensis* ZKA7, a value that is in accordance with other proteomic studies. Upon normalization of the data and differential expression analysis in individual treatment pairs, 79 proteins were found with statistical significance to be upregulated in lignin, while 98 proteins were downregulated, in comparison to the reference substrate (acetate). Correspondingly, 102 proteins were upregulated and 195 downregulated in ferulic acid, 98 proteins were upregulated and 78 downregulated in caffeic acid, and 101 proteins were upregulated and 161 downregulated in vanillic acid. Scatter plots of differentially expressed proteins in each treatment pair are shown in Figure A7 (Appendix). Analysis of the upregulated intracellular proteins revealed the activation of pathways and mechanisms described below.

Upper and central degradation pathways for lignin and lignin-derived aromatic compounds

Analysis of the differential expression of proteins on all four substrates compared to the reference substrate revealed the upregulation of proteins that form part of the upper catabolic pathway for the catabolism of guaiacyl-type lignin-derived aromatic compounds (G-units). The results indicate that the catabolism of G-units in ZKA7 proceeds through the coenzyme A

(CoA)-dependent non-β-oxidation pathway, conversion into vanillin, and subsequent oxidation of vanillin into vanillic acid. Vanillic acid is then funneled into protocatechuic acid (PCA) *via* demethylation, and degradation of PCA proceeds *via* the 3,4 *ortho*-cleavage pathway. It is interesting that, although ZKA7 carries two copies of the vanillate O-demethylase monooxygenase subunit gene (JGI Locus tags: Ga0244586_2571 and Ga0244586_3190) and three copies of vanillate O-demethylase ferredoxin subunit gene (Ga0244586_2572, Ga0244586_3189 and Ga0244586_3225), only one set of genes was induced (Ga0244586_2571 and Ga0244586_2572). Specific enzymes of the above-mentioned pathways, upregulated in lignin and lignin-derived compound cultures of this study are shown in Figure 57.
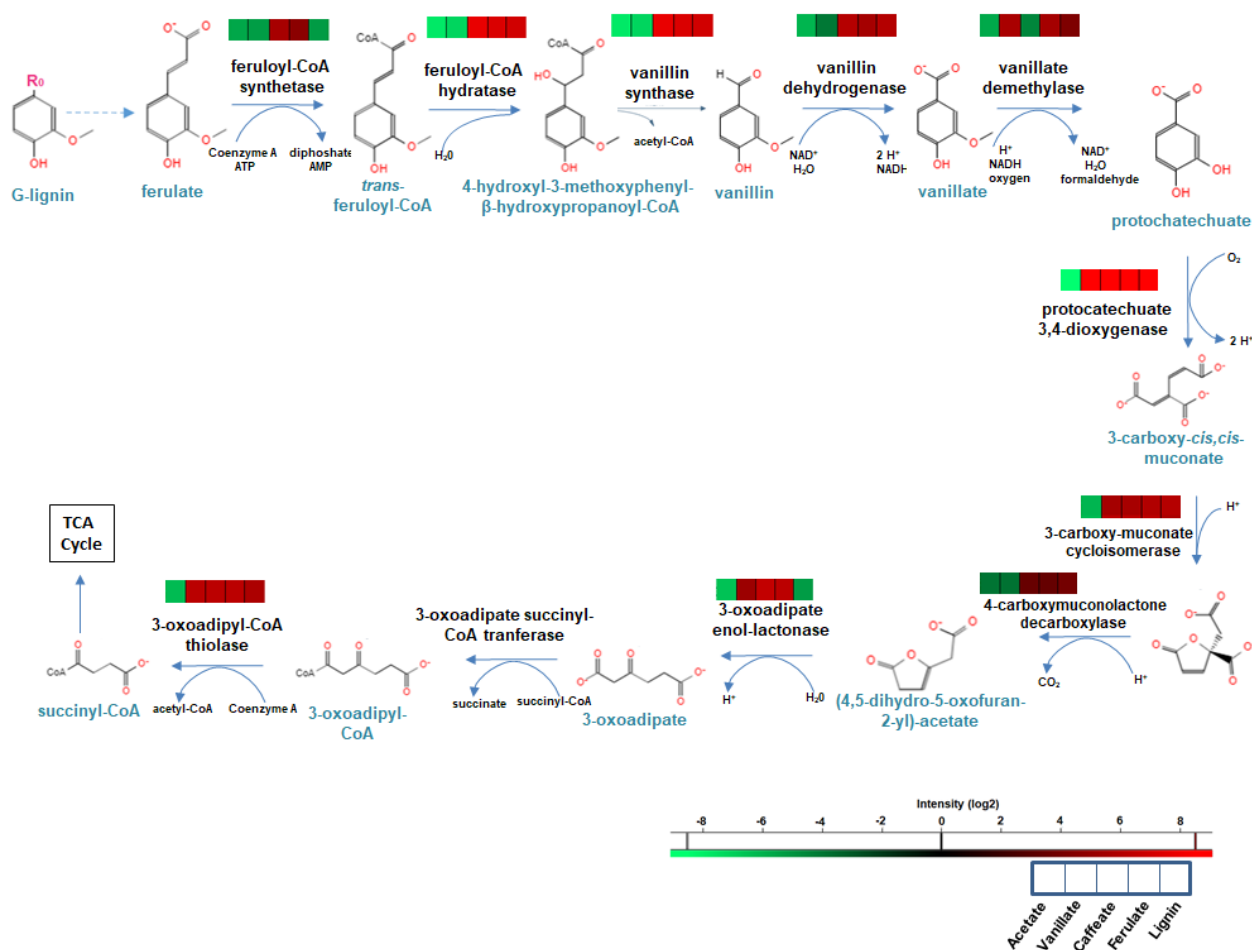
Fig. 57. Proposed metabolic pathway for degradation of lignin from alkali pretreated corn stover and lignin-related aromatic monomers in *Pseudomonas kilonensis* ZKA7. Differential expression of relevant enzymes is shown by heatmaps. Colors represent the Log2 Fold change (i.e. the ratio of each protein's expression level between each substrate and the reference substrate). The proposed pathway involves degradation of guaiacyl units via coenzyme A (CoA)-dependent non-β-oxidation pathway and ring cleavage of protocatechuate *via* the 3,4 *ortho*-cleavage pathway.

One of the most heavily induced genes in all substrates was the gene encoding the alpha and beta subunits of protocatechuate 3,4-dioxygenase, those encoding 3-carboxy-cis,cis-muconate cycloisomerase, vanillin synthase /trans-feruloyl-CoA hydratase and the alpha and beta subunits of glutaconate CoA-transferase (Table 16). Non-activation of the enzymes feruloyl-CoA synthetase and hydratase, vanillin synthase and dehydrogenase, upstream of vanillate formation, further supports the validity of these findings.

Table 16. Top five upregulated proteins in lignin and lignin-derived monoaromatic compounds.

Substrate	Protein	Fold change	JGI Locus Tag
Lignin	protocatechuate 3,4-dioxygenase alpha subunit	114	Ga0244586_4176
	vanillin synthase /trans-feruloyl-CoA hydratase	55	Ga0244586_2712
	glutaconate CoA-transferase subunit A	27	Ga0244586_4180
	3-oxoadipyl-CoA thiolase	22	Ga0244586_4178
	protocatechuate 3,4-dioxygenase beta subunit	21	Ga0244586_6136
Ferulate	protocatechuate 3,4-dioxygenase beta subunit	560	Ga0244586_4177
	3-carboxy-cis,cis-muconate cycloisomerase	500	Ga0244586_4174
	p-hydroxybenzoate 3-monooxygenase	184	Ga0244586_4258
	glutaconate CoA-transferase subunit B	100	Ga0244586_4179
	vanillate O-demethylase monooxygenase subunit	100	Ga0244586_2571
Caffeate	3-carboxy-cis,cis-muconate cycloisomerase	370	Ga0244586_4174
	protocatechuate 3,4-dioxygenase beta subunit	275	Ga0244586_4177
	glutaconate CoA-transferase subunit B	210	Ga0244586_4179
	vanillin dehydrogenase	42	Ga0244586_2711
	LSU ribosomal protein L35P	25	Ga0244586_1533
Vanillate	3-carboxy-cis,cis-muconate cycloisomerase	500	Ga0244586_4174
	vanillate O-demethylase ferredoxin subunit	430	Ga0244586_2572
	p-hydroxybenzoate 3-monooxygenase	130	Ga0244586_4258
	dihydropyrimidinase	70	Ga0244586_1973
	glutaconate CoA-transferase subunit B	53	Ga0244586_4179

Transport proteins

Two outer membrane OprD family porins were induced in lignin and caffeate grown cells (genes Ga0244586_5899, Ga0244586_2714) and a third one was also induced in ferulic acid grown cells (gene Ga0244586_4171). Proteins belonging to the outer membrane porin D family (OprD) are assumed to be involved in the passive diffusion of various aromatic compounds across the outer membrane of Gram-negative bacteria (Tamber *et al.*, 2006). Specifically, the Ga0244586_4171 gene encodes a PCA importer gene *pca*K, found in the protocatechuic acid catabolic cluster, and may be transcribed along with PCA-utilization genes or may be actively involved in the uptake of ferulic acid. A tripartite ATP-independent transporter belonging to DctP family (Ga0244586_2347) was also induced in ferulic, caffeic and vanillic acid cultures. The tripartite ATP-independent periplasmic (TRAP) transporters are unidirectional secondary transporters with a broad substrate specificity (Mulligan *et al.*, 2011). Their involvement in the active transport of p-coumarate, caffeate, ferulate and cinnamate across the inner membrane of *Rhodopseudomonas palustris* CGA009 has been

reported (Salmon *et al.*, 2013). Our results indicate that this protein may also be implicated in the transport of vanillate. Another protein whose expression was upregulated in vanillate in this study was a mechanosensitive ion channel-like protein (Ga0244586_3714). Transporters belonging to the ATP-binding cassette transporters superfamily (ABC transporters) were also induced in all four substrates of this study, in accordance with previous studies (MacLean *et al.*, 2011, Michalska *et al.*, 2012).

Transcriptional regulators

A transcriptional regulator belonging to the MarR family (Ga0244586_2713) was induced in ZKA7 cells grown on lignin, ferulic and caffeic acid. This protein is located upstream of the operon (ferBA operon) that encodes the genes responsible for ferulate metabolism (*fcs*, *ech*). Homologs of this transcriptional regulator have been previously shown to regulate the transcription of the ferBA operon in bacteria such as *Sphingomonas paucimobilis* SYK-6, *Pseudomonas fluorescens* BF13, *Rhodococcus jostii* RHA1 and *Corynebacterium glutamicum* ATCC (Calisti *et al.*, 2008, Kasai *et al.*, 2012, Otani *et al.*, 2014, Kallscheuer *et al.*, 2016). A MarR family transcriptional regulator was induced in ferulate, caffeate and vanillate cultures of this study (Ga0244586_3981), however, its genomic position gives no further information of controlling the expression of a specific catabolic gene. A transcriptional factor belonging to the XRE family (Ga0244586_5799) was also induced in ferulate cultures. Members of this family have been shown to be involved in resistance mechanisms towards oxidative stress (Hu *et al.*, 2019).

Stress response and detoxification proteins

Several stress response proteins were overexpressed on cells grown on lignin and on monoaromatic substrates. Proteins induced on lignin include a protein refolding chaperone of the Spy/CpxP family (Ga0244586_0808), two catalases (Ga0244586_0970 and Ga0244586_0063), a peroxiredoxin (Ga0244586_1926) and a methyl-accepting chemotaxis protein (Ga0244586_5111). An efflux transporter belonging to the Resistance-Nodulation-Division (RND) family (Ga0244586_4224) was also induced in lignin grown cells and a protein annotated as membrane fusion protein associated with the multidrug efflux system (Ga0244586_4166) was upregulated in caffeic acid grown cells. Universal stress protein A (Ga0244586_3643) and two different putative cold-shock DNA-binding proteins (Ga0244586_0745 and Ga0244586_4429) were upregulated in both ferulic and caffeic grown

cells. The expression of a 1-Cys peroxiredoxin was also increased in caffeic acid. Peroxiredoxins (Prxs) constitute a large family of thiol-dependent peroxidases that protect bacteria from H_2O_2 (Kaihami *et al.*, 2014). In vanillate, among stress-induced proteins were a heat shock protein Hsp33 chaperone (Ga0244586_5241), and three different chemotaxis-associated proteins (Ga0244586_5111 Ga0244586_3916 and Ga0244586_3654). These results confirm the fact that aromatic substrates used in this study can serve as potential bacterial carbon sources but also as cellular stressors.

Other proteins

Several dehydrogenases were induced in all four substrates, such as a pyruvate dehydrogenase, a NAD(P)-dependent dehydrogenase, an acyl-CoA dehydrogenase, a flavin-dependent dehydrogenase, a butyryl-CoA dehydrogenase, aldehyde dehydrogenases, a FAD/FMN-containing dehydrogenase, a glutaryl-CoA dehydrogenase, cytochrome c related proteins and many others. Proteins whose function has not been annotated were also induced in these substrates. Interestingly, the protein Ga0244586_2747, which was originally not annotated and was almost 50 times upregulated in caffeate and vanillate cultures, shares a high identity with an uncharacterized periplasmic protein of *P. fluorescens* F113, putatively involved in iron transport.

To conclude, this proteomic study proves that the upper aromatic catabolic pathway for degradation of guaiacyl type lignin units and subsequently the central pathway for cleavage of aromatic compounds can be induced in cells of *Pseudomonas kilonensis* ZKA7 grown on a lignin substrate generated through a mild alkaline pretreatment of plant biomass. Proteomic studies on bacterial lignin degradation are limited, and up to now have used commercially available lignin preparations (Kumar *et al.*, 2017, Lin *et al.*, 2019). Further analysis of the data produced by this proteomic analysis is required to unravel the expression profile of ZKA7 cells grown on lignin substrates.

3.22 Genomic sequencing of lignin-degrading bacterial strains

During this study, the genomes of 15 bacterial strains, able to grow on lignin or lignin-derived aromatic compounds, have been sequenced for a future comparative genomic analysis, along with genome sequences from well-known bacterial lignin degraders. This whole-genome shotgun project has been deposited at NCBI under Accession no. PRJNA580915.

Bacterial strain	NCBI Reference sequence
Pseudomonas plecoglossicida ZKA3	NZ_RBLH00000000.1
Pseudomonas kilonensis ZKA7	NZ_QEKL00000000
Cellulomonas hominis ZKA19	NZ_JACCAG000000000.1
Rhodococcus pyridinivorans ZKA33	NZ_RAPW00000000.1
Pseudomonas putida ZKA37	NZ_QXDD00000000.1
Microbacterium trichothecenolyticum ZKA46	NZ_QTTZ00000000.1
Cellulosimicrobium cellulans ZKA48	NZ_QUMZ00000000.1
Rhodococcus pyridinivorans ZKA49	NZ_RAPW00000000.1
Pseudomonas pseudoalcaligenes ZKA50	NZ_JACCCX000000000.1
Pseudomonas kunmingensis ZKA55	NZ_JACCAJ000000000.1
Pseudomonas sp. ZKA12	Pending
Pseudomonas sp. ZKA5	Pending
Pseudomonas sp. ZKA21	Pending
Pseudomonas sp. ZKA39	Pending
Stenotrophomonas sp. ZKA40	Pending

Final conclusions

The aim of this Ph.D. thesis was to study the functional microbial diversity of the unique environment in Keri Lake at Zakynthos Island to (i) discover novel bacteria with the ability to degrade lignin and plant polysaccharides, (ii) identify efficient hydrolytic and oxidative enzymes with robust activity towards lignocellulose and (iii) elucidate the mechanisms of lignin degradation. The obtained knowledge is expected to contribute to the efforts towards the development of efficient biocatalysts (both enzymatic and microbial) for the efficient valorization of residual lignocellulosic biomass and production of lignin-based high-added value chemicals.

Keri area represents a unique ecosystem in Greece, due to the long-term presence of natural asphalt springs and the decay of plant biomass, providing a natural habitat for the proliferation of aromatics and polysaccharide degrading microorganisms. The enrichment strategy employed for the isolation of bacterial lignocellulose degraders from this environment, yielded a wide diversity of *Pseudomona*s species from the cultures with organosolv lignin as sole carbon source, as well as diverse Actinobacteria, Proteobacteria, Bacilli, Sphingobacteriia and Flavobacteria species from the corresponding cultures with amorphous cellulose and xylan.

A series of screening growth tests on industrial lignin substrates, lignin-derived aromatic substances, and cellulosic and hemicellulosic substrates has highlighted the ability of several individual strains to utilize several of these substrates as a sole carbon and energy source. Screening on xylan and amorphous and microcrystalline cellulose has revealed the distinctive potential of isolates belonging to genera such as *Pseudomonas*, *Advenella*, *Fictibacillus*, *Ochrobactrum*, *Paracoccus* and *Shinella* to produce an array of cellulases such as endo-1,4-β-glucanases, β-glucosidases and exoglucanases and of xylanases such as endo-β-1,4-xylanases and β-xylosidases, for many of which no biochemical characterization exists in literature. Five *Pseudomonas* strains were able to utilize industrial organosolv lignin as a sole carbon and energy source, providing one of the few reports of the utilization of this substrate and suggesting the potential of applying these strains in an organosolv lignin valorization scheme.

A lignin hydrolysate was generated from agricultural residues of corn stover and wheat straw, by implementing a mild alkali pretreatment method. Characterization of the lignin hydrolysates revealed typical structural features of lignin preparations and very low sugar content. Screening of bacterial isolates on these substrates proved that both sources could

support the growth of certain bacterial isolates, featuring the isolates' potential to proliferate in a lignin substrate produced through a biorefinery-scale pretreatment process, deprived of extra carbon sources and without the need to remove any potential inhibitors. Screening on lignin-derived aromatic substances also revealed the ability of several *Pseudomonas* strains to assimilate hydroxycinnamates, such as ferulate, caffeate, and vanillic acid. The results also highlight the ability of a certain strain, *Pseudomonas* sp. ZKA12, to assimilate a wider range of lignin-derived aromatics, with guaiacyl and syringyl nuclei, providing a source for future studies on designing a single microbe with multiple catabolic pathways for lignin degradation. Strain *Pseudomonas kilonensis* ZKA7 was distinguished due to its ability to efficiently grow on lignin hydrolysate from corn stover, its ability to grow in organosolv lignin and degrade the aromatic monomers ferulic, caffeic and vanillic acid. NMR analysis revealed that strain *Pseudomonas kilonensis* ZKA7 was also able to generate structural modifications in corn stover lignin hydrolysate, arising from degradation of lignin aromatic moieties, proving that it can utilize the aromatic constituents of a lignin feedstock.

The proteomic profiling of strain *Pseudomonas kilonensis* ZKA7 proves that the genes involved in the mechanism for degradation of guaiacyl type lignin monomers are functionally active and significantly induced in the presence of corn stover lignin hydrolysate as a sole carbon and energy source. The induction of the same pathway in cells grown on guaiacyl type monomers and lignin degradation intermediates clearly corroborated this finding. The results also feature a significant induction of genes encoding transporter proteins that may be actively involved in the transport of lignin-derived monoaromatic compounds, and genes involved in detoxification mechanisms required for survival of cells under the potentially toxic environment of aromatic compounds.

Three novel lignin related oxidoreductases were selected from the genome of strain *P. kilonensis* ZKA7 and functionally expressed in *Escherichia coli*: a multicopper oxidase, Pk-CopA, a dye-decolorizing peroxidase, Pk-DypB, and a catalase-peroxidase, Pk-KatG. The biochemical characterization of the recombinant multicopper oxidase Pk-CopA, revealed properties of a laccase-like multicopper oxidase. Pk-CopA was able to oxidize lignin prepared from alkali pretreated corn stover, in the presence of ABTS as a mediator, and generate a new product, whose structure will be elucidated in future studies. What is more, this study expands the substrate range of this enzyme towards lignin-derived monoaromatic compounds such as ferulic acid, caffeic acid, syringic acid and catechol. Pk-CopA also presented activity at a wider and more alkaline pH range than other characterized bacterial laccases, tolerance to temperatures as high as 60 ° C, stability at alkaline pH, and resistance to well-known

enzymatic inhibitors. Such features are considered important for the industrial application of enzymes with lignin oxidative activity, and provide the basis for future improvement efforts, raising the possibility to overcome other enzymes in industrial suitability.

The biochemical characterization of the dye-decolorizing peroxidase Pk-DypB revealed its oxidative activity towards ABTS, a typical substrate for oxidoreductases, and its ability to act at a wider and higher pH range than other bacterial dyp-type peroxidases. However, its stability at alkaline pH and higher temperatures was poorer than other functionally similar enzymes. Under the conditions implemented in this study, no lignin oxidative activity was observed for this enzyme, while oxidation of lignin-associated monoaromatic compounds or aromatic synthetic dyes was minimal.

The recombinant catalase-peroxidase Pk-KatG exhibited both catalase and peroxidase activity though it had a higher affinity and catalytic efficiency towards peroxidase substrates than the natural catalase substrate, H_2O_2. The results also provided the first proof of syringaldazine oxidation by a catalase-peroxidase, which is a typical substrate for established ligninolytic enzymes. Furthermore, this is the first report of a catalase-peroxidase oxidation of the aromatic monomers catechol and pyrogallol, mediated by the presence of ABTS. These results, combined with the enzyme's ability to oxidize synthetic aromatic dyes and specifically Remazol Brilliant Blue R, a substrate used to detect ligninolytic activity, may indicate oxidative activity against lignin, too. This hypothesis remains to be investigated.

Future prospects

Biological lignin valorization is a new and challenging biotechnological field, with tremendous application potential. The present work has provided a solid contribution to this field, by the isolation of a set of bacteria that can grow and modify lignin and lignin related compounds. These strains, along with their genomes, metabolic pathways and enzymes represent a valuable toolset for efficient and economically sustainable lignin valorization that can fuel a number of diverse future research directions.

In this respect, the genetic basis of the 15 lignin-degrading bacterial isolates of this study should be elucidated through a comparative genomic analysis with other known bacterial lignin degraders. The analysis will aid the designing, through synthetic biology tools, of a single isolate able to assimilate diverse lignin-derived aromatic compounds and efficiently produce high-added value compounds.

The proteomic profiling of strain *Pseudomonas kilonensis* ZKA7 should also be further analyzed to elucidate genes whose expression was induced but their function is not yet properly understood. Genes whose expression was downregulated should also be analyzed, as well as interactions between differentially expressed proteins. The results of this proteomic analysis can be further supported by a transcriptomic and metabolomic analysis that may also reveal the production of valuable metabolites.

The above analyses are expected to benefit from a more detailed structural analysis of the lignin hydrolysates prior to and after bacterial treatment that will further reveal the properties of the substrate and elucidate the structural changes mediated by the bacterial isolates.

As far as the enzymes are concerned, the recombinant enzyme Pk-CopA can be further evaluated for its potential application in a lignin valorization scheme, by standardizing the conditions under which it reacts with lignin hydrolysates, and elucidating the structure of the product(s) generated by this reaction. Its substrate range should be investigated towards different lignin-derived compounds and a structure-to-function analysis may contribute to further improvement of its properties. A comparison with commercial enzymes will further assess its potential for industrial applications. The lignin oxidating activity of Pk-KatG must also be investigated.

References

"IEA Bioenergy Task 42 (2009) Biorefineries: adding value to the sustainable utilisation of biomass."

Abdelaziz, O. Y., D. P. Brink, J. Prothmann, K. Ravi, M. Sun, J. García-Hidalgo, M. Sandahl, C. P. Hulteberg, C. Turner, G. Lidén and M. F. Gorwa-Grauslund (2016). "Biological valorization of low molecular weight lignin." *Biotechnol Adv* 34(8): 1318-1346.

Abe, T., E. Masai, K. Miyauchi, Y. Katayama and M. Fukuda (2005). "A tetrahydrofolate-dependent O-demethylase, LigM, is crucial for catabolism of vanillate and syringate in Sphingomonas paucimobilis SYK-6." *J Bacteriol* 187(6): 2030-2037.

Adaikkalam, V. and S. Swarup (2005). "Characterization of copABCD operon from a copper-sensitive Pseudomonas putida strain." *Can J Microbiol* 51(3): 209-216.

Aebi, H. (1984). [13] Catalase in vitro. Methods in Enzymology, Academic Press. **105:** 121-126.

Ahmad, M., J. N. Roberts, E. M. Hardiman, R. Singh, L. D. Eltis and T. D. H. Bugg (2011). "Identification of DypB from *Rhodococcus jostii* RHA1 as a Lignin Peroxidase." *Biochemistry* 50(23): 5096-5107.

Ahmad, M., C. R. Taylor, D. Pink, K. Burton, D. Eastwood, G. D. Bending and T. D. Bugg (2010). "Development of novel assays for lignin degradation: comparative analysis of bacterial and fungal lignin degraders." *Molecular Biosystems* 6(5): 815-821.

Akiyama, T., K. Magara, Y. Matsumoto, G. Meshitsuka, A. Ishizu and K. Lundquist (2000). "Proof of the presence of racemic forms of arylglycerol-B-aryl ether structure in lignin: studies on the stereo structure of lignin by ozonation." *Journal of Wood Science* 46(5): 414-415.

Alcalde, M. (2007). Laccases: Biological Functions, Molecular Structure and Industrial Applications. Industrial Enzymes: Structure, Function and Applications. J. Polaina and A. P. MacCabe. Dordrecht, Springer Netherlands**:** 461-476.

Alvira, P., E. Tomás-Pejó, M. Ballesteros and M. J. Negro (2010). "Pretreatment technologies for an efficient bioethanol production process based on enzymatic hydrolysis: A review." *Bioresour Technol* 101(13): 4851-4861.

Andreini, C., I. Bertini, G. Cavallaro, G. L. Holliday and J. M. Thornton (2008). "Metal ions in biological catalysis: from enzyme databases to general principles." *JBIC Journal of Biological Inorganic Chemistry* 13(8): 1205-1218.

Arias, M. E., M. Arenas, J. Rodriguez, J. Soliveri, A. S. Ball and M. Hernandez (2003). "Kraft pulp biobleaching and mediated oxidation of a nonphenolic substrate by laccase from *Streptomyces cyaneus* CECT 3335." *Appl Environ Microbiol* 69(4): 1953-1958.

Arregui, L., M. Ayala, X. Gómez-Gil, G. Gutiérrez-Soto, C. E. Hernández-Luna, M. Herrera de los Santos, L. Levin, A. Rojo-Domínguez, D. Romero-Martínez, M. C. N. Saparrat, M. A. Trujillo-Roldán and N. A. Valdez-Cruz (2019). "Laccases: structure, function, and potential application in water bioremediation." *Microbial Cell Factories* 18(1): 200.

Asina, F. N. U., I. Brzonova, E. Kozliak, A. Kubátová and Y. Ji (2017). "Microbial treatment of industrial lignin: Successes, problems and challenges." *Renewable and Sustainable Energy Reviews* 77: 1179-1205.

Avramidis, P., S. Kalaitzidis, G. Iliopoulos, P. Papadopoulou, K. Nikolaou, S. Papazisimou, K. Christanis and G. J. van Wijngaarden (2017). "The so called 'Herodotus Springs' at 'Keri Lake' in Zakynthos Island western Greece: A palaeoenvironmental and palaeoecological approach." *Quaternary International* 439: 37-51.

Aziz, R. K., D. Bartels, A. A. Best, M. DeJongh, T. Disz, R. A. Edwards, K. Formsma, S. Gerdes, E. M. Glass, M. Kubal, F. Meyer, G. J. Olsen, R. Olson, A. L. Osterman, R. A. Overbeek, L. K. McNeil, D. Paarmann, T. Paczian, B. Parrello, G. D. Pusch, C. Reich, R. Stevens, O. Vassieva, V. Vonstein, A. Wilke and O. Zagnitko (2008). "The RAST Server: rapid annotations using subsystems technology." *BMC Genomics* 9: 75.

Baldrian, P. (2006). "Fungal laccases – occurrence and properties." *FEMS Microbiology Reviews* 30(2): 215-242.

Bandounas, L., N. Wierckx, J. de Winde and H. Ruijssenaars (2011). "Isolation and characterization of novel bacterial strains exhibiting ligninolytic potential." *BMC Biotechnology* 11(1): 94.

Banka, A. L., S. A. Guralp and E. Gulari (2014). "Secretory expression and characterization of two hemicellulases, xylanase, and β-xylosidase, isolated from Bacillus subtilis M015." *Appl Biochem Biotechnol* 174(8): 2702-2710.

Barabote, R. D., J. V. Parales, Y.-Y. Guo, J. M. Labavitch, R. E. Parales and A. M. Berry (2010). "Xyn10A, a thermostable endoxylanase from Acidothermus cellulolyticus 11B." *Appl Environ Microbiol* 76(21): 7363-7366.

Barder, M. J. and D. L. Crawford (1981). "Effects of carbon and nitrogen supplementation on lignin and cellulose decomposition by a Streptomyces." *Can J Microbiol* 27(8): 859-863.

Barreca, A., M. Fabbrini, C. Galli, P. Gentili and S. Ljunggren (2003). "Laccase/mediated oxidation of a lignin model for improved delignification procedures." *Journal of Molecular Catalysis B: Enzymatic* 26: 105-110.

Batista, R. (2014). Uses and Potential Applications of Ferulic Acid**:** 39-70.

Bauer, S., H. Sorek, V. D. Mitchell, A. B. Ibáñez and D. E. Wemmer (2012). "Characterization of Miscanthus giganteus Lignin Isolated by Ethanol Organosolv Process under Reflux Condition." *J Agric Food Chem* 60(33): 8203-8212.

Bayer, E. A., J. P. Belaich, Y. Shoham and R. Lamed (2004). "The cellulosomes: multienzyme machines for degradation of plant cell wall polysaccharides." *Annu Rev Microbiol* 58: 521-554.

Bayer, E. A., H. Chanzy, R. Lamed and Y. Shoham (1998). "Cellulose, cellulases and cellulosomes." *Curr Opin Struct Biol* 8(5): 548-557.

Beckham, G. T. (2018). Lignin Valorization: Emerging Approaches, London, UK: The Royal Society of Chemisty (RSC); National Renewable Energy Lab. (NREL), Golden, CO (United States).

Beckham, G. T., C. W. Johnson, E. M. Karp, D. Salvachúa and D. R. Vardon (2016). "Opportunities and challenges in biological lignin valorization." *Current Opinion in Biotechnology* 42: 40-53.

Beeson, W. T., V. V. Vu, E. A. Span, C. M. Phillips and M. A. Marletta (2015). "Cellulose degradation by polysaccharide monooxygenases." *Annu Rev Biochem* 84: 923-946.

Bekiari, V. and P. Avramidis (2014). "Data quality in water analysis: validation of combustion-infrared and combustion-chemiluminescence methods for the simultaneous determination of Total Organic Carbon (TOC) and Total Nitrogen (TN)." *International Journal of Environmental Analytical Chemistry* 94(1): 65-76.

Belda, E., R. G. van Heck, M. Jose Lopez-Sanchez, S. Cruveiller, V. Barbe, C. Fraser, H. P. Klenk, J. Petersen, A. Morgat, P. I. Nikel, D. Vallenet, Z. Rouy, A. Sekowska, V. A. Martins Dos Santos, V. de Lorenzo, A. Danchin and C. Medigue (2016). "The revisited genome of Pseudomonas putida KT2440 enlightens its value as a robust metabolic chassis." *Environ Microbiol* 18(10): 3403-3424.

Berg, J. M., J. L. Tymoczko and L. Stryer (2012). Biochemistry. New York, N.Y, W. H. Freeman and Company.

Bertrand, T., N. A. Eady, J. N. Jones, Jesmin, J. M. Nagy, B. Jamart-Grégoire, E. L. Raven and K. A. Brown (2004). "Crystal structure of Mycobacterium tuberculosis catalase-peroxidase." *J Biol Chem* 279(37): 38991-38999.

Biermann, C. J. (1996). 3 - Pulping Fundamentals. Handbook of Pulping and Papermaking (Second Edition). C. J. Biermann. San Diego, Academic Press**:** 55-100.

Biswas, S., M. M. Mohammad, L. Movileanu and B. van den Berg (2008). "Crystal Structure of the Outer Membrane Protein OpdK from Pseudomonas aeruginosa." *Structure* 16(7): 1027-1035.

Bourbonnais, R., D. Leech and M. G. Paice (1998). "Electrochemical analysis of the interactions of laccase mediators with lignin model compounds." *Biochim Biophys Acta* 1379(3): 381-390.

Bourbonnais, R. and M. G. Paice (1990). "Oxidation of non-phenolic substrates. An expanded role for laccase in lignin biodegradation." *FEBS Lett* 267(1): 99-102.

Bourne, Y. and B. Henrissat (2001). "Glycoside hydrolases and glycosyltransferases: families and functional modules." *Curr Opin Struct Biol* 11(5): 593-600.

Bowyer, Q. N. a. J. (2017). Global Production of second generation biofuels: Trends and influences. DOVETAIL PARTNERS, INC.

Bracmort, K. (2019). "The Renewable Fuel Standard (RFS): An Overview." *Congressional Research Service Report prepeared for Members and Committees of Congress*.

Bradford, M. M. (1976). "A rapid and sensitive method for the quantitation of microgram quantities of protein utilizing the principle of protein-dye binding." *Analytical Biochemistry* 72: 248-254.

Brink, D. P., K. Ravi, G. Liden and M. F. Gorwa-Grauslund (2019). "Mapping the diversity of microbial lignin catabolism: experiences from the eLignin database." *Appl Microbiol Biotechnol* 103(10): 3979-4002.

Brown, M. E. and M. C. Y. Chang (2014). "Exploring bacterial lignin degradation." *Current Opinion in Chemical Biology* 19(0): 1-7.

Brown, M. E., M. C. Walker, T. G. Nakashige, A. T. Iavarone and M. C. Chang (2011). "Discovery and characterization of heme enzymes from unsequenced bacteria: application to microbial lignin degradation." *J Am Chem Soc* 133(45): 18006-18009.

Brunel, F. and J. Davison (1988). "Cloning and sequencing of Pseudomonas genes encoding vanillate demethylase." *J Bacteriol* 170(10): 4924-4930.

Bugg, T. D. H., M. Ahmad, E. M. Hardiman and R. Rahmanpour (2011). "Pathways for degradation of lignin in bacteria and fungi." *Natural Product Reports* 28(12): 1883-1896.

Bugg, T. D. H., M. Ahmad, E. M. Hardiman and R. Singh (2011). "The emerging role for bacteria in lignin degradation and bio-product formation." *Current Opinion in Biotechnology* 22(3): 394-400.

Bugg, T. D. H. and R. Rahmanpour (2015). "Enzymatic conversion of lignin into renewable chemicals." *Current Opinion in Chemical Biology* 29: 10-17.

Bush, M. F., J. Oomens, R. J. Saykally and E. R. Williams (2008). "Effects of Alkaline Earth Metal Ion Complexation on Amino Acid Zwitterion Stability: Results from Infrared Action Spectroscopy." *J Am Chem Soc* 130(20): 6463-6471.

Calandrelli, V., A. Gambacorta, I. Romano, V. Carratore and L. Lama (2008). "A novel thermo-alkali stable catalase–peroxidase from Oceanobacillus oncorhynchi subsp. incaldaniensis: purification and characterization." *World Journal of Microbiology and Biotechnology* 24(10): 2269.

Calisti, C., A. G. Ficca, P. Barghini and M. Ruzzi (2008). "Regulation of ferulic catabolic genes in Pseudomonas fluorescens BF13: involvement of a MarR family regulator." *Applied Microbiology and Biotechnology* 80(3): 475-483.

Camarero, S., D. Ibarra, M. J. Martinez and A. T. Martinez (2005). "Lignin-derived compounds as efficient laccase mediators for decolorization of different types of recalcitrant dyes." *Appl Environ Microbiol* 71(4): 1775-1784.

Carpena, X., S. Loprasert, S. Mongkolsuk, J. Switala, P. C. Loewen and I. Fita (2003). "Catalase-peroxidase KatG of Burkholderia pseudomallei at 1.7A resolution." *J Mol Biol* 327(2): 475-489.

Carpena, X., B. Wiseman, T. Deemagarn, R. Singh, J. Switala, A. Ivancich, I. Fita and P. C. Loewen (2005). "A molecular switch and electronic circuit modulate catalase activity in catalase-peroxidases." *EMBO Rep* 6(12): 1156-1162.

Cha, J. S. and D. A. Cooksey (1991). "Copper resistance in Pseudomonas syringae mediated by periplasmic and outer membrane proteins." *Proc Natl Acad Sci U S A* 88(20): 8915-8919.

Chakar, F. S. and A. J. Ragauskas (2004). "Review of current and future softwood kraft lignin process chemistry." *Industrial Crops and Products* 20(2): 131-141.

Chakdar, H., M. Kumar, K. Pandiyan, A. Singh, K. Nanjappan, P. L. Kashyap and A. K. Srivastava (2016). "Bacterial xylanases: biology to biotechnology." *3 Biotech* 6(2): 150.

Chandra, R. and P. Chowdhary (2015). "Properties of bacterial laccases and their application in bioremediation of industrial wastes." *Environ Sci Process Impacts* 17(2): 326-342.

Chandra, R. P. and A. J. Ragauskas (2002). "Evaluating laccase-facilitated coupling of phenolic acids to high-yield kraft pulps." *Enzyme and Microbial Technology* 30(7): 855-861.

Charalabous, P., J. M. Risk, R. Jenkins, A. J. Birss, C. A. Hart and J. W. Smalley (2007). "Characterization of a bifunctional catalase-peroxidase of Burkholderia cenocepacia." *FEMS Immunol Med Microbiol* 50(1): 37-44.

Chauhan, P. S., B. Goradia and A. Saxena (2017). "Bacterial laccase: recent update on production, properties and industrial applications." *3 Biotech* 7(5): 323.

Chen, C. and T. Li (2016). "Bacterial dye-decolorizing peroxidases: Biochemical properties and biotechnological opportunities." *Physical Sciences Reviews* 1.

Chen, C., R. Shrestha, K. Jia, P. F. Gao, B. V. Geisbrecht, S. H. Bossmann, J. Shi and P. Li (2015). "Characterization of Dye-decolorizing Peroxidase (DyP) from Thermomonospora curvata Reveals Unique Catalytic Properties of A-type DyPs." *J Biol Chem* 290(38): 23447-23463.

Chen, H. (2014). Chemical Composition and Structure of Natural Lignocellulose. . <u>Biotechnology of Lignocellulose: Theory and Practice</u>, Springer, Dordrecht.

Chen, H., J. Liu, X. Chang, D. Chen, Y. Xue, P. Liu, H. Lin and S. Han (2017). "A review on the pretreatment of lignocellulose for high-value chemicals." *Fuel Processing Technology* 160: 196-206.

Chen, Y., M. A. Stevens, Y. Zhu, J. Holmes and H. Xu (2013). "Understanding of alkaline pretreatment parameters for corn stover enzymatic saccharification." *Biotechnol Biofuels* 6(1): 8.

Cherubini, F. (2010). "The biorefinery concept: Using biomass instead of oil for producing energy and chemicals." *Energy Conversion and Management* 51(7): 1412-1421.

Chin, C. S., D. H. Alexander, P. Marks, A. A. Klammer, J. Drake, C. Heiner, A. Clum, A. Copeland, J. Huddleston, E. E. Eichler, S. W. Turner and J. Korlach (2013). "Nonhybrid, finished microbial genome assemblies from long-read SMRT sequencing data." *Nat Methods* 10(6): 563-569.

Colpa, D. I., M. W. Fraaije and E. van Bloois (2014). "DyP-type peroxidases: a promising and versatile class of enzymes." *J Ind Microbiol Biotechnol* 41(1): 1-7.

Constant, S., H. L. J. Wienk, A. E. Frissen, P. d. Peinder, R. Boelens, D. S. van Es, R. J. H. Grisel, B. M. Weckhuysen, W. J. J. Huijgen, R. J. A. Gosselink and P. C. A. Bruijnincx (2016). "New insights into the structure and composition of technical lignins: a comparative characterisation study." *Green Chemistry* 18(9): 2651-2665.

Cortes, L., A. G. Wedd and Z. Xiao (2015). "The functional roles of the three copper sites associated with the methionine-rich insert in the multicopper oxidase CueO from E. coli." *Metallomics* 7(5): 776-785.

Dailey, H. A., A. N. Septer, L. Daugherty, D. Thames, S. Gerdes, E. V. Stabb, A. K. Dunn, T. A. Dailey and J. D. Phillips (2011). "The Escherichia coli protein YfeX functions as a porphyrinogen oxidase, not a heme dechelatase." *mBio* 2(6): e00248-00211.

Daniel, R., M. Danson, R. Eisenthal, C. Lee and M. Peterson (2008). "The effect of temperature on enzyme activity: New insights and their implications." *Extremophiles : life under extreme conditions* 12: 51-59.

Daniel, R. M. and M. J. Danson (2013). "Temperature and the catalytic activity of enzymes: A fresh understanding." *FEBS Lett* 587(17): 2738-2743.

Das, R., Z. Liang, G. Li and T. An (2020). "A non-blue laccase of Bacillus sp. GZB displays manganese-oxidase activity: A study of laccase characterization, Mn(II) oxidation and prediction of Mn(II) oxidation mechanism." *Chemosphere* 252: 126619.

de Gonzalo, G., D. I. Colpa, M. H. M. Habib and M. W. Fraaije (2016). "Bacterial enzymes involved in lignin degradation." *Journal of Biotechnology* 236: 110-119.

de Jong, E. a. v. R., R. (2009). Biorefineries: adding value to the sustainable utilisation of biomass. IEA Bioenergy:T42:2009:01.

de la Torre, M. J., A. Moral, M. D. Hernández, E. Cabeza and A. Tijero (2013). "Organosolv lignin for biofuel." *Industrial Crops and Products* 45(0): 58-63.

del Rio, J. C., J. Rencoret, P. Prinsen, A. T. Martinez, J. Ralph and A. Gutierrez (2012). "Structural characterization of wheat straw lignin as revealed by analytical pyrolysis, 2D-NMR, and reductive cleavage methods." *J Agric Food Chem* 60(23): 5922-5935.

Doherty, W. O. S., P. Mousavioun and C. M. Fellows (2011). "Value-adding to cellulosic ethanol: Lignin polymers." *Industrial Crops and Products* 33(2): 259-276.

Dos Santos, V. A., S. Heim, E. R. Moore, M. Stratz and K. N. Timmis (2004). "Insights into the genomic basis of niche specificity of Pseudomonas putida KT2440." *Environ Microbiol* 6(12): 1264-1286.

Dumon, C., L. Song, S. Bozonnet, R. Fauré and M. J. O'Donohue (2012). "Progress and future prospects for pentose-specific biocatalysts in biorefining." *Process Biochemistry* 47(3): 346-357.

Durão, P., Z. Chen, A. T. Fernandes, P. Hildebrandt, D. H. Murgida, S. Todorovic, M. M. Pereira, E. P. Melo and L. O. Martins (2008). "Copper incorporation into recombinant CotA laccase from Bacillus subtilis: characterization of fully copper loaded enzymes." *J Biol Inorg Chem* 13(2): 183-193.

Dwivedi, U. N., P. Singh, V. P. Pandey and A. Kumar (2011). "Structure–function relationship among bacterial, fungal and plant laccases." *Journal of Molecular Catalysis B: Enzymatic* 68(2): 117-128.

Dworkin, M., S. Falkow, E. Rosenberg, K.-H. Schleifer and E. Stackebrandt (2006). The Prokaryotes Vol. 5: Proteobacteria: Alpha and Beta Subclasses, Springer-Verlag New York.

Ebringerová, A., Z. Hromádková and T. Heinze (2005). Hemicellulose. Polysaccharides I. T. Heinze, Springer Berlin Heidelberg. **186:** 1-67.

Eitinger, T. and M. A. Mandrand-Berthelot (2000). "Nickel transport systems in microorganisms." *Archives of Microbiology* 173(1): 1-9.

Elegir, G., A. Kindl, P. Sadocco and M. Orlandi (2008). "Development of antimicrobial cellulose packaging through laccase-mediated grafting of phenolic compounds." *Enzyme and Microbial Technology* 43: 84-92.

Endo, K., Y. Hayashi, T. Hibi, K. Hosono, T. Beppu and K. Ueda (2003). "Enzymological characterization of EpoA, a laccase-like phenol oxidase produced by Streptomyces griseus." *J Biochem* 133(5): 671-677.

Endo, K., K. Hosono, T. Beppu and K. Ueda (2002). "A novel extracytoplasmic phenol oxidase of Streptomyces: its possible involvement in the onset of morphogenesis." *Microbiology (Reading)* 148(Pt 6): 1767-1776.

Enguita, F. J., L. O. Martins, A. O. Henriques and M. A. Carrondo (2003). "Crystal structure of a bacterial endospore coat component. A laccase with enhanced thermostability properties." *J Biol Chem* 278(21): 19416-19425.

Escovar-Kousen, J. M., D. Wilson and D. Irwin (2004). "Integration of computer modeling and initial studies of site-directed mutagenesis to improve cellulase activity on Cel9A from Thermobifida fusca." *Appl Biochem Biotechnol* 113(1): 287.

Ethiraj, S., S. V and S. S (2018). Xylanases - For Sustainable Bioproduct Production.

Eugenio, M. E., M. Hrenández, R. Moya, R. Martín-Sampedro, J. C. Villar and M. E. Arias (2011). "Evaluation of a new laccase produced by Streptomyces ipomoea on biobleaching and ageing of kraft pulps." *2011* 6(3): 11.

Everette, J. D., Q. M. Bryant, A. M. Green, Y. A. Abbey, G. W. Wangila and R. B. Walker (2010). "Thorough study of reactivity of various compound classes toward the Folin-Ciocalteu reagent." *J Agric Food Chem* 58(14): 8139-8144.

Fabbrini, M., C. Galli and P. Gentili (2002). "Comparing the catalytic efficiency of some mediators of laccase." *Journal of Molecular Catalysis B: Enzymatic* 16(5): 231-240.

Fan, L. T. and Y. H. Lee (1983). "Kinetic studies of enzymatic hydrolysis of insoluble cellulose: Derivation of a mechanistic kinetic model." *Biotechnol Bioeng* 25(11): 2707-2733.

Fernandes, T., Silveira, W. , Passos, F. and Zucchi, T. (2014). "Laccases from Actinobacteria—What We Have and What to Expect." *Advances in Microbiology* 4: 285-296.

Fernández-Fueyo, E., D. Linde, D. Almendral, M. F. López-Lucendo, F. J. Ruiz-Dueñas and A. T. Martínez (2015). "Description of the first fungal dye-decolorizing peroxidase oxidizing manganese(II)." *Appl Microbiol Biotechnol* 99(21): 8927-8942.

Ferreira, A. F. (2017). Biorefinery Concept. Biorefineries: Targeting Energy, High Value Products and Waste Valorisation. M. Rabaçal, A. F. Ferreira, C. A. M. Silva and M. Costa. Cham, Springer International Publishing**:** 1-20.

Fisher, F. (2014). "Lignin biodegradation and industrial implications." *AIMS Bioengineering* 1(2): 92-112.

Fleurbaey, M., S. Kartha, Y. L. Bolwig, Y. Chee, E. Chen, F. Corbera, W. Lecocq, M. S. Lutz, R. B. Muylaert, C. Norgaard, C. Okereke and A. D. Sagar (2014). Sustainable Development and Equity. In: Climate Change 2014: Mitigation of Climate Change.

Contribution of Working Group III to the Fifth Assessment Report of the Intergovernmental Panel on Climate Change Cambridge University Press, Cambridge, United Kingdom and New York, NY, USA.

Fuchs, G., M. Boll and J. Heider (2011). "Microbial degradation of aromatic compounds — from one strategy to four." *Nature Reviews Microbiology* 9(11): 803-816.

Galai, S., F. Limam and M. N. Marzouki (2009). "A New *Stenotrophomonas maltophilia* Strain Producing Laccase. Use in Decolorization of Synthetics Dyes." *Appl Biochem Biotechnol* 158(2): 416-431.

Gallage, Nethaji J. and Birger L. Møller (2015). "Vanillin–Bioconversion and Bioengineering of the Most Popular Plant Flavor and Its De Novo Biosynthesis in the Vanilla Orchid." *Molecular Plant* 8(1): 40-57.

Gasson, M. J., Y. Kitamura, W. R. McLauchlan, A. Narbad, A. J. Parr, E. L. Parsons, J. Payne, M. J. Rhodes and N. J. Walton (1998). "Metabolism of ferulic acid to vanillin. A bacterial gene of the enoyl-SCoA hydratase/isomerase superfamily encodes an enzyme for the hydration and cleavage of a hydroxycinnamic acid SCoA thioester." *J Biol Chem* 273(7): 4163-4170.

Ghoul, M. and L. Chebil (2012). Enzymatic Polymerization of Phenolic Compounds by Oxidoreductases. Enzymatic polymerization of phenolic compounds by oxidoreductases. Dordrecht, Springer Netherlands**:** 1-46.

Gillet, L. C., P. Navarro, S. Tate, H. Röst, N. Selevsek, L. Reiter, R. Bonner and R. Aebersold (2012). "Targeted Data Extraction of the MS/MS Spectra Generated by Data-independent Acquisition: A New Concept for Consistent and Accurate Proteome Analysis." *Molecular & Cellular Proteomics* 11(6): O111.016717.

Giroux, H., P. Vidal, J. Bouchard and F. Lamy (1988). "Degradation of Kraft Indulin Lignin by Streptomyces viridosporus and Streptomyces badius." *Appl Environ Microbiol* 54(12): 3064-3070.

Godden, B., A. S. Ball, P. Helvenstein, A. J. Mccarthy and M. J. Penninckx (1992). "Towards elucidation of the lignin degradation pathway in actinomycetes." *Microbiology* 138(11): 2441-2448.

Gorbacheva, M., O. Morozova, G. Shumakovich, A. Streltsov, S. Shleev and A. Yaropolov (2009). "Enzymatic oxidation of manganese ions catalysed by laccase." *Bioorganic Chemistry* 37(1): 1-5.

Granja-Travez, R. S. and T. D. H. Bugg (2018). "Characterization of multicopper oxidase CopA from Pseudomonas putida KT2440 and Pseudomonas fluorescens Pf-5: Involvement in bacterial lignin oxidation." *Arch Biochem Biophys* 660: 97-107.

Granja-Travez, R. S., R. C. Wilkinson, G. F. Persinoti, F. M. Squina, V. Fülöp and T. D. H. Bugg (2018). "Structural and functional characterisation of multi-copper oxidase CueO from lignin-degrading bacterium Ochrobactrum sp. reveal its activity towards lignin model compounds and lignosulfonate." *FEBS Journal* 285(9): 1684-1700.

Guan, Z. B., Q. Luo, H. R. Wang, Y. Chen and X. R. Liao (2018). "Bacterial laccases: promising biological green tools for industrial applications." *Cell Mol Life Sci* 75(19): 3569-3592.

Gunne, M. and V. B. Urlacher (2012). "Characterization of the alkaline laccase Ssl1 from Streptomyces sviceus with unusual properties discovered by genome mining." *PLoS One* 7(12): e52360-e52360.

Gupta, V., S. Garg, N. Capalash, N. Gupta and P. Sharma (2015). "Production of thermo-alkali-stable laccase and xylanase by co-culturing of Bacillus sp. and B. halodurans for biobleaching of kraft pulp and deinking of waste paper." *Bioprocess Biosyst Eng* 38(5): 947-956.

Haki, G. D. and S. K. Rakshit (2003). "Developments in industrially important thermostable enzymes: a review." *Bioresour Technol* 89(1): 17-34.

Hakulinen, N. and J. Rouvinen (2015). "Three-dimensional structures of laccases." *Cellular and Molecular Life Sciences* 72(5): 857-868.

Hämäläinen, V., T. Grönroos, A. Suonpää, M. W. Heikkilä, B. Romein, P. Ihalainen, S. Malandra and K. R. Birikh (2018). "Enzymatic Processes to Unlock the Lignin Value." *Front Bioeng Biotechnol* 6: 20.

Hammel, K. E., P. J. Tardone, M. A. Moen and L. A. Price (1989). "Biomimetic oxidation of nonphenolic lignin models by Mn(III): New observations on the oxidizability of guaiacyl and syringyl substructures." *Archives of biochemistry and biophysics* 270(1): 404-409.

Hansen, J. H., S. V. Petersen, K. K. Andersen, J. J. Enghild, T. Damhus and D. Otzen (2009). "Stable intermediates determine proteins' primary unfolding sites in the presence of surfactants." *Biopolymers* 91(3): 221-231.

Hartmann, E. M. and J. Armengaud (2014). "Shotgun proteomics suggests involvement of additional enzymes in dioxin degradation by Sphingomonas wittichii RW1." *Environ Microbiol* 16(1): 162-176.

Hatfield, R. and W. Vermerris (2001). "Lignin formation in plants. The dilemma of linkage specificity." *Plant Physiol* 126(4): 1351-1357.

Heck, J. X., S. H. Flôres, P. F. Hertz and M. A. Z. Ayub (2006). "Statistical optimization of thermo-tolerant xylanase activity from Amazon isolated Bacillus circulans on solid-state cultivation." *Bioresour Technol* 97(15): 1902-1906.

Hernández, M., M. J. Hernández-Coronado, A. S. Ball and M. E. Arias (2001). "Degradation of alkali-lignin residues from solid-state fermentation of wheat straw by streptomycetes." *Biodegradation* 12(4): 219-223.

Hill, J., E. Nelson, D. Tilman, S. Polasky and D. Tiffany (2006). "Environmental, economic, and energetic costs and benefits of biodiesel and ethanol biofuels." *Proc Natl Acad Sci U S A* 103(30): 11206-11210.

Hirose, J., A. Nagayoshi, N. Yamanaka, Y. Araki and H. Yokoi (2013). "Isolation and characterization of bacteria capable of metabolizing lignin-derived low molecular weight compounds." *Biotechnology and Bioprocess Engineering* 18(4): 736-741.

Hochman, A. and I. Goldberg (1991). "Purification and characterization of a catalase-peroxidase and a typical catalase from the bacterium Klebsiella pneumoniae." *Biochim Biophys Acta* 1077(3): 299-307.

Hofrichter, M. (2002). "Review: lignin conversion by manganese peroxidase (MnP)." *Enzyme and Microbial Technology* 30(4): 454-466.

Hu, Y., Q. Hu, R. Wei, R. Li, D. Zhao, M. Ge, Q. Yao and X. Yu (2019). "The XRE Family Transcriptional Regulator SrtR in Streptococcus suis Is Involved in Oxidant Tolerance and Virulence." *Frontiers in cellular and infection microbiology* 8: 452-452.

Huang, X. F., N. Santhanam, D. V. Badri, W. J. Hunter, D. K. Manter, S. R. Decker, J. M. Vivanco and K. F. Reardon (2013). "Isolation and characterization of lignin-degrading bacteria from rainforest soils." *Biotechnol Bioeng* 110(6): 1616-1626.

Huntemann, M., N. N. Ivanova, K. Mavromatis, H. J. Tripp, D. Paez-Espino, K. Palaniappan, E. Szeto, M. Pillay, I. M. Chen, A. Pati, T. Nielsen, V. M. Markowitz and N. C. Kyrpides (2015).

"The standard operating procedure of the DOE-JGI Microbial Genome Annotation Pipeline (MGAP v.4)." *Stand Genomic Sci* 10: 86.

Ibrahim, R., L. Melton, s. B.G and R. Schroeder (2009). "Mannans in primary and secondary plant cell walls." *New Zealand Journal of Forestry Science* 39: 153-160.

Iglesias, M., D. Gomez -Maldonado, M. Peresin, B. Via and Z. Jiang (2019). "Comparison of kraft and sulfite pulping processes and Their Effects on Cellulose Fibers and Nanofibrillated Cellulose Properties: A Review." *Forest Products Journal*.

Ihssen, J., D. Jankowska, T. Ramsauer, R. Reiss, R. Luchsinger, L. Wiesli, M. Schubert, L. Thöny-Meyer and G. Faccio (2017). "Engineered Bacillus pumilus laccase-like multi-copper oxidase for enhanced oxidation of the lignin model compound guaiacol." *Protein Eng Des Sel* 30(6): 449-453.

Ishida, N., A. Okubo, H. Kawai, S. Yamazaki and S. Toda (1980). "Interaction of Amino Acids with Transition Metal Ions in Solution (I) Solution Structure of l-Lysine with Co(II) and Cu(II) Ions as Studied by Nuclear Magnetic Resonance Spectroscopy." *Agricultural and Biological Chemistry* 44(2): 263-270.

Jakopitsch, C., F. Rüker, G. Regelsberger, M. Dockal, G. A. Peschek and C. Obinger (1999). "Catalase-peroxidase from the cyanobacterium Synechocystis PCC 6803: cloning, overexpression in Escherichia coli, and kinetic characterization." *Biol Chem* 380(9): 1087-1096.

Jambo, S. A., R. Abdulla, S. H. Mohd Azhar, H. Marbawi, J. A. Gansau and P. Ravindra (2016). "A review on third generation bioethanol feedstock." *Renewable and Sustainable Energy Reviews* 65: 756-769.

Jiménez, J. I., J. Nogales, J. L. García and E. Díaz (2010). A Genomic View of the Catabolism of Aromatic Compounds in Pseudomonas. Handbook of Hydrocarbon and Lipid Microbiology. K. N. Timmis. Berlin, Heidelberg, Springer Berlin Heidelberg: 1297-1325.

Johnsson, K., W. A. Froland and P. G. Schultz (1997). "Overexpression, purification, and characterization of the catalase-peroxidase KatG from Mycobacterium tuberculosis." *J Biol Chem* 272(5): 2834-2840.

Jönsson, L. J. and C. Martín (2016). "Pretreatment of lignocellulose: Formation of inhibitory by-products and strategies for minimizing their effects." *Bioresour Technol* 199: 103-112.

Joo, J. C., S. P. Pack, Y. H. Kim and Y. J. Yoo (2011). "Thermostabilization of Bacillus circulans xylanase: Computational optimization of unstable residues based on thermal fluctuation analysis." *Journal of Biotechnology* 151(1): 56-65.

Jung, D.-H., E.-J. Kim, E. Jung, R. J. Kazlauskas, K.-Y. Choi and B.-G. Kim (2016). "Production of p-hydroxybenzoic acid from p-coumaric acid by Burkholderia glumae BGR1." *Biotechnol Bioeng* 113(7): 1493-1503.

Kaihami, G. H., J. R. Almeida, S. S. Santos, L. E. Netto, S. R. Almeida and R. L. Baldini (2014). "Involvement of a 1-Cys peroxiredoxin in bacterial virulence." *PLoS Pathog* 10(10): e1004442.

Kallscheuer, N., M. Vogt, J. Kappelmann, K. Krumbach, S. Noack, M. Bott and J. Marienhagen (2016). "Identification of the phd gene cluster responsible for phenylpropanoid utilization in Corynebacterium glutamicum." *Appl Microbiol Biotechnol* 100(4): 1871-1881.

Kamimura, N. and E. Masai (2014). The Protocatechuate 4,5-Cleavage Pathway: Overview and New Findings. Biodegradative Bacteria: How Bacteria Degrade, Survive, Adapt, and Evolve. H. Nojiri, M. Tsuda, M. Fukuda and Y. Kamagata. Tokyo, Springer Japan: 207-226.

Kamimura, N., K. Takahashi, K. Mori, T. Araki, M. Fujita, Y. Higuchi and E. Masai (2017). "Bacterial catabolism of lignin-derived aromatics: New findings in a recent decade: Update on bacterial lignin catabolism." *Environ Microbiol Rep* 9(6): 679-705.

Kamm, B., P. R. Gruber and M. Kamm (2008). "Biorefineries - Industrial Processes and Products." *Ullmann's Encycl Ind Chem* 5: 659-683.

Kane, S. D. and C. E. French (2018). "Characterisation of novel biomass degradation enzymes from the genome of Cellulomonas fimi." *Enzyme and Microbial Technology* 113: 9-17.

Karlen, S. D., C. Zhang, M. L. Peck, R. A. Smith, D. Padmakshan, K. E. Helmich, H. C. Free, S. Lee, B. G. Smith, F. Lu, J. C. Sedbrook, R. Sibout, J. H. Grabber, T. M. Runge, K. S. Mysore, P. J. Harris, L. E. Bartley and J. Ralph (2016). "Monolignol ferulate conjugates are naturally incorporated into plant lignins." *Sci Adv* 2(10): e1600393.

Kasai, D., T. Fujinami, T. Abe, K. Mase, Y. Katayama, M. Fukuda and E. Masai (2009). "Uncovering the protocatechuate 2,3-cleavage pathway genes." *J Bacteriol* 191(21): 6758-6768.

Kasai, D., N. Kamimura, K. Tani, S. Umeda, T. Abe, M. Fukuda and E. Masai (2012). "Characterization of FerC, a MarR-type transcriptional regulator, involved in transcriptional regulation of the ferulate catabolic operon in Sphingobium sp. strain SYK-6." *FEMS Microbiol Lett* 332(1): 68-75.

Kasai, D., E. Masai, Y. Katayama and M. Fukuda (2007). "Degradation of 3-O-methylgallate in Sphingomonas paucimobilis SYK-6 by pathways involving protocatechuate 4,5-dioxygenase." *FEMS Microbiol Lett* 274(2): 323-328.

Kasai, D., E. Masai, K. Miyauchi, Y. Katayama and M. Fukuda (2004). "Characterization of the 3-O-methylgallate dioxygenase gene and evidence of multiple 3-O-methylgallate catabolic pathways in Sphingomonas paucimobilis SYK-6." *J Bacteriol* 186(15): 4951-4959.

Katayama, Y., S. Nishikawa, A. Murayama, M. Yamasaki, N. Morohoshi and T. Haraguchi (1988). "The metabolism of biphenyl structures in lignin by the soil bacterium (Pseudomonas paucimobilis SYK-6)." *FEBS Lett* 233(1): 129-133.

Katoh, K. and D. M. Standley (2013). "MAFFT Multiple Sequence Alignment Software Version 7: Improvements in Performance and Usability." *Molecular Biology and Evolution* 30(4): 772-780.

Kavanagh, K. L., H. Jörnvall, B. Persson and U. Oppermann (2008). "Medium- and short-chain dehydrogenase/reductase gene and protein families : the SDR superfamily: functional and structural diversity within a family of metabolic and regulatory enzymes." *Cell Mol Life Sci* 65(24): 3895-3906.

Kelley, L. A., S. Mezulis, C. M. Yates, M. N. Wass and M. J. E. Sternberg (2015). "The Phyre2 web portal for protein modeling, prediction and analysis." *Nat Protoc* 10(6): 845-858.

Kiiskinen, L. L., K. Kruus, M. Bailey, E. Ylösmäki, M. Siika-Aho and M. Saloheimo (2004). "Expression of Melanocarpus albomyces laccase in Trichoderma reesei and characterization of the purified enzyme." *Microbiology (Reading)* 150(Pt 9): 3065-3074.

Kim, D. Y., D. H. Shin, S. Jung, H. Kim, J. S. Lee, H. Y. Cho, K. S. Bae, C. K. Sung, Y. H. Rhee, K. H. Son and H. Y. Park (2014). "Novel alkali-tolerant GH10 endo-β-1,4-xylanase with broad substrate specificity from Microbacterium trichothecenolyticum HY-17, a gut bacterium of the mole cricket Gryllotalpa orientalis." *J Microbiol Biotechnol* 24(7): 943-953.

Kirk, T. K. and R. L. Farrell (1987). "Enzymatic "combustion": the microbial degradation of lignin." *Annu Rev Microbiol* 41: 465-505.

Kita, A., S.-i. Kita, I. Fujisawa, K. Inaka, T. Ishida, K. Horiike, M. Nozaki and K. Miki (1999). "An archetypical extradiol-cleaving catecholic dioxygenase: the crystal structure of catechol 2,3-dioxygenase (metapyrocatechase) from Pseudomonas putida mt-2." *Structure* 7(1): 25-34.

Koeck, D. E., A. Pechtl, V. V. Zverlov and W. H. Schwarz (2014). "Genomics of cellulolytic bacteria." *Curr Opin Biotechnol* 29: 171-183.

Koschorreck, K., S. M. Richter, A. B. Ene, E. Roduner, R. D. Schmid and V. B. Urlacher (2008). "Cloning and characterization of a new laccase from *Bacillus licheniformis* catalyzing dimerization of phenolic acids." *Applied Microbiology and Biotechnology* 79(2): 217-224.

Koschorreck, K., R. D. Schmid and V. B. Urlacher (2009). "Improving the functional expression of a Bacillus licheniformislaccase by random and site-directed mutagenesis." *BMC Biotechnology* 9(1): 12.

Kozlowski, L. P. (2017). "Proteome-pI: proteome isoelectric point database." *Nucleic Acids Res* 45(D1): D1112-D1116.

Kudakasseril, J., G. Raveendran Nair, A. Hussain and G. S. Vijaya Raghavan (2013). "Feedstocks, logistics and pre-treatment processes for sustainable lignocellulosic biorefineries: A comprehensive review." *Renewable and Sustainable Energy Reviews* 25: 205-219.

Kudanga, T. and M. Le Roes-Hill (2014). "Laccase applications in biofuels production: current status and future prospects." *Applied Microbiology and Biotechnology* 98(15): 6525-6542.

Kumar, M., A. Singhal, P. K. Verma and I. S. Thakur (2017). "Production and Characterization of Polyhydroxyalkanoate from Lignin Derivatives by Pandoraea sp. ISTKB." *ACS Omega* 2(12): 9156-9163.

Kumar, S. and R. Nussinov (2001). "How do thermophilic proteins deal with heat?" *Cellular and Molecular Life Sciences CMLS* 58(9): 1216-1233.

Kunamneni, A., F. Plou, A. Ballesteros and M. Alcalde (2008). "Laccases and their applications: a patent review." *Recent Pat Biotechnol* 2(1): 10-24.

Lan, W., J. Rencoret, F. Lu, S. D. Karlen, B. G. Smith, P. J. Harris, J. C. del Río and J. Ralph (2016). "Tricin-lignins: occurrence and quantitation of tricin in relation to phylogeny." *The Plant Journal*: Medium: ED; Size: p. 1046-1057.

Larrabee, J. A. and T. G. Spiro (1979). "Cobalt II substitution in the type 1 site of the multi-copper oxidase Rhus laccase." *Biochem Biophys Res Commun* 88(3): 753-760.

Laurichesse, S. and L. Avérous (2014). "Chemical modification of lignins: Towards biobased polymers." *Progress in Polymer Science* 39(7): 1266-1290.

Le, R. K., T. Wells Jr, P. Das, X. Meng, R. J. Stoklosa, A. Bhalla, D. B. Hodge, J. S. Yuan and A. J. Ragauskas (2017). "Conversion of corn stover alkaline pre-treatment waste streams into biodiesel via Rhodococci." *RSC Advances* 7(7): 4108-4115.

Lee, J. (1997). "Biological conversion of lignocellulosic biomass to ethanol." *Journal of Biotechnology* 56(1): 1-24.

Leontievsky, A., N. Myasoedova, N. Pozdnyakova and L. Golovleva (1997). "'Yellow' laccase of Panus tigrinus oxidizes non-phenolic substrates without electron-transfer mediators." *FEBS Lett* 413(3): 446-448.

Leontievsky, A. A., T. Vares, P. Lankinen, J. K. Shergill, N. N. Pozdnyakova, N. M. Myasoedova, N. Kalkkinen, L. A. Golovleva, R. Cammack, C. F. Thurston and A. Hatakka (1997). "Blue and yellow laccases of ligninolytic fungi." *FEMS Microbiol Lett* 156(1): 9-14.

Li, J., C. Liu, B. Li, H. Yuan, J. Yang and B. Zheng (2012). "Identification and molecular characterization of a novel DyP-type peroxidase from Pseudomonas aeruginosa PKE117." *Appl Biochem Biotechnol* 166(3): 774-785.

Li, M., K. Eskridge, E. Liu and M. Wilkins (2019). "Enhancement of polyhydroxybutyrate (PHB) production by 10-fold from alkaline pretreatment liquor with an oxidative enzyme-mediator-surfactant system under Plackett-Burman and central composite designs." *Bioresour Technol* 281: 99-106.

Li, S. and K. Lundquist (1994). "A new method for the analysis of phenolic groups in lignins by ′H NMR spectrometry." *Nordic Pulp & Paper Research Journal* 9(3): 191.

Li, W., W.-W. Zhang, M.-M. Yang and Y.-L. Chen (2008). "Cloning of the Thermostable Cellulase Gene from Newly Isolated Bacillus subtilis and its Expression in Escherichia coli." *Molecular Biotechnology* 40(2): 195-201.

Lin, L., X. Wang, L. Cao and M. Xu (2019). "Lignin catabolic pathways reveal unique characteristics of dye-decolorizing peroxidases in Pseudomonas putida." *Environ Microbiol* 21(5): 1847-1863.

Linde, D., C. Coscolín, C. Liers, M. Hofrichter, A. T. Martínez and F. J. Ruiz-Dueñas (2014). "Heterologous expression and physicochemical characterization of a fungal dye-decolorizing peroxidase from Auricularia auricula-judae." *Protein Expr Purif* 103: 28-37.

Linger, J. G., D. R. Vardon, M. T. Guarnieri, E. M. Karp, G. B. Hunsinger, M. A. Franden, C. W. Johnson, G. Chupka, T. J. Strathmann, P. T. Pienkos and G. T. Beckham (2014). "Lignin valorization through integrated biological funneling and chemical catalysis." *Proc Natl Acad Sci U S A* 111(33): 12013-12018.

Liu, H., Y. Cheng, B. Du, C. Tong, S. Liang, S. Han, S. Zheng and Y. Lin (2015). "Overexpression of a novel thermostable and chloride-tolerant laccase from Thermus thermophilus SG0.5JP17-16 in Pichia pastoris and its application in synthetic dye decolorization." *PLoS One* 10(3): e0119833.

Liu, W., J. Hong, D. R. Bevan and Y. H. Zhang (2009). "Fast identification of thermostable beta-glucosidase mutants on cellobiose by a novel combinatorial selection/screening approach." *Biotechnol Bioeng* 103(6): 1087-1094.

Liu, X., Z. Yuan, J. Wang, Y. Cui, S. Liu, Y. Ma, L. Gu and S. Xu (2017). "Crystal structure and biochemical features of dye-decolorizing peroxidase YfeX from Escherichia coli O157 Asp(143) and Arg(232) play divergent roles toward different substrates." *Biochem Biophys Res Commun* 484(1): 40-44.

Liu, Y., L. Huang, W. Guo, L. Jia, Y. Fu, S. Gui and F. Lu (2017). "Cloning, expression, and characterization of a thermostable and pH-stable laccase from Klebsiella pneumoniae and its application to dye decolorization." *Process Biochemistry* 53: 125-134.

Lombard, V., H. Golaconda Ramulu, E. Drula, P. M. Coutinho and B. Henrissat (2014). "The carbohydrate-active enzymes database (CAZy) in 2013." *Nucleic Acids Res* 42(Database issue): D490-495.

Lončar, N., D. I. Colpa and M. W. Fraaije (2016). "Exploring the biocatalytic potential of a DyP-type peroxidase by profiling the substrate acceptance of Thermobifida fusca DyP peroxidase." *Tetrahedron* 72(46): 7276-7281.

Lopez-Mondejar, R., C. Algora and P. Baldrian (2019). "Lignocellulolytic systems of soil bacteria: A vast and diverse toolbox for biotechnological conversion processes." *Biotechnol Adv* 37(6): 107374.

Lora, J. H., C. F. Wu, E. K. Pye and J. J. Balatinecz (1989). Characteristics and Potential Applications of Lignin Produced by an Organosolv Pulping Process. Lignin, American Chemical Society. **397:** 312-323.

Lu, L., G. Zeng, C. Fan, X. Ren, C. Wang, Q. Zhao, J. Zhang, M. Chen, A. Chen and M. Jiang (2013). "Characterization of a laccase-like multicopper oxidase from newly isolated Streptomyces sp. C1 in agricultural waste compost and enzymatic decolorization of azo dyes." *Biochemical Engineering Journal* 72: 70-76.

Lundquist, K. (1987). "On the Occurrence of β-1 Structures in Lignins." *Journal of Wood Chemistry and Technology* 7(2): 179-185.

Lundquist, K., T. Olsson, P. M. Boll, H. Hope, A. Christensen and G. Schroll (1977). <u>NMR Studies of lignins. 1. Signals due to protons in formyl groups.</u>

Luo, L., J. Cai, C. Wang, J. Lin, X. Du, A. Zhou and X. Mengxiong (2015). "Purification and characterization of an alkaliphilic endo-xylanase from Streptomyces althioticus LMZM and utilization in pulp industry." *Journal of Chemical Technology and Biotechnology* 91.

Lynd, L. R., M. S. Laser, D. Bransby, B. E. Dale, B. Davison, R. Hamilton, M. Himmel, M. Keller, J. D. McMillan, J. Sheehan and C. E. Wyman (2008). "How biotech can transform biofuels." *Nature Biotechnology* 26(2): 169-172.

Machczynski, M. C., E. Vijgenboom, B. Samyn and G. W. Canters (2004). "Characterization of SLAC: a small laccase from *Streptomyces coelicolor* with unprecedented activity." *Protein Science* 13(9): 2388-2397.

MacLean, A. M., W. Haerty, G. B. Golding and T. M. Finan (2011). "The LysR-type PcaQ protein regulates expression of a protocatechuate-inducible ABC-type transport system in Sinorhizobium meliloti." *Microbiology* 157(Pt 9): 2522-2533.

Mai, C., O. Milstein and A. Hüttermann (2000). "Chemoenzymatical grafting of acrylamide onto lignin." *Journal of Biotechnology* 79(2): 173-183.

Majumdar, S., T. Lukk, J. O. Solbiati, S. Bauer, S. K. Nair, J. E. Cronan and J. A. Gerlt (2014). "Roles of small laccases from Streptomyces in lignin degradation." *Biochemistry* 53(24): 4047-4058.

Malherbe, S. and T. E. Cloete (2002). "Lignocellulose biodegradation: Fundamentals and applications." *Reviews in Environmental Science and Biotechnology* 1(2): 105-114.

Manju, S. and B. Singh Chadha (2011). Chapter 9 - Production of Hemicellulolytic Enzymes for Hydrolysis of Lignocellulosic Biomass. <u>Biofuels</u>. A. Pandey, C. Larroche, S. C. Ricke, C.-G. Dussap and E. Gnansounou. Amsterdam, Academic Press**:** 203-228.

Marcinkeviciene, J. A., R. S. Magliozzo and J. S. Blanchard (1995). "Purification and characterization of the Mycobacterium smegmatis catalase-peroxidase involved in isoniazid activation." *J Biol Chem* 270(38): 22290-22295.

Marques De Souza, C. G. and R. M. Peralta (2003). "Purification and characterization of the main laccase produced by the white-rot fungus Pleurotus pulmonarius on wheat bran solid state medium." *J Basic Microbiol* 43(4): 278-286.

Martínez, A. T., F. J. Ruiz-Dueñas, S. Camarero, A. Serrano, D. Linde, H. Lund, J. Vind, M. Tovborg, O. M. Herold-Majumdar, M. Hofrichter, C. Liers, R. Ullrich, K. Scheibner, G. Sannia, A. Piscitelli, C. Pezzella, M. E. Sener, S. Kılıç, W. J. H. van Berkel, V. Guallar, M. F. Lucas, R. Zuhse, R. Ludwig, F. Hollmann, E. Fernández-Fueyo, E. Record, C. B. Faulds, M. Tortajada, I. Winckelmann, J.-A. Rasmussen, M. Gelo-Pujic, A. Gutiérrez, J. C. del Río, J. Rencoret and M. Alcalde (2017). "Oxidoreductases on their way to industrial biotransformations." *Biotechnol Adv* 35(6): 815-831.

Martins, L. g. O., C. M. Soares, M. M. Pereira, M. Teixeira, T. Costa, G. H. Jones and A. O. Henriques (2002). "Molecular and Biochemical Characterization of a Highly Stable Bacterial Laccase That Occurs as a Structural Component of theBacillus subtilis Endospore Coat." *Journal of Biological Chemistry* 277(21): 18849-18859.

Masai, E., Y. Katayama and M. Fukuda (2007). "Genetic and biochemical investigations on bacterial catabolic pathways for lignin-derived aromatic compounds." *Bioscience, Biotechnology, and Biochemistry* 71(1): 1 - 15.

Masai, E., Y. Katayama, S. Nishikawa, M. Yamasaki, N. Morohoshi and T. Haraguchi (1989). "Detection and localization of a new enzyme catalyzing the beta-aryl ether cleavage in the soil bacterium (Pseudomonas paucimobilis SYK-6)." *FEBS Lett* 249(2): 348-352.

Masai, E., S. Kubota, Y. Katayama, S. Kawai, M. Yamasaki and N. Morohoshi (1993). "Characterization of the C alpha-dehydrogenase gene involved in the cleavage of beta-aryl ether by Pseudomonas paucimobilis." *Biosci Biotechnol Biochem* 57(10): 1655-1659.

Masai, E., M. Sasaki, Y. Minakawa, T. Abe, T. Sonoki, K. Miyauchi, Y. Katayama and M. Fukuda (2004). "A novel tetrahydrofolate-dependent O-demethylase gene is essential for growth of Sphingomonas paucimobilis SYK-6 with syringate." *J Bacteriol* 186(9): 2757-2765.

Master, S., T. C. Zahrt, J. Song and V. Deretic (2001). "Mapping of Mycobacterium tuberculosis katG Promoters and Their Differential Expression in Infected Macrophages." *J Bacteriol* 183(13): 4033.

Mathews, S. L., J. Pawlak and A. M. Grunden (2015). "Bacterial biodegradation and bioconversion of industrial lignocellulosic streams." *Applied Microbiology and Biotechnology* 99(7): 2939-2954.

McCord, J. M. and E. D. Day, Jr. (1978). "Superoxide-dependent production of hydroxyl radical catalyzed by iron-EDTA complex." *FEBS Lett* 86(1): 139-142.

McDonald, J. E., D. J. Rooks and A. J. McCarthy (2012). Chapter nineteen - Methods for the Isolation of Cellulose-Degrading Microorganisms. <u>Methods in Enzymology</u>. J. G. Harry, Academic Press. **Volume 510:** 349-374.

Meijnen, J. P., S. Verhoef, A. A. Briedjlal, J. H. de Winde and H. J. Ruijssenaars (2011). "Improved p-hydroxybenzoate production by engineered Pseudomonas putida S12 by using a mixed-substrate feeding strategy." *Appl Microbiol Biotechnol* 90(3): 885-893.

Mellano, M. A. and D. A. Cooksey (1988). "Nucleotide sequence and organization of copper resistance genes from Pseudomonas syringae pv. tomato." *J Bacteriol* 170(6): 2879-2883.

Menon, V. and M. Rao (2012). "Trends in bioconversion of lignocellulose: Biofuels, platform chemicals & biorefinery concept." *Progress in Energy and Combustion Science* 38(4): 522-550.

Michalska, K., C. Chang, J. C. Mack, S. Zerbs, A. Joachimiak and F. R. Collart (2012). "Characterization of transport proteins for aromatic compounds derived from lignin: benzoate derivative binding proteins." *J Mol Biol* 423(4): 555-575.

Michas, A., G. Vestergaard, K. Trautwein, P. Avramidis, D. G. Hatzinikolaou, C. E. Vorgias, H. Wilkes, R. Rabus, M. Schloter and A. Schöler (2017). "More than 2500 years of oil exposure shape sediment microbiomes with the potential for syntrophic degradation of hydrocarbons linked to methanogenesis." *Microbiome* 5(1): 118.

Miethke, M., C. G. Monteferrante, M. A. Marahiel and J. M. van Dijl (2013). "The Bacillus subtilis EfeUOB transporter is essential for high-affinity acquisition of ferrous and ferric iron." *Biochimica et Biophysica Acta (BBA) - Molecular Cell Research* 1833(10): 2267-2278.

Miller, G. L. (1959). "Use of Dinitrosalicylic Acid Reagent for Determination of Reducing Sugar." *Analytical Chemistry* 31(3): 426-428.

Min, D., S. F. Wang, H. M. Chang, H. Jameel and L. Lucia (2017). "Molecular changes in corn stover lignin resulting from pretreatment chemistry." *BioResources* 12(3): 6262-6275.

Min, K., G. Gong, H. M. Woo, Y. Kim and Y. Um (2015). "A dye-decolorizing peroxidase from Bacillus subtilis exhibiting substrate-dependent optimum temperature for dyes and β-ether lignin dimer." *Sci. Rep.* 5.

Mishra, S., A. Sachan, A. Vidyarthi and S. Ghosh Sachan (2014). "Transformation of ferulic acid to 4-vinyl guaiacol as a major metabolite: a microbial approach." *Reviews in Environmental Science and Bio/Technology* 13.

Mitra, A., Y. Kitamura, M. J. Gasson, A. Narbad, A. J. Parr, J. Payne, M. J. Rhodes, C. Sewter and N. J. Walton (1999). "4-hydroxycinnamoyl-CoA hydratase/lyase (HCHL)--An enzyme of phenylpropanoid chain cleavage from Pseudomonas." *Arch Biochem Biophys* 365(1): 10-16.

Miyazaki, K. (2005). "A hyperthermophilic laccase from Thermus thermophilus HB27." *Extremophiles* 9(6): 415-425.

Molina-Guijarro, J. M., J. Perez, J. Munoz-Dorado, F. Guillen, R. Moya, M. Hernandez and M. E. Arias (2009). "Detoxification of azo dyes by a novel pH-versatile, salt-resistant laccase from *Streptomyces ipomoea.*" *International Microbiology* 12(1): 13-21.

Mollania, N., K. Khajeh, B. Ranjbar and S. Hosseinkhani (2011). "Enhancement of a bacterial laccase thermostability through directed mutagenesis of a surface loop." *Enzyme and Microbial Technology* 49(5): 446-452.

Moon, R. J., A. Martini, J. Nairn, J. Simonsen and J. Youngblood (2011). "Cellulose nanomaterials review: structure, properties and nanocomposites." *Chem Soc Rev* 40(7): 3941-3994.

Moore, E. R. B., M. Mau, A. Arnscheidt, E. C. Böttger, R. A. Hutson, M. D. Collins, Y. Van De Peer, R. De Wachter and K. N. Timmis (1996). "The Determination and Comparison of the 16S rRNA Gene Sequences of Species of the Genus Pseudomonas (sensu stricto and Estimation of the Natural Intrageneric Relationships." *Systematic and Applied Microbiology* 19(4): 478-492.

Moore, R. L., L. J. Powell and D. C. Goodwin (2008). "The kinetic properties producing the perfunctory pH profiles of catalase-peroxidases." *Biochimica et Biophysica Acta (BBA) - Proteins and Proteomics* 1784(6): 900-907.

Moreno, A., D. Ibarra, M. Eugenio and E. Tomas-Pejo (2019). "Laccases as versatile enzymes: From industrial uses to novel applications."

Mulligan, C., M. Fischer and G. H. Thomas (2011). "Tripartite ATP-independent periplasmic (TRAP) transporters in bacteria and archaea." *FEMS Microbiol Rev* 35(1): 68-86.

Murinova, S. and K. Dercova (2014). "Response mechanisms of bacterial degraders to environmental contaminants on the level of cell walls and cytoplasmic membrane." *Int J Microbiol* 2014: 873081.

Mussatto, S. I., G. Dragone and I. C. Roberto (2007). "Ferulic and p-coumaric acids extraction by alkaline hydrolysis of brewer's spent grain." *Industrial Crops and Products* 25(2): 231-237.

Nadler, V., I. Goldberg and A. Hochman (1986). "Comparative study of bacterial catalases." *Biochimica et Biophysica Acta (BBA) - General Subjects* 882(2): 234-241.

Naresh Kumar, M., R. Ravikumar, S. Thenmozhi, M. Ranjith Kumar and M. Kirupa Shankar (2019). "Choice of Pretreatment Technology for Sustainable Production of Bioethanol from Lignocellulosic Biomass: Bottle Necks and Recommendations." *Waste and Biomass Valorization* 10(6): 1693-1709.

Nawapan, S., N. Charoenlap, A. Charoenwuttitam, P. Saenkham, S. Mongkolsuk and P. Vattanaviboon (2009). "Functional and expression analyses of the cop operon, required for copper resistance in Agrobacterium tumefaciens." *J Bacteriol* 191(16): 5159-5168.

Ndontsa, E. N., R. L. Moore and D. C. Goodwin (2012). "Stimulation of KatG catalase activity by peroxidatic electron donors." *Archives of biochemistry and biophysics* 525(2): 215-222.

Ndontsa, E. N., R. L. Moore and D. C. Goodwin (2012). "Stimulation of KatG catalase activity by peroxidatic electron donors." *Arch Biochem Biophys* 525(2): 215-222.

Neher, T. M. and D. R. Lueking (2009). "Pseudomonas fluorescens ompW: plasmid localization and requirement for naphthalene uptake." *Can J Microbiol* 55(5): 553-563.

Nguyen, L.-T., H. A. Schmidt, A. von Haeseler and B. Q. Minh (2014). "IQ-TREE: A Fast and Effective Stochastic Algorithm for Estimating Maximum-Likelihood Phylogenies." *Molecular Biology and Evolution* 32(1): 268-274.

Nichols, N. N. and C. S. Harwood (1997). "PcaK, a high-affinity permease for the aromatic compounds 4-hydroxybenzoate and protocatechuate from Pseudomonas putida." *J Bacteriol* 179(16): 5056-5061.

Niladevi, K. N., N. Jacob and P. Prema (2008). "Evidence for a halotolerant-alkaline laccase in Streptomyces psammoticus: Purification and characterization." *Process Biochemistry* 43(6): 654-660.

Niladevi, K. N. and P. Prema (2008). "Effect of inducers and process parameters on laccase production by Streptomyces psammoticus and its application in dye decolourization." *Bioresour Technol* 99(11): 4583-4589.

Nogales, J., A. Canales, J. Jimenez-Barbero, J. L. Garcia and E. Diaz (2005). "Molecular characterization of the gallate dioxygenase from Pseudomonas putida KT2440. The prototype of a new subgroup of extradiol dioxygenases." *J Biol Chem* 280(42): 35382-35390.

Noinaj, N., M. Guillier, T. J. Barnard and S. K. Buchanan (2010). "TonB-dependent transporters: regulation, structure, and function." *Annu Rev Microbiol* 64: 43-60.

Novoa, C., G. V. Dhoke, D. M. Mate, R. Martínez, T. Haarmann, M. Schreiter, J. Eidner, R. Schwerdtfeger, P. Lorenz, M. D. Davari, F. Jakob and U. Schwaneberg (2019). "KnowVolution of a Fungal Laccase toward Alkaline pH." *Chembiochem* 20(11): 1458-1466.

Numata, K. and K. Morisaki (2015). "Screening of Marine Bacteria To Synthesize Polyhydroxyalkanoate from Lignin: Contribution of Lignin Derivatives to Biosynthesis by Oceanimonas doudoroffii." *ACS sustainable chemistry & engineering* 3(4): 569-573.

Obel, N., L. Neumetzler and M. Pauly (2007). Hemicelluloses and Cell Expansion. The Expanding Cell. J.-P. Verbelen and K. Vissenberg. Berlin, Heidelberg, Springer Berlin Heidelberg**:** 57-88.

Ogola, H., O. Ogola, H. Ashida, T. Ishikawa and Y. Sawa (2015). Explorations and Applications of Enzyme-linked Bioremediation of Synthetic Dyes.

Oh, H., S.-Y. Heo, D. Y. Kim, D. Park, K. S. Bae and H.-Y. Park (2008). "Biochemical characterization and sequence analysis of a xylanase produced by an exo-symbiotic bacterium of Gryllotalpa orientalis, Cellulosimicrobium sp. HY-12." *Antonie Van Leeuwenhoek* 93: 437-442.

Ohara, H. (2003). "Biorefinery." *Appl Microbiol Biotechnol* 62(5-6): 474-477.

Ohta, Y., S. Nishi, R. Hasegawa and Y. Hatada (2015). "Combination of six enzymes of a marine Novosphingobium converts the stereoisomers of β-O-4 lignin model dimers into the respective monomers." *Sci Rep* 5: 15105.

Orencio-Trejo, M., S. De la Torre-Zavala, A. Rodriguez-Garcia, H. Avilés-Arnaut and A. Gastelum-Arellanez (2016). "Assessing the Performance of Bacterial Cellulases: the Use of Bacillus and Paenibacillus Strains as Enzyme Sources for Lignocellulose Saccharification." *BioEnergy Research* 9(4): 1023-1033.

Otani, H., Y.-E. Lee, I. Casabon and L. D. Eltis (2014). "Characterization of p-Hydroxycinnamate Catabolism in a Soil Actinobacterium." *J Bacteriol* 196(24): 4293.

Oviedo, C. and J. Rodríguez (2003). "EDTA: the chelating agent under environmental scrutiny." *Química Nova* 26: 901-905.

Palacas, J. G., D. Monopolis, C. A. Nicolaou and D. E. Anders (1986). "Geochemical correlation of surface and subsurface oils, western Greece." *Organic Geochemistry* 10(1): 417-423.

Pasadakis, N., V. Dagounaki and E. Chamilaki (2016). "A comparative organic geochemical study of oils seeps in Western Greece." *Energy Sources, Part A: Recovery, Utilization and Environmental Effects* 38(3): 362-369.

Peng, X., E. Masai, Y. Katayama and M. Fukuda (1999). "Characterization of the meta-Cleavage Compound Hydrolase Gene Involved in Degradation of the Lignin-Related Biphenyl Structure by Sphingomonas paucimobilis SYK-6." *Appl Environ Microbiol* 65(6): 2789-2793.

Pereira, J., E. Giese, M. Moretti, A. Santos, O. Micali Perrone, M. Boscolo, R. Da Silva, E. Gomes, D. Martins and A. Santos Gomes (2017). Effect of Metal Ions, Chemical Agents and Organic Compounds on Lignocellulolytic Enzymes Activities: 139-164.

Perez, J. M., W. S. Kontur, M. Alherech, J. Coplien, S. D. Karlen, S. S. Stahl, T. J. Donohue and D. R. Noguera (2019). "Funneling aromatic products of chemically depolymerized lignin into 2-pyrone-4-6-dicarboxylic acid with Novosphingobium aromaticivorans." *Green Chemistry* 21(6): 1340-1350.

Petersen, T. N., S. Brunak, G. von Heijne and H. Nielsen (2011). "SignalP 4.0: discriminating signal peptides from transmembrane regions." *Nat Methods* 8(10): 785-786.

Pettersen, E. F., T. D. Goddard, C. C. Huang, G. S. Couch, D. M. Greenblatt, E. C. Meng and T. E. Ferrin (2004). "UCSF Chimera--a visualization system for exploratory research and analysis." *J Comput Chem* 25(13): 1605-1612.

Peyrado, G. M., S. M. de Forchetti, H. Tigier and E. Taleisnik (1996). "Tissue Printing for Peroxidases Associated with Lignification." *Biotechnic & Histochemistry* 71(5): 258-262.

Philibert, T., Z. Rao, T. Yang, J. Zhou, G. Huang, K. Irene and N. Samuel (2016). "Heterologous expression and characterization of a new heme-catalase in Bacillus subtilis 168." *Journal of Industrial Microbiology & Biotechnology* 43(6): 729-740.

Pozdnyakova, N., O. Turkovskaya, E. N. Yudina and Y. Rodakiewicz-Nowak (2006). "Yellow laccase from the fungus Pleurotus ostreatus D1: Purification and characterization." *Applied Biochemistry and Microbiology* 42: 56-61.

Prakash, N., N. Sharma, R. Prakash and R. Acharya (2010). "Removal of selenium from Se enriched natural soils by a consortium of Bacillus isolates." *Bulletin of environmental contamination and toxicology* 85(2): 214 - 218.

Qiao, W., J. Chu, S. Ding, X. Song and L. Yu (2017). "Characterization of a thermo-alkali-stable laccase from Bacillus subtilis cjp3 and its application in dyes decolorization." *J Environ Sci Health A Tox Hazard Subst Environ Eng* 52(8): 710-717.

Ragauskas, A. J., G. T. Beckham, M. J. Biddy, R. Chandra, F. Chen, M. F. Davis, B. H. Davison, R. A. Dixon, P. Gilna, M. Keller, P. Langan, A. K. Naskar, J. N. Saddler, T. J. Tschaplinski, G. A. Tuskan and C. E. Wyman (2014). "Lignin Valorization: Improving Lignin Processing in the Biorefinery." *Science* 344(6185).

Rahmanpour, R. and T. D. Bugg (2015). "Characterisation of Dyp-type peroxidases from Pseudomonas fluorescens Pf-5: Oxidation of Mn(II) and polymeric lignin by Dyp1B." *Arch Biochem Biophys* 574: 93-98.

Rahmanpour, R. and T. D. H. Bugg (2013). "Assembly in vitro of Rhodococcus jostii RHA1 encapsulin and peroxidase DypB to form a nanocompartment." *FEBS Journal* 280(9): 2097-2104.

Rahmanpour, R., D. Rea, S. Jamshidi, V. Fülöp and T. D. Bugg (2016). "Structure of Thermobifida fusca DyP-type peroxidase and activity towards Kraft lignin and lignin model compounds." *Arch Biochem Biophys* 594: 54-60.

Raj, A., S. Kumar and S. Singh (2013). "A Highly Thermostable Xylanase from Stenotrophomonas maltophilia: Purification and Partial Characterization." *Enzyme Res* 2013: 429305.

Rajasekaran, M. B., S. Nilapwar, S. C. Andrews and K. A. Watson (2009). "EfeO-cupredoxins: major new members of the cupredoxin superfamily with roles in bacterial iron transport." *BioMetals* 23(1): 1.

Ralph, J. (2010). "Hydroxycinnamates in lignification." *Phytochemistry Reviews* 9(1): 65-83.

Raven, E. L. (2013). Heme Peroxidases. Encyclopedia of Biophysics. G. C. K. Roberts. Berlin, Heidelberg, Springer Berlin Heidelberg: 962-965.

Ravi, K., O. Y. Abdelaziz, M. Nobel, J. Garcia-Hidalgo, M. F. Gorwa-Grauslund, C. P. Hulteberg and G. Liden (2019). "Bacterial conversion of depolymerized Kraft lignin." *Biotechnol Biofuels* 12: 56.

Ravi, K., J. Garcia-Hidalgo, M. F. Gorwa-Grauslund and G. Liden (2017). "Conversion of lignin model compounds by Pseudomonas putida KT2440 and isolates from compost." *Appl Microbiol Biotechnol* 101(12): 5059-5070.

Reiss, R., J. Ihssen, M. Richter, E. Eichhorn, B. Schilling and L. Thöny-Meyer (2013). "Laccase versus Laccase-Like Multi-Copper Oxidase: A Comparative Study of Similar Enzymes with Diverse Substrate Spectra." *PLoS One* 8(6): e65633.

Rekik, H., Z. J. Nadia, W. Bejar, S. Kourdali, M. Belhoul, M. Hmidi, A. Benkiar, A. Badis, N. Sallem, S. Bejar and B. Jaouadi (2015). "Characterization of a purified decolorizing detergent-stable peroxidase from Streptomyces griseosporeus SN9." *Int J Biol Macromol* 73: 253-263.

Reverón, I., N. Jiménez, J. A. Curiel, E. Peñas, F. López de Felipe, B. de Las Rivas and R. Muñoz (2017). "Differential Gene Expression by Lactobacillus plantarum WCFS1 in Response to Phenolic Compounds Reveals New Genes Involved in Tannin Degradation." *Appl Environ Microbiol* 83(7).

Reyes-Ortiz, V., R. A. Heins, G. Cheng, E. Y. Kim, B. C. Vernon, R. B. Elandt, P. D. Adams, K. L. Sale, M. Z. Hadi, B. A. Simmons, M. S. Kent and D. Tullman-Ercek (2013). "Addition of a carbohydrate-binding module enhances cellulase penetration into cellulose substrates." *Biotechnol Biofuels* 6(1): 93.

Ro, Y. T., H. I. Lee, E. J. Kim, J. H. Koo, E. Kim and Y. M. Kim (2003). "Purification, characterization, and physiological response of a catalase-peroxidase in Mycobacterium sp. strain JC1 DSM 3803 grown on methanol." *FEMS Microbiol Lett* 226(2): 397-403.

Roberts, J. N., R. Singh, J. C. Grigg, M. E. Murphy, T. D. Bugg and L. D. Eltis (2011). "Characterization of dye-decolorizing peroxidases from Rhodococcus jostii RHA1." *Biochemistry* 50(23): 5108-5119.

Roberts, S. A., A. Weichsel, G. Grass, K. Thakali, J. T. Hazzard, G. Tollin, C. Rensing and W. R. Montfort (2002). "Crystal structure and electron transfer kinetics of CueO, a multicopper oxidase required for copper homeostasis in Escherichia coli." *Proc Natl Acad Sci U S A* 99(5): 2766-2771.

Rodriguez, A., D. Salvachúa, R. Katahira, B. A. Black, N. S. Cleveland, M. Reed, H. Smith, E. E. K. Baidoo, J. D. Keasling, B. A. Simmons, G. T. Beckham and J. M. Gladden (2017). "Base-Catalyzed Depolymerization of Solid Lignin-Rich Streams Enables Microbial Conversion." *ACS sustainable chemistry & engineering* 5(9): 8171-8180.

Rulíšek, L. and U. Ryde (2013). "Theoretical studies of the active-site structure, spectroscopic and thermodynamic properties, and reaction mechanism of multicopper oxidases." *Coordination Chemistry Reviews* 257(2): 445-458.

S. Miller Jr, E. and S. W. Peretti (1999). "Bioconversion of toluene to p-hydroxybenzoate . via the construction and characterization of a recombinant Pseudomonas putida." *Green Chemistry* 1(3): 143-152.

Sainsbury, P. D., E. M. Hardiman, M. Ahmad, H. Otani, N. Seghezzi, L. D. Eltis and T. D. Bugg (2013). "Breaking down lignin to high-value chemicals: the conversion of lignocellulose to vanillin in a gene deletion mutant of Rhodococcus jostii RHA1." *ACS Chem Biol* 8(10): 2151-2156.

Salmon, R. C., M. J. Cliff, J. B. Rafferty and D. J. Kelly (2013). "The CouPSTU and TarPQM transporters in Rhodopseudomonas palustris: redundant, promiscuous uptake systems for lignin-derived aromatic substrates." *PLoS One* 8(3): e59844-e59844.

Salvachúa, D., E. M. Karp, C. T. Nimlos, D. R. Vardon and G. T. Beckham (2015). "Towards lignin consolidated bioprocessing: simultaneous lignin depolymerization and product generation by bacteria." *Green Chemistry* 17(11): 4951-4967.

Salvachúa, D., A. Prieto, M. L. Mattinen, T. Tamminen, T. Liitiä, M. Lille, S. Willför, A. T. Martínez, M. J. Martínez and C. B. Faulds (2013). "Versatile peroxidase as a valuable tool for generating new biomolecules by homogeneous and heterogeneous cross-linking." *Enzyme Microb Technol* 52(6-7): 303-311.

Sammons, R., D. Harper, N. Labbé, J. Bozell, T. Elder and T. Rials (2013). "Characterization of Organosolv Lignins using Thermal and FT-IR Spectroscopic Analysis." *BioResources* 8.

Santos, A., S. Mendes, V. Brissos and L. O. Martins (2014). "New dye-decolorizing peroxidases from Bacillus subtilis and Pseudomonas putida MET94: towards biotechnological applications." *Appl Microbiol Biotechnol* 98(5): 2053-2065.

Sato, Y., H. Moriuchi, S. Hishiyama, Y. Otsuka, K. Oshima, D. Kasai, M. Nakamura, S. Ohara, Y. Katayama, M. Fukuda and E. Masai (2009). "Identification of three alcohol dehydrogenase genes involved in the stereospecific catabolism of arylglycerol-beta-aryl ether by Sphingobium sp. strain SYK-6." *Appl Environ Microbiol* 75(16): 5195-5201.

Savelli, B., Q. Li, M. Webber, A. M. Jemmat, A. Robitaille, M. Zamocky, C. Mathé and C. Dunand (2019). "RedoxiBase: A database for ROS homeostasis regulated proteins." *Redox Biol* 26: 101247.

Scheiblbrandner, S., E. Breslmayr, F. Csarman, R. Paukner, J. Führer, P. L. Herzog, S. V. Shleev, E. M. Osipov, T. V. Tikhonova, V. O. Popov, D. Haltrich, R. Ludwig and R. Kittl (2017). "Evolving stability and pH-dependent activity of the high redox potential Botrytis aclada laccase for enzymatic fuel cells." *Sci Rep* 7(1): 13688.

Scheibner, M., B. Hülsdau, K. Zelena, M. Nimtz, L. de Boer, R. G. Berger and H. Zorn (2008). "Novel peroxidases of Marasmius scorodonius degrade β-carotene." *Applied Microbiology and Biotechnology* 77(6): 1241-1250.

Schlosser, D. and C. Höfer (2002). "Laccase-catalyzed oxidation of Mn2+ in the presence of natural Mn3+ chelators as a novel source of extracellular H2O2 production and its impact on manganese peroxidase." *Appl Environ Microbiol* 68(7): 3514-3521.

Schoenherr, S., M. Ebrahimi and P. Czermak (2018). Lignin Degradation Processes and the Purification of Valuable Products.

Seca, A. M. L., J. A. S. Cavaleiro, F. M. J. Domingues, A. J. D. Silvestre, D. Evtuguin and C. P. Neto (2000). "Structural Characterization of the Lignin from the Nodes and Internodes of Arundo donax Reed." *J Agric Food Chem* 48(3): 817-824.

Shallom, D. and Y. Shoham (2003). "Microbial hemicellulases." *Curr Opin Microbiol* 6(3): 219-228.

Sharma, M., B. S. Chadha and H. S. Saini (2010). "Purification and characterization of two thermostable xylanases from Malbranchea flava active under alkaline conditions." *Bioresour Technol* 101(22): 8834-8842.

She, D., F. Xu, Z. Geng, R. Sun, G. L. Jones and M. S. Baird (2010). "Physicochemical characterization of extracted lignin from sweet sorghum stem." *Industrial Crops and Products* 32(1): 21-28.

Shi, H., Y. Zhang, H. Zhong, Y. Huang, X. Li and F. Wang (2014). "Cloning, over-expression and characterization of a thermo-tolerant xylanase from Thermotoga thermarum." *Biotechnol Lett* 36(3): 587-593.

Shi, X., Q. Liu, J. Ma, H. Liao, X. Xiong, K. Zhang, T. Wang, X. Liu, T. Xu, S. Yuan, Z. Xin and Y. Zhu (2015). "An acid-stable bacterial laccase identified from the endophyte Pantoea ananatis Sd-1 genome exhibiting lignin degradation and dye decolorization abilities." *Biotechnol Lett* 37.

Shi, Y., L. Chai, C. Tang, Z. Yang, Y. Zheng, Y. Chen and Q. Jing (2013). "Biochemical investigation of kraft lignin degradation by *Pandoraea* sp. B-6 isolated from bamboo slips." *Bioprocess Biosyst Eng* 36(12): 1957-1965.

Shin, K., I. Oh and C. Kim (1997). "Production and Purification of Remazol Brilliant Blue R Decolorizing Peroxidase from the Culture Filtrate of Pleurotus ostreatus." *Appl Environ Microbiol* 63(5): 1744-1748.

Si, W., Z. Wu, L. Wang, M. Yang and X. Zhao (2015). "Enzymological Characterization of Atm, the First Laccase from Agrobacterium sp. S5-1, with the Ability to Enhance In Vitro digestibility of Maize Straw." *PLoS One* 10(5): e0128204.

Simon, O., I. Klaiber, A. Huber and J. Pfannstiel (2014). "Comprehensive proteome analysis of the response of Pseudomonas putida KT2440 to the flavor compound vanillin." *J Proteomics* 109: 212-227.

Singh, R. and L. D. Eltis (2015). "The multihued palette of dye-decolorizing peroxidases." *Arch Biochem Biophys* 574: 56-65.

Singh, R., J. C. Grigg, Z. Armstrong, M. E. Murphy and L. D. Eltis (2012). "Distal heme pocket residues of B-type dye-decolorizing peroxidase: arginine but not aspartate is essential for peroxidase activity." *J Biol Chem* 287(13): 10623-10630.

Singh, R., J. C. Grigg, W. Qin, J. F. Kadla, M. E. P. Murphy and L. D. Eltis (2013). "Improved Manganese-Oxidizing Activity of DypB, a Peroxidase from a Lignolytic Bacterium." *ACS Chem Biol* 8(4): 700-706.

Singh, R., B. Wiseman, T. Deemagarn, L. J. Donald, H. W. Duckworth, X. Carpena, I. Fita and P. C. Loewen (2004). "Catalase-peroxidases (KatG) exhibit NADH oxidase activity." *J Biol Chem* 279(41): 43098-43106.

Singh, R., B. Wiseman, T. Deemagarn, V. Jha, J. Switala and P. C. Loewen (2008). "Comparative study of catalase-peroxidases (KatGs)." *Arch Biochem Biophys* 471(2): 207-214.

Singleton, V. L. and J. A. Rossi (1965). "Colorimetry of Total Phenolics with Phosphomolybdic-Phosphotungstic Acid Reagents." *American Journal of Enology and Viticulture* 16(3): 144.

Sitthisak, S., K. Howieson, C. Amezola and R. K. Jayaswal (2005). "Characterization of a multicopper oxidase gene from Staphylococcus aureus." *Appl Environ Microbiol* 71(9): 5650-5653.

Smulevich, G., C. Jakopitsch, E. Droghetti and C. Obinger (2006). "Probing the structure and bifunctionality of catalase-peroxidase (KatG)." *J Inorg Biochem* 100(4): 568-585.

Solioz, M. and J. V. Stoyanov (2003). "Copper homeostasis in Enterococcus hirae." *FEMS Microbiol Rev* 27(2-3): 183-195.

Solomon, E. I., U. M. Sundaram and T. E. Machonkin (1996). "Multicopper Oxidases and Oxygenases." *Chem Rev* 96(7): 2563-2606.

Sonoki, T., K. Takahashi, H. Sugita, M. Hatamura, Y. Azuma, T. Sato, S. Suzuki, N. Kamimura and E. Masai (2018). "Glucose-Free cis,cis-Muconic Acid Production via New Metabolic Designs Corresponding to the Heterogeneity of Lignin." *ACS sustainable chemistry & engineering* 6(1): 1256-1264.

Spezio, M., D. B. Wilson and P. A. Karplus (1993). "Crystal structure of the catalytic domain of a thermophilic endocellulase." *Biochemistry* 32(38): 9906-9916.

Srivastava, L. M. (2002). CHAPTER 2 - Cell Wall, Cell Division, and Cell Growth. Plant Growth and Development. L. M. Srivastava. San Diego, Academic Press**:** 23-74.

Srivastava, N., M. Srivastava, P. K. Mishra, V. K. Gupta, G. Molina, S. Rodriguez-Couto, A. Manikanta and P. W. Ramteke (2018). "Applications of fungal cellulases in biofuel production: Advances and limitations." *Renewable and Sustainable Energy Reviews* 82: 2379-2386.

Stanzione, I., C. Pezzella, P. Giardina, G. Sannia and A. Piscitelli (2020). "Beyond natural laccases: extension of their potential applications by protein engineering." *Applied Microbiology and Biotechnology* 104(3): 915-924.

Strassberger, Z., S. Tanase and G. Rothenberg (2014). "The pros and cons of lignin valorisation in an integrated biorefinery." *RSC Advances* 4(48): 25310-25318.

Strong, P. J. and H. Claus (2011). "Laccase: A review of its past and its future in bioremediation." *Critical Reviews in Environmental Science and Technology* 41(4): 373-434.

Sugano, Y. (2009). "DyP-type peroxidases comprise a novel heme peroxidase family." *Cellular and Molecular Life Sciences* 66(8): 1387-1403.

Sugano, Y., R. Muramatsu, A. Ichiyanagi, T. Sato and M. Shoda (2007). "DyP, a unique dye-decolorizing peroxidase, represents a novel heme peroxidase family: ASP171 replaces the distal histidine of classical peroxidases." *J Biol Chem* 282(50): 36652-36658.

Sugawara, K., Y. Nishihashi, T. Narioka, T. Yoshida, M. Morita and Y. Sugano (2017). "Characterization of a novel DyP-type peroxidase from Streptomyces avermitilis." *J Biosci Bioeng* 123(4): 425-430.

Suman, S. K., M. Dhawaria, D. Tripathi, V. Raturi, D. K. Adhikari and P. K. Kanaujia (2016). "Investigation of lignin biodegradation by Trabulsiella sp. isolated from termite gut." *International Biodeterioration & Biodegradation* 112: 12-17.

Sun, R., J. M. Lawther and W. B. Banks (1996). "Effects of pretreatment temperature and alkali concentration on the composition of alkali-soluble lignins from wheat straw." *Journal of Applied Polymer Science* 62(9): 1473-1481.

Suzuki, T., K. Endo, M. Ito, H. Tsujibo, K. Miyamoto and Y. Inamori (2003). "A Thermostable Laccase from <i>Streptomyces lavendulae</i> REN-7: Purification, Characterization, Nucleotide Sequence, and Expression." *Bioscience, Biotechnology, and Biochemistry* 67(10): 2167-2175.

Tamber, S., M. M. Ochs and R. E. Hancock (2006). "Role of the novel OprD family of porins in nutrient uptake in Pseudomonas aeruginosa." *J Bacteriol* 188(1): 45-54.

Tanamura, K., T. Abe, N. Kamimura, D. Kasai, S. Hishiyama, Y. Otsuka, M. Nakamura, S. Kajita, Y. Katayama, M. Fukuda and E. Masai (2011). "Characterization of the third glutathione S-transferase gene involved in enantioselective cleavage of the β-aryl ether by Sphingobium sp. strain SYK-6." *Biosci Biotechnol Biochem* 75(12): 2404-2407.

Taylor, C., E. Hardiman, M. Ahmad, P. Sainsbury, P. Norris and T. Bugg (2012). "Isolation of bacterial strains able to metabolize lignin from screening of environmental samples." *J Appl Microbiol* 113(3): 521-530.

Teather, R. M. and P. J. Wood (1982). "Use of Congo red-polysaccharide interactions in enumeration and characterization of cellulolytic bacteria from the bovine rumen." *Appl Environ Microbiol* 43(4): 777-780.

Teeri, T. T. (1997). "Crystalline cellulose degradation: new insight into the function of cellobiohydrolases." *Trends in Biotechnology* 15(5): 160-167.

Tejado, A., C. Peña, J. Labidi, J. M. Echeverria and I. Mondragon (2007). "Physico-chemical characterization of lignins from different sources for use in phenol-formaldehyde resin synthesis." *Bioresour Technol* 98(8): 1655-1663.

ten Have, R. and P. J. Teunissen (2001). "Oxidative mechanisms involved in lignin degradation by white-rot fungi." *Chem Rev* 101(11): 3397-3413.

Thomas, L., M. V. Ushasree and A. Pandey (2014). "An alkali-thermostable xylanase from Bacillus pumilus functionally expressed in Kluyveromyces lactis and evaluation of its deinking efficiency." *Bioresour Technol* 165: 309-313.

Tian, J. H., A. M. Pourcher and P. Peu (2016). "Isolation of bacterial strains able to metabolize lignin and lignin-related compounds." *Lett Appl Microbiol* 63(1): 30-37.

Tiwari, R., L. Nain, N. E. Labrou and P. Shukla (2018). "Bioprospecting of functional cellulases from metagenome for second generation biofuel production: a review." *Crit Rev Microbiol* 44(2): 244-257.

Tonin, F., E. Rosini, L. Piubelli, A. Sanchez-Amat and L. Pollegioni (2016). "Different recombinant forms of polyphenol oxidase A, a laccase from Marinomonas mediterranea." *Protein Expr Purif* 123: 60-69.

Trautwein, K., H. Wilkes and R. Rabus (2012). "Proteogenomic evidence for β-oxidation of plant-derived 3-phenylpropanoids in " Aromatoleum aromaticum " EbN1." *Proteomics* 12: 1402-1413.

Uchida, T., M. Sasaki, Y. Tanaka and K. Ishimori (2015). "A Dye-Decolorizing Peroxidase from Vibrio cholerae." *Biochemistry* 54(43): 6610-6621.

Vaaje-Kolstad, G., B. Westereng, S. J. Horn, Z. Liu, H. Zhai, M. Sørlie and V. G. Eijsink (2010). "An oxidative enzyme boosting the enzymatic conversion of recalcitrant polysaccharides." *Science* 330(6001): 219-222.

van Bloois, E., D. E. Torres Pazmiño, R. T. Winter and M. W. Fraaije (2010). "A robust and extracellular heme-containing peroxidase from Thermobifida fusca as prototype of a bacterial peroxidase superfamily." *Appl Microbiol Biotechnol* 86(5): 1419-1430.

Vanholme, R., B. Demedts, K. Morreel, J. Ralph and W. Boerjan (2010). "Lignin Biosynthesis and Structure." *Plant Physiol* 153(3): 895-905.

Vardon, D. R., N. A. Rorrer, D. Salvachúa, A. E. Settle, C. W. Johnson, M. J. Menart, N. S. Cleveland, P. N. Ciesielski, K. X. Steirer, J. R. Dorgan and G. T. Beckham (2016). "cis,cis-Muconic acid: separation and catalysis to bio-adipic acid for nylon-6,6 polymerization." *Green Chemistry*: p. 3397-3413.

Verhoef, S., N. Gao, H. J. Ruijssenaars and J. H. de Winde (2014). "Crude glycerol as feedstock for the sustainable production of p-hydroxybenzoate by Pseudomonas putida S12." *N Biotechnol* 31(1): 114-119.

Verma, D. and T. Satyanarayana (2012). "Molecular approaches for ameliorating microbial xylanases." *Bioresour Technol* 117: 360-367.

Veselý, M., M. Knoppová, J. Nesvera and M. Pátek (2007). "Analysis of catRABC operon for catechol degradation from phenol-degrading Rhodococcus erythropolis." *Appl Microbiol Biotechnol* 76(1): 159-168.

Vicuña, R. (1988). "Bacterial degradation of lignin." *Enzyme and Microbial Technology* 10(11): 646-655.

Vicuña, R., B. González, M. D. Mozuch and T. K. Kirk (1987). "Metabolism of Lignin Model Compounds of the Arylglycerol-beta-Aryl Ether Type by Pseudomonas acidovorans D(3)." *Appl Environ Microbiol* 53(11): 2605-2609.

Vishtal, A. and A. Kraslawski (2011). "Challenges in industrial applications of technical lignins." *BioResources* 6(3): 3547-3568.

Walia, A., P. Mehta, A. Chauhan and S. C.K (2012). "Production of Alkalophilic Xylanases by Paenibacillus polymyxa CKWX1 Isolated from Decomposing Wood." *Proceedings of the National Academy of Sciences, India Section B: Biological Sciences* 83.

Wang, T.-N., L. Lu, J.-Y. Wang, T.-F. Xu, J. Li and M. Zhao (2015). "Enhanced expression of an industry applicable CotA laccase from Bacillus subtilis in Pichia pastoris by non-repressing carbon sources together with pH adjustment: Recombinant enzyme characterization and dye decolorization." *Process Biochemistry* 50(1): 97-103.

Wang, Z., Y. Cai, X. Liao, F. Zhang, D. Zhang and Z. Li (2010). "Production and characterization of a novel laccase with cold adaptation and high thermal stability from an isolated fungus." *Appl Biochem Biotechnol* 162(1): 280-294.

Welinder, K. G. (1991). "Bacterial catalase-peroxidases are gene duplicated members of the plant peroxidase superfamily." *Biochimica et Biophysica Acta (BBA) - Protein Structure and Molecular Enzymology* 1080(3): 215-220.

Wells, T., Jr. and A. J. Ragauskas (2012). "Biotechnological opportunities with the β-ketoadipate pathway." *Trends Biotechnol* 30(12): 627-637.

Wells, T., Z. Wei and A. Ragauskas (2015). "Bioconversion of lignocellulosic pretreatment effluent via oleaginous Rhodococcus opacus DSM 1069." *Biomass and Bioenergy* 72: 200-205.

Widsten, P. and A. Kandelbauer (2008). "Adhesion improvement of lignocellulosic products by enzymatic pre-treatment." *Biotechnol Adv* 26(4): 379-386.

William, S., H. Feil and A. Copeland (2012). "Bacterial genomic DNA isolation using CTAB." http://1ofdmq2n8tc36m6i46scovo2e.wpengine.netdna-cdn.com/wp-content/uploads/2014/02/JGI-Bacterial-DNA-isolation-CTAB-Protocol-2012.pdf.

Windeisen, E. and G. Wegener (2016). Lignin as Building Unit for Polymers.

Wong, D. W. (2009). "Structure and action mechanism of ligninolytic enzymes." *Appl Biochem Biotechnol* 157(2): 174-209.

Wu, W., T. Dutta, A. M. Varman, A. Eudes, B. Manalansan, D. Loqué and S. Singh (2017). "Lignin Valorization: Two Hybrid Biochemical Routes for the Conversion of Polymeric Lignin into Value-added Chemicals." *Sci Rep* 7(1): 8420.

Xia, Z., T. Yoshida and M. Funaoka (2003). "Enzymatic synthesis of polyphenols from highly phenolic lignin-based polymers (lignophenols)." *Biotechnol Lett* 25(1): 9-12.

Xu, C., J. Zhang, Y. Zhang, Y. Guo, H. Xu, J. Xu and Z. Wang (2019). "Enhancement of high-solids enzymatic hydrolysis efficiency of alkali pretreated sugarcane bagasse at low cellulase dosage by fed-batch strategy based on optimized accessory enzymes and additives." *Bioresour Technol* 292: 121993.

Xu, F., T. Damhus, S. Danielsen and L. Østergaard (2007). Catalytic Applications of Laccase**:** 43-75.

Xu, F., W. Shin, S. H. Brown, J. A. Wahleithner, U. M. Sundaram and E. I. Solomon (1996). "A study of a series of recombinant fungal laccases and bilirubin oxidase that exhibit significant differences in redox potential, substrate specificity, and stability." *Biochim Biophys Acta* 1292(2): 303-311.

Xu, H., Y. Z. Lai, D. Slomczynski, J. P. Nakas and S. W. Tanenbaum (1997). "Mediator-assisted selective oxidation of lignin model compounds by laccase from Botrytis cinerea." *Biotechnol Lett* 19(10): 957-960.

Xu, Z., P. Lei, R. Zhai, Z. Wen and M. Jin (2019). "Recent advances in lignin valorization with bacterial cultures: microorganisms, metabolic pathways, and bio-products." *Biotechnol Biofuels* 12: 32.

Xu, Z., L. Qin, M. Cai, W. Hua and M. Jin (2018). "Biodegradation of kraft lignin by newly isolated Klebsiella pneumoniae, Pseudomonas putida, and Ochrobactrum tritici strains." *Environmental Science and Pollution Research* 25(14): 14171-14181.

Yamada, Y., T. Fujiwara, T. Sato, N. Igarashi and N. Tanaka (2002). "The 2.0 A crystal structure of catalase-peroxidase from Haloarcula marismortui." *Nat Struct Biol* 9(9): 691-695.

Yamanashi, T., S. Y. Kim, H. Hara and N. Funa (2015). "In vitro reconstitution of the catabolic reactions catalyzed by PcaHG, PcaB, and PcaL: the protocatechuate branch of the β-ketoadipate pathway in Rhodococcus jostii RHA1." *Biosci Biotechnol Biochem* 79(5): 830-835.

Yang, C., G. Cao, Y. Li, X. Zhang, H. Ren, X. Wang, J. Feng, L. Zhao and P. Xu (2008). "A constructed alkaline consortium and its dynamics in treating alkaline black liquor with very high pollution load." *PLoS One* 3(11): e3777.

Yang, W., H. Tang, J. Ni, Q. Wu, D. Hua, F. Tao and P. Xu (2013). "Characterization of Two Streptomyces Enzymes That Convert Ferulic Acid to Vanillin." *PLoS One* 8(6): e67339.

Yang, Y., H. R. Wang and H. M. Zhou (1996). "Kinetics of inhibition of aminoacylase activity by dithiothreitol or 2-mercaptoethanol." *Int J Pept Protein Res* 48(6): 532-538.

Yoon, S. H., S. M. Ha, S. Kwon, J. Lim, Y. Kim, H. Seo and J. Chun (2017). "Introducing EzBioCloud: a taxonomically united database of 16S rRNA gene sequences and whole-genome assemblies." *Int J Syst Evol Microbiol* 67(5): 1613-1617.

Yoshikata, T., K. Suzuki, N. Kamimura, M. Namiki, S. Hishiyama, T. Araki, D. Kasai, Y. Otsuka, M. Nakamura, M. Fukuda, Y. Katayama and E. Masai (2014). "Three-Component O-Demethylase System Essential for Catabolism of a Lignin-Derived Biphenyl Compound in Sphingobium sp. Strain SYK-6." *Appl Environ Microbiol* 80(23): 7142-7153.

Yoshino, M. and K. Murakami (2015). "Analysis of the substrate inhibition of complete and partial types." *SpringerPlus* 4(1): 292.

Yu, W., W. Liu, H. Huang, F. Zheng, X. Wang, Y. Wu, K. Li, X. Xie and Y. Jin (2014). "Application of a novel alkali-tolerant thermostable DyP-type peroxidase from Saccharomonospora viridis DSM 43017 in biobleaching of eucalyptus kraft pulp." *PLoS One* 9(10): e110319.

Yun, S. H., C. W. Choi, S. Y. Lee, Y. G. Lee, J. Kwon, S. H. Leem, Y. H. Chung, H. Y. Kahng, S. J. Kim, K. K. Kwon and S. I. Kim (2014). "Proteomic characterization of plasmid pLA1 for biodegradation of polycyclic aromatic hydrocarbons in the marine bacterium, Novosphingobium pentaromativorans US6-1." *PLoS One* 9(6): e90812.

Zakzeski, J., P. C. A. Bruijnincx, A. L. Jongerius and B. M. Weckhuysen (2010). "The Catalytic Valorization of Lignin for the Production of Renewable Chemicals." *Chem Rev* 110(6): 3552-3599.

Zámocký, M., S. Hofbauer, I. Schaffner, B. Gasselhuber, A. Nicolussi, M. Soudi, K. F. Pirker, P. G. Furtmüller and C. Obinger (2015). "Independent evolution of four heme peroxidase superfamilies." *Archives of biochemistry and biophysics* 574: 108-119.

Zámocký, M., G. Regelsberger, C. Jakopitsch and C. Obinger (2001). "The molecular peculiarities of catalase-peroxidases." *FEBS Lett* 492(3): 177-182.

Zeng, J., X. Lin, J. Zhang, X. Li and M. H. Wong (2011). "Oxidation of polycyclic aromatic hydrocarbons by the bacterial laccase CueO from *E. coli*." *Applied Microbiology and Biotechnology* 89(6): 1841-1849.

Zeng, J., D. Singh, D. D. Laskar and S. Chen (2012). "Degradation of native wheat straw lignin by Streptomyces viridosporus T7A." *International Journal of Environmental Science and Technology* 10(1): 165-174.

Zhang, X.-Z. and Y.-H. P. Zhang (2013). Cellulases: Characteristics, Sources, Production, and Applications. <u>Bioprocessing Technologies in Biorefinery for Sustainable Production of Fuels, Chemicals, and Polymers,</u> John Wiley & Sons, Inc.**:** 131-146.

Zhang, Y. H. and L. R. Lynd (2004). "Toward an aggregated understanding of enzymatic hydrolysis of cellulose: noncomplexed cellulase systems." *Biotechnol Bioeng* 88(7): 797-824.

Zhang, Z.-G., Z.-L. Yi, X.-Q. Pei and Z.-L. Wu (2010). "Improving the thermostability of Geobacillus stearothermophilus xylanase XT6 by directed evolution and site-directed mutagenesis." *Bioresour Technol* 101(23): 9272-9278.

Zhao, X., K. Cheng and D. Liu (2009). "Organosolv pretreatment of lignocellulosic biomass for enzymatic hydrolysis." *Applied Microbiology and Biotechnology* 82(5): 815-827.

Zheng, Z., H. Li, L. Li and W. Shao (2012). "Biobleaching of wheat straw pulp with recombinant laccase from the hyperthermophilic *Thermus thermophilus*." *Biotechnol Lett* 34(3): 541-547.

Zhou, X., W. Li, R. Mabon and L. J. Broadbelt (2017). "A critical review on hemicellulose pyrolysis." *Energy Technology* 5(1): 52-79.

Zhu, C., Z. Xu and R. Song (2011). "The endoglucanase from Bacillus subtilis BEC-1 bears halo-tolerant, acidophilic and dithiothreitol-stimulated enzyme activity." *World Journal of Microbiology and Biotechnology* 27(12): 2863-2871.

Zhu, Z., N. Sathitsuksanoh and Y. H. Percival Zhang (2009). "Direct quantitative determination of adsorbed cellulase on lignocellulosic biomass with its application to study cellulase desorption for potential recycling." *Analyst* 134(11): 2267-2272.

Zimmermann, W. (1990). "Degradation of lignin by bacteria." *Journal of Biotechnology* 13: 119 - 130.

Zwietering, M. H., I. Jongenburger, F. M. Rombouts and K. van 't Riet (1990). "Modeling of the Bacterial Growth Curve." *Appl Environ Microbiol* 56(6): 1875-1881.

<u>Websites</u>

www.dovetailinc.org

https://digitalinsights.qiagen.com

https://genome.jgi.doe.gov/portal/

Appendix
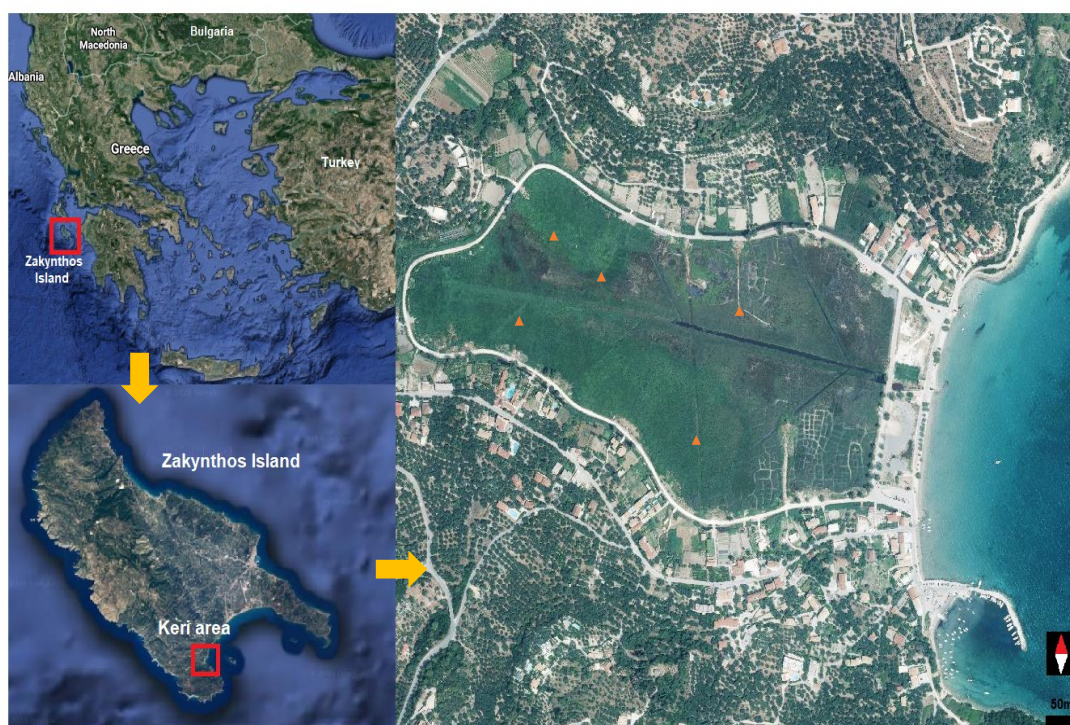
Figure A1. The Keri Lake, at Zakynthos Island, western Greece. The sampling sites are indicated with orange triangles.

Table A1. Taxonomic identification of Keri isolates, based on 16S rRNA sequences. The highest score candidates from GenBank and EzBioCloud database are shown.

Isolate	ATHUBA Culture Collection Acc. No.	16S rRna GenBank Acc. No.	GenBank		EzBioCloud	
			Strain	Identity (%)	Strain	Identity (%)
ZKA1	ATHUBa1401	MT683172	*Achromobacter pulmonis* R-16442	100	*Achromobacter pulmonis* LMG 26696	99.85
ZKA2	ATHUBa1402	MT683173	*Pseudomonas aeruginosa* DSM 50071	100	*Pseudomonas aeruginosa* JCM 5962	100
ZKA3	ATHUBa1403	MT683174	*Pseudomonas plecoglossicida* NBRC 103162	99	*Pseudomonas putida* KT2440	100
ZKA4	ATHUBa1404	MT683175	*Bordetella tumbae* T6713-1-3b	99	*Bordetella tumbae* T6713-1-3b	99.62
ZKA5	ATHUBa1405	MT683176	*Pseudomonas pseudoalcaligenes* Stanier 63	99	*Pseudomonas oleovorans* subsp. oleovorans DSM 1045	98.73
ZKA6	ATHUBa1406	MT683177	*Pseudomonas plecoglossicida* NBRC 103162	99	*Pseudomonas* sp. R17(2017)	100
ZKA7	ATHUBa1407	MT683178	*Pseudomonas kilonensis* 520-20	99	*Pseudomonas fluorescens* 2P24	99.86
ZKA8	ATHUBa1408	MT683179	*Achromobacter pulmonis* R-16442	100	*Achromobacter pulmonis* LMG 26696	99.86
ZKA9	ATHUBa1409	MT683180	*Pseudomonas resinovorans* ATCC 14235	100	*Pseudomonas resinovorans* LMG 26696	99.15
ZKA10	ATHUBa1410	MT683181	*Pseudomonas plecoglossicida* NBRC 103162	100	*Pseudomonas* sp. R17(2017)	100
ZKA11	ATHUBa1411	MT683182	*Pseudomonas oryzihabitans* L-1	99	*Pseudomonas capeferrum* WCS358	99.93
ZKA12	ATHUBa1412	MT683183	*Pseudomonas plecoglossicida* NBRC 103162	99	*Pseudomonas* sp. R17(2017)	100
ZKA13	ATHUBa1413	MT683184	*Pseudomonas oryzihabitans* L-1	99	*Pseudomonas capeferrum* WCS358	99.93

ZKA14	ATHUBa1414	MT683185	*Sphingobium yanoikuyae* NBRC 15102	99	*Sphingobium yanoikuyae* ATCC 51230	99.78
ZKA15	ATHUBa1415	MT683186	*Microbacterium ginsengiterrae* DCY37	98	*Microbacterium shaanxiense* CCNWSP60(T)	98.34
ZKA16	ATHUBa1416	MT683187	*Paracandidimonas soli* IMT-305	97	*Paracandidimonas soli* IMT-305	98.43
ZKA17	ATHUBa1417	MT683188	*Cellulosimicrobium cellulans* DSM 43879	99	*Cellulosimicrobium funkei* ATCC BAA-886	99.64
ZKA18	ATHUBa1418	MT683189	*Paracandidimonas soli* IMT-305	98	*Paracandidimonas soli* IMT-305	98.65
ZKA19	ATHUBa1419	MT683190	*Cellulomonas pakistanensis* NCCP-11	98	*Cellulomonas hominis* JCM 12133	98.5
ZKA20	ATHUBa1420	MT683191	*Klebsiella aerogenes* NBRC 13534	99	*Klebsiella aerogenes* KCTC 2190	99.86
ZKA21	ATHUBa1421	MT683192	*Microbacterium thalassium* DSM 12511	99	*Microbacterium thalassium* IFO 16060	98.42
ZKA22	ATHUBa1422	MT683193	*Stenotrophomonas maltophilia* IAM 12423	99	*Stenotrophomonas maltophilia* MTCC 434	99.72
ZKA23	ATHUBa1423	MT683194	*Shinella kummerowiae* CCBAU 25048	98	*Sinorhizobium* sp. RAC02	98.46
ZKA24	ATHUBa1424	MT683195	*Ochrobactrum rhizosphaerae* PR17	99	*Ochrobactrum pituitosum* CCUG 50899	99.71
ZKA25	ATHUBa1425	MT683196	*Sphingobium yanoikuyae* NBRC 15102	99	*Sphingobium* sp. AP49	99.27
ZKA26	ATHUBa1426	MT683197	*Advenella kashmirensis* WT001	99	*Advenella kashmirensis* subsp. *methylica* PK1	99.93
ZKA27	ATHUBa1427	MT683198	*Microbacterium sorbitolivorans* SZDIS-1-1	99	*Microbacterium sorbitolivorans* SZDIS-1-1	99.86
ZKA28	ATHUBa1428	MT683199	*Pseudomonas composti* C2	100	*Pseudomonas composti* CCUG 59231	100
ZKA29	ATHUBa1429	MT683200	*Paracoccus caeni* MJ17	99	*Paracoccus caeni* MJ17	100
ZKA30	ATHUBa1430	MT683201	*Microbacterium pumilum* KV-488	99	*Microbacterium pumilum* KV-488	99.21
ZKA31	ATHUBa1431	MT683202	*Advenella kashmirensis* WT001	99	*Advenella kashmirensis* subsp. *methylica* PK1	99.93
ZKA32	ATHUBa1432	MT683203	*Pseudomonas plecoglossicida* NBRC 103162	99	*Pseudomonas* sp. R17(2017)	100
ZKA33	ATHUBa1433	MT683204	*Rhodococcus pyridinivorans* PDB9	100	*Rhodococcus pyridinivorans* DSM 44555	99.86
ZKA34	ATHUBa1434	MT683205	*Parapedobacter pyrenivorans* P-4	99	*Parapedobacter pyrenivorans* P-4	98.85
ZKA35	ATHUBa1435	MT683206	*Pseudomonas plecoglossicida* NBRC 103162	99	*Pseudomonas* sp. R17(2017)	100
ZKA36	ATHUBa1436	MT683207	*Pseudomonas aeruginosa* DSM 50071	99	*Pseudomonas aeruginosa* JCM 5962	99.86
ZKA37	ATHUBa1437	MT683208	*Pseudomonas putida* NBRC 14164	99	*Pseudomonas putida* ATH-43	99.86
ZKA38	ATHUBa1438	MT683209	*Achromobacter pulmonis* R-16442	100	*Achromobacter pulmonis* LMG 26696	100
ZKA39	ATHUBa1439	MT683210	*Pseudomonas songnenensis* NEAU-ST5-5	98	*Pseudomonas stutzeri* DSM 17088	99.78
ZKA40	ATHUBa1440	MT683211	*Stenotrophomonas pavanii* strain LMG 25348	98	*Stenotrophomonas indicatrix* WS40	100
ZKA41	ATHUBa1441	MT683212	*Pseudomonas plecoglossicida* NBRC 103162	99	*Pseudomonas putida* KT2440	100
ZKA42	ATHUBa1442	MT683213	*Sphingomonas sanxanigenens* NX02	99	*Sphingomonas sanxanigenens* DSM 19645	99.93
ZKA43	ATHUBa1443	MT683214	*Microbacterium resistens* DMMZ 1710	98	*Microbacterium shaanxiense* CCNWSP60(T)	98.34
ZKA44	ATHUBa1444	MT683215	*Sphingobacterium pakistanense* NCCP-246	98	*Sphingobacterium pakistanense* NCCP-246	98.29
ZKA45	ATHUBa1445	MT683216	*Bordetella tumbae* T6713-1-3b	99	*Bordetella tumbae* T6713-1-3b	99.65
ZKA46	ATHUBa1446	MT683217	*Microbacterium trichothecenolyticum* DSM 8608	99	*Microbacterium trichothecenolyticum* DSM 8608	99.14

ZKA47	ATHUBa1447	MT683218	*Pseudomonas aeruginosa* DSM 50071	100	*Pseudomonas aeruginosa* JCM 5962	100
ZKA48	ATHUBa1448	MT683219	*Cellulosimicrobium cellulans* DSM 43879	99	*Cellulosimicrobium funkei* ATCC BAA-886	99.5
ZKA49	ATHUBa1449	MT683220	*Rhodococcus pyridinivorans* PDB9	99	*Rhodococcus pyridinivorans* DSM 44555	99.86
ZKA50	ATHUBa1450	MT683221	*Pseudomonas pseudoalcaligenes* Stanier 63	99	*Pseudomonas oleovorans* subsp. *Oleovorans* DSM 1045	98.73
ZKA51	ATHUBa1451	MT683222	*Pseudomonas pseudoalcaligenes* Stanier 63	99	*Pseudomonas oleovorans* subsp. *Oleovorans* DSM 1045	98.8
ZKA52	ATHUBa1452	MT683223	*Alcanivorax dieselolei* B5	99	*Alcanivorax dieselolei* B-5	99.86
ZKA53	ATHUBa1453	MT683224	*Ancylobacter pratisalsi* E130	99	*Ancylobacter pratisalsi* E130	99.41
ZKA54	ATHUBa1454	MT683225	*Sinomicrobium oceani* SCSIO 03483	99	*Sinomicrobium oceani* SCSIO 03483	100
ZKA55	ATHUBa1455	MT683226	*Pseudomonas knackmussii* B13	99	*Pseudomonas kunmingensis* HL22-2	99.29
ZKA56	ATHUBa1456	MT683227	*Microbacterium esteraromaticum* DSM 8609	99	*Microbacterium esteraromaticum* DSM 8609	99.64
ZKA57	ATHUBa1457	MT683228	*Microbacterium esteraromaticum* DSM 8609	99	*Microbacterium esteraromaticum* DSM 8609	99.64
ZKA58	ATHUBa1458	MT683229	*Bacillus thuringiensis* ATCC 10792	100	*Bacillus mobilis* 0711P9-1	100
ZKA59	ATHUBa1459	MT683230	*Fictibacillus nanhaiensis* JSM 082006	99	*Fictibacillus nanhaiensis* JSM 082006	99.44
ZKA60	ATHUBa1460	MT683231	*Bacillus mojavensis* NBRC 15718	99	*Bacillus halotolerans* ATCC 25096	99.93
ZKA61	ATHUBa1461	MT683232	*Bacillus thuringiensis* ATCC 10792	99	*Bacillus mobilis* 0711P9-1	99.93
ZKA62	ATHUBa1462	MT683233	*Enterobacter tabaci* YIM Hb-3	99	*Enterobacter tabaci* YIM Hb-3	99.86
ZKA63	ATHUBa1463	MT683234	*Sphingobacterium siyangense* SY1	99	*Sphingobacterium siyangense* SY1	99.25
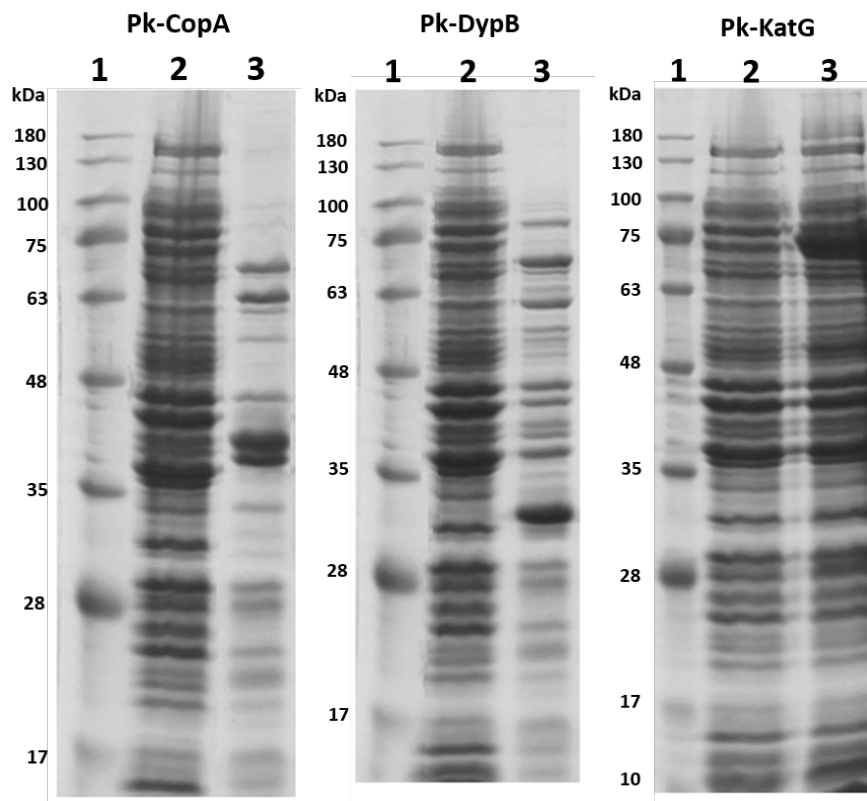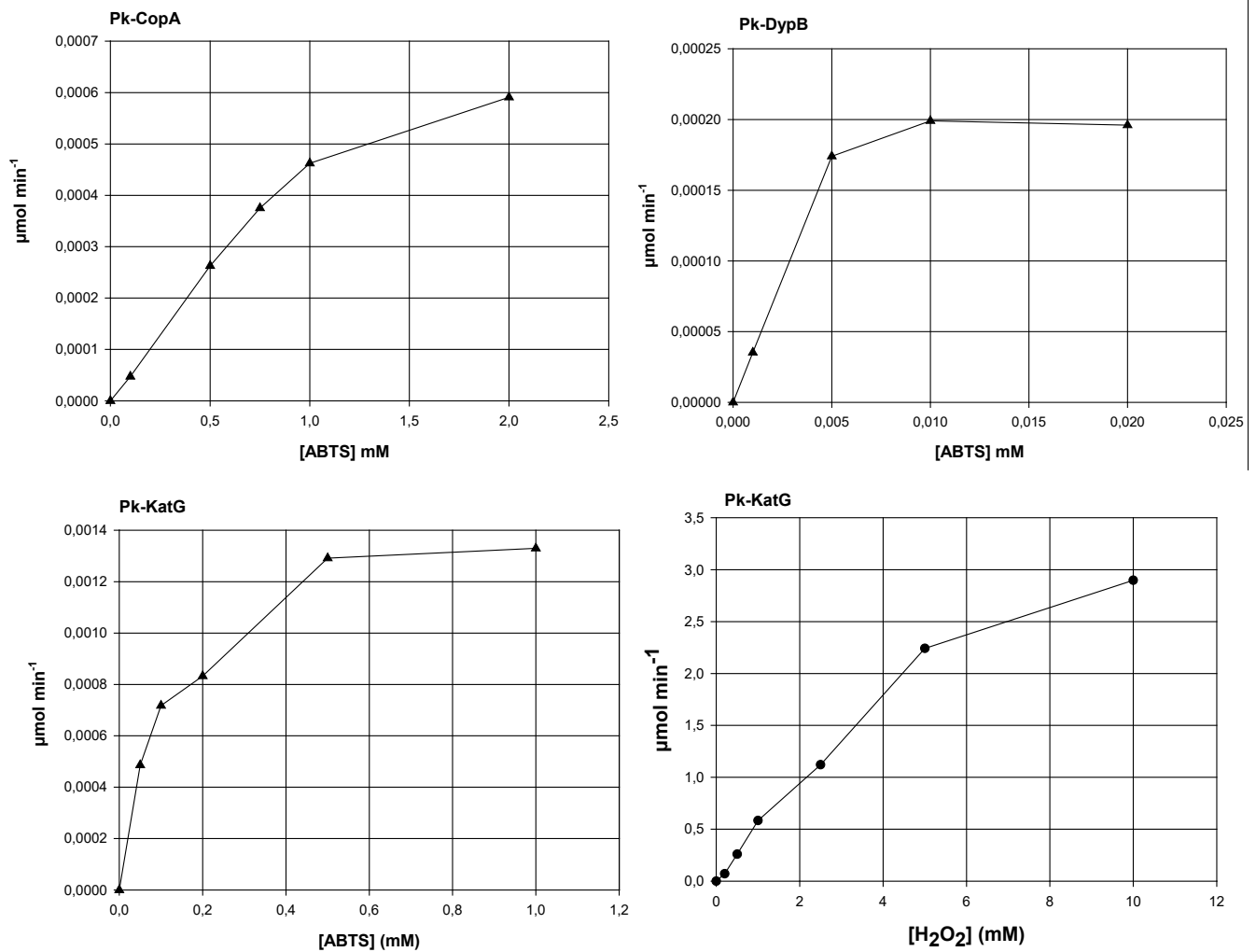
Fig. A3. The initial reaction rates of Pk-CopA, Pk-DypB and Pk-KatG against different ABTS concentrations and of Pk-KatG against different H_2O_2 concentrations. The reaction rates are expressed in µmoles of product formed for ABTS or µmoles of substrate consumed for H_2O_2, per minute of reaction. The substrate concentration giving the highest reaction rate in the linear part of the plot was chosen for further kinetic studies of the enzymes.
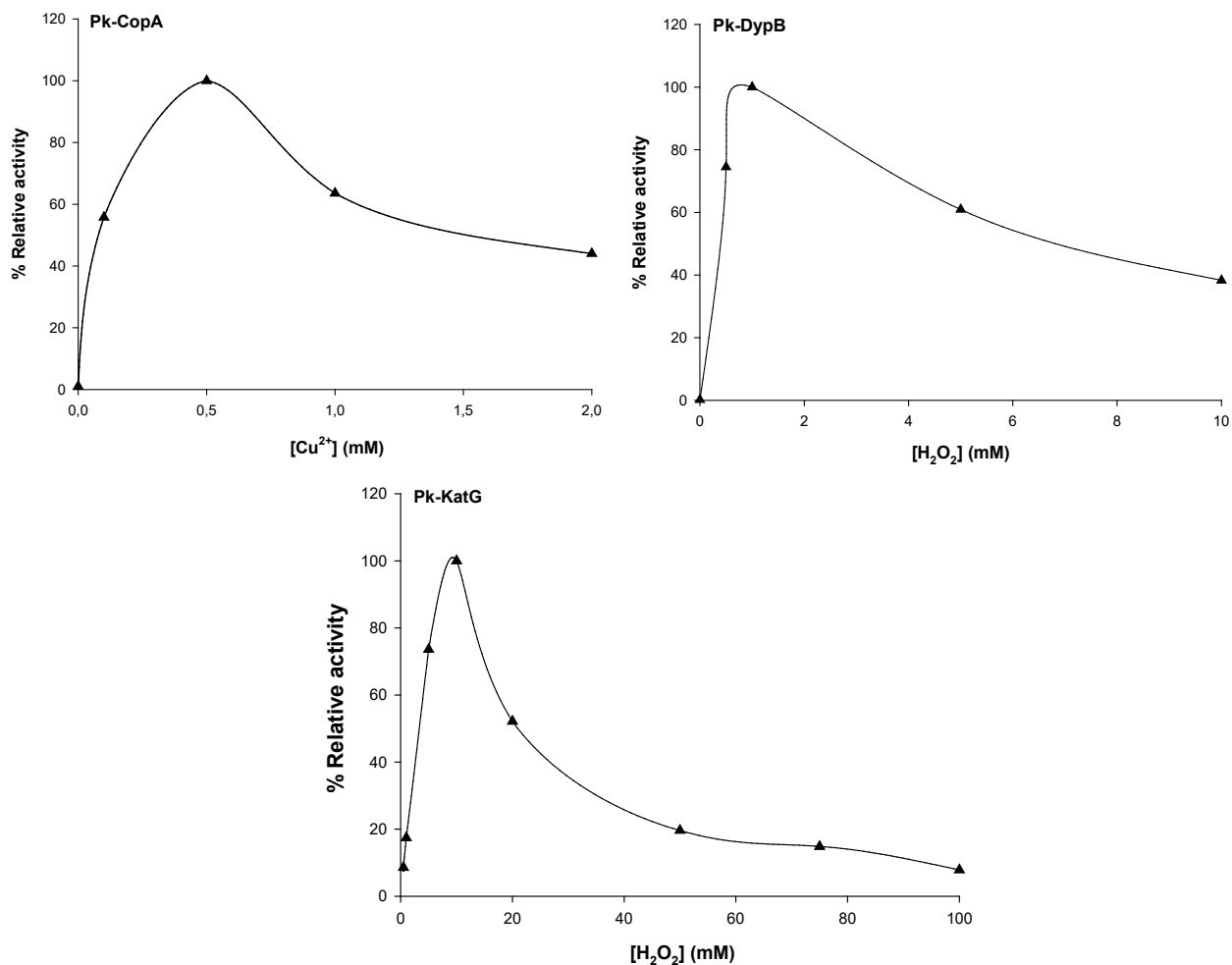
Fig. A4. The effect of copper concentration on the ABTS activity of Pk-CopA, and the effect of hydrogen peroxide concentration on the ABTS activity of Pk-DypB and Pk-KatG. Reactions were conducted in a 100 mM phosphate buffer, with 1.0 mM, 0.01 mM and 0.1 mM ABTS for Pk-CopA, Pk-DypB and Pk-KatG, respectively, at 30 °C. Relative activity is expressed as a percentage of the optimum initial reaction rate.
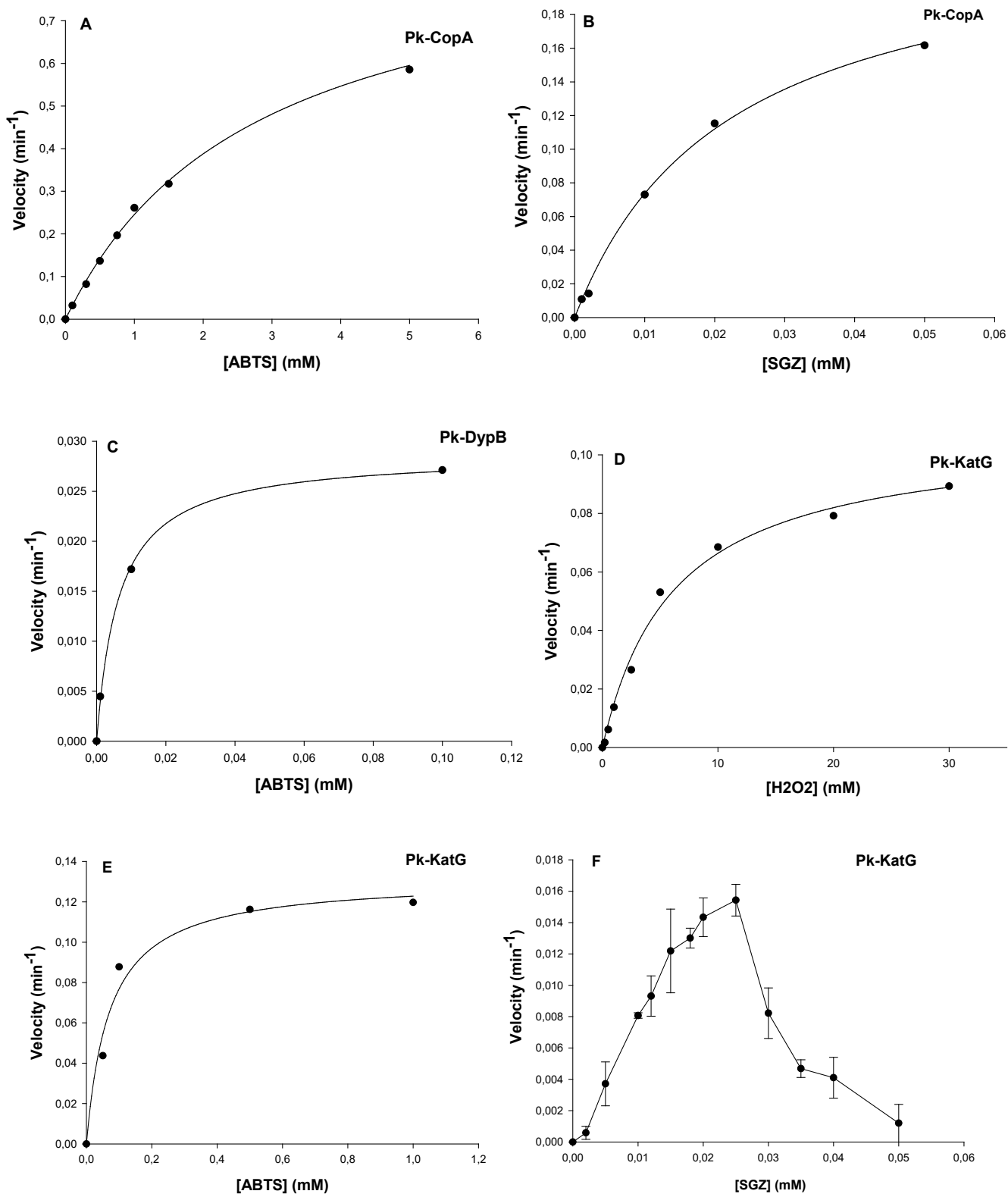
Fig. A5. The Michaelis-Menten plots from which the Km constant and the maximum reaction rate (Vmax) of the enzymatic reactions were calculated.
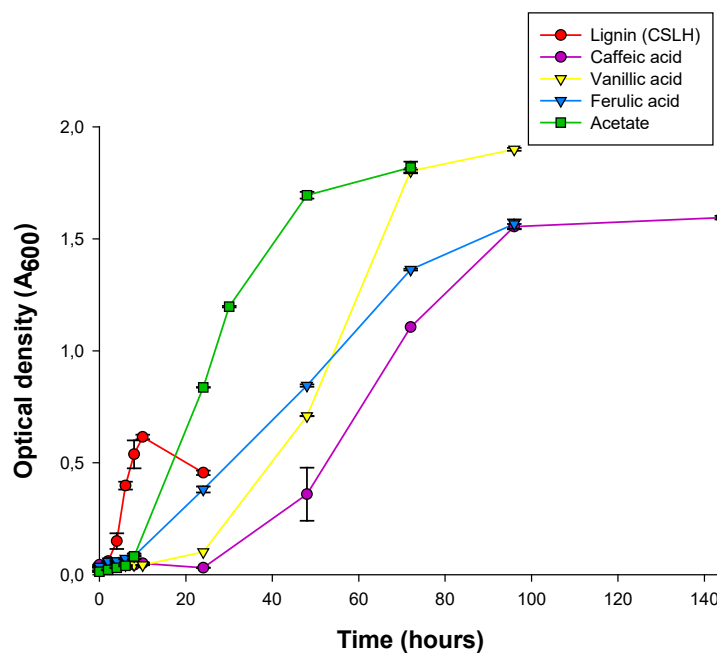
Fig. A6. Growth curves of *Pseudomonas kilonensis* ZKA7 cells grown on mineral salt medium supplemented with 1.5 TOC lignin hydrolysate from alkali pretreated corn stover, 1.0 TOC ferulic acid, TOC caffeic acid, 1.0 TOC vanillic acid and 0.5 TOC acetate. Incubation was performed at 30 °C, at 180 rpm.
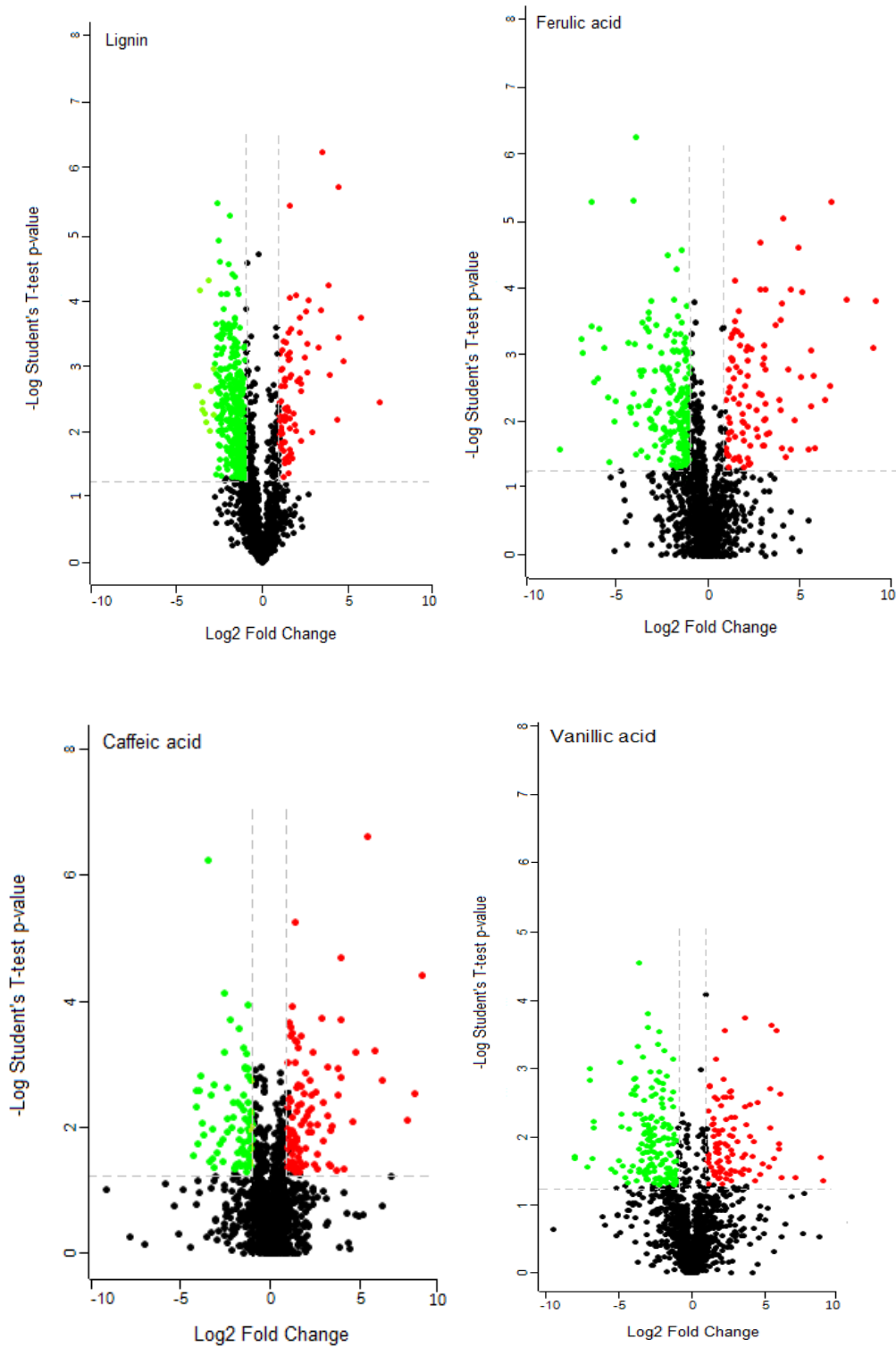
Fig. A7. Scatter plot of differential gene expression of *P. kilonensis* ZKA7 cells grown on lignin from alkali pretreated corn stover, ferulic acid, caffeic acid or vanillic acid. Acetate was used as a reference substrate for each treatment. Each dot represents a gene, and its position in the x-axis corresponds to the log2 fold change (ratio of expression level in substrate vs reference substrate), whereas its position in the y-axis corresponds to the negative logarithm of the p-value (p-value = 0.05. Vertical grey lines correspond to 2.0-fold upregulation and 2.0-fold downregulation of expression, and horizontal grey lines indicate p=0.05. Red dots represent upregulated genes with statistical significance, and green dots represent downregulated genes with statistical significance.